School of Biological Sciences

Study of Neuropilin-1 interactions

Thesis submitted in accordance with the requirements of the University of Liverpool for the degree of Doctor in Philosophy

by

Katarzyna Adela Uniewicz

October 2010

"The most beautiful thing we can experience is the mysterious. It is the source of all true art and all science"

Albert Einstein

Abstract

Neuropilin-1 (NRP-1) was discovered in the 1990's as a powerful cellular membrane protein involved in the control of axon migration and angiogenesis. Owing to its large multidomain structure, it was thought to interact with multiple molecules present in its environment, and thus, play an important role as a molecular network hub regulating the local multi-component signalling flow. While NRP-1 does not posses any intrinsic tyrosine kinase activity on its own, it was suggested to act via formation of signalling complexes with other receptors and affect their signalling properties in response to their soluble ligands. Importantly, as a part of the extracellular matrix, NRP-1 was also suggested to be further regulated by interaction with cell surface heparan sulfate.

The doctoral project targeted several principle ideas of the field. First of all, the extensive analysis of NRP-1's interaction with the proxy of heparan sulfate, heparin, was undertaken. The characterisation of NRP-1's preference for the sulfation pattern and length of oligosaccharide is the first obtained for the recombinant NRP-1 species. An additional attempt to map major areas involved in interaction with heparin within recombinant NRP-1 revealed possible sites of heparin interaction and intramolecular interactions occurring due to the binding of the protein to the polysaccharide. Since the study used a dimeric Fc fusion construct, a set of experiments were designed to identify the importance of functional properties that derived from NRP-1's dimerisation, the regions that may be important in driving dimerisation and so explain the differences observed between monomeric and dimeric NRP-1 species.

Another part of the project was focused on the functional aspect of the recombinant NRP-

1 species and demonstrated an exciting new property of the protein, namely that contrary to the current view that defines NRP-1 as an enhancer of VEGF-A_{165}-driven angiogenesis, the dimeric NRP-1 independently induced tubular differentiation of endothelial cells. This was observed even in the presence of a VEGF-A sequestering antibody and was mediated by direct VEGFR-2 activation. This finding undermines the current model of NPR-1's mechanism of function and also indicates putative pharmacological applications of recombinant NRP-1.

Finally, the work on the NRP-1 biochemical and functional properties was complemented by the development of a novel method of analysis of interactions of polysaccharides with proteins. The method records the thermostabilisation effect that polysaccharide bestows on an interacting protein partner and provides numerical values of detected melting temperatures. Adapted to a multiwell format, the assay allows investigation of the specificity of binding in a high-throughput manner.

Overall, the thesis provides new insights into NRP-1 structure-function relationship and advances several aspects of understanding of its nature. The thermostability assay developed and described alongside goes beyond the NRP-1 field, and permits high quality data to be obtained for any protein that is stabilised by polysaccharides or other small molecules.

Acknowledgments

The work was supported by the European Commission (Marie Curie Early Stage Training Fellowship), the North West Cancer Research Fund and the Cancer and Polio Research Fund.

The author would like to thank **Prof David Fernig** for appointing her for the project on Neuropilin-1 structure-function relationship and guiding in the development of her scientific independence. This was probably the most character shaping experience ever. She would also like to thank for three years of scientific discussions, which broadened her views on importance of having imagination and freedom of mind in science.

The author would like to thank to her assessor, **Dr. Roger Barraclough**, for extremely important indications in career development.

The author would like to thank to her assessor, **Prof Philip Rudland**, for help in estimating the best pathway choice in managing the project.

The author would like to thank to her collaborator, **Dr. Michael Cross**, for showing to her superb quality in lab practice and high professionalism.

The author would like to thank to her other collaborator, **Dr. Ed Yates**, for introducing to sophisticated written English and spreading good common sense irony.

The author would like to thank to her other collaborator, **Dr. Daniel Rigden**, for presenting

the fascinating world of *in silico* approach towards understanding biological data.

Above all, the author would like to thank to all the members of the Fernig, Cross, Yates, Barraclough, Turnbull, Mayans, Murray, Levy, Fisher, Barsukov groups and any people that provided help and support in discussions, demonstrations, or simply, for being there in everyday lab life.

Separate acknowledgements are directed to the companies' representatives that helped to obtain some of the described results, **Jonathan Popplewell** of Farfield group, and **Liam Brady** of Waters.

The main expression of gratitude goes to **Dr. Alessandro Ori**, for enormous support in performance of this impossible project and believing in the intellectual skills of the author. The project would have never been accomplished without his help and the presentation of this thesis is a proof of determination of the author fueled by his boundless care.

Contents

Abstract iii

Acknowledgments v

Contents vii

List of Figures x

List of Tables xii

List of Abbreviations xiv

1 Introduction **1**

1.1 NRP-1 state of knowledge 1

1.2 Things about NRP-1 that we know and we do not know 2

1.3 Thesis objectives 11

2 Materials and Methods **12**

2.1 Materials 12

2.2 Protein biochemical methods 13

2.2.1 N-glycanase digest 13

2.2.2 Selective labelling and identification of the heparin-binding peptides derived from Fc rNRP1 13

2.2.3 Peptide analysis 15

2.2.4 Binding to heparin affinity minicolumns 15

2.2.5 Differential Scanning Fluorimetry (DSF) 16

2.2.6 DSF data analysis 16
2.2.7 Native proteolytic digest 17
2.2.8 Crosslinking 17
2.3 Surface-based methods 18
2.3.1 Heparin surface preparation 18
2.3.2 Binding assays 18
2.3.3 Biosensor data analysis 20
2.3.4 Dual polarisation interferometry (DPI) 20
2.3.5 DPI data analysis 21
2.4 Tissue culture methods 22
2.4.1 BaF3 proliferation assay 22
2.4.2 Tissue culture of HDMECs 23
2.4.3 Tube formation assay 23
2.4.4 Data analysis of the tube formation 24
2.4.5 Signalling assay 25
2.4.6 Data analysis of the signalling assay 25
2.5 PAGE, western blot and silver staining 26
2.5.1 Biochemical analysis 26
2.5.2 Gel electrophoresis and western blot of HDMECs samples 26
2.6 Bioinformatics 27
2.6.1 General bioinformatics 27
2.6.2 Homology modelling of the c domain 27
2.6.3 Docking analysis of the c domain 28
2.6.4 Homology modelling of NRP-1 28
2.6.5 Sequence alignments of NRP sequences 29
2.6.6 Visualisation of the structures 29

3 Development of the differential scanning fluorimetry method to probe protein-glycosaminoglycans interactions 32

4 Biochemical analysis of the interaction of Neuropilin-1 with heparin 38

4.1 Structural characterisation of NRP-1 proteins 42

4.2 Determination of interaction of shNRP-1 and Fc rNRP-1 with heparin 46

4.3 Characterisation of the Fc rNRP-1 interaction with heparin by optical biosensor . 49

4.4 Identification of the protected/ buried regions of Fc rNRP-1 upon interaction with heparin 59

4.5 Further verification of shNRP-1 binding to heparin 71

4.6 Investigation of relationship between monomeric/ dimeric state of NRP-1 and heparin-binding ability 75

4.7 Investigation of importance of the c domain of NRP-1 and heparin-binding ability 78

5 Exogenous recombinant dimeric Fc rNRP-1 is sufficient to drive angiogenesis in human dermal microvascular endothelial cells 90

5.1 Characterisation of recombinant soluble NRP-1s 93

5.2 Induction of tube formation by Fc rNRP-1 and shNRP-1 via VEGFR-2 activation . 95

5.3 Fc rNRP-1 response is blocked by a VEGFR-2 specific inhibitor ZM323881 . . . 101

5.4 Fc rNRP-1-driven tube formation occurs in VEGF-A_{165} depleted cells 101

5.5 Sequestration of VEGFs with anti-VEGF-A antibody does not block tube formation105

6 General Discussion 110

Supplemental paper 1 117

Supplemental paper 2 140

Supplemental data 3 148

Bibliography 165

List of Figures

1.1 Postulated Neuropilin-1 extracellular and intracellular interactions 4

1.2 Challenging novel aspects of NRP-1 biology 10

2.1 Crosslinking reagents used in the study 30

3.1 Typical recording of fluorescence intensity versus temperature for the unfolding of protein in the presence of Sypro® Orange 34

3.2 Denaturation curves of the proteins tested by DSF applying Sypro® Orange dye . 37

4.1 Analysis of the disorder of the structures of human NRP-1 and FGF-1 43

4.2 Analysis of recombinant NRP-1 species 45

4.3 Characterisation of the interaction of Fc rNRP-1 and shNRP-1 with heparin in an optical biosensor and a BaF3 cell assay 48

4.4 Kinetic analysis of Fc rNRP-1 binding to heparin surface in biosensor IAsys . . . 50

4.5 Additional information on oligosaccharides used in the competition assays 53

4.6 Schematic presentation of the modified heparin derivatives used in the competition assays 53

4.7 Competition experiments defining length of heparin-derived oligosaccharide requirement that enable Fc rNRP-1 binding 54

4.8 Competition experiments defining heparin sulfation pattern requirements that enable Fc rNRP-1 binding 56

4.9 Competition experiments defining heparin cationic forms requirements that enable Fc rNRP-1 binding 58

4.10 Analysis of protein in the course of the P&L procedure 60

4.11 Clustal W alignment of the NRP sequences 64

4.12 Approximate localisation of the identified rat NRP-1 peptides on the human NRP-2 crystal structure (2QQL) presented in the proposed dimeric form [1] . . . 66

4.13 Localisation of the identified rat NRP-1 peptides in the human c domain obtained by *in silico* modelling 68

4.14 Approximate localisation of the identified rat NRP-1 peptides in the human NRP-1 obtained by *in silico* modelling 69

4.15 Comparison of Fc rNRP-1 and shNRP-1 binding to two different heparin affinity resins 72

4.16 Sypro stability assay of recombinant NRP-1s 74

4.17 Tryptic digests of recombinant NRP-1s 76

4.18 Dual polarisation interferometry analysis of binding of recombinant NRP-1 isoforms to dp 16 77

4.19 Bioinformatics analysis of the potential docking sites for protein interactions within the c domain 80

4.20 The cross-eye stereo picture of the c domains dimer according to the HADDOCK prediction 81

4.21 The analysis of the binding capacities of the two different products of native tryptic digest of the Fc rNRP-1 83

4.22 Schematic representation of the truncated Fc rNRP-1-derived proteins obtained in trypsin digests 85

5.1 Sequence analysis of recombinant NRP-1 proteins and human wild-type NRP-1 94

5.2 Recombinant NRP-1 proteins stimulate tube formation in HDMECs 96

5.3 Western blot result of experiment with HDMECs cultured on a layer of collagen . 98

5.4 Western blot result of experiment with HDMECs cultured on a layer of gelatin . . 99

5.5 Western blot for phosphotyrosine-containing proteins in the HDMECs lysates . . 100

5.6 The effect of the VEGFR-2 kinase inhibitor (ZM323881) on tube formation 102

5.7 Western blot result of the effect of addition of VEGFR-2 inhibitor to the HDMECs cultured on collagen 103

5.8 Western blot result of the effect of addition of VEGFR-2 inhibitor to the HDMECs cultured on gelatin 104

5.9 The tube formation induced by Fc rNRP-1 depends on VEGFR-2 kinase activity but not on isoform of the VEGF-A in HDMECs 106

5.10 Effect of a sequestering antibody to VEGF-A on tube formation by HDMECs . . . 107

List of Tables

1.1 An up-to-date list of proteins that interact with NRP-1 4

4.1 Kinetic result of Fc rNRP-1 binding to heparin surface in biosensor IAsys 50

4.2 List of peptides identified in the P&L experiment 62

List of Abbreviations

BMPH	N-(β-maleimidopropionic acid) hydrazide
BSA	Bovine serum albumin
CDK	Cyclin dependent kinase
crNRP-1	c domain containing rat NRP-1
CV	Column volume
CyPB	CyclophilinB
DMSO	Dimethyl sulfoxide
dp	Degree of polimerisation
DPI	Dual polarisation interferometry
DSCR-1	Down syndrome critical region-1
DSF	Differential scanning fluorimetry
DTT	Dithiothreitol
ECM	Extracellular matrix
EDC	1-Ethyl-3-(3-dimethylaminopropyl) carbodiimide hydrochloride
EDTA	ethylenediaminetetraacetic acid
EPCR	Endothelial cell protein C receptor
ERK	Extracellular signal regulated kinase
Fc rNRP-1	Recombinant Fc fused rat Neuropilin-1
FGF	Fibroblast growth factor
FGFR	FGF receptor

GAG	Glycosaminoglycan
HDMECs	Human Dermal Microvascular Endothelial Cells
HGF/ SF	Hepatocyte growth factor/ Scatter factor
HPLC	High-performance liquid chromatography
HRP	Horseraddish peroxidase
HS	Heparan sulfate
HUVECs	Human Umbilical Vein Endothelial Cells
IC50	Half maximal inhibitory concentration
IL	Interleukin
IgG1	Immunoglobulin G1
k_{ass}	Association rate constant
k_{diss}	Dissociation rate constant
K_d	Dissociation equilibrium constant
k_{off}	Dissociation rate
k_{on}	Association rate
MALDI-Q-TOF	Matrix-assisted laser desorption ionisation quadrupole-time of flight
MTT	3-(4,5-Dimethylthiazol-2-yl)-2,5-diphenyltetrazolium bromide
MWCO	Molecular weight cut-off
NHS	N-hydroxysuccinimide
NIP	Neuropilin interacting protein
NRP	Neuropilin
PBS	Phosphate-buffered saline
PBST	Phosphate-buffered saline with Tween
PDGF	Platelet-derived growth factor
PEG-CHO	Aldehyde-functionalised poly(ethylene glycol)
PF-4	Platelet factor 4
PIR	Protein Information Resource

PLCγ-1	Phospholipase C- gamma 1
PlGF-2	Placenta growth factor 2
PMSF	Phenylmethanesulfonylfluoride
PTN	Pleiotrophin
RAGE	Receptor for advanced glycation products
RCAN	Regulator of Calcineurin
SD	Standard deviation
SDS-PAGE	Sodium dodecyl sulfate polyacrylamide gel electrophoresis
SE	Standard error
SEMA	Semaphorin
shNRP-1	Soluble human Neuropilin-1
TBS	Tris-buffered saline
TGF-β	Transforming/ Tumour growth factor-β
trNRP-1	Truncated rat Neuropilin-1
VEGF-A	Vascular endothelial growth factor A
VEGFR	VEGF receptor

Chapter 1

Introduction

1.1 NRP-1 state of knowledge

In 2006, when the doctoral project was commenced, there were ca 500 publications focused on Neuropilin-1 (NRP-1), with the first publications appearing in 1990-91 [2, 3], which described NRP-1 as the antigen A5. This means that during 16 years 462 publications on NRP-1 emerged, while during the length of the subsequent doctoral study, which is 3.5 years, 272 novel findings were published. This number reflects the dynamics of the NRP-1 field, and when compared with the p53 protein, and its total publication record - ca 53000 (http://www.ncbi.nlm.nih.gov/sites/entrez), it illustrates the potential capacity for growth. Much of the data on NRP-1 that has been published up to 2007 was collated and published in the form of a comprehensive review [4] - **Supplemental paper 1**. Additionally, each chapter of this thesis commences with a small review of papers that are directly relevant to the focus of the chapter. This Introduction Chapter provides an overview and, in particular, aims to highlight some of the intriguing aspects of NRP-1.

1.2 Things about NRP-1 that we know and we do not know

It is a well known fact that the vascular and nervous systems show high degree of similarity at the level of organisation and development [5]. First of all, the general architecture of both systems is analogous, where nerves are built of neural cells supported by glial cells, while blood vessels are built of endothelial cells supported by vascular smooth muscle cells and pericytes. Also the co-patterning across the organism and their coordination in responding to the same growth factors is a feature that highlights their likeness [5]. NRP-1 is one of the several molecules, which are expressed by cells in both systems, and is typically listed among strong candidates that indicate the coordination and co-dependence of these systems. This feature makes NRP-1 a very interesting target of studies that aim to investigate the more generic features of the regulation of the neurovascular niche [6], in contrast to the dominating approaches that focus on each system separately. Albeit NRP-1 is a powerful linking argument for the existence of the neurovascular niche, it is its interacting partner molecules that are directly involved in mediating specific responses. The partners use NRP-1 as a non-signalling co-receptor, and it is their presence that allows NRP-1 to be involved in the complex regulation of their action. This is why NRP-1 for most, but not all of its functions, is described in the context of its ligands' properties and their respective signalling receptors.

The interactions of NRP-1 have been described in several publications [4,6–8], and can occur between NRP-1 and other membrane receptors (including NRPs), soluble species (including growth factors and possibly soluble NRPs), and intracellular proteins (Figure 1.1, Table 1.1). Importantly, although more data on NRP-1 interactions is possible to retrieve, some of it is based on techniques such as co-immunoprecipitation and should be treated with caution [9], as they do not necessarily prove a direct interaction. Similarly, a novel source of information on proteins' interactions are multiple online databases, however, they also should be treated cautiously. The main reason is that as they progress by collecting records of possible interactions and arrange them in clusters, some of them remain functional clusters although there is no evidence for a direct physical interaction (http://genomeknowledge.org and [10]). Still, most of

the collected research articles tackling particular interactions of NRP-1 will present reasonable biochemical and/ or biophysical data, however, in a few cases a number of uncertainties arise and a list of articles illustrating the argument is provided. This applies especially in the case of the interactions of NRP-1 with tyrosine kinase receptors, where a direct interaction and bridging through a ligand were initially two parallel concepts present in the field, until more data was provided to support the latter mechanism. Such observations were made for VEGFR-2 and PDGFR, where the most popular view, namely ligand mediated bridging of the NRP: receptor complex, is supported by [11–13] and [14], respectively. A related aspect of the NRP-1 function, although no physical interaction has been confirmed, is the synergism occurring between pathways where NRP-1 is indicated as a linking component. Such synergism was observed between FGF-2 and VEGF-A_{165} [15], but is not supported by biophysical evidence of a direct complex formation between FGF-2 and NRP-1 and VEGFR-2. Thus, alternative mechanisms are equally likely, involving other pathway(s) of NRP-1 function. Until more data are available it is impossible to distinguish between the prevalent view and the alternatives.

Importantly, due to its large size and complex multidomain structure, NRP-1 was suggested to be a hub protein involved in coordinating of the numerous interactions, and probably, in the coming future more proteins will be identified as its interacting partners. Indeed, *in silico* analysis by the InterDom server (http://interdom.i2r.a-star.edu.sg/) estimated that the a1a2 domains could interact with 177 other types of domains, the b1b2 domains with 121, and the c domain with 31 [16]. Additionally, the extracellular domains' loops and unstructured intracellular domain may provide a backbone for more interactions. This contrasts with the up-to-date state of knowledge on NRP-1, which lists ca 30 interacting partners of NRP-1 (Figure 1.1, Table 1.1).

Another group of molecules that interact with NRP-1 are polysaccharides. With regard to the NRP-1 localisation in the pericellular and extracellular matrix (ECM) compartment, the fact that polysaccharides may regulate NRP-1 function is not surprising, given the primordial role of sugars in regulating cell-cell communication [17].

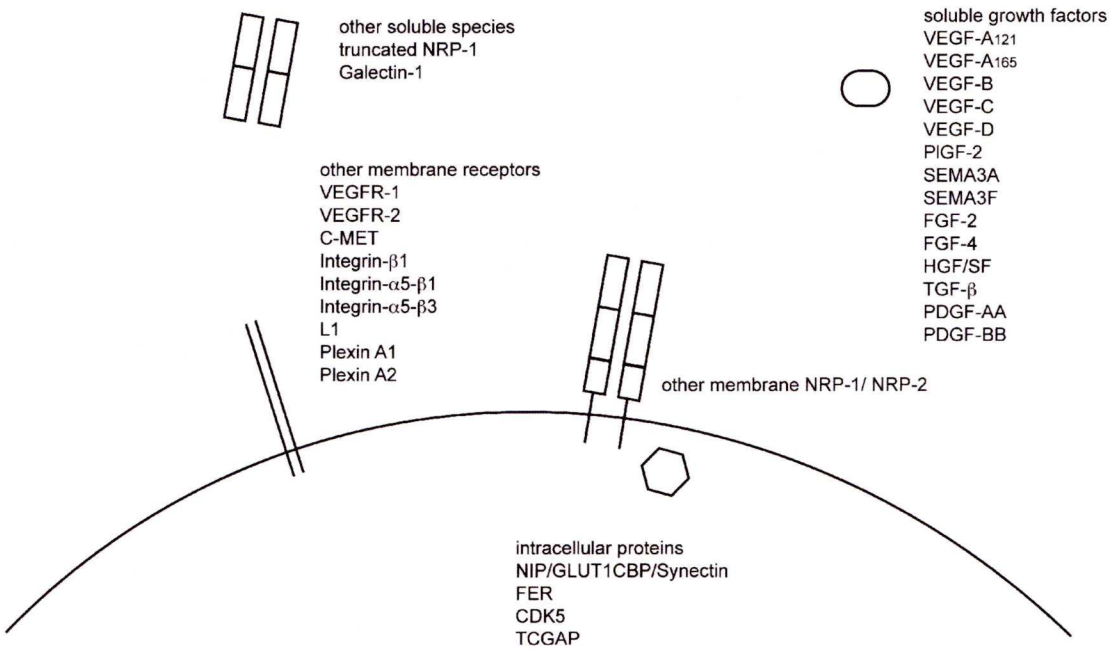

Figure 1.1: Postulated Neuropilin-1 extracellular and intracellular interactions.

The molecules that are putative NRP-1 interaction partners were classified into subgroups according to their type and location. Thus in separate groups gathered are soluble growth factors, other soluble proteins, membrane receptors, intracellular proteins, with indication of possible homophilic interactions with other NRPs.

Interacting partner	References
VEGF-A_{121}	[12, 18–20]
VEGF-A_{165}	[18, 21–29]
VEGF-B	[30]
VEGF-C	[31]
VEGF-D	[31]
PlGF-2	[18, 29, 32]
SEMA3A	[25, 28, 33–35]
SEMA3F	[25]
FGF-2	[36]
FGF-4	[36]
HGF/SF	[36, 37]
TGF-β	[38]
PDGF-AA	[14]
PDGF-BB	[14]
NRPs	[25, 34, 36, 39, 40]
Galectin-1	[41]
VEGFR-1	[26]
VEGFR-2	[11–13, 18, 24, 28, 42, 43]
C-MET	[44]
Integrin-β1	[45]
Integrin-α5-β1	[46]
Integrin-α5-β3	[47]
L1	[48]
Plexin-A1	[9, 28, 49, 50]
Plexin-A2	[50]
NIP/GLUT1CBP/Synectin	[9, 42, 46, 51, 52]
FER	[9]
CDK5	[9]
TCGAP	[9]

Table 1.1: An up-to-date list of proteins that interact with NRP-1 with appropriate references documenting the discovery and functionality of the interaction.

Initial studies suggested that interaction of NRP-1 with an exogenously administered drug - heparin - enhanced VEGF-A_{165} [21,22,24,26,53], PlGF-2 [29,32], and SEMA3A [53,54] binding. Moreover, binding of VEGF-C and VEGF-D to NRP-1 seemed to be heparin-dependent [31]. Interestingly, at the same time, using biophysical methods heparin appeared to have an antagonistic effect on the interaction of NRP-1 and VEGFR-1 [26]. Together these data suggest that interactions with polysaccharides can mediate both enhancing and inhibitory effects. The current mainstream explanation of the function of the NRP1-heparin interaction is that it increases the number of VEGF binding sites [21] without changing the overall affinity for VEGF binding [18,22]. Although these observations were obtained mainly using heparin, there are studies that indicate that similar processes might take place in the presence of native cell-surface heparan sulfate (HS) [55]. Recently, more polysaccharide-based compounds were tested for their impact on NRP-1. Lake and co-workers investigated NRP-1 interaction with low-molecular weight fucoidan [56] and showed that it causes, in a similar manner to heparin, enhanced binding of VEGF-A_{165} to VEGFR-2 and NRP-1 complexes on the endothelial cells. It is noteworthy, that for technical reasons, it is impossible to differentiate between enhanced growth factor binding to NRP-1 in the presence of heparin and growth factor binding to the heparin chain that is already bound to the NRP-1. Thus, none of these mechanisms can be excluded.

On the other hand, another exogenous compound, a non-sulfated analogue of heparin - phenylacetate carboxymethyl benzylamine dextran - was observed to convey an exactly contrary effect and inhibited growth factor binding and signalling [57]. Additionally, sulfated polysaccharides - fucoidan and dextran - both were shown to enhance the internalisation of cell-surface NRP-1 providing a direct tool to control the level of responsiveness of the cells to the NRP-1 ligands [58]. The latter studies used different polysaccharides to obtain contrasting results, and these results were reflected in the angiogenic properties of the cells and had clear functional outputs. This means that polysaccharides may be a good source of regulatory/ therapeutic molecules affecting NRP-1 function.

Most of the classical NRP-1 studies describe NRP-1 as a derivative of its extracellular interactions. Nevertheless, some studies indicate that there are functions of NRP-1 that are independent of its main ligands, VEGF and semaphorins, and rely on other intrinsic properties of NRP-1 [59]. It is especially evident in the case of some NRP-1 functions, which appear to be VEGFR-2 independent [24, 60–62], where the link between NRP-1 and its extracellular ligands is less obvious. For example, the fact that several cell lines express only NRP-1, but not any known tyrosine kinase receptor that interacts with NRP-1, has been a puzzle for a long time [24]. A possible explanation is that NRP-1 maintains cell survival and supports VEGF autocrine function either alone or together with other receptors [60]. On the other hand, no link with classical NRP-1 co-partners was found in a study that showed direct involvement of NRP-1 in the adhesion process [61]. The explanation indicated that the intracellular part of NRP-1 was responsible for such behaviour, which was in disagreement with the apparent independence of Plexin-NRP-1 signalling from the cytoplasmic domain of NRP-1 [34, 49]. In contrast, in a number of studies the presence or lack of the intracellular domain of NRP-1 was a critical factor in driving NRP-1-dependent responses, such as migration and angiogenesis [52, 62]. Thus, in addition to supporting the interaction of NRP-1 and VEGFR-2 [42], it was suggested that NRP-1 was involved in other mechanisms of control due to the intracellular interactions it can promote (Figure 1.1, Table 1.1). Additionally, Abcam has developed an antibody against phosphorylated threonine 916 of NRP-1, which has confirmed the presence of a substantial pool of intracellularly phosphorylated NRP-1. Again, this suggests further function of the intracellular domain. Therefore, it is highly plausible that the intracellular part of NRP-1 will bring a lot more functional discovery to the field.

Another interesting aspect of the NRP-1 is its c domain, which spans a meprin (MAM) domain and is considered to be responsible for protein-protein interactions [63, 64]. It was discovered to be essential for signal transduction of the NRP-1: Plexin-A complex [34, 49, 65], and this property was in fact used to raise anti-MAM blocking antibodies and peptides to inhibit this pathway [9, 25, 66]. Initially, it was postulated to mediate NRP-1 oligomerisation [26, 34],

however, later on, it was shown that it was not absolutely required for such dimerisation [1,25]. At the same time the c domain was shown to be not critical for the binding of extracellular ligands, such as SEMA3A [25,34,39,49], VEGF-A_{165} [25], VEGF-C [31]. Overall, the observed functions of the c domain remain largely unexplained. The contemporary hypothesis is that it contributes to some other interactions [34,65] and helps in orientating the NRP-1 in relation to other molecules [67].

The next interesting aspect of NRP-1s are its soluble isoforms. They were described at both theoretical and experimental levels [4,68], and comprise several different empirically confirmed proteins. In humans, the first described isoform was a 90 kDa truncated NRP-1, comprising the a1a2b1b2 domains [27], which was subsequently confirmed in other studies, that also identified 75 kDa and 120 kDa truncated NRP-1s [68, 69]. While the former is probably the 90 kDa variant with small truncation in the C-terminal part [70], the latter comprises the entire extracellular part of NRP-1 (a1a2b1b2c domains). Interestingly, while the 90 kDa variant is produced as a result of alternative splicing, the 120 kDa variant is suggested to be a product of membrane shedding, and the 75 kDa can be produced either by alternative splicing or membrane shedding [68,71]. Therefore, different mechanisms contribute to the formation of a pool of molecules that encode the part of the NRP-1 responsible for its extracellular interactions. How the production of these NRP-1 variants is controlled is not known. Additionally, the fact that soluble species of the same protein may have different domain compositions implies important functional differences between them, and highlights how little is known on the roles of the particular domains. The notion of soluble NRP-1 dimerisation and its subsequent effect on ligand binding (growth factors, receptors, glycosaminoglycans) in comparison to its membrane counterpart is also largely unknown.

Another complication associated with the soluble isoforms of NRP-1 followed several contradictory studies that identified soluble NRP-1 isoforms as agonists or antagonists of membrane NRP-1. Although most data indicate that exogenously added NRP-1 is an antagonist of membrane NRP-1 [27,34,53,72–78], some studies were able to show the opposite.

Thus, when NRP-1 was provided as a soluble dimer, it could bind to the cell surface and mediate agonistic responses in the presence of VEGF-A_{165} [11, 73], however, again, not in all cases [74, 79]. Occasionally, monomeric NRP-1 was also found to mediate agonistic responses [80]. Importantly, all the tested dimeric forms were artificial Fc-fusions. Consequently, the hypothesis was put forward that some of the soluble NRP-1 variants, which have been identified *in silico*, might have similar property of dimerisation *in vivo* [81]. Together with the suggestion that NRP-1 can act both *in cis* and *in trans* [11], this led to a rather unclear picture of the physical state of soluble NRP-1 (monomeric or dimeric) and its actual mechanism of action (soluble antagonist, cell-surface attached agonist) [82].

Another developing aspect of our understanding of the NRP-1 function is its internalisation. Several studies indicated that different molecules caused the internalisation of NRP-1, e.g., VEGF-A_{165} [53, 83], SEMA3A [53, 84], HGF/ SF [44], NIP [46], sulfated polyoligosaccharides [58]. In fact, a short sequence, R/K/XXR/K, was described as a recognition motif driving NRP-1-dependent internalisation, and was identified in several known NRP-1 ligands [85]. The fact that various NRP-1 ligands are causing the internalisation of NRP-1 and the rest of the signalling complex is not surprising, however, the mechanisms underlying this process are diverse and have important implications. Thus, NRP-1 can be internalised via a clathrin-dependent mechanism [13, 46, 84, 86], [46] or clathrin-independent caveolar mechanism initiated in lipid rafts [13], although the latter was based solely on the location of NRP-1 within rafts [87, 88]. The differences between these processes are substantial, as they determine subsequent intracellular signalling, degradation, or translocation to the nucleus, and this potentially provides another regulatory mechanism of NRP-1 [89].

Another significant feature of NRP-1 that has resulted in substantial confusion is ligand competition. In the early days of NRP-1 research there were two dominant experimental approaches, one solely focused on its function in neural system in association with semaphorins, and the other focused on its angiogenic function in concert with VEGFs. These approaches were subsequently combined and the notion of crosstalk between the two signalling pathways

was investigated. Initially, the competition between VEGF-A_{165} and various semaphorins was considered relevant at the molecular and functional level [25, 35, 53, 90]. However, later studies suggested that no direct competition takes place, and that there are other mechanisms controlling the selectivity of response, such as downstream signalling, affinity and preferential binding or internalisation [1, 28, 91, 92]. Nonetheless, for some ligands the overlapping binding sites were documented, and the discussion remains open on the NRP-1-dependent selectivity of signal transduction. Among those are PlGF-2 and VEGF-A_{165} [29], VEGFR-1 and VEGF-A_{165} [26], SEMA3F and VEGF-C [31], TGF-β and VEGF-A_{165} [38]. Interestingly, these data, although they provide a rather hazy insight into the functions of NRP-1, they have the potential to become a source of predictive data through the use of various mathematical approaches that aim to combine in an algorithm-based manner several input parameters in order to interpret and estimate further outputs. To date Wu and co-workers have performed extensive modelling of the angiogenic processes, so far based on various characteristics of VEGFR-2, VEGFR-1, soluble VEGFR-1 and membrane NRP-1 (see [93]). With regard to the enormous advances in the classical and 'omics data acquisition methods, it is plausible that this type of analysis will expand quickly, to provide a means of generating novel hypotheses and so indicate new directions of research.

The description above of NRP-1 provides a lot of information on possible functions and mechanisms of regulation of NRP-1, however, at the same time, it opens several discussions and indicates important questions that need to be answered (Figure 1.2). This thesis attempted to target some of these questions, and provide further explanations of some of the NRP-1 properties.

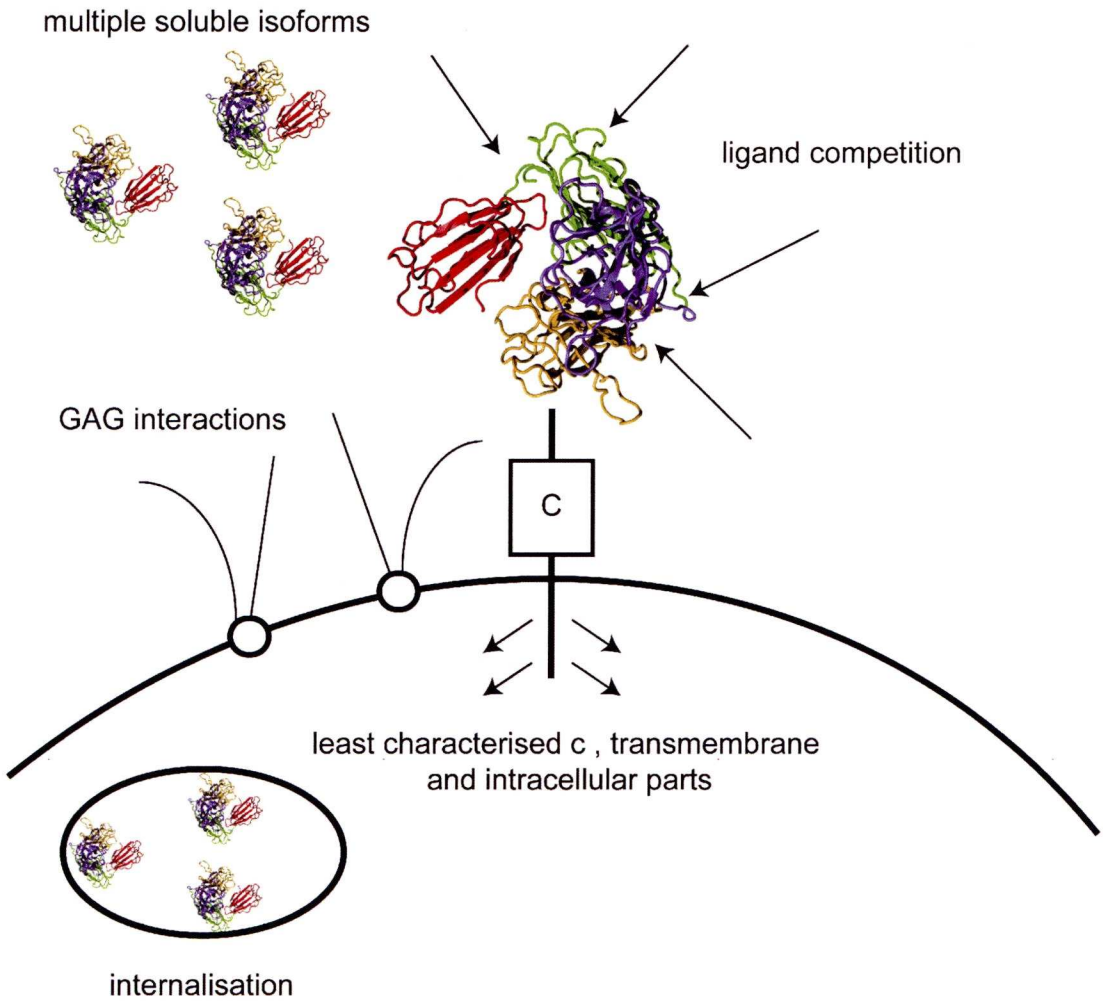

Figure 1.2: Challenging novel aspects of NRP-1 biology.

The figure illustrates phenomena described in the text, that are raising a lot of interest in the field, often remain not characterised and await clarification. The pool of soluble NRP-1 molecules symbolises multiplicity of such isoforms *in vivo*, which are produced either via alternative splicing or as a result of the surface shedding. They may have monomeric or dimeric properties, and no knowledge on their exact mechanism of function is available at the moment. Another aspect of NRP-1 biology is the multitude of its interacting ligands, which mediate various cellular responses and might act via NRP-1 either in an agonistic or antagonistic manner, possibly undergoing functional and structural competition. GAG interactions with NRP-1 might be a means of modulating NRP-1 interactions with the ligands and cell surface receptors, thus, might be responsible for the regulation of the signalling responses. The c domain, transmembrane and intracellular parts remain the least characterised parts of the NRP-1 and are suggested to bestow important interactions and, at the same time, allow NRP-1 functions that are independent from its extracellular-interactions. Internalisation might be a novel mechanism of regulation of NRP-1 function related to the properties of the membrane *milieu* where it forms signalling complexes. This mechanism would allow another level of regulation, responsible for the ligand selectivity and secondary signalling effects occurring after complex internalisation.

1.3 Thesis objectives

This study begins with a presentation of a novel method for the measurement of the interactions of proteins and polysaccharides in a high-throughput manner. The method is briefly introduced in Chapter 3 and is described in a peer-reviewed publication (**Supplemental paper 2**).

The NRP-1 part of the study is focused on two important aspects of NRP-1 function, namely its interactions with the polysaccharide heparin, an experimental proxy for cellular HS and its pro-angiogenic activity.

Chapter 4 aims to define the interaction of NRP-1 with heparin, as a model for cellular HS. In this part of the thesis, the structural requirements for this interaction are established from both the perspective of the polysaccharide and the protein. In the latter instance, the impact of NRP-1 dimerisation and of the c domain of NRP-1 on the interaction is established.

Chapter 5 is focused on the functional aspect of the NRP-1 in the context of a 3-dimensional angiogenesis assay. Here it is shown that a dimeric form of NRP-1 elicits a strong proangiogenic response, independently of VEGF-A, on the endothelial cells. It also provides confirmation of the agonistic character of the soluble dimeric form of the protein, and, surprisingly, possibly also for the truncated monomer.

Overall, the thesis introduces advances to the methodology of studying protein-polysaccharide interactions and broadens our contemporary view on NRP-1-polysaccharide interactions and angiogenic functions.

Chapter 2

Materials and Methods

2.1 Materials

Recombinant rat NRP-1 chimera (Fc rNRP-1), soluble human truncated variant (shNRP-1), human Fc and human IL-2 were purchased from R&D Systems (Abingdon, Oxon, UK), VEGF-A_{121} was purchased from PeproTech EC Ltd (London, UK). VEGF-A_{165} and IL-6 were kindly provided by NCI-Frederick (Frederick, MD, USA). Human lactoferrin and BSA were purchased from Sigma-Aldrich (Gillingham, Kent, UK). S100A4 was a kind gift from Dr Thamir Ismail. The same heparin (17 kDa avarage molecular weight) (Celsus Lab, Cincinnati, OH, USA) was used in the assay and for the production of modified derivatives, cationic forms and oligosaccharide fragments. The HDMECs and tissue culture reagents were purchased from Promocell GmbH (Heidelberg, Germany) and Lonza (Wokingham, Berks, UK). Antibodies against phospho-VEGFR-2 clone 19A10 (Y1175), VEGFR-2 clone 55B11, phospho-PLCγ (Y783), phospho ERK-1/2 (Y202,204/Y185,187) were purchased from Cell Signaling Technology (NEB, Hitchin, Herts, UK); against RCAN-1.4 (DSCR-1/ ADAPT78/ Calcipressin-1) and against His-tag from Sigma-Aldrich; against actin from Santa Cruz Biotechnology (Insight Biotechnology, Wembley, Middx, UK); against phospho-tyrosine clone 4G10 from Upstate Biotechnology (Buckingham, Bucks, UK); anti-mouse-HRP and anti-rabbit-HRP antibodies were purchased from GE Health-

care (Amersham, Bucks, UK); sequestering anti-VEGF and anti-rNRP-1 antibodies were from R&D Systems. VEGFR-2 kinase inhibitor (ZM323881) [94] was purchased from Tocris Bioscience (Bristol, Avon, UK).

2.2 Protein biochemical methods

2.2.1 N-glycanase digest

One μg of Fc rNRP-1, shNRP-1 and Fc were diluted in 50 μL phosphate-buffered saline (PBS, 150 mM NaCl, 2.7 mM KCl, 1.5 mM KH_2PO_4, 10 mM Na_2HPO_4 pH 7.4) and incubated overnight at 37°C with or without (mock control) 2.5 mU N-glycanase (Glyko, Prozyme, Ely, Cambs, UK). One hundred ng samples were subsequently analysed by SDS-PAGE; Fc rNRP1 and shNRP1 on 8 % (w/v) SDS-PAGE, Fc on 15 % (w/v) SDS-PAGE. Proteins were visualised by silver staining.

2.2.2 Selective labelling and identification of the heparin-binding peptides derived from Fc rNRP1

Mapping of the heparin-binding site has been performed as described previously [95], with some modifications. To 20 μL of AF-heparin beads packed in a minitip column and equilibrated in buffer A (17.6 mM Na_2HPO_4, 2.6 mM NaH_2PO_4, 100 mM NaCl, pH 7.6, 0.02 % Tween), 4 μg of Fc rNRP-1 was added in a total volume of 80 μL of buffer A. The loading was repeated three times. After the minicolumn has been washed with the buffer A, the lysines not involved in heparin binding were acetylated by means of 50 mM sulfo-NHS-acetate (Thermo, Pierce, Perbio Science, Cramlington, Northumberland, UK) (Figure 2.1) in buffer B (18.3 mM Na_2HPO_4, 1.7 mM NaH_2PO_4, pH 7.8) during 5 min incubation. The reaction was stopped by washing the microcolumn with buffer B. Acetylated proteins bound to the column were eluted with buffer C (45.75 mM Na_2HPO_4, 4.25 mM NaH_2PO_4, 2M NaCl pH 7.8). The elution was buffer exchanged into buffer D (45.75 mM Na_2HPO_4, 4.25 mM NaH_2PO_4, pH 7.8) using a

Vivaspin 100 kDa MWCO centrifugal filter (Sartorius Stedim, Epsom, Surrey, UK) blocked previously in BSA to avoid Fc rNRP1 nonspecific binding to the filter. Subsequently, the lysines that were protected by heparin interaction were biotinylated using a final concentration of 10 mM NHS-biotin in DMSO (Thermo) (Figure 2.1) (added as 7 % v/v) during 30 min incubation at room temperature. The reaction was quenched by the addition of a final concentration of 100 mM Tris pH 6.8 (added as 9 % v/v). Next, the solution was buffer exchanged into buffer E (4.58 mM Na_2HPO_4, 0.43 mM NaH_2PO_4, pH 7.8) using new Vivaspin 100 kDa MWCO centrifugal filter also blocked previously in BSA, and the remaining sample was dried by rotary evaporation. Afterwards, it was dissolved in buffer F (8 M urea, 400 mM NH_4HCO_3 pH 7.8, 2.5 μL 45 mM DTT) and incubated for 15 min in 56°C. Next, protein was carbamidomethylated using a final concentration of 9 mM iodoacetamide (added as 9 % v/v) during 15 min incubation at room temperature in the dark. After dilution 1: 4 with HPLC grade water, the sample was digested with 1.5 μg of chymotrypsin (Sigma-Aldrich) overnight at 37°C (cuts after T, F, W, L, M, N and Q). The digest mixture was diluted a further four times with HPLC grade water and applied to a 40 μL Strep-Tactin® Sepharose® (IBA, Stratech, Newmarket, Suffolk, UK) minitip column equilibrated previously in sixteen times diluted buffer F (500 mM urea, 25 mM NH_4HCO_3). The microcolumn was washed with the same buffer and HPLC grade water and the bound biotinylated peptides were eluted with buffer G (80 % v/v, acetonitrile, 20 % v/v, trifluoroacetic acid, 5 mM biotin). The elution was dried by rotary evaporation down to 4 μL and topped up with 50 μL of 0.1 % (v/v) trifluoroacetic acid. Subsequently, the sample was desalted by C18 ZipTip™ (Millipore, Watford, Herts, UK) according to the manufacturer's instruction and the peptides were eluted with buffer H (60 % v/v, acetonitrile, 0.1 % v/v, trifluoroacetic acid). The sample was analysed by MALDI-Q-TOF Premier mass spectrometer (Waters-Micromass, Manchester, UK).

2.2.3 Peptide analysis

Biotinylated peptides obtained from MALDI analysis were analysed using MassLynx software (Waters - Micromass, Manchester, UK) and identified with Protein Prospector MS-Tag (UCSF, San Francisco, CA, USA). The settings included: chymotrypsin digest, nonspecific cleavage on one peptide termini, a set of variable modificiations, as acetylation and biotinylation of lysines, carbamidomethylation and carboxymethylation of cysteines (occurring due to iodoacetamide presence in the procedure), and oxidation of methionines (related to the sample handling). The analysis was performed for monoisotopic ions with error tolerance of 100 ppm for parental ions, and 300 ppm for fragmented ions in MALDI-Q-TOF instrument setting. The peptides were ascribed to the regions of rat NRP-1 (Uniprot accession number Q9QWJ9) or human IgG1 (Uniprot accession number P01857) and were presented in the text.

2.2.4 Binding to heparin affinity minicolumns

Two types of heparin resins, Affi-gel heparin (Bio-Rad) and Toyopearl AF-heparin 650M (Tosoh Bioscience, Redditch, Worcs, UK), were used to analyse Fc rNRP-1 and shNRP-1 binding to heparin. The minicolumns were assembled in a minitip (0.1-10 μL range) fitted with a filter and approximately 25 μL of slurry of the respective resins. In order to eliminate the residual contamination with the storage buffer the minicolumns were washed with 4 column volums (CV) of water and, subsequently, with 8 CV of PBST identical to the buffer used in the Biosensor analysis. Next, 50 μL of 20 μg/ mL of Fc rNRP-1 and shNRP-1 (1 μg) was applied 3 times on the minicolumn. The load (LD) and flow through (FT) fractions were collected and 100 ng samples were resolved on 8 % (w/v) SDS-PAGE and visualised by silver staining. Concurrently, 100 μL of each resin was washed with excessive amount of water and heparinase digest buffer 5x (500mM CH_3COONa, 0.5 mM $(CH_3COO)_2Ca$ pH 7.0). Subsequently, the resins were resuspended in 800 μL of heparinase digest buffer 1x (100mM CH_3COONa, 0.1 mM $(CH_3COO)_2Ca$ pH 7.0) supplemented with 2.5 mU heparinases I/II/III (IBEX Technologies, Montreal, Canada). The digest samples were incubated on tube rotator at 37°C overnight. Afterwards, the resins

were extensively washed and packed into minicolumns of the same volume as the original ones and, the proteins were analysed for binding to the resins as previously.

2.2.5 Differential Scanning Fluorimetry (DSF)

DSF was performed as described previously (see [96] , Chapter 3 and **Supplemental paper 2**). Briefly, a final concentration of 0.57 μM (136 μg/ mL) Fc rNRP1 was tested alone or with 1.132 μM (19 μg/ mL) heparin or 11.32 μM (190 μg/ mL) heparin, which gave respectively 1: 2 and 1: 20 ratios of dimeric Fc rNRP1 versus heparin. Similarily, a final concentration of 1.132 μM shNRP1 was tested with 1.132 μM heparin or 11.32 μM heparin, which gave respectively 1: 1 and 1: 10 monomeric truncated shNRP1 versus heparin. The assay was performed in 96-Well Reaction Plate (Applied Biosystems, Warrington, Cheshire, UK). The final volume per well (25 μL) comprised of the protein dissolved in PBS (20 % v/v), heparin dissolved in HPLC grade water (10 % v/v), PBS (60 % v/v or 70 % v/v in case of the condition containing no heparin) and a freshly prepared 100x water based dilution of Sypro® Orange 5000x (Invitrogen) (10 % v/v), added in the given order. During the preparation, the plate was kept on ice and immediately afterwards, it was sealed with Optical Adhesive Film (Applied Biosystems) and directly analysed in a 7500 Fast Real Time PCR System (software version 1.4.0) (Applied Biosystems) instrument. The heating cycle comprised of a 120 s pre-warming step at 31 °C and a subsequent gradient between 32 and 81 °C obtained in 99 steps of 20 s, each of 0.5 °C ramp. Data were collected using the calibration setting for TAMRA™ dye detection (λex 560 nm; λem 582 nm) installed on the instrument (as compared to Sypro® Orange ideal settings λex 492 nm; λem 610 nm).

2.2.6 DSF data analysis

The data were analysed using the Plot v. 0.997 software for Mac OS X (http://plot.micw.eu/) by application of an exponential correlation function approximation of the first derivative for each melting curve.

2.2.7 Native proteolytic digest

The native proteolytic digest experiments were performed in fresh tubes to obtain the best efficiency of the digests not affected by the interaction between the protein and the plastic tube following freezing. Both digestes were performed in the volume not larger than 30 μL. In a digest A 2 μg of Fc rNRP-1 in 0.1 M phosphate buffer pH 7.7, 75 mM NaCl supplemented with 50 ng of trypsin (porcine trypsin sequence grade modified) (Promega, Southampton, Hants, UK) was incubated in 37°C for 30 min. For a digest B 2 μg of Fc rNRP-1 in 0.5 M NaCl supplemented with 75 ng of the same trypsin stock was incubated in 12°C for 90 min. Each digest was reproducible as confirmed by three independent repeats visualised by SDS-PAGE, where amounts equivalent to 90 ng of Fc rNRP-1 of each digest were resolved. Prior to Dual Polarisation Interferometry (DPI) analysis the digest solutions were supplemented with PBS to the final volume of 600 μL. The final NaCl concentration in the samples used for the binding experiments was approximately 0.15 M, while the final Fc rNRP-1 concentration was 14 nM.

2.2.8 Crosslinking

Following the digest procedure, each sample was diluted either with PBS or phosphate buffer pH 7.7 to contain a final concentration of 0.14 M NaCl. Subsequently, 6 mM of fresh 1-Ethyl-3-(3-dimethylaminopropyl) carbodiimide hydrochloride (EDC) (Thermo) and 15 mM of N-hydroxysuccinimide (NHS) (Thermo) from DMSO-based stock were added (Figure 2.1). The mixtures were incubated for 45 min at room temperature and analysed on SDS-PAGE where amounts equivalent to 90 ng of Fc rNRP-1 of each digest were resolved.

2.3 Surface-based methods

2.3.1 Heparin surface preparation

Surfaces were prepared in an Iasys optical biosensor running IAsys plus software version 3.01 (NeoSensors, Sedgefield, Cleveland, UK). Biotin functionalised surfaces were derivatised with streptavidin to enable subsequent capture of internally biotinylated heparin (via internal free amino groups). The usual volume added to the cuvette was 50 μL, unless indicated otherwise. Most of the precedure was performed at 20°C. Briefly, biotin functionalised surface cuvette (NeoSensors) after regeneration with acidic wash solution A (20 mM HCl) and basic wash solution B (20 mM NaOH 2 M NaCl) was washed with PBST (140 mM NaCl, 5 mM NaH_2PO_4, 5 mM Na_2HPO_4, 0.02 % (v/v) Tween, 0.02 % (w/v) sodium azide) and subsequently incubated for 40 minutes with 20 μL of 2.5 mg/ mL streptavidin (Sigma-Aldrich, Gillingham, Kent, UK) and 10 μL of PBST. After thorough PBST washes the surface was incubated overnight at 4°C with 20 μL of 10 mg/ mL heparin internally biotinylated on free amines (kind gift from Yassir Ahmed) protected against evaporation and drying. The resonance scan confirmed that the surface was modified uniformly.

2.3.2 Binding assays

The binding assays were performed in automated IAsys optical biosensor device controled by IAsys Auto Plus software version 3.01 applying appropriate scripts for kinetic association and competition assays. The initial binding tests and kinetic dissociation assay was performed in a manually operated IAsys. The total volume of solution over the surface was constant for each step of the experiment and equal 50 μL. The temperature of the experiments was 20°C.

For the initial binding tests of Fc rNRP-1, shNRP-1 and Fc, to 45 μL of PBST 5 μL of the tested protein was added. The final concentration of the proteins in the cuvette was 0.5 μg/ mL.

In kinetic association assays the binding solution consisted of 45 μL of PBST and 5 μL of Fc

rNRP-1 at 10 times final concentration. Fc rNRP-1 final concentration range was 0.25 nM-1.6 nM. The experimental steps consisted of setting a PBST baseline (500s), an association phase (240s), followed by a dissociation phase (60s). The regeneration of the surface was achieved by washing with solution B. The needle was washed with wash solution A. The association experiment was repeated 5 times to provide the k_{ass} values used for further calculation of K_d.

In dissociation assays, higher concentrations of Fc rNRP-1 were used, 1.2 μg/ mL in 50 μL of PBST, to reduce the probability of re-binding. Following association and washing, dissociation was initiated by the addition of 40 μg/ mL heparin in PBST; the competing heparin also reduced the probablitly of re-binding. The experiment steps consisted of acquiring a baseline (60s), an association phase (240s), dissociation with PBST (120s) and dissociation with 1 μL of 2 mg/ mL porcine heparin (at least 60s). Regeneration was achieved with wash solution B. The dissociation experiment was repeated 5 times to provide the k_{off} values used for further calculation of K_d.

In competition assays the binding solution consisted of 40 μL of PBST, 5 μL of Fc rNRP-1 at 10 times the final concentration, and 5 μL of competing sugar at 10 times the final concentration added from a 96-well plate where a range of appropriate solutions were prepared. The sugars used in the competition assay were either modified heparin derivatives (kind gift from Dr Ed Yates) [97, 98] or heparin derived oligosaccharides obtained from partial heparinase I (IBEX Technologies) digest of porcine heparin (Celsus Lab) performed as described previously [99]. The range of concentration of competing sugars did not exceed 0.01-100 μg/ mL. The Fc rNRP-1 was aliquoted from 10 times concentrated solution (5 μg/ mL). The final concentration of sugars varied within the experimental range, while the Fc rNRP-1 concentration was constant (0.5 μg/ mL). The experimental steps consisted of setting a PBST baseline (30s), acquiring a baseline after sugar addition (150-450s), and the association phase (300s). Regeneration was achieved with wash solution B and the needle was washed with wash solution A. As Fc rNRP-1 seemed to loose its heparin-binding activity, no more than 25 binding curves were collected from a single stock tube of the protein. Each set of data for each sugar was collected at least

twice.

2.3.3 Biosensor data analysis

The analysis was done using FastFit software version 2.03 (NeoSensors). The collected data were analysed using single-site binding model. For the analysis of the kinetic data the FastFit software provided distribution of the data around the one site model and a measure of the consequent variation, the slope of initial rate, k_{on} and the extent of binding in a graphical and numerical output. The FastPlot software version 2.0 juxtaposed the binding curves for each Fc rNRP-1 concentration. The dissociation data were analysed in FastFit where 60s of the heparin-dependent dissociation was used for the calculation. K_d calculation was based on the values of k_{ass} and k_{diss} obtained in association and dissociation assays, respectively. The final kinetic values and their respective standard errors (SE) were calculated basing on 5 independent association experiments, and 6 independent dissociation experiments.

The competition assay data were normalised by comparison of extent of response of Fc rNRP-1 binding to the heparin surface versus the extents of Fc rNRP-1 response in the presence of sugar. This allowed a comparison to be made between sets of binding curves comprising of a control Fc rNRP-1 and a range of concentrations of the competitor. The control extent of binding was defined as 100 %, while the following values of Fc rNRP-1 extent of binding in the presence of inhibiting compounds were calculated as fractions of 100 %. The IC_{50} values were calculated using Origin 8 (OriginLab Corporation, Northampton, MA, USA) applying a non-linear curve fit.

2.3.4 Dual polarisation interferometry (DPI)

DPI analysis was performed on an AnaLight® Bio200 System (Farfield Scientific, Crewe, Cheshire, UK) equipped with a 632.8 nm laser. The experiment was performed as described previously [100]. Briefly, the thiol chip was verified for sufficient polarisation pattern characterised by T_e and T_m values over 0.6. Next, the chip was calibrated with 80 % (w/v) ethanol and water at

20 °C at 50 µL/ min flow. Subsequently, the temperature of the flow cell was set to 30 °C and 180 µL of freshly prepared 5 mg/ mL N-(β-maleimidopropionic acid) hydrazide (BMPH) (Thermo) (Figure 2.1) dissolved in PBS was applied at 8 µL/ min to each flow cell. In this way reactive thiol groups of the chip reacted with maleimide groups of BMPH to form stable thioether bonds, and consequently, a new surface with reactive hydrazide groups was obtained. This step was followed by extensive PBS washing at 50 µL/ min. Next, the flow cell destined to be modified with oligosaccharide was injected with 180 µL of 2 mg/ mL hexadecasaccharide (dp 16) dissolved in PBS pH 5 at 2 µL/ min. Thereupon, aldehyde groups of dp 16 produced by partial nitrous acid digest (on reducing end) [99] created stable hydrazone bonds with the hydrazide groups of immobilised BMPH. Subsequently, both flow cells were modified with aldehyde-functionalised poly(ethylene glycol) (PEG-CHO) (Rapp Polymere, Tübingen, Germany) used here as a blocking reagent. PEG-CHO (180 µL of 20 mg/ mL) dissolved in PBS was applied at 1 µL/ min and incubated overnight resulting in blocking of the remaining hydrazide groups of the oligosaccharide flow cell and hydrazide groups of the second flow cell. The injection of PEG-CHO was repeated to ensure full modification of the surface. After extensive PBS washes the temperature was returned to 20 °C and the surface was regenerated with 2 M NaCl phosphate buffer pH 7.5. The binding assays of each molecule were repeated three times and each binding was followed by regeneration with 20 mM HCl. The molecules were tested at 3.33 µg/ mL, which equals to 14 nM (Fc rNRP-1), 47 nM (hNRP1) and 123 nM (control Fc). The native digest samples were prepared for analysis as described in the previous section.

2.3.5 DPI data analysis

The surface preparation and binding events were analysed applying Analight Explorer 1.5.2.17946 software version according to the manufacturer's instructions. For the illustrations, the mass readings of the binding events were normalised to start from 0 value. The thickness and density readings are presented according to the experimental recordings.

2.4 Tissue culture methods

2.4.1 BaF3 proliferation assay

The BaF3 assay was performed as described previously [101]. Briefly, the cells were cultured in RPMI-1640 medium (Sigma-Aldrich) supplemented with 10 % (v/v) fetal calf serum (Gibco, Invitrogen, Paisley, Scotland, UK), 50 μM L-glutamine (Gibco), 100 U/ mL penicillin G, 50 μg/ mL streptomycin sulfate (Gibco) and 2 ng/ mL murine IL-3 (R&D Systems) at 37°C and 5 % (v/v) CO_2.

The assays were performed in 96-well tissue culture plates and consisted of standard controls (negative, positive, FGF-2 alone and FGF-2 in combination with heparin) and a dilution curve of total 6 points spanning the range of concentrations of the antagonists (Fc rNRP-1, shNRP-1, Fc) of a step dilution factor of 3. Each variant was prepared in 3 repeats.

The control wells were supplemented with 50 μL of the basic medium without IL-3 (negative control), medium containing 4 ng/ mL IL-3 (final 2 ng/ mL) (positive control), medium containing 2 nM FGF-2 (final 1 nM) and medium containing 2 nM FGF-2 and 20 μg/ mL heparin (final 1 nM FGF-2 and 10 μg/ mL heparin).

The wells prepared for the dilution curve were supplemented with 50 μL of the basic medium with the addition of appropriate amounts of FGF-2 and heparin in order to obtain 4 variants of final concentrations (0.1 nM FGF-2 and 0.1 μg/ mL heparin, 0.1 nM FGF-2 and 1 μg/ mL heparin, 0.3 nM FGF-2 and 0.1 μg/ mL heparin and 0.3 nM FGF-2 and 1 μg/ mL heparin).

The wells designed to contain the highest concentration of the antagonists (30 nM) were supplemented with 75 μL of the medium containing appropriate concentrations of FGF-2, heparin (consistent with the variant) and antagonists (Fc rNRP-1, shNRP-1, Fc). Subsequently, 25 μL of the solution containing the antagonists was transfered to the next set of wells, and the operation was repeated to obtain a full set of dilutions.

Finally, to the wells containing 50 μL of the 2 x concentrated IL-3, FGF-2, heparin and

antagonists, the cells, which were previously washed twice in the basic medium, were added in 50 μL at 1 x 10^4 per well in the basic medium.

After 72h of incubation in 37℃ 10 μL of MTT solution (5 mg/ mL in PBS) was added to each well and incubation was continued for a further 4h. Finally, 100 μL of solubilising solution (10 % (w/v) SDS, 0.01M HCl) was added to each well and incubation in 37℃ was continued overnight. The plate was subsequently analysed by reading OD_{590} values for each well. The presented result is illustrated by the mean values and SD of readings for each variant.

2.4.2 Tissue culture of HDMECs

HDMECs were purchased from Promocell and were cultured with the Endothelial Cell Growth Medium MV2 Kit (Promocell) consisting of the Endothelial Cell Basal Medium with appropriate supplements provided by the manufacturer (5 % v/v fetal calf serum, 5 ng/ mL human epidermal growth factor, 10 ng/ mL FGF-2, 20 ng/ mL insulin-like growth factor, 0.5 ng/ mL VEGF-A_{165}, 1 μg/ mL ascorbic acid, 0.2 μg/ mL hydrocortisone). Alternatively, the cells were grown with 0.5 ng/ mL VEGF-A_{121} instead of VEGF-A_{165} where indicated. Cells were used until passage 10. For routine cell maintenance, HDMECs were grown on 1 % (w/v) gelatin-coated plates at 37℃ and 5 % (v/v) CO_2. Twenty four hours prior to the experiments, the cells were serum-starved by replacing the fully supplemented medium with 1 % (v/v) fetal calf serum Endothelial Cell Basal Medium. For regular maintenance, cells were detached from the plates using solution of 0.05 % (w/v) trypsin in 0.53 mM EDTA (Invitrogen, Paisley, UK). For the experiments the cells were detached using Accutase solution (Promocell) to preserve the extracellular membrane proteins.

2.4.3 Tube formation assay

The tube formation assay was performed as described previously [102]. Collagen type I (Vitrogen, Cohesion Technologies, Palo Alto, CA, USA) was mixed at a ratio 8: 1: 1 with 0.1 M NaOH and 10x concentrated Ham's F-12 medium (Promocell). The solution was supplemented to

contain 0.02 M Hepes, 0.1 % (w/v) sodium bicarbonate and 2 mM Glutamax-I (Invitrogen), and kept on ice until placed into the wells. The assay was prepared in 24-well plate format and the bottom layer of collagen was formed by adding 300 μL of the solution per well and allowing subsequent gelation at 37°C overnight. Following serum starvation, cells were plated at 8-9 x 10^4 in 500 μL per well in 1 % (v/v) fetal calf serum Endothelial Cell Basal Medium. After 120 min the medium was aspirated and a second layer of collagen (200 μL per well) was prepared according to the same protocol and gently placed on top of the cell layer. After 90 min of incubation at 37°C, the medium was returned to the wells. The photos were taken after 17h to 20h incubation at 37°C from approximately the same coordinates in each well within the experimental plate.

The final volume of the assay was 1 mL, comprising of 0.5 mL of the collagen layers and 0.5 mL of medium. Depending on the ligand type, various orders of addition were employed. The higher molecular weight ligands, such as Fc, shNRP-1 and Fc rNRP-1 were added to the cells at the adhesion step (final concentration 5 nM, unless indicated otherwise), while smaller molecular weight ligands, such as VEGF-A_{165} (final concentration 10 ng/ mL) and VEGFR-2 inhibitor ZM323881 (final concentration 3 μM) were added to the medium after formation of the top layer of collagen. In experiments using sequestering VEGF-A antibody, the antibody (20 μg/ mL) was incubated with VEGF-A_{165} (10 ng/ mL) for 60 min at room temperature and added after formation of the top layer of collagen. For experiments with the Fc rNRP-1/ shNRP-1 variants the antibody was added directly to the medium.

2.4.4 Data analysis of the tube formation

Photographs of HDMECs in the tube formation assays were analysed with Adobe® Photoshop® CS3 Extended version 10.0 (San Jose, CA, USA). For each experimental condition three squares of 400 x 400 pixels were selected in the photograph and on each, the area covered by tubes was calculated. The output values were used for the Student's t test evaluation of the significant difference between the experiments. To allow comparison between experi-

ments, the mean value of the tubes' surface in the control containing no agonist was set as a reference value 1, and used to normalise all other experimental values.

2.4.5 Signalling assay

Serum-starved cells were plated at 1.8 x 10^5 cells in 500 μL per well of 12-well plates either on collagen or a layer of 1 % (w/v) gelatin in 1 % (v/v) fetal calf serum Endothelial Cell Basal Medium. Two hours later the medium with appropriate ligands was added to the wells and the plate was returned to the incubator. After an appropriate time of incubation (10 min and 180 min), plates were placed on ice and the cells were lysed by 3 min incubation with RIPA buffer (20 mM Tris pH 7.5, 150 mM NaCl, 2.5 mM EDTA, 10 % (w/v) glycerol, 1 % (w/v) Triton-X-100, 1 mM sodium vanadate, 10 mg/ mL aprotinin, 10 mg/ mL leupeptin, 1 mM PMSF, 0.1 % (w/v) SDS, 0.5 % (w/v) sodium deoxycholate). The lysates were collected, clarified by centrifugation at 11000 RPM (ca 13000 g) at 4°C for 20 min, boiled with NuPAGE LDS Sample Buffer and analysed by SDS-PAGE.

2.4.6 Data analysis of the signalling assay

The band intensities in analysed western blots were estimated using Adobe® Photoshop® CS3 Extended version 10.0 and presented as relative values compared to the control. To do so, the pictures were converted to their respective negatives, and the same surface for each condition was analysed for the light intensity profile.

2.5 PAGE, western blot and silver staining

2.5.1 Biochemical analysis

Eight or 15 % (w/v) SDS-PAGE gels were resolved at 200 V constant voltage and where required transferred for 2 h at 100 V by wet transfer onto nitrocellulose membranes (GE Healthcare, Amersham, Bucks, UK) using a Bio-Rad Laboratories apparatus (Hemel Hempstead, Herts, UK). The membranes were blocked for 1 h at room temperature in PBS, 0.1 % (v/v) Tween, 5 mg/ ml BSA. Subsequently, they were incubated with the primary antibody solution (PBS 0.1 % (v/v) Tween, 5 mg/ ml BSA, 1: 250 anti-rat NRP-1 antibody raised in mouse (R&D Systems)) for 1 h at room temperature. After washing they were incubated with the secondary antibody solution (PBS 0.1 % (v/v) Tween, 5 mg/ ml BSA, 1: 250 anti-mouse antibody raised in goat conjugated with HRP (Pierce)) for 1 h at room temperaure. Afterwards, the membranes were extensively washed with PBS 0.1 % (v/v) Tween and developed using Super Signal West Dura Extended Duration Substrate kit (Thermo). Silver staining of recombinant proteins was performed as described previously [103].

Native PAGE was performed as SDS-PAGE with the exception of omission of SDS, β-mercaptoethanol and sample boiling. One μg samples of heparin, dp 24 and dp 26 were analysed on 33 % (w/v) Tris-acetate gels resolved in Tris-Mes running buffer initially at 200 V for 4 h, then, overnight at 75 V [104]. The gels were stained for 10 min with 0.08 % (w/v) azure A, due to its property to interact with sulfate groups, briefly washed, and photographed.

2.5.2 Gel electrophoresis and western blot of HDMECs samples

For gel electrophoresis the NuPAGE Bis-Tris system was used (Invitrogen). The gradient 4-12 % (w/v polyacrylamide) gels were resolved at 50 mA constant current and transferred onto nitrocellulose membranes (GE Healthcare) using XCell II^{TM} Blot Module for 120 min at 140 mA (Invitrogen). The membranes were blocked in 5 % (w/v) BSA, 0.1 % (v/v) Tween-20 in Tris-buffered saline (TBS) for 60 min at room temperature and subsequently incubated overnight

in the cold room with the appropriate antibody solution prepared in 2 % (w/v) BSA, 0.1 % (v/v) Tween-20 in TBS. After washing, the membranes were incubated with the appropriate secondary antibodies in 2 % (w/v) BSA in TBS 0.1 % (v/v) Tween-20 for 60 min in the cold room. The membranes were developed using Super Signal West Dura Extended Duration Substrate kit (Pierce, Perbio Science, Cramlington, Northumberland, UK).

2.6 Bioinformatics

2.6.1 General bioinformatics

The preliminary characterisation of the NRP-1 publication record was made using PubMed (http://www.ncbi.nlm.nih.gov/sites/entrez). The putative interaction record was obtained with the help of the InterDom server (http://interdom.i2r.a-star.edu.sg/).

2.6.2 Homology modelling of the c domain

The sequence of the c domain (Uniprot accession number O14786, residues 645-804) was used to search HHPred algorithm in search for the most similar available templates (http://toolkit.tuebingen.mpg.de/hhpred) [105]. The best templates indicated by the software, 2C9A (2.7 Å resolution) [106] and 2V5Y (3.1 Å resolution) [107] both contained the immunoglobulin domain of the Receptor-type tyrosine-protein phosphatase MU that served for the further modelling of the c domain. It is noteworthy that the sequence similarity between the c domain and both templates within the matching region was low, and with the 2C9A was 24 % identity and 38.6 % similarity, and with 2V5Y was 24.1 % identity and 38.8 % similarity as shown by Emboss pairwise alignment (http://www.ebi.ac.uk/Tools/emboss/align/index.html). The consistency of the secondary structures within the templates was verified by Dalilite (http://www.ebi.ac.uk/Tools/dalilite/index.html) [108]. The alignment of the c domain and the two structures was performed by Clustal W (http://align.genome.jp/) [109] and its PIR presentation served to prepare the input file for Modeller 9v7 (http://www.salilab.org/modeller/) [110].

Subsequent modelling produced five initial structures which were verified by DOPE score in Modeller 9v7, and the lowest score model (most energetically favoured) was further optimised. In order to do so, the Ramachandran plot of the chosen model was examined (http://mordred.bioc.cam.ac.uk/ rapper/rampage.php), and residues in the outlier region were remodelled to obtain correct biophysical properties. Again, the best model was validated by the DOPE score, and additionally inspected by Model Quality Assesment Suite (http://ika.bwh.harvard.edu/testmod/Qasmod.html), and compared with the template structural files. This showed that the obtained model was of medium quality, however, at the same time it did not differ substantially in its properties from the input templates and it had no major structural constrains. The final model was used to visualise the peptides identified in the P&L experiment.

2.6.3 Docking analysis of the c domain

The obtained model of the c domain was subsequently analysed by PPI-Pred (http://bmbpcu36.leeds.ac.uk/ppi_pred/index.html [111], meta-PPISP (http://pipe.scs.fsu.edu/meta-ppisp.html) [112] and WHISCY (http://nmr.chem.uu.nl/Software/whiscy/index.html) [113]. The output residues were suggested to be involved in protein-protein interactions. The final consensus sequence was subsequently used to model a putative dimer of the c domain by HADDOCK server.

2.6.4 Homology modelling of NRP-1

The sequence of NRP-1 (Uniprot accession number O14786, residues 22-808) was homology-modelled basing on the 2QQM and 2QQK structures, and previously homology-modelled a1 and c domains. The standard procedure as described above was applied for a1, c, and the final NRP-1 modelling.

2.6.5 Sequence alignments of NRP sequences

Alignments of rat NRP-1 versus human NRP-2 sequence covered by the 2QQL structure and human NRP-1 were performed by Clustal W [109] (http://align.genome.jp/) and served to reflect best fitting of the identified peptides on the available crystal structure. The level of identity and similarity of the sequences was calculated using Emboss pairwise alignment (http://www.ebi.ac.uk/Tools/emboss/align/index.html).

2.6.6 Visualisation of the structures

In order to present approximated location of the identified biotinylated peptides of rat NRP-1, either a human NRP-2 structure covering all a1a2b1b2 domains (the 2QQL) [1] or the homology-modelled c domain or human NRP-1 were used. Subsequently, the Pymol software (http://pymol.org/) was used to illustrate the above regions.

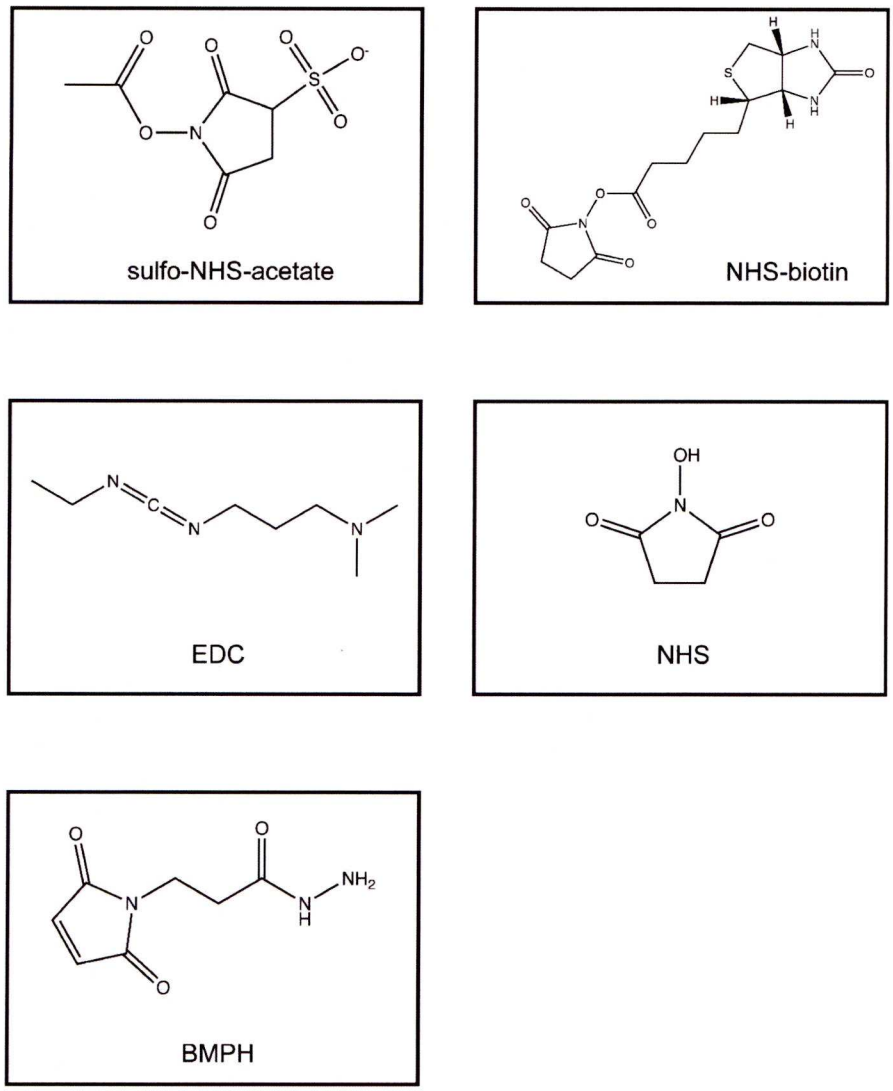

Figure 2.1: Crosslinking reagents used in the study.

Results and Discussion

Chapter 3

Development of the differential scanning fluorimetry method to probe protein-glycosaminoglycans interactions

Abstract

This chapter presents a novel method that investigates protein-polysaccharide interactions in a high-throughput manner. The method provides a direct rapid measurement of the melting temperature shifts of the studied protein-polysaccharide complexes and allows simultaneous analysis of up to 96 possible conditions. The method was based on work of Niesen et al., [114], and was additionally used in Chapter 4 to confirm the binding of heparin to recombinant NRP-1s (see Figure 4.16). The choice of FGFs as test proteins resulted from a relatively solid knowledge on the chosen - FGF-1, FGF-2, and partially FGF-18 - interaction with various heparin-derived molecules. This knowledge allowed the verification of the method's applicabil-

ity to screen in a high-throughput manner structural requirements of molecules that can bestow changes in thermostability of their protein partners. The method appeared successful for the tested proteins, and allowed to follow several aspects of the polysaccharide: FGF interactions. First of all, the heparin-concentration dependent elevation of stability was observed, secondly, oligosaccharide size influence on stability, thirdly, sulfation pattern of the polysaccharide requirement to bestow stability. Such a set of data provides information on the thermostabilising aspect of the given interactions, however, it might be very useful as a partial characterisation of the binding events. It is important to note that in order to obtain a full picture of the functional aspect of the interaction more assays are indispensable (e.g. structural shift characterisation, signalling capability correlation).

The publication describing the method is attached as a **Supplemental paper 2**.

Introduction

The name *Differential scanning fluorimetry* (DSF) derives from the measurements of small differences in fluorescence of an analysed sample. When combined with a gradient of temperature it allows collection of data points in defined temperature and time intervals in order to build a thermal profile of an unfolding protein. Although in general, due to the presence of aromatic amino acids, proteins possess intrinsic fluorescence properties, the application of the method detecting the intrinsic fluorescence is limited to proteins containing at least one of those amino acids. Using an additional dye to detect fluorescence measurements is therefore useful due to its independence of amino acid content. Additionally, in case of Sypro® Orange dye, its high signal-to-noise ratio makes it an excellent probe enhancing the detection of unfolding [82]. Application of Sypro® Orange dye is also useful as it allows the experiment to be run in a standard RT-PCR machines, which usually have a default setting for detection of similar dyes, thus, does not require a specific calibration, and is available in most molecular biology laboratories.

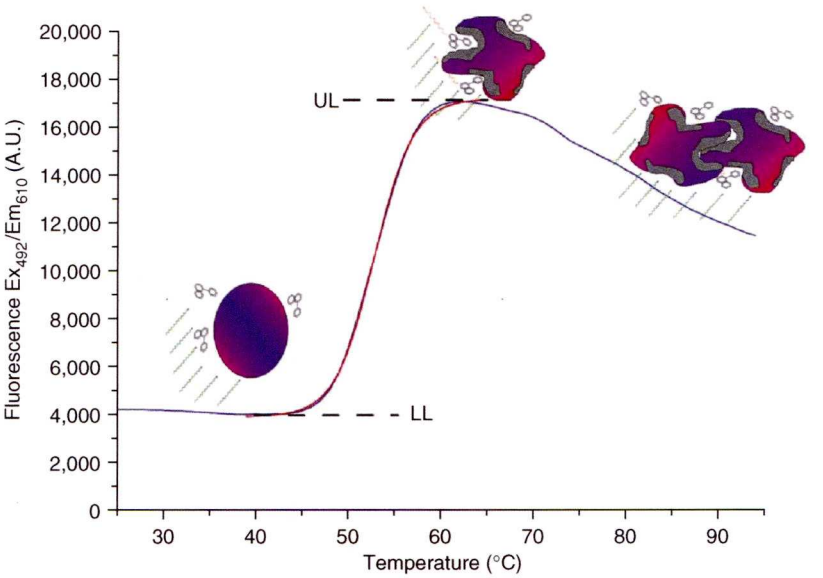

Figure 3.1: Typical recording of fluorescence intensity versus temperature for the unfolding of protein (citrate synthase) in the presence of Sypro® Orange (adapted from [114]).

The dye is symbolised as a three-ring aromatic molecule. In the presence of a globular protein (spherical shape at the baseline of the curve) the dye does not interact with the protein and the basic fluorescence intensity is low. Through unfolding of the protein, hydrophobic patches (in gray) become exposed, the dye binds to them, and strong fluorescent light (depicted by orange curved arrows) is emitted by the dye molecules bound to them. Following the peak in the intensity, a gradual decrease is observed, which is mainly explained by protein being removed from solution owing to precipitation and aggregation. The lower and upper level in the fluorescence intensity are marked LL and UL, respectively.

The Sypro® Orange is a commercial dye of a classified structure that was initially developed as an SDS-PAGE stain. Its mechanism of interaction with proteins is driven by hydrophobic forces. Namely, in native conditions when the protein is folded and its hydrophobic residues are buried inside the structure the dye remains largely free *in solution* and its fluorescence is low. However, upon transition of the protein into an unfolded state, as the hydrophobic residues become exposed, the dye interacts with them, and this causes a significant rise in its fluorescence signal (Figure 3.1). Thus, so that the method was suitable for the protein analysis, first of all, the dye needs to have no background affinity for the protein in its native state, secondly, a more universal requirement for the protein to undergo a state transition denaturation is fundamental.

In most cases, the shape of the thermal (denaturation) curve recorded by the RT-PCR machine will resemble a two-state transition curve (Figure 3.1), and this is a prerequisite for the further analysis. The inflection point, defined by the maximum of the first derivative of the thermal curve, is a melting temperature (T_m) of the protein, and is a direct output value allowing data interpretation.

Several proteins were tested to confirm that the method could be ubiquitously applied for the protein studies (Figure 3.2). Among proteins belonging to *All* α protein class were Interleukin-6 (IL-6), BSA and S100A4 [115–117], in α *and* β class was lactoferrin [118], and in *All* β class were FGFs presented in the **Supplemental paper 2**. All of them required 5 μM concentration to provide detectable signal. IL-6 and lactoferrin underwent denaturation according to the two-state model. BSA and S100A4 had less evident melting curves, nonetheless, the estimation of their respective T_m values was possible. It is important to remember, as in the latter cases, when the first derivatives were based on shallow thermal profiles, that the precision, repeatability, and, consequently, the errors of the measurement can be affected by the shape of the thermal curves. Overall, the chosen test proteins allowed the determination of the output T_m values, which was a good prognostic for the method.

Next, the obtained T_m values were compared with the literature-derived values. Only for

lactoferrin and BSA [119] was such comparison possible, and revealed that the method was providing values in a close range to the published data [119, 120], for lactoferrin 66°C as compared with the published 72°C, for BSA 61°C as compared with the published 59°C. The 66°C for IL-6 and 52°C for S100A4 are to the author's knowledge the first determinations of their respective T_m values.

This initial experimental stage led to a further development of the application of this method to studying protein-polysaccharide complexes. Detailed description of this part of the project is presented in the **Supplemental paper 2**.

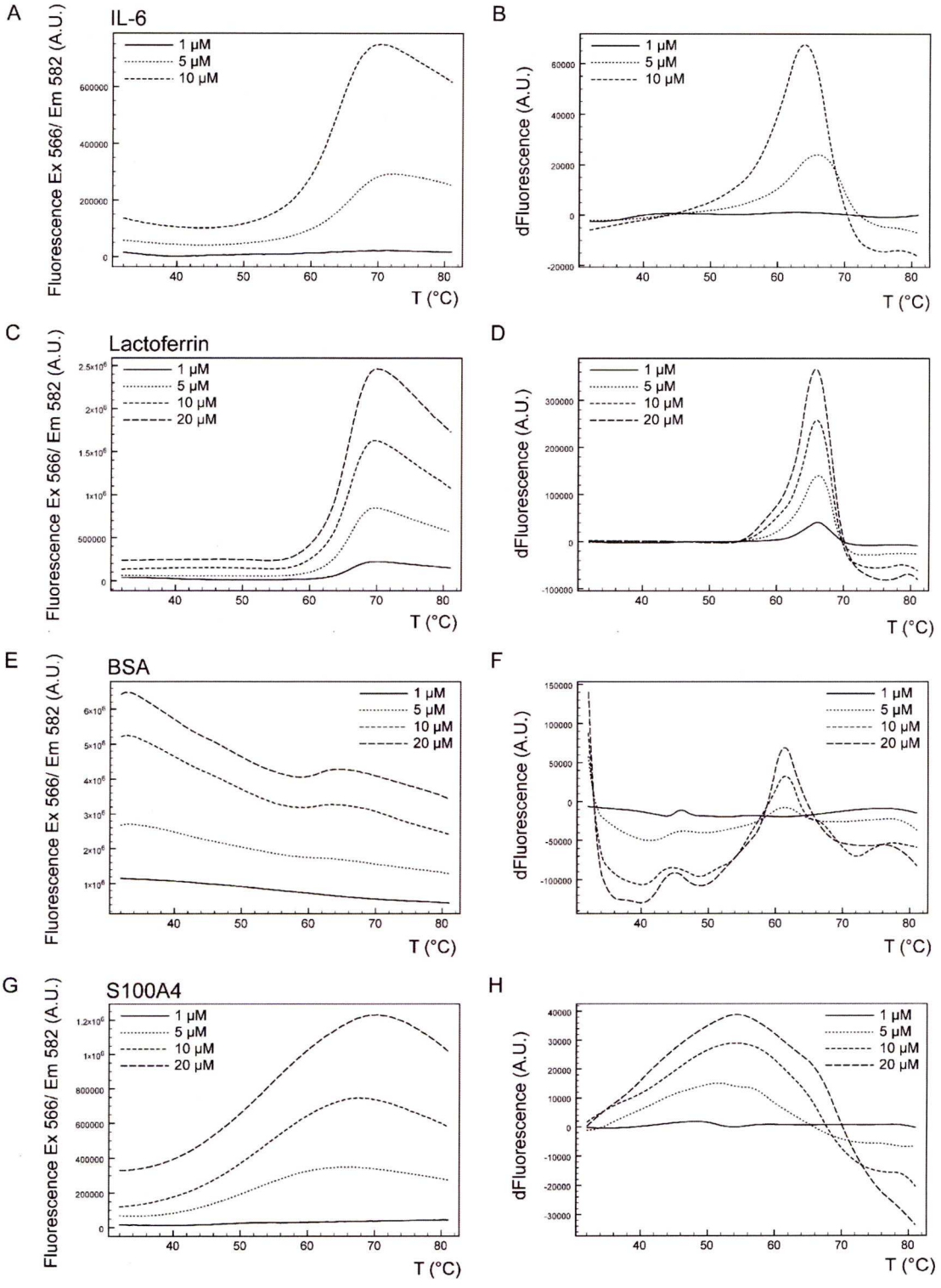

Figure 3.2: Denaturation curves of the proteins tested by DSF applying Sypro® Orange dye.

The figure presents denaturation curves of the chosen test proteins (left panels) and their respective first derivatives (right panels) calculated as described in the Section 2.2.6. The indicated molar amounts of the proteins were subjected to the procedure described in the Section 2.2.5. A, B) IL-6. C, D) Lactoferrin. E, F) BSA. G, H) S100A4. The experiment was performed in 2 repeats for each concentration variant and one representative curve is plotted and analysed on the figure.

Chapter 4

Biochemical analysis of the interaction of Neuropilin-1 with heparin

Abstract

Neuropilin-1 (NRP-1) is a vertebrate specific molecule recognised for its involvement in the development of vasculature, neural patterning, immunological responses and pathological angiogenesis. It is a large multidomain membrane protein involved in a complex interaction network with other membrane receptors, such as VEGFRs, plexins, c-MET, and their respective ligands, VEGFs, PlGF-2, SEMA-3A, and HGF/ SF. As a co-receptor, lacking an intracellular domain with an enzyme activity or an obvious motif to dock to such an enzyme, its function is either to allow signal transduction to occur or modulate its strength. Besides membrane location, NRP-1 exists also as several truncated soluble isoforms, resulting from alternative splicing, which additionally increase the complexity of possible interactions and mechanisms of control. This study applied two different commercially available NRP-1 isoforms, and showed

that, depending on the structure context, distinct NRP-1 isoforms can have altered heparin-binding properties. The recombinant dimeric Fc fusion of rat NRP-1 bound to heparin with high affinity (2.5 nM), which permitted thorough characterisation of the interaction, whereas monomeric human NRP-1 displayed weak binding, detectable only by certain methodologies. The investigation of the origin of the difference revealed the requirement of the Fc domain, but not the c domain, to bestow the heparin-binding property. Basing on the findings and contemporary views on the cell surface *milieu*, a hypothesis defining possible biochemical differences between populations of NRP-1 molecules present in the cell environment has been proposed.

Introduction

Neuropilin-1 (NRP-1) was first described in 1987 as antigen A5 [121] expressed by neural cells of *Xenopus* tadpoles. Its role in the neural system was subsequently confirmed in several studies where it was defined as a neuronal recognition molecule responsible for, e.g., neural path finding and cell differentiation [122, 123]. Additionally, it was shown to play an important role in the vascular system, where its overexpression resulted in excessive vascularisation *in vivo* [124]. Consistently, depletion of NRP-1 impaired the development of both neural and vascular systems and had a lethal effect on developing embryos [125–127]. Its leading role in angiogenesis is considered of high significance, as this allows wound healing [128] and ischemic revascularisation [129], however, at the same time mobilises tumour angiogenesis (reviewed in [130]. A consecutive set of NRP-1 functions comprises immunological responses [131], where NRP-1 was discovered to be a T lymphocyte marker [132], important in the antigen recognition process [133], and adhesion, due to its interaction with integrins [45,46]. The latter interaction is proposed to negatively regulate other NRP-1 functions [47].

As a large multidomain protein with no intrinsic signalling properties, NRP-1 is suggested to form functional complexes with other molecules in its environment and affect the overall response [4]. The precise mechanism of NRP-1 function is thus likely to be highly dependent on the interaction networks of NRP-1. Briefly, NRP-1 is claimed to regulate several signalling

pathways via the interactions of its extracellular domain with soluble ligands and membrane receptors. Thus, among the ligands present in the extracellular environment that can interact with NRP-1 are VEGF-A_{165} via its exon 7 and exon 8 encoded amino acid sequence [23, 24], VEGF-A_{121} (lacking exon 6 and 7) via its exon exon 8 [12, 19], VEGF-B_{167} and VEGF-B_{186} [30], via exon 6B and proteolytically processed 6A, respectively, VEGF-C and VEGF-D, although they require heparin to bind to NRP-1 [31], PlGF-2 via its exon 6 and 7 [32], SEMA-3A via the SEMA and the c domain [33], FGF-2 and FGF-4 [36], HGF/ SF [36] via its N-terminus [37], and TGF-β [38]. Importantly, some of the listed interactions remain arguable, and especially for VEGF-A_{121}, an opinion that it does not bind NRP-1 is widespread [22, 24, 27, 134, 135]. Interactions of NRP-1 with cell surface receptors can occur either directly, or via ligand bridging, and comprise VEGFR-1 [26], VEGFR-2 [18], PDGFR-α/β [14], c-MET [44], plexin-A1 [28,49], L1 [136] and the above mentioned integrins. Additionally to these molecules, NRP-1 can also interact with itself [25, 34], and, possibly, its own truncated variants produced, e.g., by alternative splicing. However, the contribution of these hypothetical interactions to the function of NRP-1 is not known. Another putative group of NRP-1-interacting partners are adaptor proteins associating with the intracellular domain of NRP-1, as NRP-1 interacting protein (NIP) [51], which is crucial for the cell signalling and response to NRP-1 [52]. It is plausible that more proteins interacting with the intracellular part of NRP-1 will be discovered, which will expand the range of NRP-1 functions and regulatory mechanisms it can undergo. This also alters the perception of NRP-1 as acting purely extracellularly.

This study focused on another interacting partner of NRP-1, which is implicated in regulation of its function, heparan sulfate (HS). HS is a heterogenic polysaccharide comprised of 1,4 linked uronic acid (α-L-iduronate or β-D-glucuronate) and α-D-glucosamine with varying patterns of 2-O-sulfate in the former and 3-O-, 6-O-sulfate and N-sulfate or N-acetyl in the latter [137]. HS is a component of heparan sulfate proteoglycans (HSPGs) present in the cellular membrane together with NRP-1 [138], however in research, it is often substituted with heparin, its more fully sulfated experimental proxy, which is available in large quantities. Up

to date, there are several putative functions of heparin or other polysaccharides characterised for NRP-1. Firstly, NRP-1 has been shown to interact with heparin through the b1b2 domain, a region directly adjacent to the VEGF-A_{165} binding pocket [1,67]. Secondly, NRP-1 is proposed to dimerise in a heparin dependent manner as a result of heparin and VEGF-A_{165} binding [67]. In fact the model of the angiogenic functional complex of NRP-1 comprises of VEGF-A_{165}: NRP-1: heparin at a ratio 2: 2: 2, and the complex formed in this way would further interact with VEGFR-2 [67]. In *in vitro* studies, addition of heparin results in enhancement of VEGF-A_{165} [21, 22, 24, 26] and PlGF-2 [29, 32] binding to NRP-1 and is suggested to elevate the number of binding sites for VEGF-A_{165} [21] in a NRP-1 dependent manner, without affecting the affinity between NRP-1 and VEGF-A_{165} [18,22]. Moreover, binding of other growth factors, such as VEGF-C and VEGF-D, to NRP-1 appears to be fully dependent on the presence of heparin [31]. An interesting aspect of heparin's impact on the interaction of NRP-1 and of VEGFR-1 was also described. Namely, as it was observed that heparin enhances VEGF-A_{165} binding to NRP-1 and VEGFR-2, at the same time it appeared to prevent NRP-1 interaction with VEGFR-1. Consistent with the fact that VEGFR-1 alone was inhibiting the interaction of NPR-1 and VEGF-A_{165}, a mechanism of functional competition was suggested, that favours the formation of complexes of NRP-1 with VEGFR-1, or NRP-1 with VEGFR-2, VEGF-A_{165} and heparin [26]. Additionally, other glycosaminoglycans can affect NRP-1 functions. Thus, highly sulfated low molecular weight fucoidan (5 kDa), similarily to heparin, enhanced VEGF-A_{165} binding to NRP-1 [56], while a mimetic of a non sulfated GAG (glycosaminoglycan), phenylacetate carboxymethyl benzylamide dextran, inhibited this binding [57].

In order to shed some more light on the interaction of NRP-1 with HS, two different commercially available NRP-1 isoforms, recombinant dimeric Fc fusion of rat NRP-1 (Fc rNRP-1) and recombinant monomeric human NRP-1 (shNRP-1), were used to examine their interactions with heparin and a series of modified heparins. Fc rNRP-1 bound to heparin with high affinity (2.5 nM). Fc rNRP-1 interacted in a charge dependent manner, displaying structural selectivity within a set of tested heparin derivatives. In contrast, monomeric shNRP-1 displayed weak

binding, detectable only by certain methodologies. The lack of substantial shNRP-1 binding to heparin was a subject of further analysis.

Results and Discussion

4.1 Structural characterisation of NRP-1 proteins

NRP-1 is a multidomain protein present either as a transmembrane cellular receptor or as a soluble truncated isoform. As often found in other large mammalian complex proteins, it contains substantial unstructured regions of unidentified function. These stretches, according to the analysis of disorder (Disembl 1.5, http://dis.embl.de/cgiDict.py), cover significant parts of NRP-1 (Figure 4.1A) and in this respect resemble FGF-1 (Figure 4.1B), a well-known model of a molten globule structure [139]. According to this analysis, NRP-1 possesses a significant number of loop/coil structures, which are the first indication of disorder, because only within these elements can higher disorder be observed. Additionally, NRP-1 contains high level of "remark 46" entries, which stand for the missing coordinates in X-ray structures, and also high motility loops, named "hot loops", based on Cα temperature factors. The latter two are considered highly indicative of disorder [140]. Therefore, *in silico* analysis of the sequence of NRP-1 complements the knowledge of the domain structure and generates a picture of a partially unstructured, dynamic and multifarious protein. Nevertheless, these features, albeit potentially advantageous for protein function, at the same time are unfavourable for protein expression, purification and its stability raising numerous technical problems [140].

The commercially available NRP-1s used in this study, Fc rNRP-1 and shNRP-1, are assumed to bypass these difficulties due to some structural amelioration. Thus, to obtain Fc rNRP-1, small parts of the protein's amino acid sequence, residues 811-828 and C-terminal transmembrane/ intracellular region, were excluded from the expression construct.

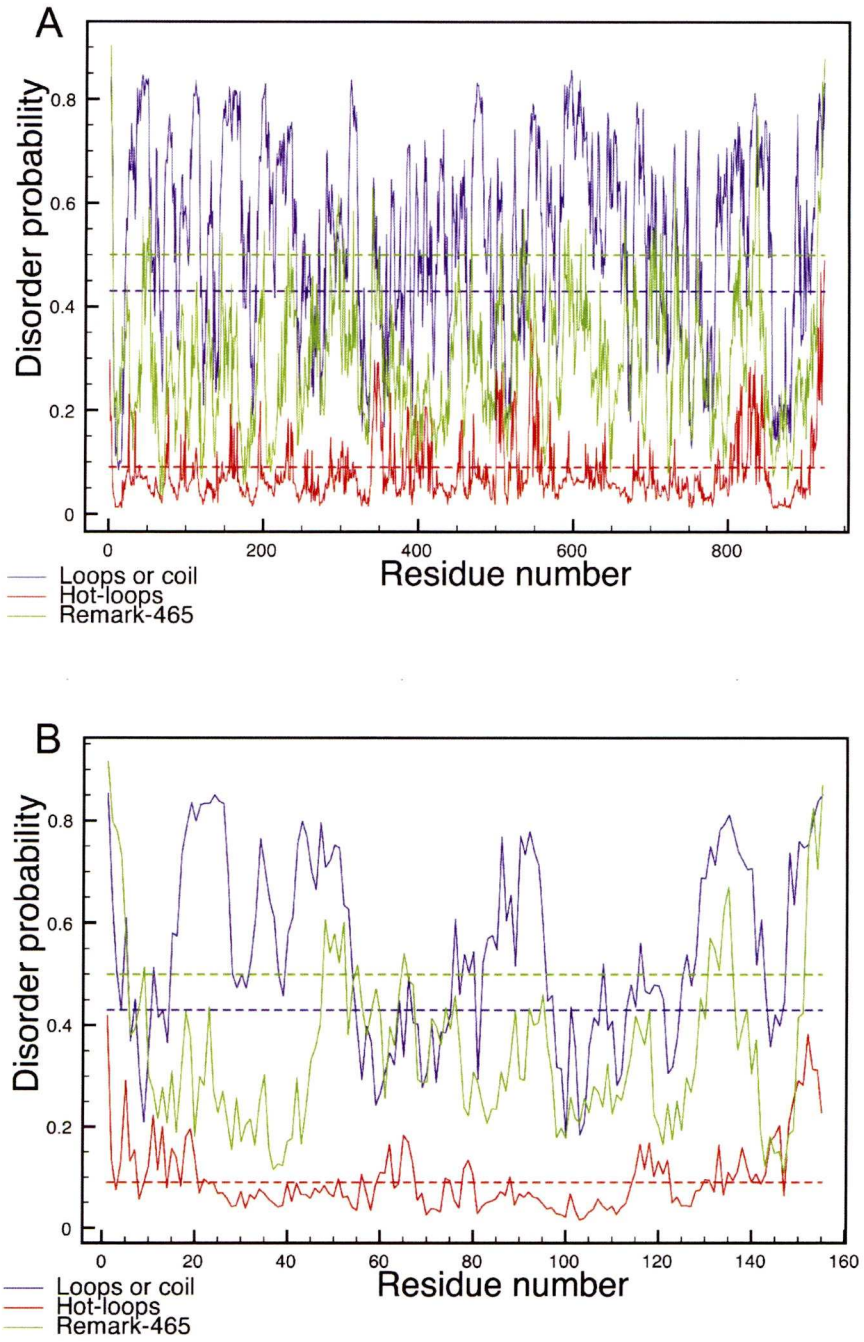

Figure 4.1: Analysis of the disorder of the structures of human NRP-1 and FGF-1 by DisEmble 1.5 application (http://dis.embl.de/cgiDict.py).

A) The analysis of disorder of full sequence of human NRP-1. B) The analysis of disorder of full sequence of human FGF-1. Several regions within FGF-1 and NRP-1 sequences exceeded the threshold values for three independent disorder probability indicators: loop/coil structures (blue), hot loops (red), Remark-454 (green). The thresholds for disorder prediction provided by the server are marked in respective colours in dashed pattern straight lines (0.43, 0.09, 0.5, respectively). The x axis spans the protein residues, while the y axis shows the disorder probability.

Whereas the deleted 17 internal amino acids might have been a source of some structural problems, as indicated by the high probability of encompassing a high motility loop (Figure 4.1A), the removal of the transmembrane/ intracellular region permitted production of the soluble protein without extra amino acids and membrane interacting structures. Secondly, the protein was expressed as a chimeric molecule, where the rat NRP-1 sequence was fused to the Xa factor cleavage site followed by the Fc part of human IgG1 sequence, where the latter has the ability to form disulfide bridges between two independent Fcs (Figure 4.2B). Consequently, the final protein is a dimer. Such an approach, where proteins are expressed as dimers, is often chosen to raise the stability of the final product. Consequently, excluding the small deletions, the assayed protein comprises most of the extracellular sequence of NRP-1 (Figure 4.2A) and is a soluble dimer. Another investigated protein, shNRP-1, covers the sequence of a naturally occurring alternatively spliced soluble human isoform (Figure 4.2C). Contrary to Fc rNRP-1, shNRP-1 is a monomer and its sequence has not been altered. Importantly, as the protein consists of 1-644 amino acids, the putatively problematic C-terminal region is absent. Both proteins were expressed with a C-terminal histidine tag.

The analysis of protein purity and size by SDS-PAGE in reducing conditions demonstrated that the Fc rNRP-1, originally estimated 238 kDa, as a dimer and expected 120 kDa as a monomer, migrated around 150 kDa, while shNRP1, anticipated 71 kDa, migrated around 90 kDa. Both NRP-1s were pure and their migration on SDS-PAGE was affected by N-glycosylation as shown by the treatment of the proteins with N-glycanase (Figure 4.2D). Additionally, whereas the band of N-glycanated Fc rNRP-1 was sharp and compact, the band of N-glycosylated shNRP-1 was blurred and indicated possible multiple glycan modifications. Importantly, it was verified that also the Fc part of Fc rNRP-1 was the subject of N-glycosylation, thus it is assumed, that in the same expression system used to produce both proteins, mouse myeloma NS0 cell line, Fc rNRP-1 is N-glycosylated on its NRP-1 moiety similarly to shNRP-1, and additionally on its Fc moiety.

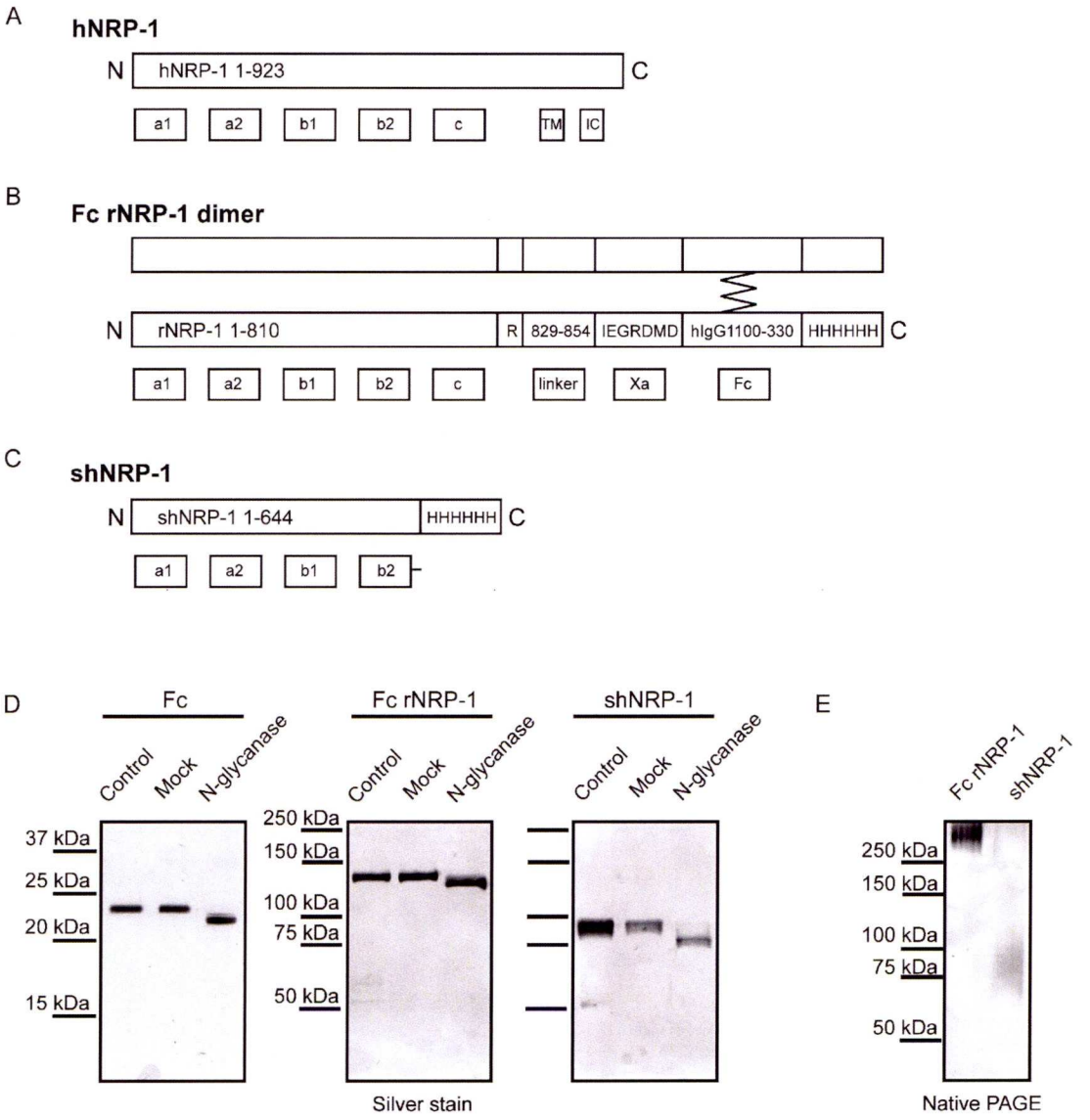

Figure 4.2: Analysis of recombinant NRP-1 species.

A, B, C) Schematic representations of the respective isoforms of NRP-1. A) Native human NRP-1 (hNRP-1) with indicated extracellular domains (a1, a2, b1, b2, and c), transmembrane (TM), and intracellular (IC) domains. B) Recombinant dimeric rat NRP-1 (Fc rNRP-1) with indicated extracellular domains and the linker sequence derived from NRP-1 sequence, and additional Xa cleavage site (Xa), Fc part of human IgG1 (Fc) and the His tag. C) Recombinant soluble isoform of human NRP-1 (shNRP-1) with indicated domains and the His tag. D) Silver staining result of N-glycanase digest, performed as described in the Section 2.2.1, of the reference Fc region, Fc rNRP-1 and shNRP-1, where control, mock digest and the digest results with indicated marker sizes are shown. E) Silver staining of the native PAGE of Fc rNRP-1 and shNRP-1 with indicated marker sizes are shown.

Furthermore, the migration of the proteins studied in native conditions revealed important differences between them. While the Fc rNRP-1 migrated as a massive aggregate exceeding the estimated size of the intact dimer, the shNRP-1 migrated roughly as the same size as under the denaturing conditions (Figure 4.2E). This observation confirmed previously observed Fc rNRP-1 behaviour in gel filtration [36] and implied an important difference between the two proteins, as, very possibly, the nature of Fc rNRP-1 is closer to a multi-component oligomer of Fc rNRP-1, contrary to the monomeric shNRP-1. Nevertheless, it was not possible to establish if the oligomerisation occured via the Fc or the NRP-1 part of the dimer, though its previously observed dependence on the concentration of electrolytes [36] suggests that both parts could be involved, as ionic bonding was observed for both molecules [36, 141].

4.2 Determination of interaction of shNRP-1 and Fc rNRP-1 with heparin

One of the recognised properties of NRP-1 is its interaction with heparin. Studies focused on functional aspects of this interaction demonstrate that heparin can enhance NRP-1 binding to VEGF-$_{165}$ [26] and placenta growth factor 2 (PlGF-2) [29] or be a prerequisite of formation of multicomponent complexes invoving NRP-1 [32]. The impact of heparin on the properties of NRP-1 observed was so substantial that, indeed, some biochemical studies of NRP-1 apply heparin as a fixed constituent in the experiments embodying its presence in overall NRP-1 function [29]. Despite this, there is not much known regarding how NRP-1 interacts with heparin.

In this study the two commercially available NRP-1s, shNRP-1 and Fc rNRP-1, were analysed in an optical biosensor, IAsys, for binding to a heparin derivatised surface. Both constructs, although they encompass the region identified to contain the heparin-binding site (the b1 and b2 domains) [29], had markedly different binding ability. Whereas the Fc rNRP-1 bound well to the surface, the shNRP-1, similarly to control Fc IgG1, showed only the small charac-

teristic bulk shift associated with the refractive index change of the PBST with protein compared to the PBST, representing no significant binding (Figure 4.3A). In order to examine this surprising result more thoroughly, a different type of experiment was designed, where a well-characterised BaF3 cell system was chosen for a perturbation experiment. In this system the murine pro-B cells, naturally deficient in cell surface glycosaminoglycans, require exogenous FGF and heparin to signal through recombinant FGFR-1c receptor in order to survive in IL-3 deficient medium. Therefore, it was hypothesised that the addition of heparin binding, and potentially sequestering, NRP-1, could affect cell survival. The experiment was designed to compare four different concentration ratios of FGF-2 versus heparin, to distinguish between NRP-1s' effect via sequestration of heparin, or potentially of FGF-2 [36]. Again, both recombinant constructs were assayed and compared with the Fc IgG1 control. In a similar manner to the biosensor experiments, only the Fc rNRP-1 appeared to reduce the survival rates of the pro-B cells, as visualised in colorimetric MTT assay (Figure 4.3B, C, D). The effect of the Fc rNRP-1 was detected at its highest employed concentrations (10 and 30 nM), in the conditions where heparin was at the lowest, more limiting, concentration (present at 0.1 μg/ ml, or 6 nM).

To conclude, the scope of recombinant NRP-1s interaction with heparin was tested either on a heparin-modified surface or *in solution.* Although for the BaF3 perturbation assay the possibility that Fc rNRP-1 exerted the observed effect via interaction with some cellular receptors cannot be fully excluded, due to the convergent result with the optical biosensor experiment, it seems reasonable to propose that Fc rNRP-1, but not shNRP-1, sequestered heparin and inhibited the activity of FGF-2. Thus, both approaches demonstrated that Fc rNRP-1, contrary to shNRP-1, had more evident heparin-binding property. This leads to conclusion that either domain composition (the missing in shNRP-1 c domain) or artificial dimerisation (via Fc IgG1) of the Fc rNRP-1 may be relevant for protein's interaction with the sugar.

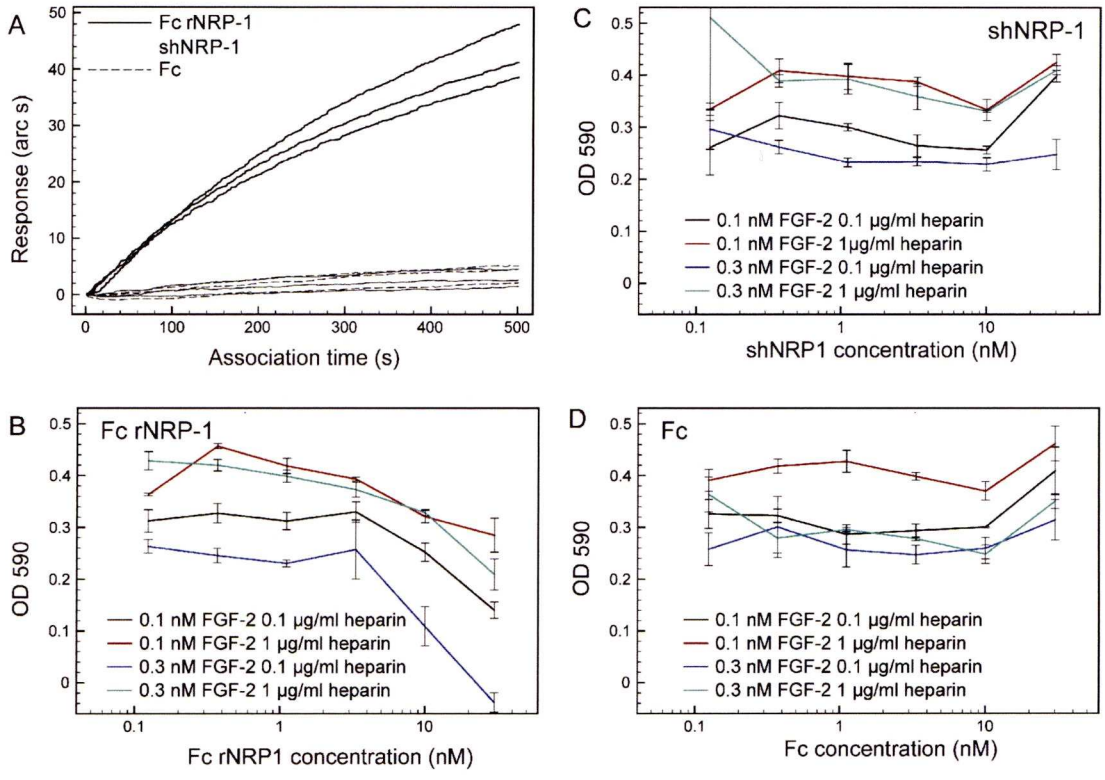

Figure 4.3: Characterisation of the interaction of Fc rNRP-1 and shNRP-1 with heparin in an optical biosensor and a BaF3 cell assay.

A) Fc, shNRP-1 and Fc rNRP-1 at final concentration of 0.5 μg/ ml were tested for binding to the heparin surface in biosensor IAsys. The x axis presents the time scale and the y axis the extent of binding expressed in [arcs s]. B, C, D) BaF3 sequestration experiment, where the BaF3 cells were grown in constant concentrations of FGF-2 and heparin, as described in the Section 2.4.1, with a range of concentrations of B) Fc rNRP-1, C) shNRP-1 and D) Fc. The graphs present the OD_{590} readings of the MTT assay of the BaF3 cells cultured in the tested conditions for 72h. Obtained values indicate the metabolic activity treated as a proxy for the number of living cells. The experiment performed in triplicate (mean$\pm$SD).

4.3 Characterisation of the Fc rNRP-1 interaction with heparin by optical biosensor

Since measurable binding to a heparin surface was observed only for Fc rNRP-1, further characterisation of this interaction was carried out with this isoform. The IAsys optical biosensor allowed two main attributes of binding, kinetics and specificity, to be established. The aim of the kinetics analysis is to calculate the rate of the association and dissociation reactions, defined by the association and dissociation rate constants, k_{ass} and k_{diss} and the affinity of the interaction, expressed as the equilibrium dissociation constant (K_d), defined by the ratio of association and dissociation rate constants (k_{diss}/ k_{ass}) and denoted in nM. The analysis of kinetics of Fc rNRP-1 binding to a heparin surface was performed after initial determination of the concentration range of the Fc rNRP-1 that only yielded monophasic binding kinetics. Heparin is a polymeric ligand possessing a range of binding sites and immobilisation of the heparin to the surface through streptavidin may result in steric hindrance of some of these sites. Thus at higher concentrations of ligate, secondary binding sites can appear in the analysis [142, 143]. As a consequence, the final concentration range of Fc rNRP-1 spanned 0.25-1.22 nM, as only within this window, the binding was uniformly presenting a one-site binding model, and at the same time was within the detection capacity of the instrument. This means that as with all such analyses, it is the interaction of Fc rNRP-1 with a class of highest affinity sites within heparin that is being measured, not the average of all the potential binding sites in heparin. Figure 4.4A-H presents analysis of the one out of five independent kinetic experiments. First of all, increasing concentration of Fc rNRP-1 showed increasing extents of binding (Figure 4.4A). Each concentration exhibited a one-site binding model, as confirmed by comparison of the binding curves versus the mathematical model of a single site interaction; the data are distributed randomly around the model (Figure 4.4B-F).

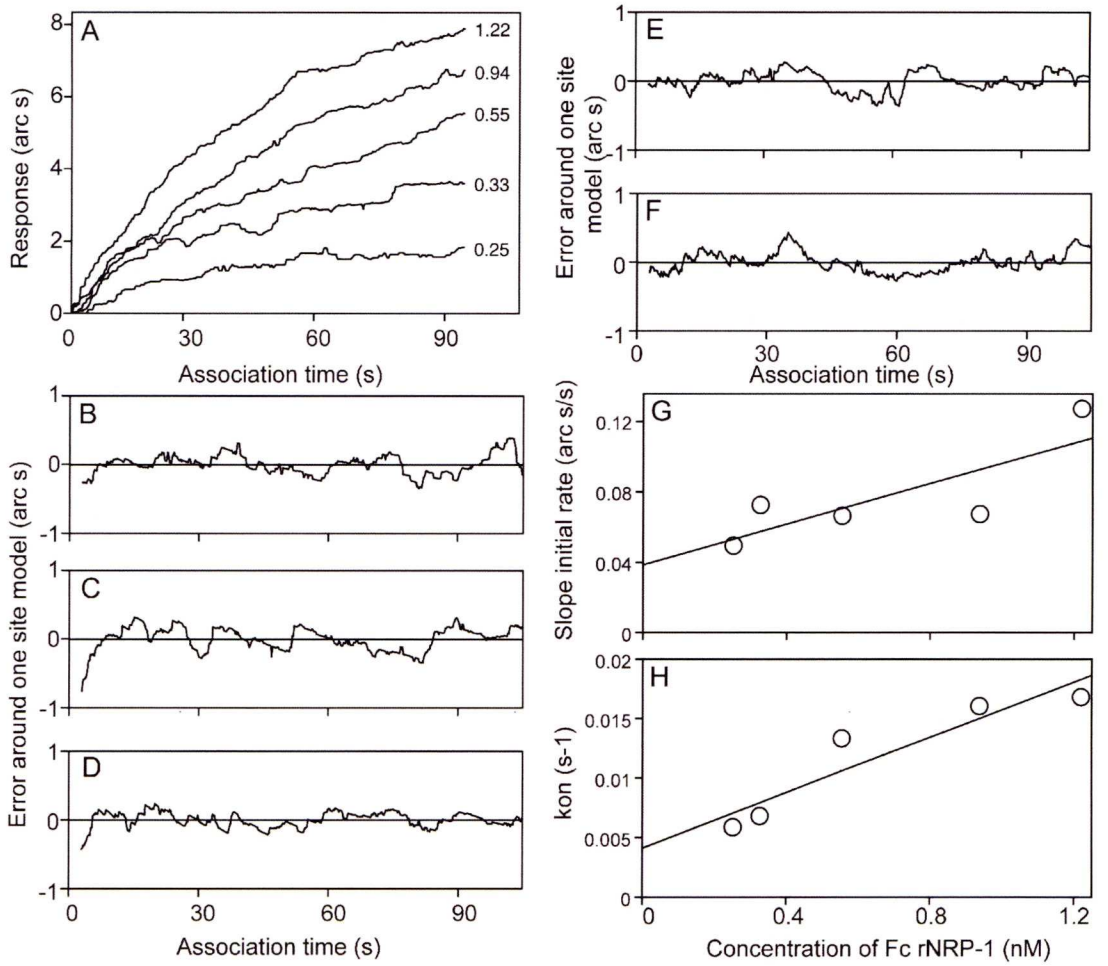

Figure 4.4: Kinetic analysis of Fc rNRP-1 binding to heparin surface in biosensor IAsys.

Data shown are a representative of a set of five independent experiments described in the Section 2.3.2. A) Extent of binding of indicated molar amounts of Fc rNRP-1 expressed in [arc s] (y axis). B-F) The distribution of the data points (jagged line) around a one site binding model (horizontal line at 0 arc s) is shown for each of the concentrations of Fc rNRP-1 used in the binding assay in panel A. B) 0.25 nM. C) 0.33 nM. D) 0.55 nM. E) 0.94 nM. F) 1.22 nM. G) Linear relationship between the slope of initial rate of association and concentration of Fc rNRP-1. H) Linear relationship between k_{on}, determined from a one-site model, and concentration of Fc rNRP-1.

k_{ass}	SE	p of line	Intercept	SE	k_{diss}	SE	K_d	SE
$(Ms)^{-1}$					s^{-1}		*nM*	
9820000	580000	0.95	0.01	0.00	0.02	0.00	2.46	0.00

Table 4.1: Kinetic result of Fc rNRP-1 binding to heparin surface in biosensor IAsys.

The table presents kinetic values characterising the Fc rNRP-1 binding to heparin, where k_{ass} is association rate constant, p value is the correlation coefficient of the linear regression through the k_{on} values, intercept is an approximate k_{diss} value obtained from k_{on} plot , k_{diss} is dissociation rate constant obtained in the dissociation experiments, and K_d is the affinity calculated from the ratio of k_{diss}/ k_{ass}. The standard errors (SE) were calculated from five independent association datasets and six independent dissociation datasets.

The initial rate of binding, defined by the binding of the soluble ligate within the first 15s of the addition of ligate was shown to increase in a linear manner with increasing concentration of Fc rNRP-1 (Figure 4.4G). This illustrated that the binding of Fc rNRP-1 to heparin was not limited by mass transport or by steric hindrance [144]. The calculated on-rate (k_{on}) was observed to increase linearly with the concentration of Fc rNRP-1, which again supports the use of a one site model to analyse the data (Figure 4.4H). The linear regression analysis of the k_{on} values allowed the calculation of k_{ass}, defined by the slope of the linear interpolation within the collected dataset. However k_{diss}, which can be also derived from the graph as a y-axis intercept value, was not taken into account, as it is more reliable to measure it directly. Thus, a separate set of dissociation experiments was performed, where dissociation of Fc rNRP-1 was enhanced by the addition of competing heparin *in solution*, to prevent the re-binding of Fc rNRP-1 to the heparin surface. Values for k_{diss} were established from 6 independent experiments. The mean k_{ass} (supported by high p value indicating variance in the measurement of the gradient of the plot of k_{on} against concentration) and k_{diss} values allowed the calculation of K_d (formally, the ratio k_{diss}/ k_{ass}), which was 2.5 nM (Table 4.1). This result was consistent with the only hitherto published affnity value for NRP-1 binding to heparin, estimated 0.69 nM, which was obtained with the same commercial isoform applying surface plasmon resonance [58]. Thus, clearly, Fc rNRP-1 can be classified among the high affinity interacting partners of heparin, though again it must be stressed that this is a measurement for the highest affinity binding sites in the sugar and there will be many lower affinity sites.

After characterisation of the kinetics of the interaction of Fc rNRP-1 with heparin, the next question was focused on the structural requirements of heparin that favour this interaction. Three different parameters were examined, namely, length of the heparin oligosaccharide, sulfation pattern of the heparin derivative and the cationic form of heparin. While the first one describes the architectural attribute of the best fitted structure within the binding site of the Fc rNRP-1, the latter two may provide additional functional information, as different sulfation patterns and cationic forms of heparin have distinct solution conformations and so functional

properties [145].

The identification of the binding preferences was established in competition tests, where Fc rNRP-1 was compelled to select between binding to the heparin immobilised on the sensor surface and a heparin-derived compound present *in solution*. In this way, the capacity of the assayed compounds to compete for Fc rNRP-1 binding to the heparin surface can be compared with the same capacity of heparin added to solution.

The analysis of the minimal length of oligosaccharide that can be accommodated by Fc rNRP-1 applied compounds defined by their degree of polymerisation (dp), where dp 2 was the minimal repeating disaccharide unit of heparin (Figure 4.5A). The range used in this study covered dp 2 - dp 26. Oligosaccharides of dp 2 - dp 8 had very weak competing potency, however, starting from dp 16, a substantial inhibition of binding of the protein to the surface was observed. However, it is noteworthy that the largest oligosaccharide tested, dp 26, was still significantly less effective than heparin (Figure 4.7), which corresponded to the difference in size between dp 26 and heparin (Figure 4.5B). This showed a direct reliance of the tested oligosaccharide size and its inhibiting property, but also suggested a complex spatial nature of the interaction between Fc rNRP-1 and heparin, as full inhibition could only be observed with native heparin (Figure 4.7). This preference for heparin, which is polydisperse in length, may reflect the recombinant dimeric structure of Fc rNRP-1 in which both NRP-1 moieties are likely to be involved in heparin binding, or the requirement for a structure for the highest affinity binding that is most common in the longest chains of heparin.

Next, the potency of variously sulfated heparin derivatives was tested. The compounds were chemically produced from native heparin and bore different substitution patterns of distribution of sulfate groups (Figure 4.6), which allowed an evaluation of the importance of specific sulfate groups for Fc rNRP-1 binding.

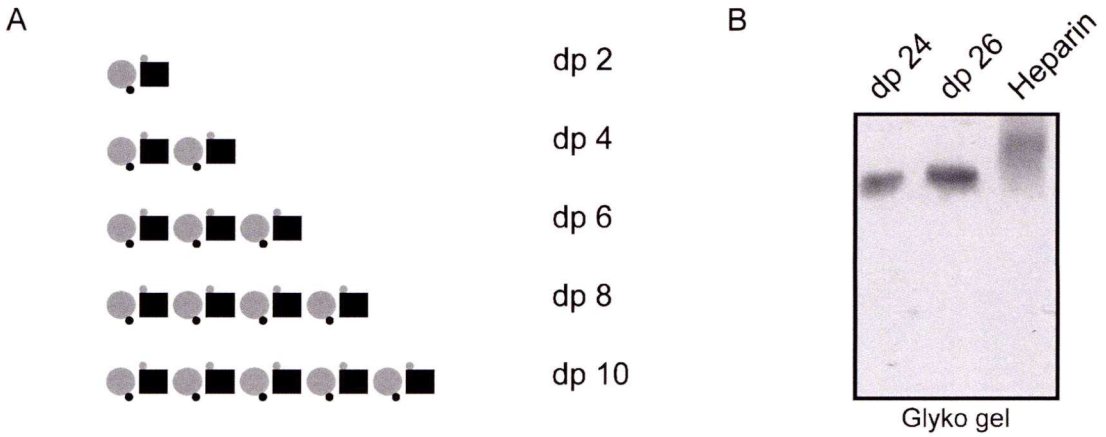

Figure 4.5: Additional information on oligosaccharides used in the competition assays.

A) Scheme of applied classification of oligosaccharide species, where grey large circle is uronic acid, small black circle is 2-O-sulfate, black rectangle is 2-N-sulfated glucosamine, and small grey circle is 6-O-sulfate. B) PAGE analysis of 1 μg of the largest dps used in the competition assay (dp 24, dp 26) and heparin was performed as described in the Section 2.5.1.

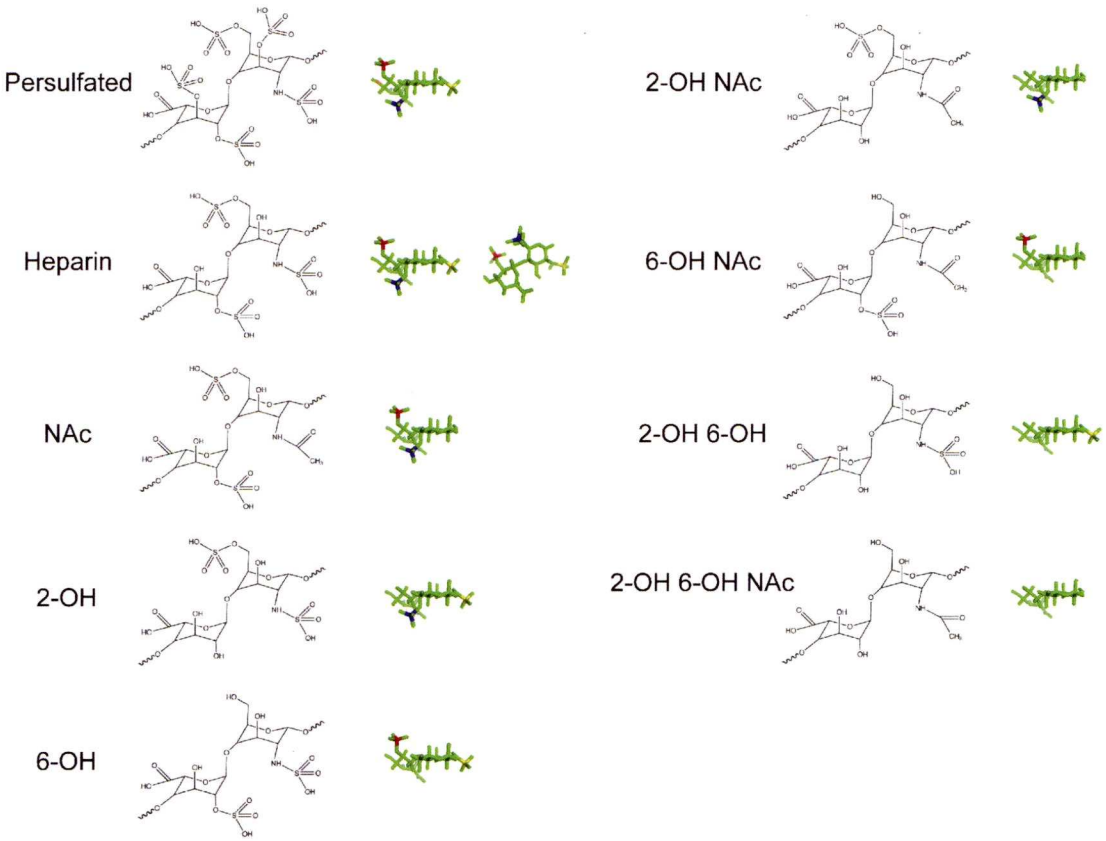

Figure 4.6: Schematic presentation of the modified heparin derivatives used in the competition assays.

Label, chemical structure and schematic stick-and-ball image of each derivative is presented, where 6-N-sulfate is marked yellow, 2-O-sulfate is red, 6-O-sulfate is blue, and two additional 3-O-sulfates of persulfated heparin are marked orange.

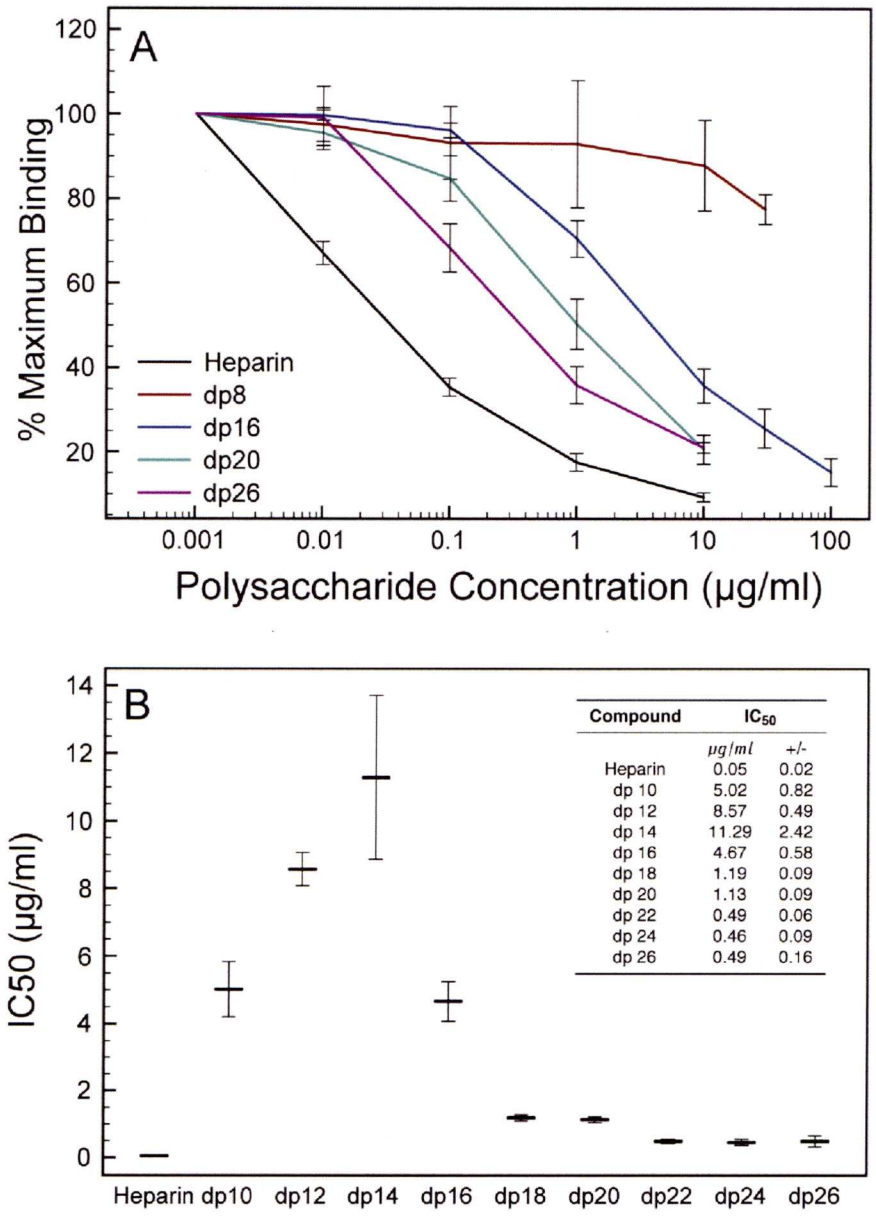

Compound	IC_{50}	
	µg/ml	+/-
Heparin	0.05	0.02
dp 10	5.02	0.82
dp 12	8.57	0.49
dp 14	11.29	2.42
dp 16	4.67	0.58
dp 18	1.19	0.09
dp 20	1.13	0.09
dp 22	0.49	0.06
dp 24	0.46	0.09
dp 26	0.49	0.16

Figure 4.7: Competition experiments defining length of heparin-derived oligosaccharide requirement that enable Fc rNRP-1 binding.

Inhibiting ability of oligosaccharides of selected lengths on Fc rNRP-1 binding to the heparin derivatised surface was tested as described in the Section 2.3.2. A) The relative binding values at presence of each concentration of added inhibiting ligand (x axis) were adjusted to 100 % of Fc rNRP-1 binding alone to heparin (measured at least between 10-40 arc s). The experiment was performed three times independently (mean±SD). B) IC_{50} values were calculated basing on the non-linear curve fit of single representatives of respective binding curves and are expressed in [µg/ml] (±SE) for the inhibiting compounds tested in panel A.

The varied sulfation patterns are considered likely to contribute to the specificity of interaction with proteins, either via alteration in conformation/ flexibility of the sugar chain, or merely the saccharide sequence [145–147], the Fc rNRP-1 did not show any selective binding preference for one sulfate group over another in the three mono sulfated heparins (Figure 4.8). Heparins desulfated at either N (in this instance re-acetylated), C6 or C2 all showed a substantial drop in IC_{50} (40- to 77-fold) compared to that of the parental heparin. This suggested that Fc rNRP-1 requires a combination of all three sulfate groups for effective binding. Nonetheless, in contrast to these results, Fc rNRP-1 bound also to a heparin lacking any of these groups, and for this species the IC_{50} value was lower than for any of the singly desulfated heparins. Similarly to the latter compound, heparin desulfated at both N and C2 appeared to be an effective inhibitor of the Fc rNRP-1 heparin surface binding and its IC_{50} was the closest to the one of heparin among the desulfated heparin derivatives. Interestingly, the other two doubly desulfated heparins were very weak competitors (Figure 4.8).

These data indicate that the binding motif of Fc rNRP-1 in heparin is more complex than one described by a simply linear sequence of sulfated sugar residues. This is in agreement with the general knowledge that interactions of proteins with polysaccharides are driven by various mechanisms including ionic forces, nonionic forces, hydrophobic interactions, hydrogen bonding and van der Waals packing [148]. In support of this contention, persulfated heparin was the strongest competitor, but completely desulfated heparin was a stronger competitor than the singly desulfated polysaccharides. Thus, it would seem that although ionic interactions are important, there are other interactions, which allow a sugar structure to bind to Fc rNRP-1 quite effectively. Moreover, persulfation places sulfate groups at the C3 position of glucosamine and it may be that this is an important requirement for Fc rNRP-1 binding. This is intriguing, since heparin-like structures are rare in most cellular HS, whereas lower sulfated structures are relatively common [149].

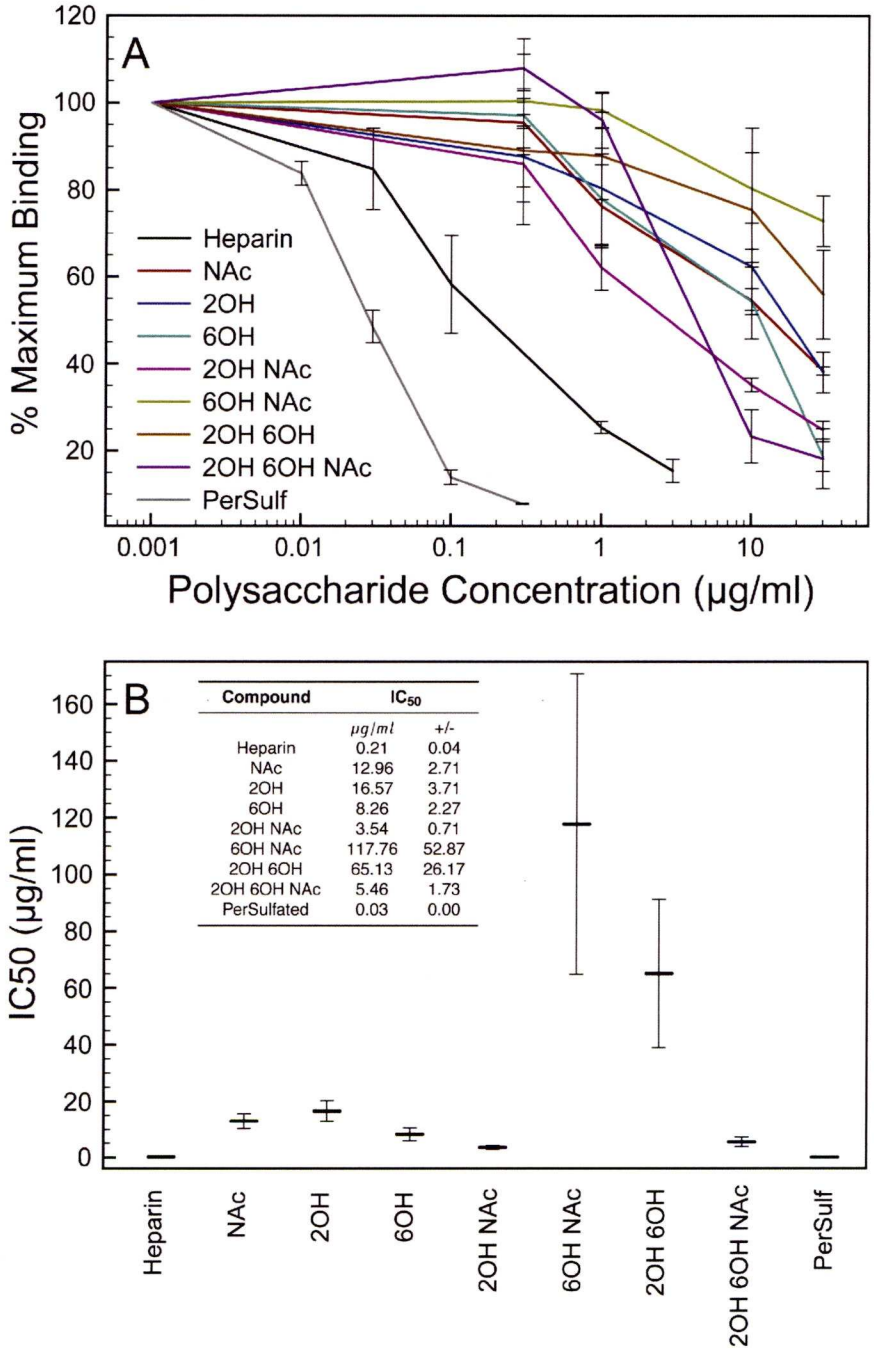

Compound	IC_{50}	
	µg/ml	+/-
Heparin	0.21	0.04
NAc	12.96	2.71
2OH	16.57	3.71
6OH	8.26	2.27
2OH NAc	3.54	0.71
6OH NAc	117.76	52.87
2OH 6OH	65.13	26.17
2OH 6OH NAc	5.46	1.73
PerSulfated	0.03	0.00

Figure 4.8: Competition experiments defining heparin sulfation pattern requirements that enable Fc rNRP-1 binding.

Inhibiting ability of modified heparin derivatives on Fc rNRP-1 binding to the heparin derivatised surface was tested as described in the Section 2.3.2. A) The relative binding values at presence of each concentration of added inhibiting ligand (x axis) were adjusted to 100 % of Fc rNRP-1 binding alone to heparin (measured at least between 10-40 arc s). The experiment was performed three times independently (mean±SD). B) IC_{50} values were calculated basing on the non-linear curve fit of single representatives of respective binding curves and are expressed in [µg/ml] (±SE) for the inhibiting compounds tested in panel A.

The last investigation of binding preferences of Fc rNRP-1 aimed to resolve if the protein distinguishes between different cationic forms of native heparin. For this purpose, the test assayed heparin was saturated with Na^+, K^+, Ca^{2+} and Cu^{2+} to form species found *in vivo* [150]. From the two main models of ion binding the tested heparins, Na^+, K^+ and Ca^{2+} forms, appear to have delocalised counterion mechanism of ion binding, and only for Cu^{2+} form, it was possible to show a site-specific mechanism of interaction [151], however, it cannot be excluded for other ion derivatives. All these complexes have distinct structural properties [145], and were shown to specifically regulate properties of interacting proteins [152, 153]. For Fc rNRP-1 all tested compounds had similar inhibiting property, therefore, they are unlikely to be distinguished by Fc rNRP-1 (Figure 4.9).

The optical biosensor study of Fc rNRP-1's interaction with heparin produced a picture of a protein that has high affinity to heparin and, though it is prone to bind to the sulfated sections of HS, it clearly can also bind to the non-sulfated regions. *In vivo* regions of low sulfation may, therefore play an important role in regulating the function of NRP-1. The issue of how NRP-1 could bind to such distinct structures remains to be established, and requires thorough structural characterisation. The minimal size of oligosaccharide required for Fc rNRP-1 binding to heparin is clearly not yet defined, however, being a complex molecule, it is plausible that the interaction with heparin involves more than one binding site, and possibly, is also affected by the presence of the IgG1 Fc parts. No detectable difference between any of the cationic forms of heparin implies no biophysical importance of their binding to NRP-1. However, in the latter case and similarly in the variously sulfated species, since these polysaccharides are known to possess very distinct structures, it is possible, that the mechanism of their binding to NRP-1 is distinct and the consequent secondary effects on NRP-1 conformation may be important for the further complex formation and signalling outcome. Additionally, the complex formation between NRP-1 and distinct heparin-derived structures may be a selective factor for assembly of other signalling complex components only on the basis of the sugar moiety preference.

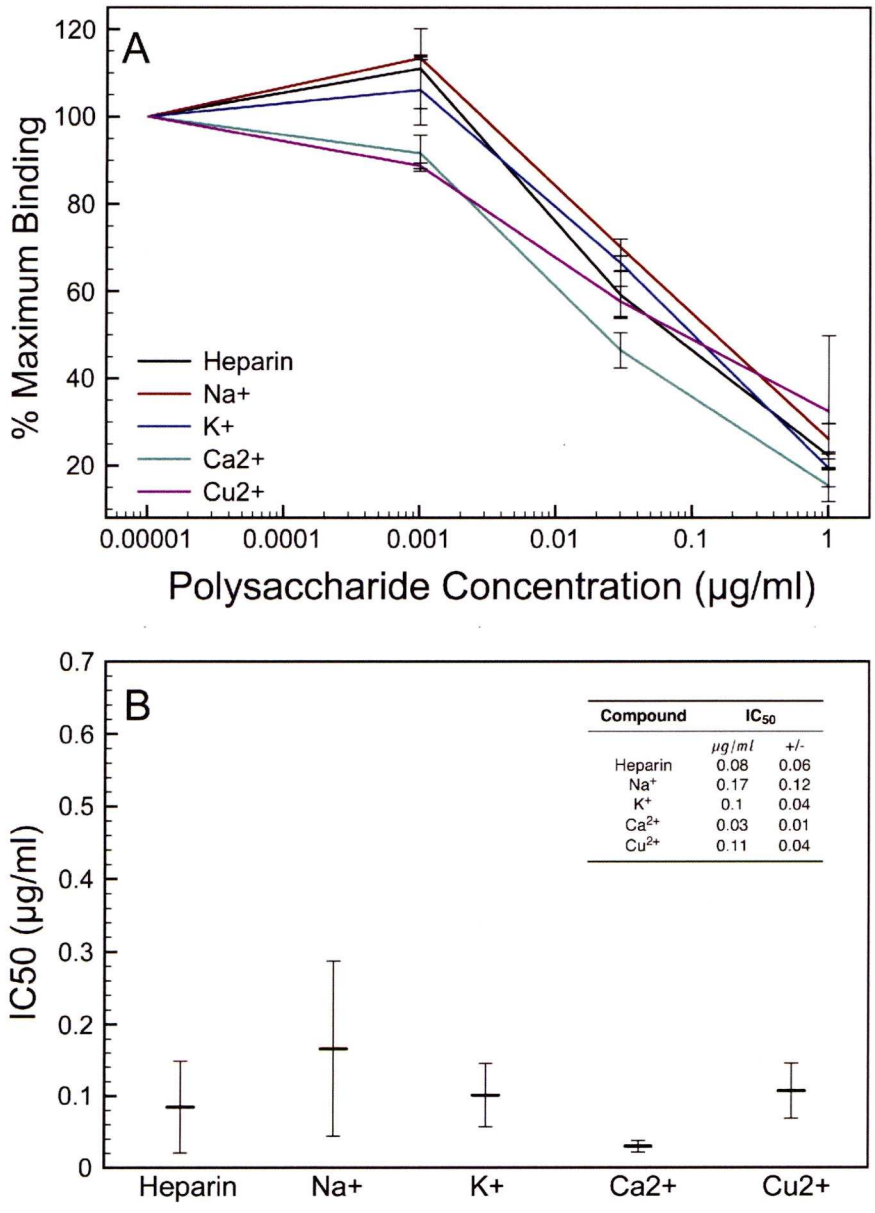

Figure 4.9: Competition experiments defining heparin cationic forms requirements that enable Fc rNRP-1 binding.

Inhibiting ability of cationic forms of heparin on Fc rNRP-1 binding to the heparin derivatised surface was tested as described in the Section 2.3.2. A) The relative binding values at presence of each concentration of added inhibiting ligand (x axis) were adjusted to 100 % of Fc rNRP-1 binding alone to heparin (measured at least between 10-40 arc s). The experiment was performed three times independently (mean±SD). B) IC_{50} values were calculated basing on the non-linear curve fit of single representatives of respective binding curves and are expressed in [µg/ml] (±SE) for the inhibiting compounds tested in panel A.

4.4 Identification of the protected/ buried regions of Fc rNRP-1 upon interaction with heparin

After the analysis of the structural features of heparin-derived polysaccharides required for strongest NRP-1 binding, the analysis of the regions of Fc rNRP-1 that mediate this interaction was undertaken. The Protect and Label (P&L) strategy [95] was designed to identify regions of a protein that contain lysines that remain protected by heparin against chemical modification. To distinguish lysines that are involved in heparin binding from those that are not, a two-step procedure was developed. Firstly, as a protein is bound to heparin, the exposed lysines are acetylated (the Protection step), secondly, after elution of the protein from the heparin resin any remaining lysines that were protected by heparin are biotinylated. Subsequently, the protein is digested by chymotrypsin and biotinylated peptides are purified and then identified using MALDI-Q-TOF. This strategy has been applied successfully to identify heparin-binding sites in small proteins, such as FGF-2, platelet factor 4 (PF-4) and pleiotrophin (PTN) [95]. Here it was used for the first time to study a multidomain protein, Fc rNRP-1.

The initial verification of the suitability of the method to study recombinant NRP-1 revealed that acetylation of Fc rNRP-1 bound to heparin resulted in its release when the experiment was conducted in PBS (data not shown). This suggested a dynamic interaction between NRP-1 and heparin, whereby the protein might "rock" on its polysaccharide-binding site. In the presence of NHS acetate, the acetylating agent, as lysines involved in heparin binding dissociatiated they would become acetylated and consequently not be able to re-bind. The result would be that the protein's interaction with heparin is lost. To overcome such dynamics, less stringent conditions of binding were used, in which there was no NaCl in the acetylation step. Under such conditions a substantial amount of the Fc rNRP-1 was retained on heparin during the acetylation step, which allowed the subsequent generation of peptides for further analysis (Figure 4.10).

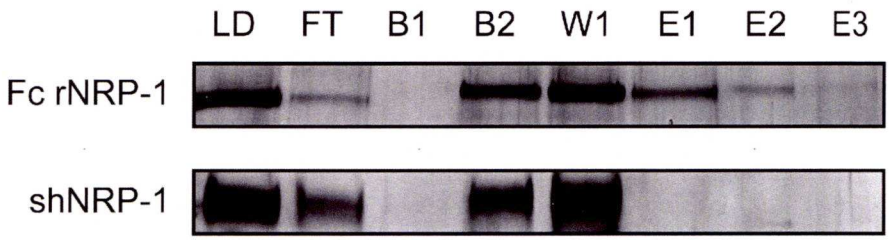

Figure 4.10: Analysis of protein in the course of the P&L procedure.

Top and bottom panels present samples for Fc rNRP-1 and shNRP-1, respectively. Lane (LD) corresponds to the sample applied to the heparin column, lane (FT) is the flow through or unbound material after applying the sample three times to the column, lanes (B1 and B2) are the two acetylation steps, lane (W1) is the post acetylation wash of the column, elution (E1) is the material eluted from the column with 2M NaCl, lane (E2) is the same material after biotinylation (E2), and (E3) is the biotinylated material after concentration and buffer exchange. Five % (v/v) of the total material, when 4 μg of the proteins was used, was analysed on SDS-PAGE and silver stained.

Importantly, the same conditions when applied to shNRP-1 did not prevent it from eluting from heparin, indicating that the interactions of Fc rNRP-1 are likely to be due to its specific high affinity binding site, despite the reduced ionic strength of the buffer used in the acetylation step (Figure 4.10).

The experiment was performed with 25 μg of Fc rNRP-1 and the analysis returned 16 peptides that were assigned to the particular sequences (Table 4.2). Five peptides were not matched to any region of the recombinant NRP-1, which might be due to modifications occuring during the experiment, which were not accounted for. All identified peptides encompassed one biotinylated lysine residue, and corresponded to the NRP-1 moiety of the fusion protein or, the IgG1 Fc moiety (Table 4.2). The peptides identified within NRP-1 moiety were mapped to the a1, b1, c domains and to the linker following the c domain (L2) (Table 4.2). Within the a1 domain two sequences were identified basing on three independent ions, whereas within the b1 domain one largely overlapping sequence was identified basing on two independent ions. Within the c domain three sequences were identified basing on one ion each, while the fragment within the L2 region was identified by two independent ions (Table 4.2). In the IgG1 Fc part of the recombinant protein four sequences were identified, where two of them based on two independent ions, two remaining on one ion each. The list of peaks with assigned values is enclosed as **Supplemental data 3**.

The interpretation of the obtained result only partially confirmed the previously identified heparin-binding region of NRP-1, which was ascribed to the b1 and b2 domains (Figure 4.11, Figure 4.12) and was functionally confirmed to be sufficient to bind to heparin [29]. Moreover, the identification of regions within the IgG1 Fc part of the recombinant protein was particularly surprising as in optical biosensor experiments the IgG1 Fc did not interact with heparin or heparin-derived oligosaccharides (Figure 4.3A, Figure 4.18A). Nevertheless, there are several reasons to suggest the presented results are of significance.

Peptide	Mass experimental	Mass calculated	Error (ppm)	Sequence	Residues	Domain
1	1800.96	1800.91	**25.8**	VRI**K**(Biotin)PASWETGISM	404-417	b1
2	1494.76	1494.6464	**76**	AGAFR(Acetyl)SD**K**(Biotin)C(Carbamidomethyl)GGT	19-30	a1
3	1926.02	1926.0953	**-39.1**	D**K**(Biotin)NISRKPGNVLKTL(Ammonium)	822-836	L2
4	2024.1	2024.0481	**25.6**	TLPPSRDELT**K**(Biotin)NQVSL	978-993	IgG1 Fc
5	2125.14	2125.0059	**63.1**	VVVDVSHEDPEV**K**(Biotin)FNW	890-905	IgG1 Fc
6	1452.74	1452.6358	**71.7**	AGAFRSD**K**(Biotin)C(Carbamidomethyl)GGT	19-30	a1
7	1790.92	1790.8643	**31.1**	TVD**K**(Biotin)SRWQQGNVF	1039-1051	IgG1 Fc
8	1381.71	1381.6603	**36**	NG**K**(Biotin)EYKCKVS	943-951	IgG1 Fc
9	1516.72	1516.7464	**-17.4**	QVIFEGEIG**K**(Biotin)GN	778-789	c
10	1811.92	1811.9069	**12.8**	SQADENQ**K**(Biotin)GK(Acetyl)VARL	695-708	c
11	2074.06	2074.0109	**23.7**	MVVGHQGDHW**K**(Biotin)EGRVL	754-769	c
12	1182.65	1182.6452	**4.05**	VRI**K**(Biotin)PASW	404-411	b1
13	1909	1909.0688	**-36**	D**K**(Biotin)NISRKPGNVLKTL	822-836	L2
14	1628.7	1628.6621	**23.3**	HSYHPSE**K**(Biotin)CEW	46-56	a1
15	2107.12	2106.9953	**59.2**	VVVDVSHEDPEV**K**(Biotin)FNW -H2O	890-905	IgG1 Fc
16	1364.69	1364.6337	**41.3**	NG**K**(Biotin)EYKCKVS -NH3	943-951	IgG1 Fc

Table 4.2: List of peptides identified in the P&L experiment of the Fc rNRP-1 binding to heparin.

The complete list of ions identified by MALDI-Q-TOF mass spectrometer is presented according to the descending intensity of the ions. The ions are presented according to their observed and theoretical masses with appropriate error values (expressed in ppm) and directly linked to the recognised sequences and their respective location within the Fc rNRP-1. The biotinylated lysines are indicated in bold. Assigned spectra are available in the **Supplemental data 3**.

First of all, the main structural study deciphering the residues involved in heparin interaction was based only on the b1b2 domain construct [67], it could not predict other areas of interaction. At the same time the lower affinity binding sites could have been neglected, while the importance of the given regions overestimated. Overall, the simplified model of the NRP-1 interaction with heparin describes specifically the heparin interaction with the b1b2 domains, but not the whole protein losing the context of the additional domains present in NRP-1. Additionally, in this study, the analysed protein is a radically different construct, not only comprising of the rat sequence, but also present in a form of a dimer of unknown overall conformation and very specific properties. Indeed, it is very probable that these specific properties might result from the proximity of the two NRP-1 moieties and novel emerging interactions.

In order to visualise the identified peptides on a 3-D structural model a search for the most complete available structure was made. Unfortunately, the best available structures of NRP protein cover only a1a2b1b2 domains of NRP-2 [1]. This part of the protein is followed by long fragments of unstructured elements, namely L1 and L2 linkers, and to date no data are available on their possible conformation, as such regions are problematic for obtaining structural data. Similarly, due to the substantial size of these elements no *in silico* approach is capable of making a prediction of their conformation. Therefore, in order to visualise the identified peptides, the most complete structure of the NRP protein was selected, 2QQL [1], covering the a1a2b1b2 domains of the human NRP-2, however lacking the subsequent c domain. Given the limited resemblance of the human NRP-2 and rat NRP-1 (53 % identity and 72 % similarity within the overlapping region), in order to identify the residues corresponding in the structure, an alignment of the human NRP-2 and rat NRP-1 was made, and appropriate residues were highlighted within the structure (Figure 4.11). Importantly, the visualised residues should be considered of approximate localisation as the sequences within 2QQL that were aligned to the identified peptide sequences from rat NRP-1 do not present significant similarity, and none of the biotinylated lysines of rat NRP-1 has an analogous lysine in human NRP-2.

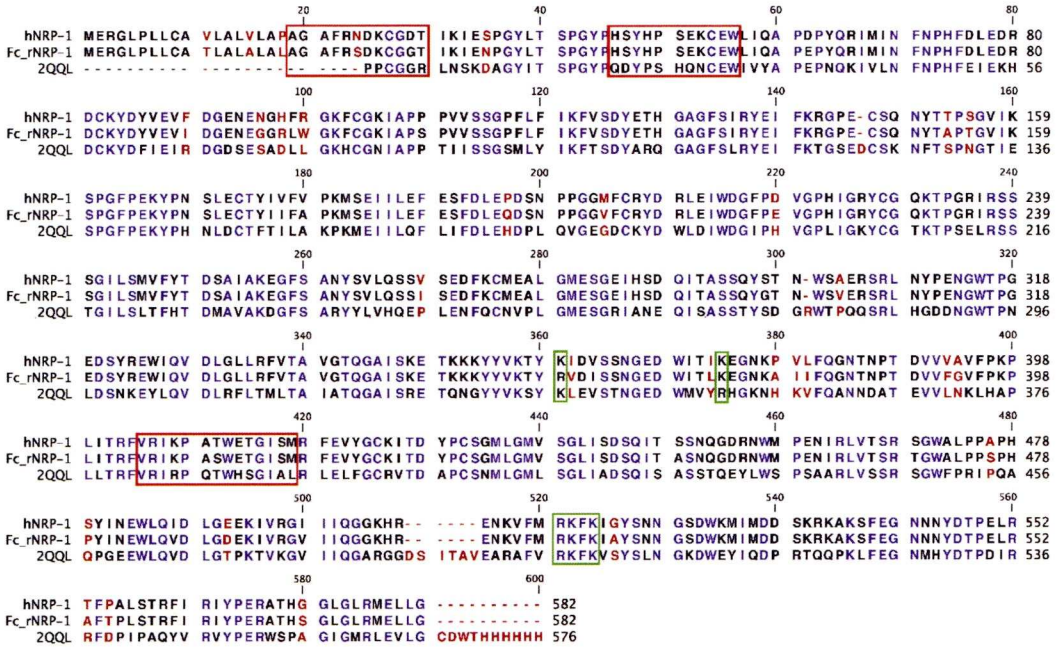

Figure 4.11: Clustal W alignment of the NRP sequences.

Clustal W alignment of the human NRP-2-derived sequence present in the QQL structure file and analogous rat NRP-1 and human NRP-1 sequences. The residues are coloured according to their level of conservation, where the rank of conservation is marked red<black<blue. The three identified peptides covered by the structure are indicated in red squares. The green squares mark the positive residues previously identified to bind to heparin [67] together with their respective residues in NRP-2.

Contrastingly, it is noteworthy that the same lysines identified by the protect and label method are fully conserved in the rat and human NRP-1 sequences (Figure 4.11).

Only five of the peptides identified in the Protect and Label experiment could be mapped on the available structure, and are indicated by 3 regions highlighted in blue. Three of them mapped to the a1 domain, while other two were found to be in close proximity of the heparin-binding site in the b2 domain identified in other experiments, which is shown in magenta [67] (Figure 4.12). Interestingly, as NRPs are supposed to form dimers, it is noteworthy that the saddle-shaped interface between the two molecules is of approximately 60-70 Å width, which could allow for flexible interactions with a chain of HS. It is especially important, if compared with the size of heparin, which is estimated around 52 Å in length for dp 12, and thus, shows, that substantial fragments of the polysaccharide can be accommodated in the crevice. As the larger fragment of HS might bear more varied modifications, this can impact the overall structure and flexibility of the molecule [154], and consequently, complex formation with NRP-1.

The structures presented here are of the dimer of NRP-2 observed upon crystallisation. In this model the magenta heparin-binding residues form a channel between molecules where heparin could be bound. Indeed, two of the peptides locate close to this area, and this would support a broader size of the binding site. Interestingly, the identification of the peptides deriving from the a1 domain coincides with the observation that exactly this part of the NRP-1 might be involved in mediating dimerisation [1]. Nevertheless, detection of the a1-driven interaction of the independent NRP-1 molecules was not confirmed by several other methods, except crystallography, and thus remains a hypothesis requiring further investigation [1]. Additionally, the identified a1-domain peptides are not located in the exact interface region between the molecules. Still, it is possible that the a1 domains of NRP-1 mediate dimerisation in a different manner than the presented a1 domains of NRP-2.

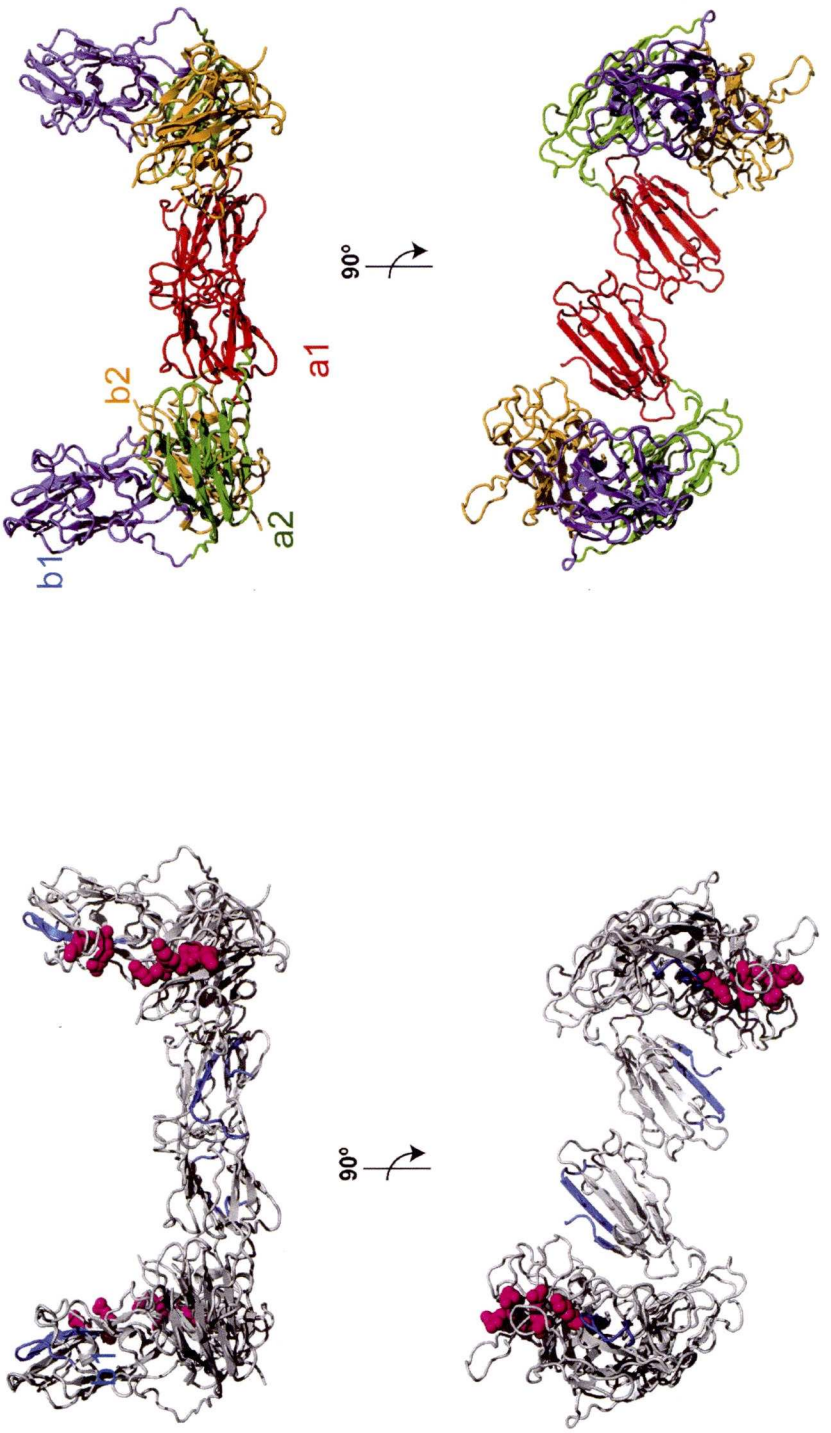

Figure 4.12: Approximate localisation of the identified rat NRP-1 peptides on the human NRP-2 crystal structure (2QQL) presented in the proposed dimeric form [1].

Illustration of the 2QQL structures in light grey, where two different perspectives of the NRP-2 dimer are shown. The three peptides identified in P&L strategy are shown in cyan. The literature-derived residues responsible for heparin interaction are labelled in magenta, where lysines and arginines are depicted in spherical mode. On the right, analogous presentation of the 2QQL structures, where each domain of NRP-2 is labelled with a different color: a2 is red, a2 is green, b1 is blue, b2 is orange.

Unfortunately, the remaining five peptides were not covered by the 2QQL structure, since they were localised in the c domain and L2 linker following the c domain. In an attempt to visualise at least some of those, a *homology modelling* approach was applied to obtain a structure of the c domain alone. The structure was modelled according to the commonly accepted steps described in the Section 2.6.2, such as identification of the best structural templates, alignment optimisation, building of an initial model, optimisation of the initial model and validation of the model according to its biophysical properties. After selection of the best model, it served to visualise the three peptides identified in P&L experiment within the c domain (Figure 4.13). Although, it is difficult to interpret this picture in the context of the remaining majority of the NRP-1 structure, still, it is apparent that the identified peptides are located on one interface of the protein and show a consistent pattern of location with clearly electropositive charge, which could be a sign of an interaction site with a negatively charged polysaccharide. This supports the hypothesis, that the identification of the peptides outside of the b1b2 region leads either to the possibility of other secondary heparin-binding sites or long-range intramolecular conformational changes occurring upon heparin binding.

An additional visualisation of the result of the P&L experiment was presented on an extended model of the NRP-1 obtained in *homolgy modelling*. Although, contrary to the QQL structure, it shows the human sequence of NRP-1, not NRP-2, and additionally, it covers the L1 linker and the c domain, it is important to note, that the unstructured L1 linker region and substantial loop region of the c domain are not possible to model, and their assignment in the model is randomised by the software. Consequently, it is not known how the c domain in reality aligns against the remaining domains. Nonetheless, this presentation provides an insight into the general distribution of the identified peptides within the structure (Figure 4.14).

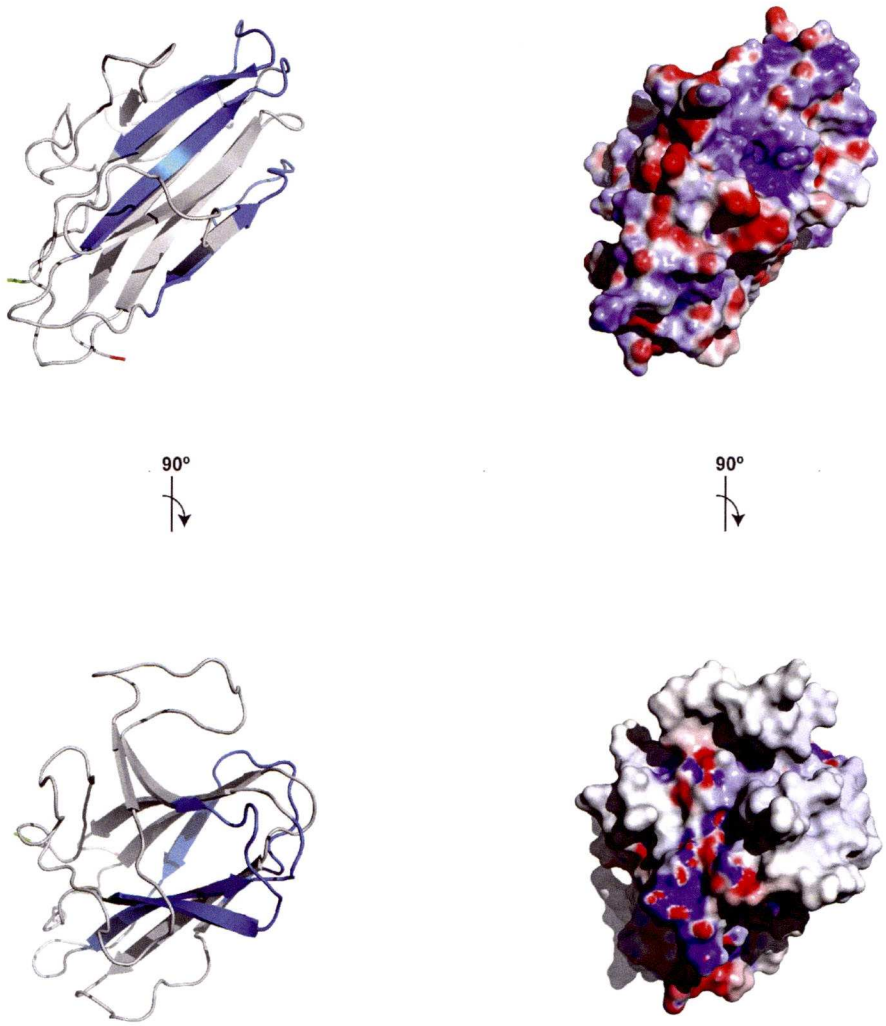

Figure 4.13: Localisation of the identified rat NRP-1 peptides in the human c domain obtained by *in silico* modelling.

Illustration of the c domain in light grey, where two different perspectives of the c domain are shown. The three identified in P&L strategy peptides are shown in cyan. On the right, analogous visualisation of the c domain coloured according to its potential is presented (blue is electropositive, red is electronegative potential).

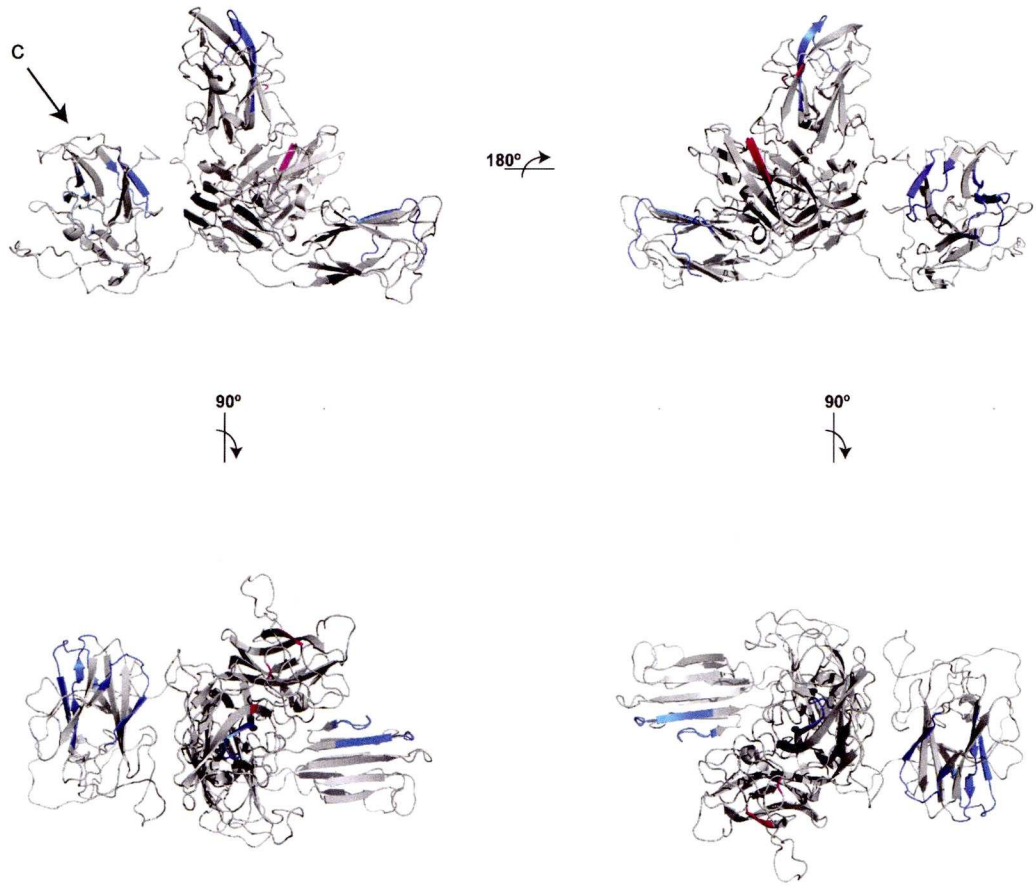

Figure 4.14: Approximate localisation of the identified rat NRP-1 peptides in the human NRP-1 obtained by *in silico* modelling.

Illustration of the NRP-1 in light grey, where four different perspectives of the NRP-1 monomer were shown. The identified peptides within a1, a2, b1, b2 and c domains are shown in cyan. The literature-derived residues responsible for heparin interaction are labelled in magenta. The c domain is indicated by an arrow.

Surprisingly, six identified peptides were mapped to the IgG1 Fc part of the recombinant fusion construct. Fc was confirmed to not bind to heparin on its own in PBS (Figure 4.3A, Figure 4.18A). Therefore, this result may either be the consequence of Fc binding heparin at low ionic strength or raises the possibility that this may occur because of its presence as a fusion partner of NRP-1. If the latter explanation was correct, the identification of the protected areas would imply possible intramolecular/ intermolecular interactions occurring upon heparin binding to the NRP-1 moiety, which may play part in stabilising of the Fc rNRP-1-heparin interaction particularly in the absence of electrolytes.

To summarise, the regions within the recombinant NRP-1 that were protected against chemical modification in the presence of heparin were mapped to the a1, b1, c domains and L2 linker of the protein, and following IgG1 Fc part. The approach allowed confirmation of the region adjacent to the heparin-binding site currently identified in the protein, however, it did not detect the binding site itself, although it does contain several lysines. It also indicated the importance of the a1 and the c domains. This result might imply other previously not described secondary heparin-binding regions, the appearance of the novel binding sites within the dimeric form of the NRP-1 or a major rearrangement within the molecule after heparin binding resulting in the protecion of lysine residues. The first hypothesis, proposing multiple heparin-binding site is supported by several examples of other molecules, such as endostatin, FGF-2, RANTES [155–157], and, considering the size of NRP-1, might be a probable interpretation of the result. Nevertheless, a set of mutagenesis experiments reinforced by more structural data could verify such an interpretation. Also the second mechanism, suggesting the crucial role of protein-protein interactions in the final definition of the heparin-binding site has been observed [158]. Namely, the complex formation between FGF and FGFR affected the mechanism of interaction with HS as compared with FGF and FGFR interacting with HS individually, and although, in this case it mainly caused a shift of hydrogen bonds, it still opens up a discussion on the impact of the dimeric fusion, proximity of the two NRP-1 moieties, and possible intramolecular interactions on final heparin interacting site.

Finally, it is possible that the lack of NaCl in the acetylation step, when exposed lysines were supposed to be labelled, was not fully efficient, and some protein parts in such conditions could be more prone to interact or have similar to aggregation behaviour. This could lead to fake positive results in identification of the heparin-binding regions and cannot be excluded.

4.5 Further verification of shNRP-1 binding to heparin

Although both tested NRP-1 proteins possess key structural regions that have been associated previously with heparin binding, the characterisation of this interaction was achievable exclusively for Fc rNRP-1, as shNRP-1 not only did not bind to the heparin surface, but also did not sequester heparin in the BaF3 experiment (Figure 4.3). Additional experiments were performed to explore in more depth the issue of shNRP-1 binding to heparin. First of all, affinity chromatography was applied on an analytical scale. The experiment employed two different heparin affinity resins, which were packed into minicolumns, and used for binding tests of the two recombinant NRP-1 proteins. The comparison of the fraction bound after triple application on the minicolumn revealed that both proteins bound to the two resins (Figure 4.15). In order to exclude the possibility that the observed binding was due to nonspecific interaction with the matrix alone, an attempt to develop a resin with reduced heparin content was undertaken. To do so, an overnight digest of both resins in appropriate buffer conditions with a mix of heparinases was done, and afterwards, the resins were used in a binding test as previously. The analysis showed noticeable reduction of shNRP-1 and Fc rNRP-1 binding to the resin, which was especially observed for the Toyopearl resin, as compared with the untreated resins (Figure 4.15A). However, as the scope for success of the digest was not technically feasible to establish, the result of the binding test should be considered with a degree of caution. Nevertheless, this opens up the possibility that shNRP-1 does indeed interact with heparin, however, in order to do so, it may require specific favouring conditions, as appropriate molecule density, which can be achieved within the void volume of the minicolumn and could facilitate behaviour similar to the dimer, resulting in shNRP-1 mimicking Fc rNRP-1.

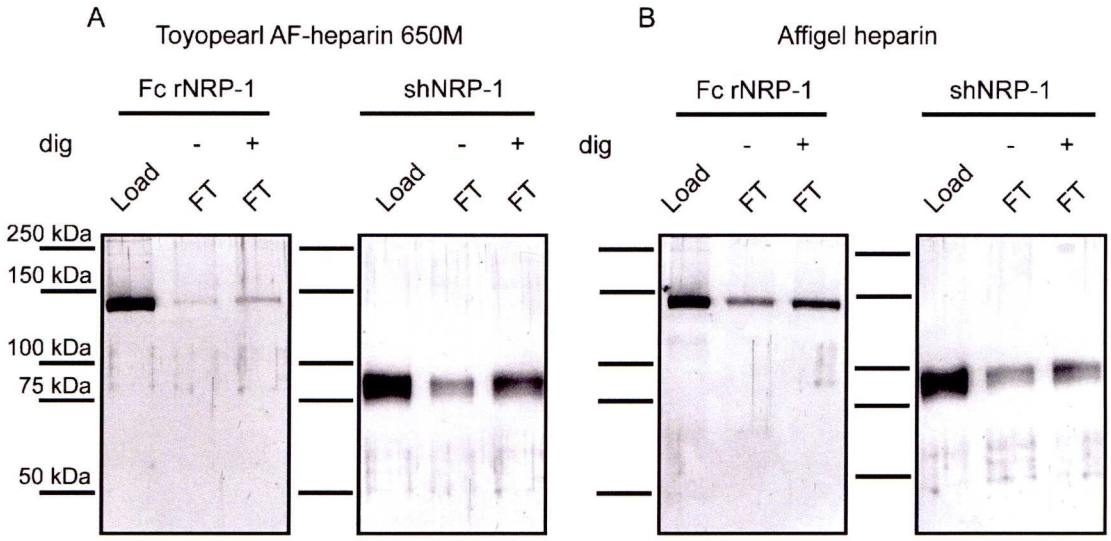

Figure 4.15: Comparison of Fc rNRP-1 and shNRP-1 binding to two different heparin affinity resins before and after heparinases digest of the resins.

A) Binding of both recombinant NRP-1 proteins to Toyopearl heparin resin. B) Binding of both recombinant NRP-1 proteins to Affigel heparin. The experiment was performed as described in the Section 2.2.4. Load and flowthrough (FT) samples are indicated together with the presence or absence of heparinases digest of the resin and the marker sizes.

Such an explanation, although alluring, falls outside the boundaries of the experimental expertise and remains solely a concept.

Nevertheless, as shNRP-1 was confirmed to bind to the heparin resin, the attempt to further characterise this interaction was undertaken by P&L strategy (Figure 4.10 bottom panel). Unfortunately, shNRP-1 after the acetylation step appeared to have lost its heparin-binding property, and consequently was eluted from the column at the washing step, thus, returning no peptides in elution for further analysis. This supported the argument of the weaker interaction of the shNRP-1 with heparin, whereby continuous rounds of association and dissociation during the protection step would result in the acetylation of all lysines, including those in the heparin-binding site. This idea is consistent with the published data on possible effects of chemical modification of lysines in some proteins, to name structural rearrangement [159], loss of stability [160] or loss of binding properties [161], as observed in this study. Therefore, more precise characterisation of shNRP-1 binding to heparin was not accomplished.

Having shown that in certain circumstances shNRP-1, contrary to the initial observations, appears to interact with heparin, one more experiment, this time exploiting the thermostabilising property of the protein as a consequence of its interaction with ligand was designed. The method had the advantage of testing protein and ligand *in solution*, whereas the previously described experimental systems, excluding the BaF3 assay, employed immobilised heparin (Figure 4.3A, Figure 4.18A). To establish comparable conditions for the analysis of recombinant NRP-1s, it was assumed that each NRP-1 moiety had the potential to bind to heparin, therefore, whereas shNRP-1 was assayed with heparin at 1: 1 and 1: 10 concentration ratios, Fc rNRP-1 was assayed at 1: 2 and 1: 20.

As in the affinity chromatography experiment, both isoforms displayed higher T_m values when analysed in the presence of heparin, which supported the capability of shNRP-1 to bind to heparin (Figure 4.16A,B). In order to clarify that the heparin effect was not an nonspecific effect, the Fc part alone was confirmed to not interact with heparin, and tested in the presence and absence of heparin (Figure 4.16C,D).

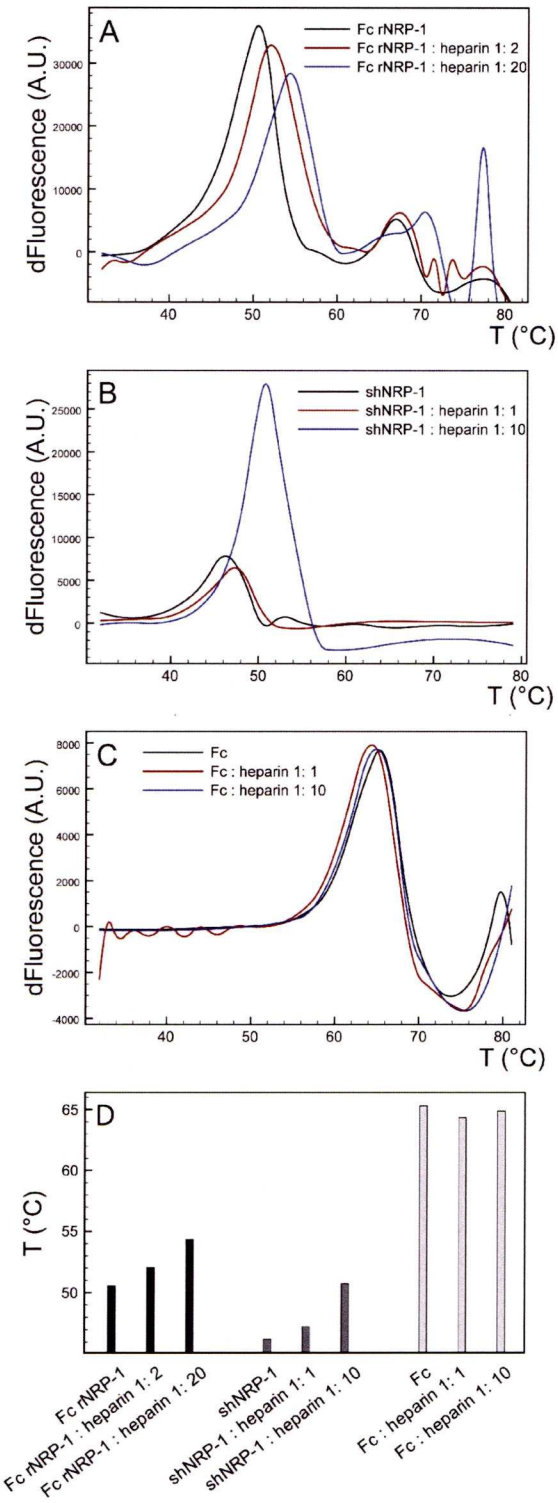

Figure 4.16: Sypro stability assay of recombinant NRP-1s in the presence and absence of heparin.

A) Fc rNRP-1, B) shNRP-1 and C) Fc region were subjected to denaturation cycle alone or with indicated amount of heparin in the presence of Sypro® Orange dye. The melting curves were recorded by RT-PCR machine and analysed as described in the Section 2.2.6. The first derivatives of the melting curves were plotted. D) Presentation of the melting temperature (T_m) values equal to the maxima of the derivatives from the panels A, B, C.

4.6 Investigation of relationship between monomeric/ dimeric state of NRP-1 and heparin-binding ability

Although in the latter experiments shNRP-1 was demonstrated to bind to heparin, the contrastingly different properties of the two NRP-1 proteins in the surface binding study (Figure 4.3) raised the questions whether the dimeric form of Fc rNRP-1 could give a rise to a monomeric NRP-1, and what would be the properties of such a protein. According to the disorder analysis of the NRP-1 sequence (Figure 4.1), there were several dynamic parts of the protein that could be accessible for a proteolytic digest, therefore, a trypsin digest of the native Fc rNRP-1 was performed to determine if truncated isoforms with a structure close to that of shNRP-1 could be produced. Manipulation of the conditions of the digest, such as NaCl concentration, temperature, time (referred to as digest A in the Section 2.2.7), permitted the production of a derivative of Fc rNRP-1 of exactly same migration pattern as shNRP1 on SDS-PAGE (Figure 4.17A), thus of comparative size. The newly produced isoform, from now referred to as trNRP-1, was recognised by N-terminus targeted antibody (Figure 4.17B), but not by anti-His antibodies targeted to the C-terminal His-tag (Figure 4.17A). This indicated that the cleavage occurred in the C-terminal part of the protein (Figure 4.22). Interestingly, in contrast to Fc rNRP-1, shNRP-1 resisted trypsin digest in the native conditions, as concluded from the retained size and the presence of the C-terminal His-tag (Figure 4.17C). Hence, it is reasonable to suggest that the trNRP-1 was indeed analogous to shNRP-1.

A polysaccharide surface-binding test of trNRP-1 was performed using a dual polarisation interferometer and a dp 16 surface (Figure 4.18A, E). Contrary to the previously applied optical biosensor, this method allows calculation of the mass, thickness and density of the bound protein layer, which provides far greater insight into the formed complexes. Alongside the analysis of trNRP-1, Fc rNRP-1, shNRP-1 and Fc were tested as characterised reference samples. The control proteins reproduced the formerly observed binding pattern. The Fc rNRP-1 showed substantial binding to dp 16.

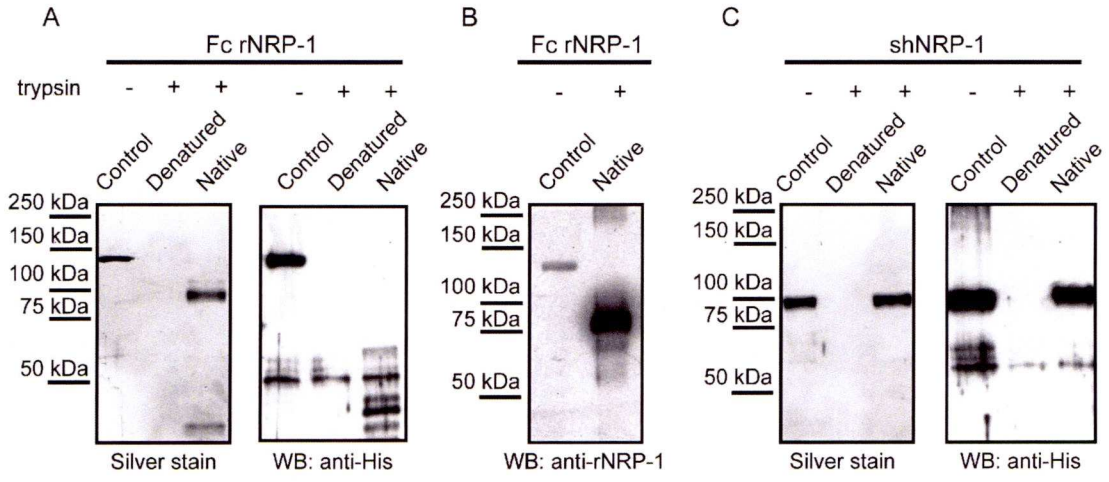

Figure 4.17: Tryptic digests of recombinant NRP-1s.

A) Tryptic digest of Fc rNRP-1 was performed either with native or denatured protein. Left panel presents result of silver staining, right panel presents western blot against the C-terminal His-tag of the protein. B) Western blot result obtained with anti-N-terminal rat NRP-1 sequence of reference Fc rNRP-1 and the native digest sample. C) Tryptic digest of shNRP-1 was performed either with native or denatured protein. Left panel presents result of silver staining, right panel presents western blot against the C-terminal His-tag of the protein. The digest was repeated three times producing the same result.

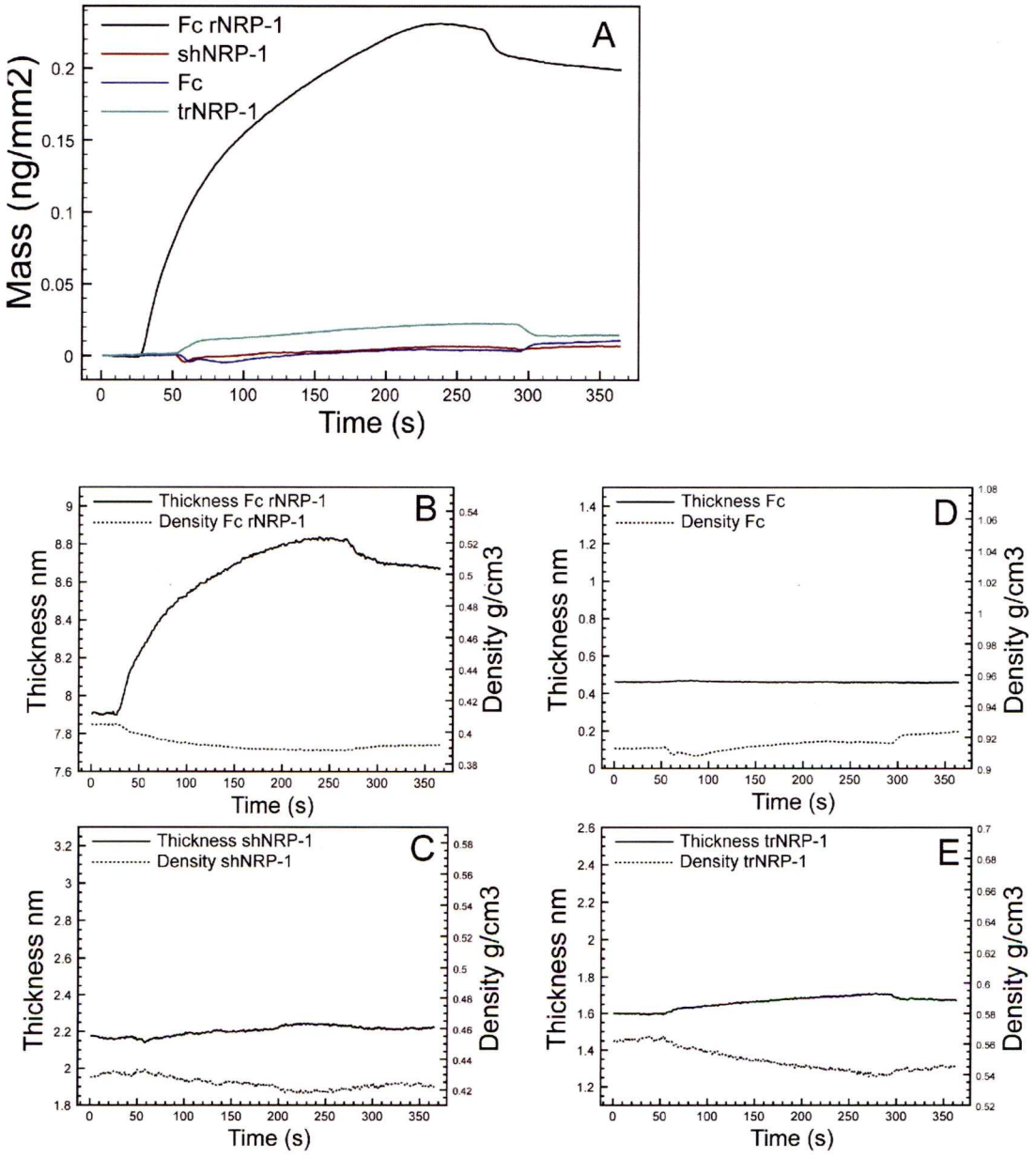

Figure 4.18: Dual polarisation interferometry analysis of binding of recombinant NRP-1 isoforms to dp 16.

Presented results are a representative of a set of three independent experiments described in the Section 2.3.4. A) Comparison of mass effect of binding of Fc rNRP-1, shNRP-1, reference Fc, and trNRP-1 expressed in [ng/ mm^2] in a function of time. B-E) Thickness and density measurements of binding of each protein in a function of time. B) Fc rNRP-1. C) shNRP-1. D) Fc. E) trNRP-1. The y1 axis is thickness [nm], the y2 axis is density [g/ cm^3].

In contrast, the trNRP-1 was observed to behave in exactly same manner as shNRP-1, it failed to bind at detectable levels to dp 16. This indicates that the high affinity of Fc rNRP-1 for heparin is likely to reflect its dimeric form, and/ or the presence of the c domain and associated linkers as these features are absent from the monomeric NRP-1 proteins, and may mediate dimerisation in an independent manner.

Unfortunately, the full benefit of the instrument, namely the measurement of the thickness and density of the layer of the bound protein, mainly Fc rNRP-1, could not be obtained, since the amount of the protein bound to the surface was too far below saturation to extract these data.

4.7 Investigation of importance of the c domain of NRP-1 and heparin-binding ability

The work described above showed that a truncated variant of Fc rNRP-1, which migrated around the size of shNRP-1, lost its heparin-binding affinity in surface-based assays. One interpretation of these data is that the dimeric state of Fc rNRP-1 was the main driver of the protein-heparin interaction. However, whereas in Fc rNRP-1 it is the IgG1 part that is responsible for the dimerisation, in native conditions, NRP-1 has its own dimerisation domain, the c domain [25, 34], which is also present in Fc rNRP-1.

Therefore, as the previous sections (Chapter 4.4, Chapter 4.6) indicated the possible importance of the c domain of NRP-1 in mediating its binding properties, its structure obtained in *homolgy modelling* was subjected to further *in silico* analysis to answer if bioinformatics can provide more data on its properties. The analysis aimed to define possible sites of protein-protein interactions, which could be responsible for either the c domain dimerisation or other heterogenous interactions. In order to do so, three different interaction interface prediction servers were employed. PPI-Pred analyses surface patches by assessing their hydrophobicity, electrostatic potential, solvent accessible surface area and surface topography to indicate

most probable interaction areas. meta-PPISP combines three independent servers, where cons-PPISP is analysing the sequence profiles and solvent accessibility of each residue on the protein surface in neural network mode, PINUP is focused on energy and structural constrains of each residue, and ProMate is calculating geometrical properties of the surface residues that could imply involvement in interaction. WHISCY uses a different approach to analyse protein structures, which is based on the sequence alignment and identification of highly conserved hydrophobic patches on the surface. The combined results of the analysis performed by these servers, intriguingly identified a region within the c domain that overlapped with the area previously identified in the P&L experiment (Table 4.2, Figure 4.19). This opened a possibility that the short sequence WKEGRVL could be involved in a protein-protein interaction specifically in homodimerisation, since the same region was protected within the Fc rNRP-1.

Therefore, subsequently, an attempt to dock two c domains via the identified region was made to illustrate a possible mechanism of the dimerisation. HADDOCK server, that predicts possible conformations of two interacting molecules requires a list of indicated active and passive residues involved in the interaction. For the purpose of this analysis the active residues chosen as an input for HADDOCK were of the peptide identified in P&L experiment comprising the WKEGRVL sequence and the passive residues were set for the automatic choice of the server. The best obtained structure according to the HADDOCK evaluation presented both c domains adjacent to each other via the indicated region and, interestingly, forming a consistent interface by the remaining P&L peptides. Thus, this analysis provided a hypothetical structure of the dimerised c domains, and putatively, it presented a consistent protein surface interface that might have been involved in heparin interaction (Figure 4.20). However, it is not possible to predict how such dimerised structure could be aligned with the remaining a1a2b1b2 NRP structure.

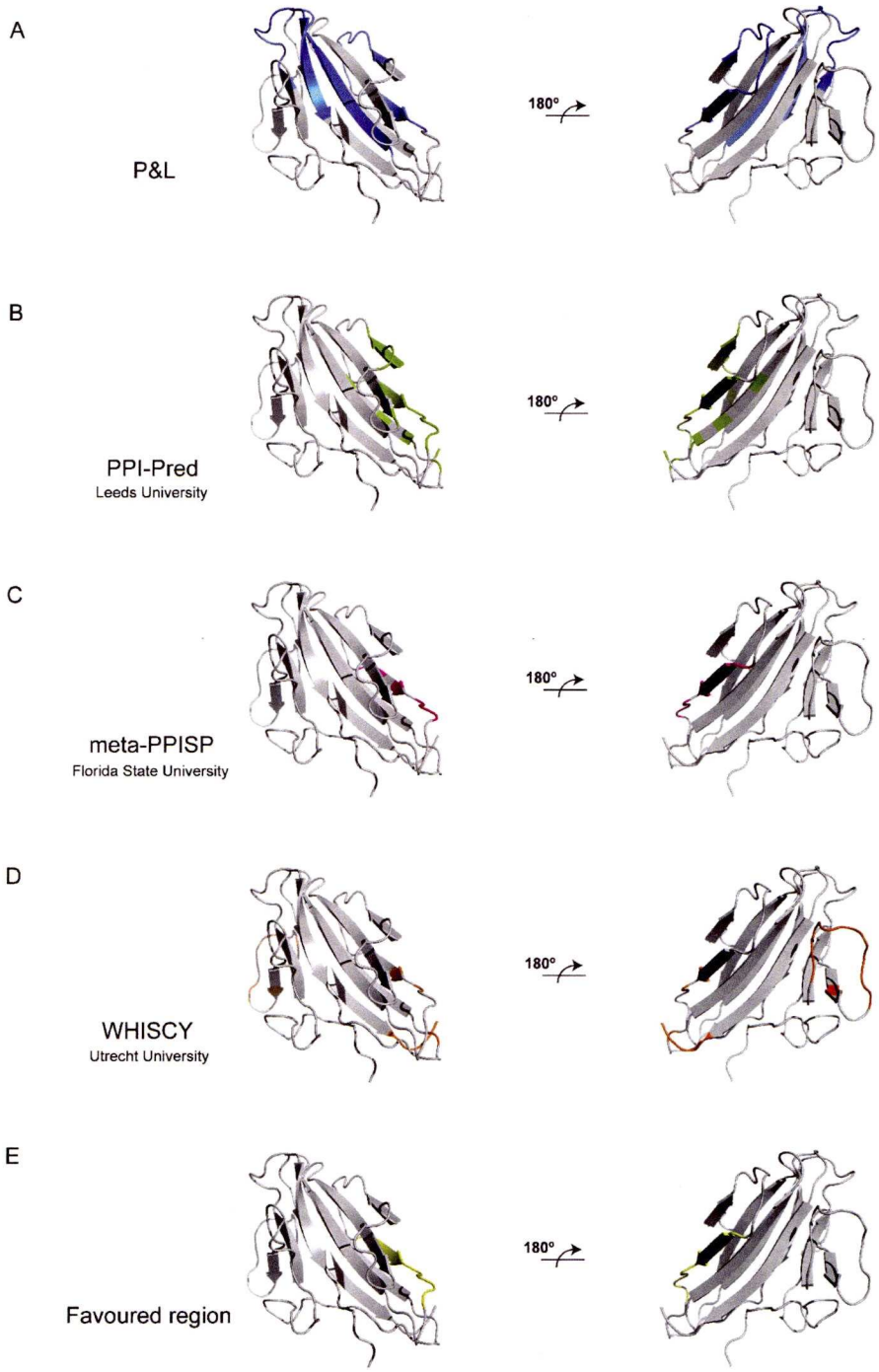

Figure 4.19: Bioinformatics analysis of the potential docking sites for protein interactions within the c domain.

The visualisations of the homology-modelled c domain with indicated interaction sites obtained by various prediction servers and compared to the output peptides of the P&L experiment. A) P&L peptides (in blue). B) PPI-Pred (in green). C) meta-PPISP (in magenta). D) WHISCY (in orange). E) the consensus WKEGRVL sequence (in yellow).

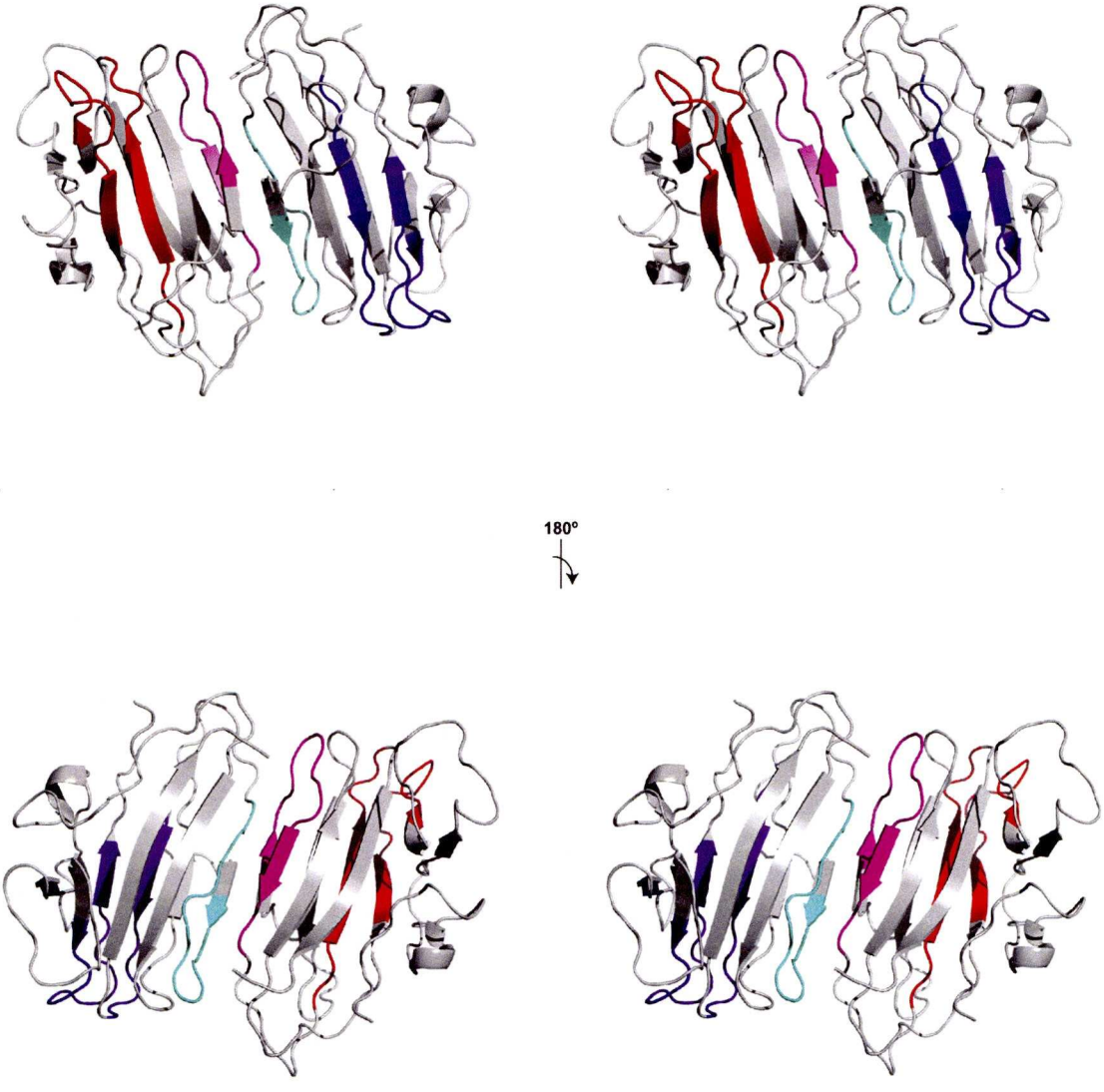

Figure 4.20: The cross-eye stereo picture of the c domains dimer according to the HADDOCK prediction.

The c domains are both presented in grey, where two different perspectives of the c domain are shown. The respective interacting sequences are labelled in pink and cyan. The remaining P&L peptides on each c domain are coloured in blue and red, respectively. In order to view the 3-D picture apply cross-eye technique (right eye focused on the left picture, left eye on the right).

In order to experimentally validate the bioinformatics data, an attempt to obtain from Fc rNRP-1 another truncated variant, this time containing all extracellular domains, was made to confirm or exclude the ability of the c domain to drive dimerisation alone. Conveniently, manipulation of the temperature and NaCl concentration during digestion (referred to as digest B in the Section 2.2.7) allowed a slightly larger protein (crNRP-1) to be obtained (Figure 4.21A, Figure 4.22), which is likely to have been digested after the c domain, as it lacked the His-tag (data not shown). At the same time a crosslinking method based on EDC/ NHS was applied to verify the possibility of the c domains serving as dimerisation platforms between two rNRP-1s. To do so, after a tryptic digest the proteins were incubated in appropriate conditions with the crosslinkers. Interestingly, according to the silver staining of the proteins, contrary to Fc rNRP-1, none of the truncation products was prone to form dimers that could be detected with the crosslinking method. Regrettably, the western blot of the N-terminal rat NRP-1 sequence did not provide clear information (Figure 4.21B), as it seems that both operations, tryptic digest and crosslinking, affected the epitopes recognised by the antibodies. However, the faint band present in crNRP-1 sample confirmed the identity of the protein by recognising its N-terminus. First of all, crosslinked Fc rNRP-1 visible on silver stained gel was not detected on western blot, secondly, the trNRP-1 was recognised as a very intense band, while crNRP-1 was hardly detectable, being accompanied by much stronger band of size of trNRP-1, which was virtually not visible on silver staining. Similarly, the crosslinked samples of trNRP-1 and crNRP-1, although not producing any defined bands indicating a larger product in silver staining, on western blot both appeared to have formed some crosslinked species of intensity proportional to its starting material. This result, though very enigmatic, does not allow solid conclusions to be drawn, however, basing on the silver staining result, it seems that none of the truncated NRP-1s formed substantial amount of dimers/multimers susceptible to EDC/ NHS crosslinking, whereas based on the western blot result, it is apparent that this method was not reliable for detection of crosslinked molecules.

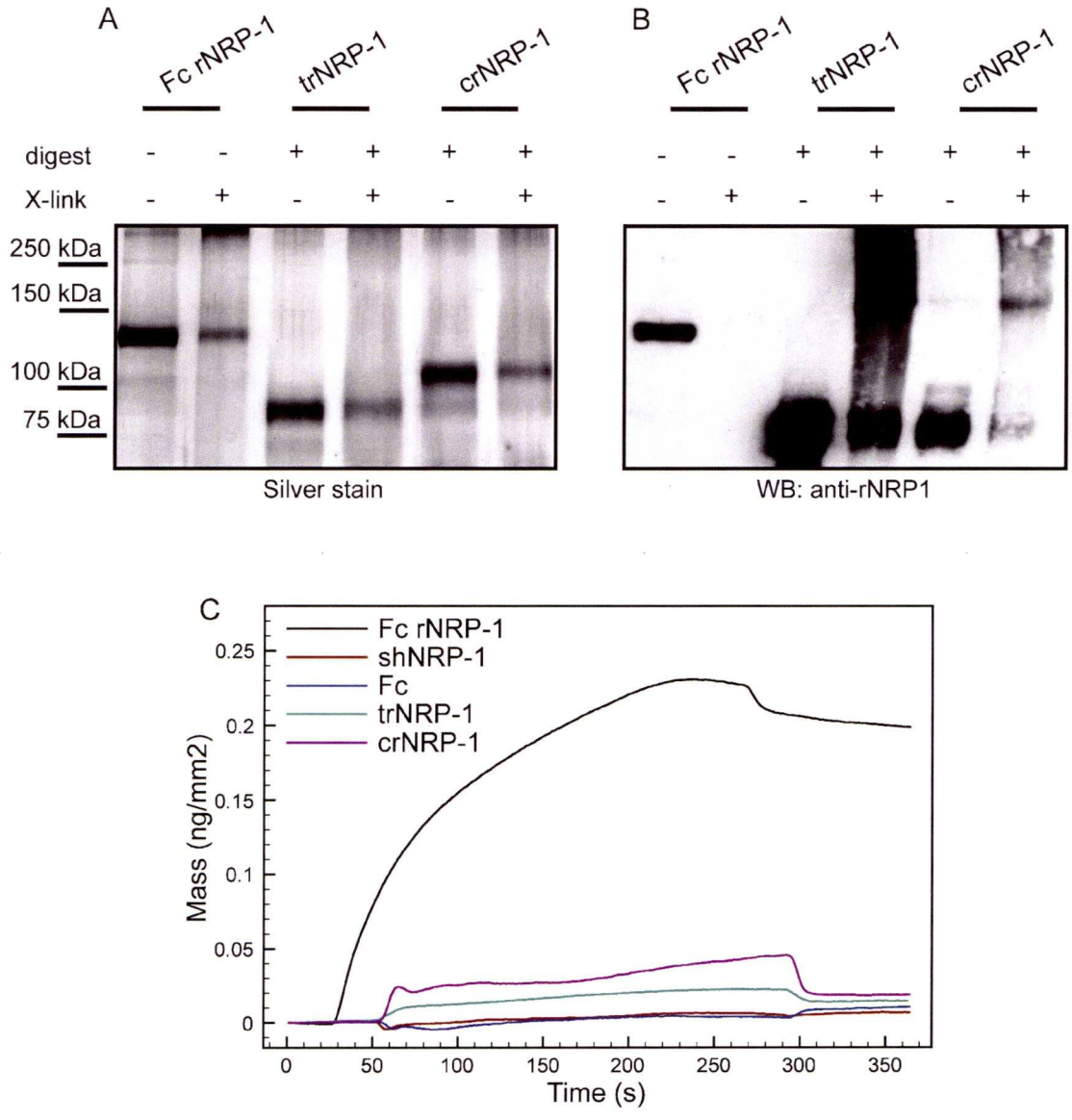

Figure 4.21: The analysis of the binding capacities of the two different products of native tryptic digest of the Fc rNRP-1.

A) Silver staining of the tryptic digests products, labelled as trNRP-1 and crNRP-1, and the control Fc rNRP-1. Additionally labelled lanes show the migration of the proteins after crosslinking. B) Anti-His tag western blot result of the analogous samples as presented on the panel A. C) Comparison of binding of Fc rNRP-1, shNRP-1, reference Fc, trNRP-1 and crNRP-1 to immobilised dp 16 expressed in [ng/mm^2] in a function of time as detected by DPI technique.

Subsequently, the obtained crNRP-1 was tested in a similar manner as trNRP-1 on the dual polarisation interferometer, where similarly to trNRP-1, it did not show any binding to the dp16 surface (Figure 4.21C). This observation was in contrast to the Fc rNRP-1 binding, which confirmed that it is capable of binding to the native functional sulfated stretches of HS, which span on average dp 6 - dp 16 [162]. This finding, and the previous silver staining result, confirmed the proposal that Fc rNRP-1 owes its heparin-binding feature to the dimeric form occuring via the recombinant Fc part, but not the c domain. However, since the docking analysis indicated a possible area of dimerisation via the c domain and presented a mutual interface that could be responsible either for heparin or further protein interaction, it is plausible that the interaction with polysaccharides could be substantial for formation of a dimer, however, this was not possible to confirm in the surface-based studies performed with the tryptic truncated NRP-1 isoform containing the c domain (crNRP-1).

To summarise, this study established some new facts about NRP-1. First of all, a major difference between recombinant dimeric Fc rNRP-1 and shNRP-1 was revealed. The dimeric species bound strongly to heparin, whereas shNRP-1 had much weaker heparin-binding affinity, detectable only by affinity chromatography or the Sypro® Orange stability test. Contrastingly to the Fc rNRP-1, shNRP-1 did not interact with heparin immobilised on optical biosensor surfaces and DPI, nor with heparin *in solution* in the BaF3 sequestration experiment.

Partially similar behaviour was previously observed for Cyclophilin B (CyPB) [163]. CyPB was able to bind to immobilised by reducing-end oligosaccharides and heparin, however, it could not bind to heparin, which was immobilised to the surface by means of biotin groups introduced to its internal free amino groups. This result was confirmed by the competition experiments where NAc derivative of heparin had very weak capacity to compete for the protein binding to the heparin. Nonetheless, in case of the shNRP-1, the protein could not bind to either of the molecules, internally biotinylated and immobilised heparin in optical biosensor, or reducing-end immobilised dp 16 in DPI. This may reflect a dissociation rate, which would render the interaction difficult to detect by these methods.

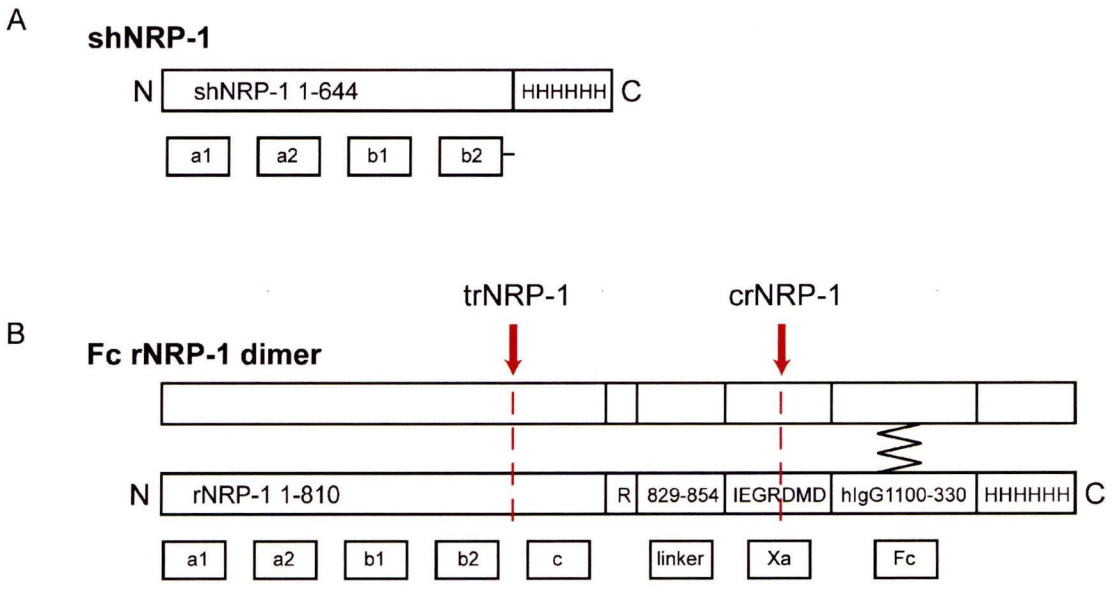

Figure 4.22: Schematic representation of the truncated Fc rNRP-1-derived proteins obtained in trypsin digests.

A) Recombinant soluble isoform of human NRP-1 (shNRP-1) with indicated domains and the His tag. B) Recombinant dimeric rat NRP-1 (Fc rNRP-1) with indicated extracellular domains and the linker sequence derived from NRP-1 sequence, and additional Xa cleavage site (Xa), Fc part of human IgG1 (Fc) and the His tag. The red arrows indicate suggested approximate areas where the trypsin could cleave the protein in order to produce trNRP-1 and crNRP-1.

The characterisation of the structural requirements of polysaccharide binding by the dimeric Fc rNRP-1 showed that it interacted with a large oligosaccharide (> dp 26), however, even dp 26 was not as effectively bound by the Fc rNRP-1 as heparin (approximately dp 50). This implies that Fc rNRP-1 interacts with a chain of a polysaccharide in a complex manner, where probably large areas of the protein are involved directly in the binding, which was investigated in detail by the P&L strategy. Further characterisation of the Fc rNRP-1 revealed that among polysaccharides bearing distinct patterns of sulfation, several different structures could maintain interaction with the Fc rNRP-1. The screening experiment revealed that to mediate strong interaction, the polysaccharide needed either all three sulfate groups (at position 2 of iduronic acid, and at positions 6 and N of glucosamine), or, surprisingly, none. Although the first requirement indicated dependence on charge, and, was additionally supported by a strong interaction with persulfated heparin bearing two additional sulfate groups, the latter requirement clearly showed that sulfate groups are not critical, though the carboxyl of the uronic acid may be. Thus, although the range of the possible structures accommodated by the Fc rNRP-1 did not follow any straightforward rule, there was clearly some selectivity mechanism that allowed the differentiation between various structures. This selectivity means that the tested interactions could be of high regulatory importance. Further assays exploring functionality of the Fc rNRP-1 interaction with fully sulfated heparin-like stretches, 3-O-sulfated and non-sulfated stretches of HS, as compared with other possible structures, could provide fuller insight into the bases of the discovered selectivity of the Fc rNRP-1 binding. At the same time, no major differences were discovered in the Fc rNRP-1 binding to the various cationic forms of heparin, implying that there is no straightforward biophysical effect of these structures on interaction with NRP-1.

The P&L experiment provided more insight into how Fc rNRP-1 could be engaged in the interaction. This approach benefited from the well-known effect of heparin of protecting the interacting residues against chemical modification [164]. In this experiment the protected residues were lysines, which were possible to identify after the chemical biotinylation and subsequent procedure of the protein digest, purification and mass spectrometry analysis of the obtained

peptides. This approach revealed that lysines within vast areas of the Fc rNRP-1 were involved in the interaction, which supported previously discovered requirement of large chains of oligosaccharides to efficiently bind to the protein. The identified peptides covered fragments of the NRP-1 a1, b1, c domains, and the L2 linker region, but also fragments within the Fc part of the protein. This was surprising as the Fc part showed no heparin-binding property in the other experiments (Figure 4.3A, Figure 4.18A). Overall, the result implies that NRP-1 might interact with heparin via more binding sites than the currently documented b1b2 domain, that was only partially confirmed by this method, and that there are other areas within the multidomain structure of NRP-1 that can mediate this interaction. Additionally, it shows that recombinant fusion proteins may have altered properties not only due to the presence in close proximity of the two NRP-1 moieties, but that the Fc part alone can be important for the binding. It is noteworthy, that in this method it is not possible to distinguish between the areas of the Fc rNRP-1 that are directly involved in the interaction, and those which are indirectly undergoing the heparin-driven protection resulting from the conformation change within such a complex protein.

Additionally, the docking analysis suggested a possible conformation of the two c domains with respect to each other, and how, possibly they could form an interface by the peptides identified in the P&L experiment. Overall, this result indicates the basis of a very interesting mechanism of the interaction and predicts further directions of investigation of the Fc rNRP-1 heparin-binding property.

Since the P&L approach highlighted the importance in the binding to the heparin of the parts of the Fc rNRP-1 that are not present in the shNRP-1, an approach that would further investigate the difference between the two species was undertaken. In order to do so, two native tryptic digests of the Fc rNRP-1 were performed resulting in two distinct Fc rNRP-1-derived monomeric proteins. The first product, trNRP-1, was highly likely to contain a similar set of domains as shNRP-1, as deduced from the pattern of migration on SDS-PAGE and the lack of the C-terminal His tag, but presence of the N-terminus. Importantly, likewise shNRP-1,

it did not show any heparin-binding property in the surface-based study (DPI).

The second product, crNRP-1, raised some uncertainties in the western blot based identification of the possible domain content, however, basing on the pattern of migration on SDS-PAGE, it was still suggested to contain all shNRP-1 domains plus the c domain, considered crucial for dimerisation. The docking analysis of the c domain supported the possibility of the dimerisation and allowed a structure of a potential c domain dimer to be built. Unfortunately, an attempt to assess experimentally the scope of mediated dimerisation between crNRP-1s in a crosslinking experiment did not identifiy major multiple migrating isoforms on SDS-PAGE, therefore, indicating rather a lack of detectable homogenic interactions. This NRP-1 also did not bind to the heparin in the surface-based study.

Unless there is a major incompatibility of the surface-based studies and detection of heparin-binding property of the monomeric NRP-1s, these observations indicate that the Fc-mediated fusion of the two rNRP-1 moieties results in unique properties of the Fc rNRP-1 protein. Heparin-binding ability is definitely one of these features.

These findings raise the question if in the physiological conditions NRP-1 may exist in a structure similar to Fc rNRP-1 dimeric/multimeric complexes and might play its functional role via interacting with various domains of heparan sulfate proteoglycans (HSPGs) present on the cell surface. Or contrastingly, both its membrane and soluble fractions may exist as monomers, and their role is not substantially affected by HSPGs, or at least not at the level of its dimeric counterparts. Owing to its native localisation (membrane) and function (co-receptor, adhesion molecule), it is plausible that native NRP-1 might share some features with other proteins of similar localisation/ function, as G-proteins coupled receptors [165] or proteins in adhesion complexes [166], which are well-known to be present on the cells in large homo- and heteromeric complexes. Nevertheless, it is important to emphasise, that the mechanism mimicking Fc fusion would need to be different from the c domain-dependent dimerisation, as according to the findings of this study, the c domain is not sufficient to bestow Fc rNRP-1 properties, at least *in solution*. However, the reduced dimensionality of the membrane may promote

dimers that are not stable *in solution*. Recently, among the mechanisms affecting clustering of the receptors in the membrane are proposed lipid rafts or galectin lattices (reviewed in [167]). Interestingly, both of them have been already proposed to control NRP-1 [41,87]. If this was the case, the picture of NRP-1 function could be as follows - membrane embedded oligomerising NRP-1 is involved in interactions with HS on the cell surface, while the soluble truncated variants are responsible for sequestration and possibly biotransport of NRP-1 interacting growth factors, similarly to soluble VEGFR-1 species [93].

Importantly, the discovery of the discrepancy between these two similar proteins provided new insights into a recently described regulatory mechanism - shedding of the NRP-1 from the membrane. Recently, two distinct soluble species of NRP-1 containing either all extracellular domains (120 kDa) [68, 69] or shNRP-1 set of domains (75 kDa) were discovered [71]. Similar processes were observed for other proteins, endothelial cell protein C receptor (EPCR) and receptor for advanced glycation products (RAGE) [168, 169], where the soluble and shedded species had similar functions in the environment, largely not overlapping with the membrane species. This reinforces the proposal that the membrane embedded NRP-1 might have different functional properties than its soluble isoforms, and, as presented in this study, the mechanism of regulation might depend on the isoform of the protein.

Chapter 5

Exogenous recombinant dimeric Fc rNRP-1 is sufficient to drive angiogenesis in human dermal microvascular endothelial cells

Abstract

Neuropilin-1 (NRP-1) is present on the cell surface of endothelial cells, or as a soluble truncated variant. Membrane NRP-1 is thought to enhance angiogenesis by promoting the formation of a signalling complex between VEGF-A_{165}, VEGFR-2 and heparan sulfate. In contrast, the truncated soluble variant of NRP-1 is postulated to act as an antagonist of signalling complex formation. In this study, the angiogenic potential of two distinct soluble NRP-1 proteins was analysed: a chimera comprising the entire extracellular NRP-1 region dimerised through an Fc IgG domain and a soluble truncated NRP-1 variant. Both NRP-1 proteins stimulated tubular morphogenesis in primary human dermal microvascular endothelial cells (HDMECs).

Surprisingly, this stimulatory activity was independent of VEGF-A_{165}. This was evidenced by depleting the cell culture of exogenous VEGF-A_{165}, replacing VEGF-A_{165} used for routine culture with VEGF-A_{121}, which does not interact with NRP-1 [22, 24, 27, 134, 135], and by the inability of VEGF-A sequestering antibodies to inhibit the angiogenic activity of the NRP proteins. The NRP proteins' angiogenic activity was mediated through VEGFR-2, since they induced its phosphorylation and the synthesis of a specific, downstream target of VEGFR-2, regulator of calcineurin-1 (RCAN-1.4). Moreover, the stimulation of tube formation and of phosphorylation of VEGFR-2 by the NRP proteins in HDMECs was blocked by ZM323881, a specific inhibitor of the VEGFR-2 kinase. Thus, it was concluded that soluble NRP-1s are VEGF-A_{165} independent agonists of VEGFR-2 that stimulate angiogenesis in HDMECs.

Introduction

NRP-1 is a protein known for playing important functions in neural and vascular systems (reviewed in [4, 7]). Initially, it was described as a regulator of axon collapse and enhancer of angiogenesis. Subsequently, new functions of NRP-1 were characterised and the expanded contemporary view of NRP-1 includes amongst its functions antigen recognition [133], adhesion via interaction with γ integrins [45, 46], activation of latent forms of cytokines [38], control of stem cell differentiation [14, 122, 170] and viral infection [171].

Many studies characterising NRP-1 focus on its ability to enhance angiogenesis and cover experiments in cell biology, animal models and patients. Thus, NRP-1 was shown to be abundantly expressed in human, mouse, and chick with highest expression in the vascular endothelium, heart and placenta [24, 124, 172]. Moreover, it was shown that a homozygous deletion of the *Nrp1* gene in mice causes embryonic lethality, due to defects in the vessels and general vascularisation [126], while exogenously overexpressed NRP-1 led to formation of excess capillaries and haemorrhages [124]. Importantly, overexpression of NRP-1 has been observed in the tumour microenvironment, where apart from endothelial cells, the tumour cells themselves were shown to express NRP-1 [173,174]. Current knowledge of NRP-1 places it among the key

drivers of angiogenesis [130], however, it must be emphasised that the exact mechanism of its action is not clear. It has been proposed that NRP-1 forms signalling complexes, where, as a co-receptor with no intrinsic kinase activity, it associates with other tyrosine kinase receptors, their ligands and heparan sulfate moieties of heparan sulfate proteoglycans [4]. The formation of such complexes is regulated by the availability of NRP-1 in the cell membrane, dependent on its down-regulation by ligand-mediated internalisation. Thus, several studies have shown that molecules interacting with NRP-1 cause its disappearance from the cell surface and this mechanism together with ligand binding preference might provide a mechanism for NRP-1 signalling selectivity [44,46,53,58,84]. The hypothesis that the internalisation process might be a means of selecting signalling pathways is supported by observations that VEGF-A_{165} induces NRP-1 internalisation at a much higher level than SEMA-3A, whereas VEGF-A_{121}, which does not bind NRP-1, fails to affect the internalisation of NRP-1 [53]. Another mechanism controlling the angiogenic activity of NRP-1 is the secretion of soluble truncated isoforms of the receptors, which bind the same ligands as membrane NRP-1. For example, in the presence of soluble NRP-1 species, which sequester VEGF-A_{165}, membrane NRP-1 cannot enhance VEGF signalling nor be internalised, which may lead to an increased probability of NRP-1 interacting with the antagonising SEMA-3A [53].

Due to its crucial role in angiogenesis, NRP-1 is currently the target of various prospective anti-cancer therapies. The most common approaches aim to inhibit NRP-1 function, and, consequently, block such phenotypes as pathological angiogenesis, and consequently tumor growth [175]. Among these are antagonistic soluble NRP-1 [75,76], VEGF-A_{165}-derived blocking peptides [75, 176, 177], siRNA against NRP-1 [75], anti-NRP-1 antibodies [178] and recently developed synthetic small molecule inhibitors [179]. Other approaches use NRP-1 to allow drug delivery inside the cells [85, 180–182], thus providing a route for selective drug delivery into the cells expressing NRP-1.

In this study it was hypothesised that dimeric NRP-1, a proxy for oligomerised membrane NRP-1, could be a potential proangiogenic agent mimicking *in trans* an intercellular activity of

NRP-1 [11]. Consequently, the molecular components required for NRP-1 to exert an angiogenic effect in human dermal microvascular endothelial cells (HDMEC) were examined. Two recombinant NRP-1 proteins were used in this study. The recombinant dimeric rat NRP-1 (Fc rNRP-1), which can be considered as a proxy for native oligomerised NRP-1 species embedded on the cell surface and a soluble human NRP-1 isoform, comprising the a and b, but not the c domains. Fc rNRP-1 contains all the main extracellular domains from a to c that are considered essential for ligand/receptor interactions and also for NRP-1 oligomerisation [4]. Surprisingly, the obtained results demonstrated that both forms of NRP-1 can cause tube formation independently of VEGF-A ligand in a collagen-based angiogenesis assay of HDMECs. The mechanism of Fc rNRP-1 action is VEGFR-2 dependent, as shown by the stimulation of VEGFR-2 phosphorylation, RCAN-1.4 induction and blockage by a VEGFR-2 kinase inhibitor. The soluble human NRP-1 isoform was similarly shown to cause tube formation, though less effectively. Thus, NRP-1 behaves as a VEGFR-2 agonist and does not require partner growth factors to exert its angiogenic activity.

Results and Discussion

5.1 Characterisation of recombinant soluble NRP-1s

The NRP-1 proteins used in this study are commercially available recombinant proteins (Figure 4.2) that were described in the previous chapter. They differ from the membrane localised NRP-1 in several aspects (Figure 4.2A). Recombinant rat NRP-1 chimera (Fc rNRP-1) has the rat sequence of NRP-1, which shows high similarity (approximately 93 % identity within the overlapping regions) to the human sequence (Figure 4.2B, Figure 5.1A). It covers all extracellular domains (a1, a2, b1, b2 and c) of the membrane NRP-1 and also fragments of the linker region that follows the c domain (where amino acids 811-828 are substituted by arginine residues, but subsequent sequence 829-854 is present). This sequence is fused to the Fc part of human IgG1 and a histidine tag.

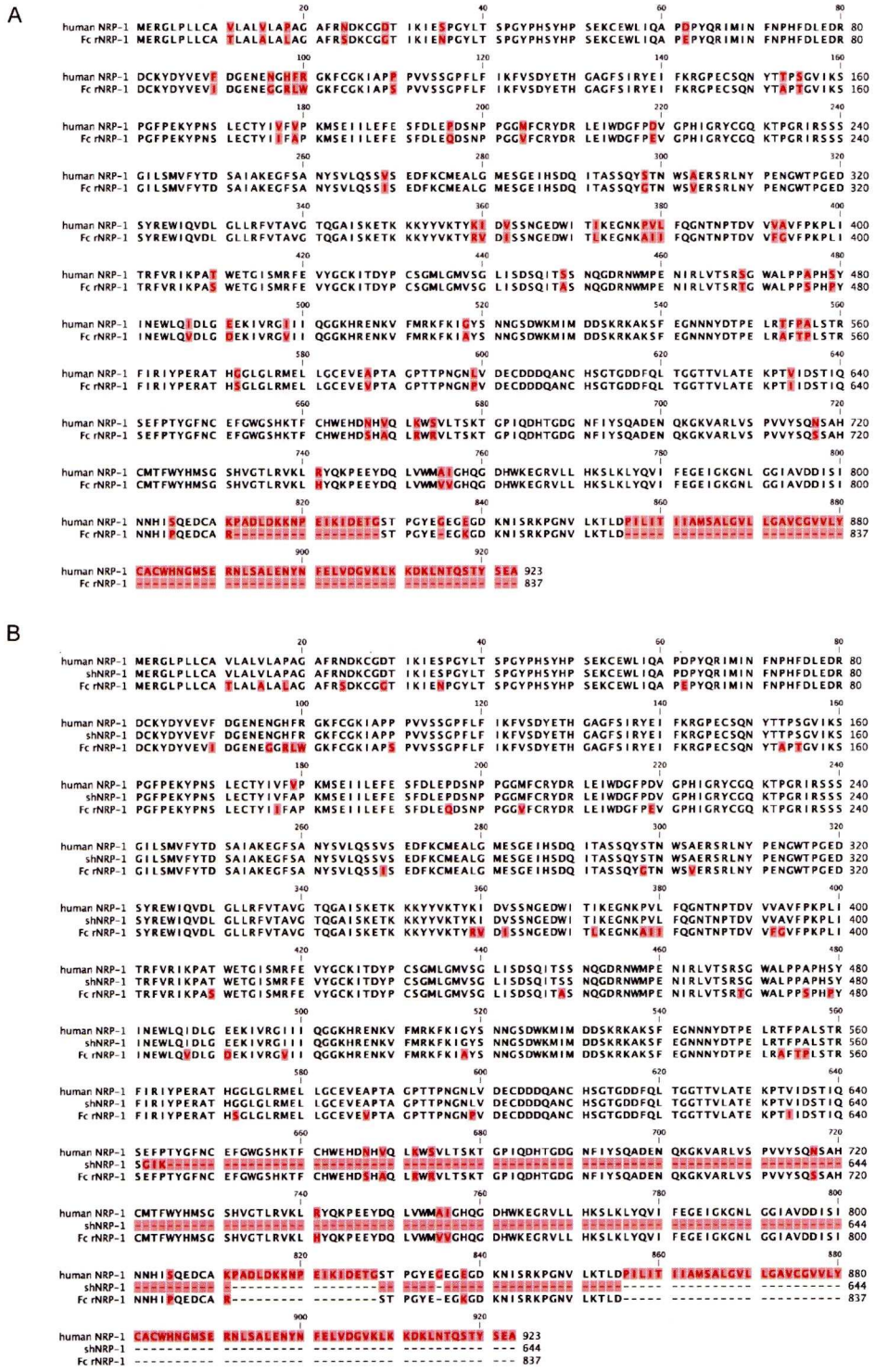

Figure 5.1: Sequence analysis of recombinant NRP-1 proteins and human wild-type NRP-1.

A) Alignment of full-length human NRP-1 and the corresponding rat sequence covered in Fc rNRP-1. B) Alignment of full-length human NRP-1 and the NRP-1 sequence covered by shNRP-1 and the rat sequence covered by Fc rNRP-1. The differing amino acids are marked in red.

Consequently, the protein is expressed as a dimer due to the formation of disulfide bridges between the Fc domains of the two identical recombinant constructs. Upon SDS-PAGE in reducing conditions it migrates as a monomer around 150 kDa (Figure 4.2D). Soluble truncated human NRP-1 (shNRP-1) encodes the human amino acid sequence of the native soluble isoform fused to a histidine tag (Figure 4.2). It differs from Fc rNRP-1 by the absence of the c domain and minor sequence variation due to alternative splicing (1) (Figure 4.2C). shNRP-1 migrates around 90 kDa upon SDS-PAGE in reducing conditions, and both proteins were confirmed to be pure as judged by silver staining (Figure 4.2D).

5.2 Induction of tube formation by Fc rNRP-1 and shNRP-1 via VEGFR-2 activation

Human Dermal Microvascular Endothelial Cells (HDMECs) were used, which are of similar characteristics to Human Umbilical Vein Endothelial Cells (HUVECs) [183]. However, in contrast to the latter, they are of micro-, not macrovascular origin. This makes them more appropriate subject of angiogenic studies, as angiogenesis is their direct physiological function [184, 185].

The tubular morphogenesis assay measures the ability of cells to form capillary-like structures in a 3-D collagen type I gel in response to growth factors and represents an *in vitro* angiogenesis assay [102, 186]. This assay confirmed the ability of VEGF-A_{165} to induce angiogenesis *in vitro*. It also demonstrated that both recombinant NRP-1 proteins induced tube formation (Figure 5.2). Fc rNRP-1 (5 nM) had the highest proangiogenic activity and appeared to be a more potent stimulator of angiogenesis than VEGF-A_{165} (10 ng/ ml; 224 pM). The Fc region (5 nM) of Fc rNRP-1 had no stimulatory effect on tube formation, demonstrating that the effects observed with the Fc rNRP-1 chimeric protein were entirely due to the NRP-1 part.

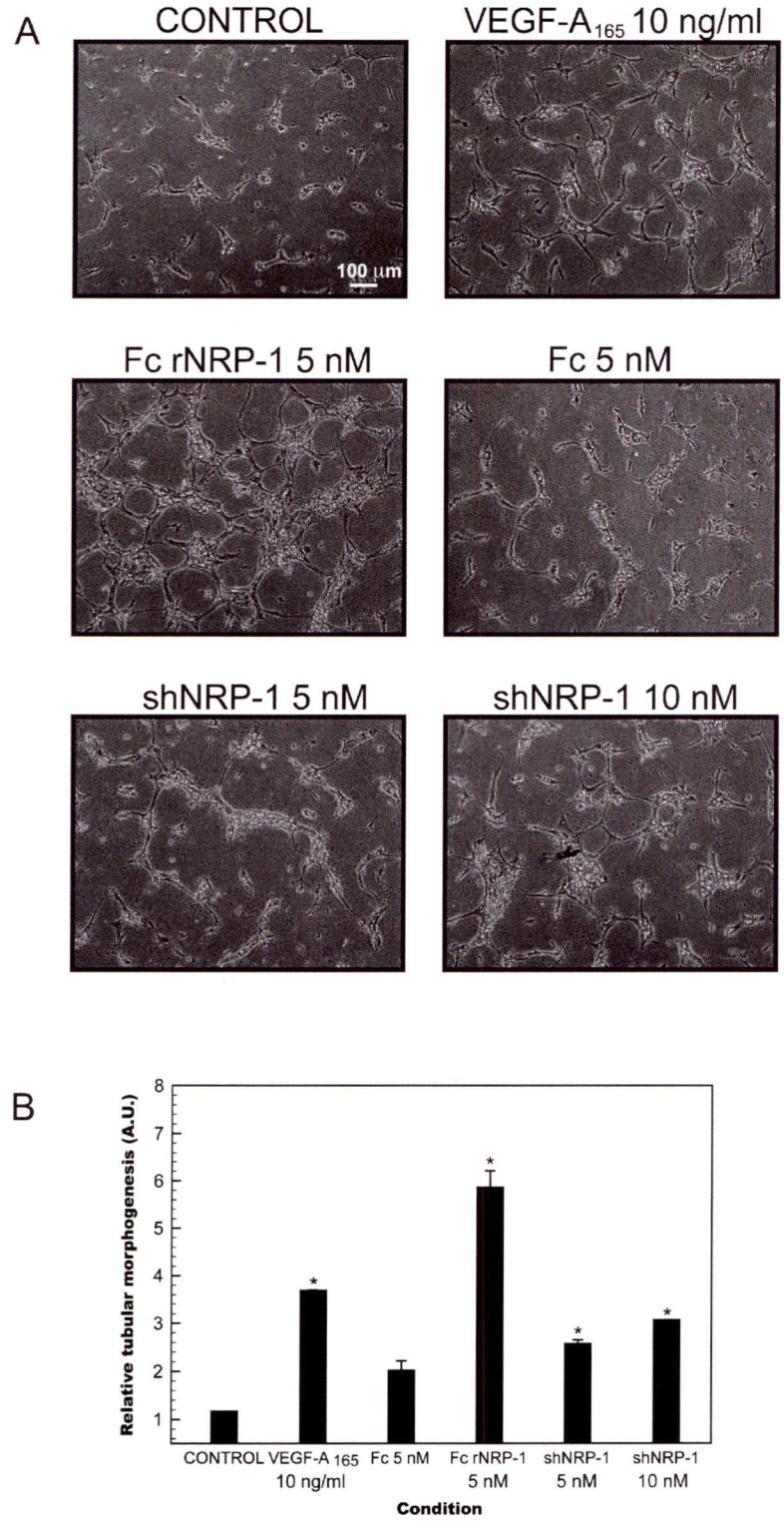

Figure 5.2: Recombinant NRP-1 proteins stimulate tube formation in HDMECs.

A, B) The influence of addition of VEGF-A_{165} (10 ng/ mL), reference Fc, shNRP-1 and Fc rNRP-1 (5 nM or 10 nM) on HDMECs tube formation on collagen substratum. The tubes were photographed and analysed as described in the Section 2.4.4. Significant differences between the tested agonists and the control were determined by Student's t test. Asterisks (*) indicate that the P values are <0.001 for comparison to control.

The monomeric shNRP-1 (5 nM) induced tube formation to a lesser extent than Fc rNRP-1. However, as NRP-1s were added at equimolar concentrations, the dimeric form of Fc rNRP-1 had double the content of NRP-1 moieties. Therefore, shNRP-1 was also tested at 10 nM, but this did not increase its ability to induce the formation of tubes (Figure 5.2), indicating that the dimerisation of Fc rNRP-1 and/ or the presence of the c domain is the most likely reason for the increased potency of the latter in this assay.

To identify the potential molecular partners of NRP-1 in the stimulation of *in vitro* angiogenesis, the activation of VEGFR-2 and induction of a downstream VEGF-responsive protein, RCAN-1.4/ DSCR-1 [187] (Uniprot accession number P53805-2) [188], were analysed by western blotting. Surprisingly, Fc rNRP-1 in the absence of exogenous VEGF-A_{165} was able to stimulate the phosphorylation of VEGFR-2 in the cells plated on collagen (Figure 5.3) and gelatin (Figure 5.4). Moreover, after 3 hours, the level of RCAN-1.4 was higher, supporting a VEGFR-2 dependent mechanism of activation of its synthesis [189]. The same molar amount of shNRP-1, however, did not have any detectable effect on the signalling proteins tested, which is in accordance with its weaker angiogenic activity, and explained by the similar, but much weaker response it can induce. Indeed, when the amount of shNRP-1 is doubled a very weak activation of VEGFR-2 and ERK-1/2 is observed (Figure 5.7), which supports the notion that the effects of shNRP-1 are the same, but less potent than those of Fc rNRP-1. As NRP-1 is also a putative co-receptor of c-MET and FGF receptors, phosphorylation of total tyrosines in the lysate samples was investigated to identify whether other pathways were strongly activated. However, no significant target phosphorylation candidate was observed other than VEGFR-2 (Figure 5.5). Consequently, these data indicate that exogenously added recombinant Fc rNRP-1 and shNRP-1 are likely to elicit their proangiogenic response in a VEGFR-2 dependent manner.

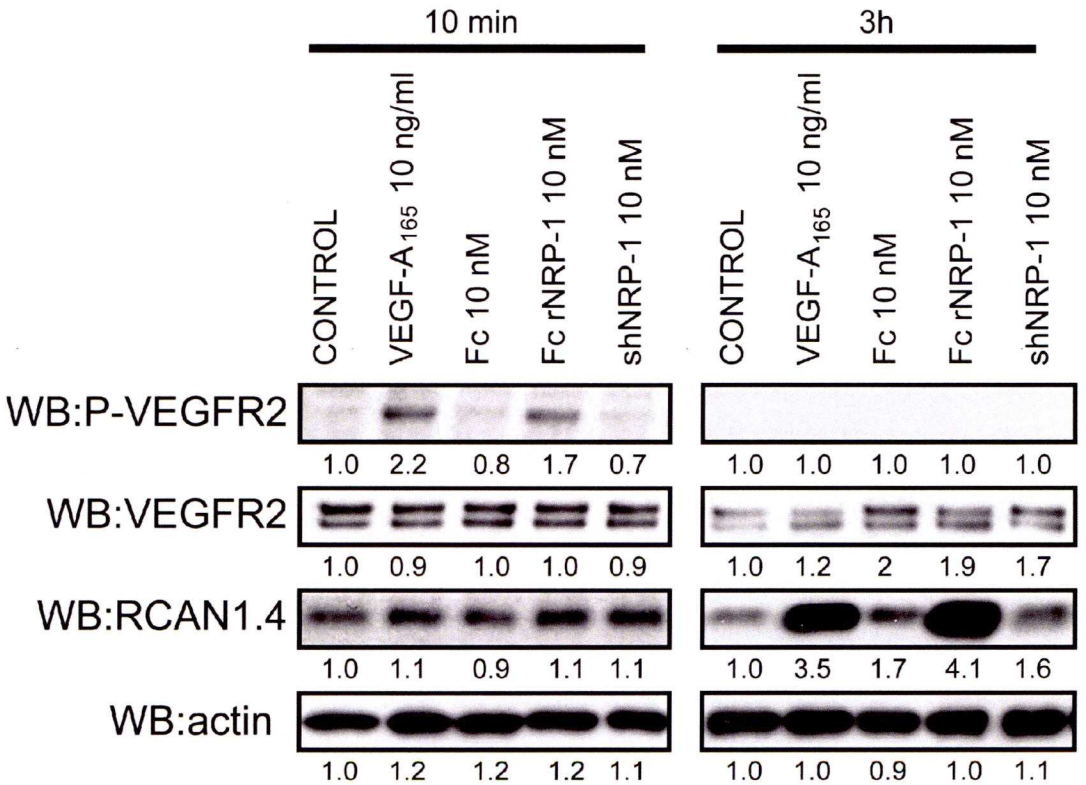

Figure 5.3: Western blot result of experiment with HDMECs cultured on a layer of collagen.

The phosphorylation of VEGFR-2 and the levels of RCAN-1 following stimulation with VEGF-A_{165} or recombinant NRP-1s are shown. The band intensities were analysed as described in the Section 2.4.6.

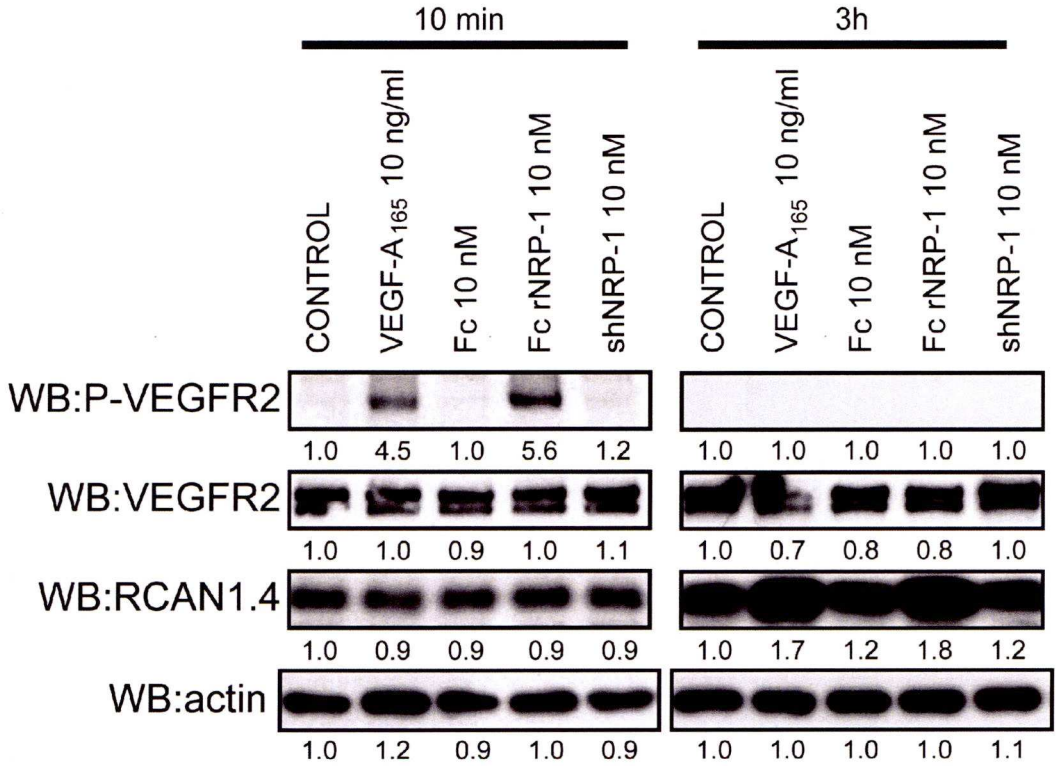

Figure 5.4: Western blot result of experiment with HDMECs cultured on a layer of gelatin.

The phosphorylation of VEGFR-2 and the levels of RCAN-1 following stimulation with VEGF-A_{165} or recombinant NRP-1s are shown. The band intensities were analysed as described in the Section 2.4.6.

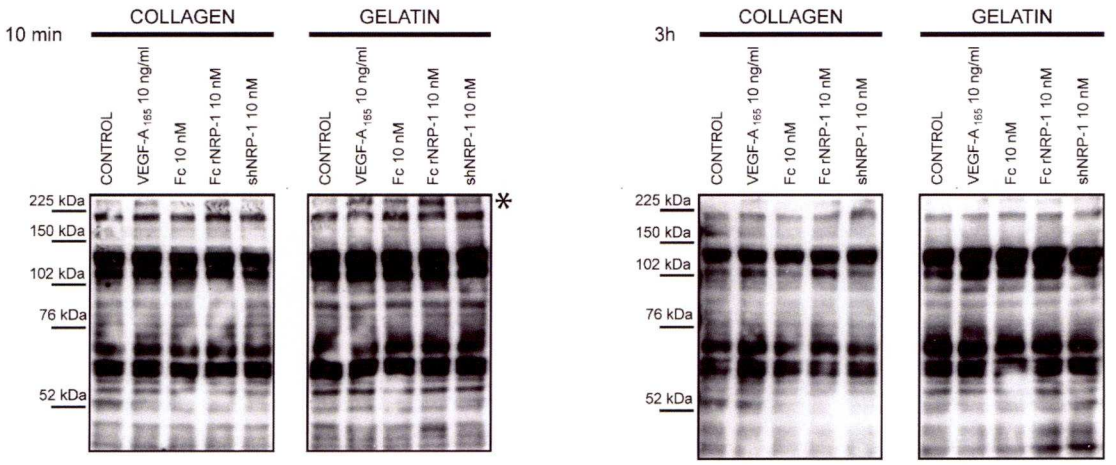

Figure 5.5: Western blot for phosphotyrosine-containing proteins in the HDMECs lysates.

The phosphorylation levels after stimulation with VEGF-A_{165} and recombinant NRP-1s are shown. Cells grown on collagen and gelatin were stimulated with VEGF-A_{165} and recombinant NRP-1 proteins for 10 min and 3 h. Asterisk indicates a band corresponding to the molecular weight of VEGFR-2 which is phosphorylated.

5.3 Fc rNRP-1 response is blocked by a VEGFR-2 specific inhibitor ZM323881

To formally establish that the activation of the VEGFR-2 pathway by Fc rNRP-1 was the cause of the stimulation of tube formation, the cells were treated with ZM323881, a potent cell-permeable inhibitor of the VEGFR-2 tyrosine kinase [94] (Figure 5.6). Under these conditions, Fc rNRP-1 stimulation of tube formation in HDMECs was fully blocked (Figure 5.6). The efficiency of the inhibitor was confirmed by western blot, where it was able to abolish detectable phosphorylation of VEGFR-2 and downstream responses induced either by VEGF-A_{165} or the recombinant NRP-1 proteins, both on collagen and gelatin substrata (Figure 5.7, Figure 5.8). These data demonstrate that NRP-1 stimulates angiogenesis solely through VEGFR-2.

5.4 Fc rNRP-1-driven tube formation occurs in VEGF-A_{165} depleted cells

The recombinant NRP-1 proteins were shown to induce angiogenesis in an exclusively VEGFR-2 dependent manner and an inhibitor of the VEGFR-2 tyrosine kinase could block this response. However, most of the published data have been interpreted to suggest that NRP-1 exerts its angiogenic effects by potentiating the effects of VEGF-A_{165}, as generally these experiments were performed in the presence of VEGF-A_{165} [11,73,74]. In contrast, the experimental design of the present study implied lack of involvement of endogenous VEGF-A_{165}, due to the 24h incubation of the HDMECs in low-serum in the absence of VEGF-A_{165}, prior to the addition of NRP-1 proteins [190–193]. To rigorously exclude the presence of small amounts of VEGF-A_{165} carried over from the culture medium or bound to extracellular matrix, the cells were grown for at least 7 days in medium containing 0.5 ng/ mL VEGF-A_{121} isoform, instead of VEGF-A_{165}.

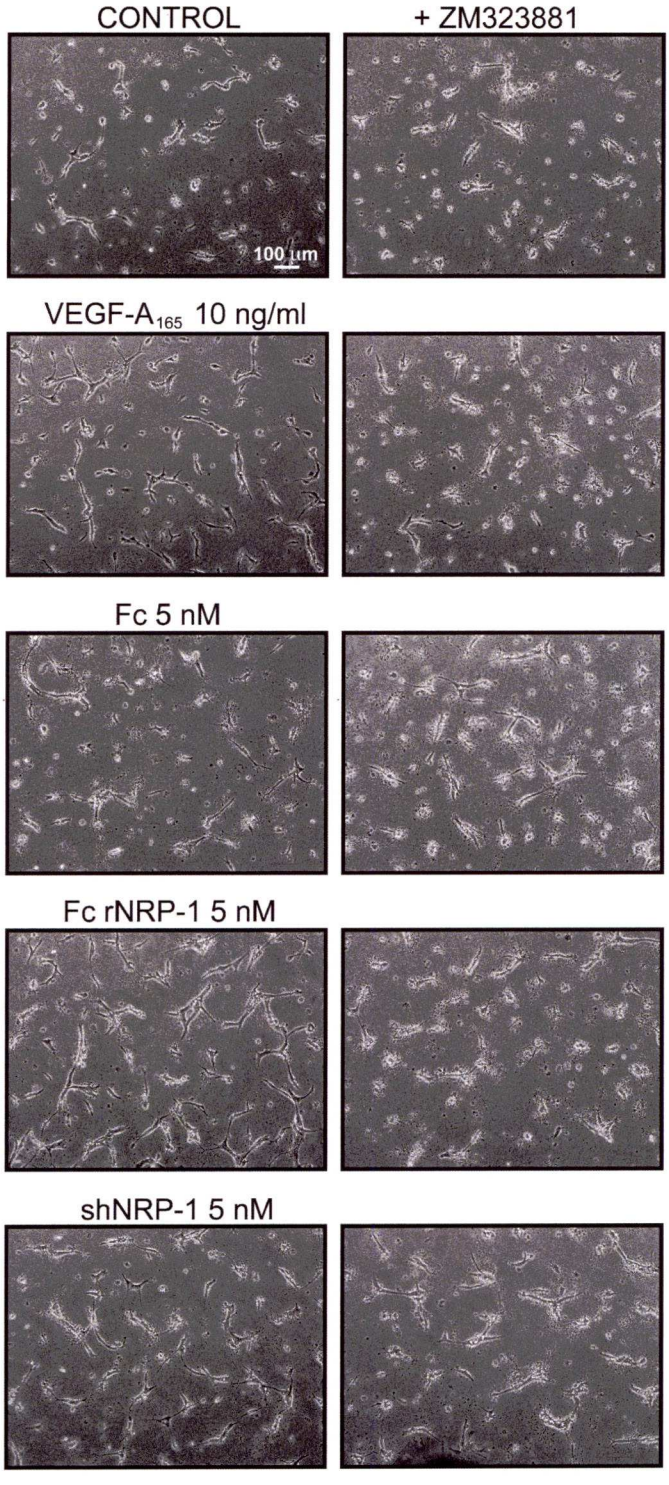

Figure 5.6: The effect of the VEGFR-2 kinase inhibitor (ZM323881) on tube formation.

The stimulation of tube formation by Fc rNRP-1 depends on VEGFR-2 kinase activity but not on VEGF-A in HDMECs. The experiment was performed as described in the Section 2.4.3. The tube formation observed in the presence of VEGF-A_{165} and recombinant NRP-1 proteins was blocked by the VEGFR-2 kinase inhibitor (ZM323881).

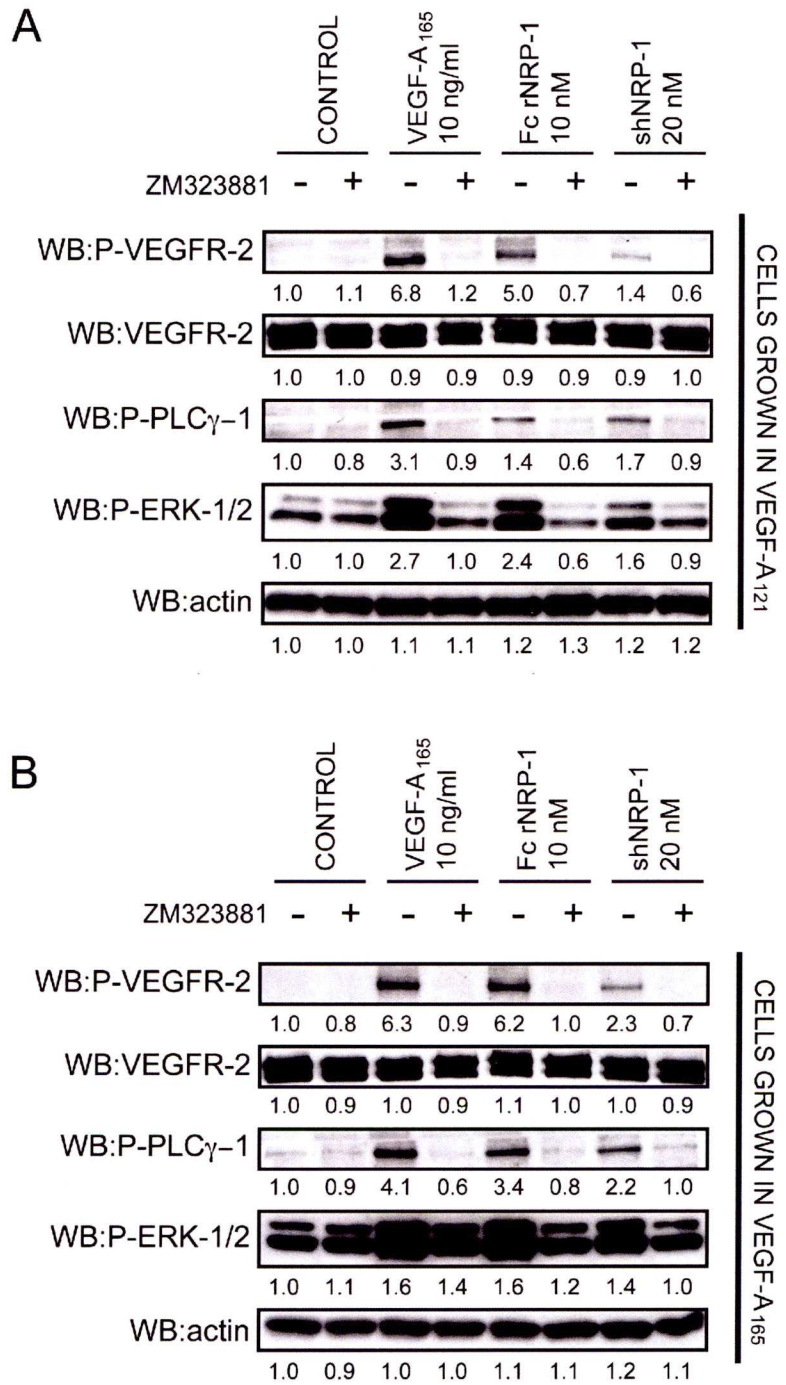

Figure 5.7: Western blot result of the effect of addition of VEGFR-2 inhibitor to the HDMECs cultured on collagen.

A) The effect of stimulation with VEGF-A_{165} and recombinant NRP-1 proteins on cells grown 7 days prior to serum starvation in medium supplemented with VEGF-A_{121}. B) An analogous experiment with cells grown in standard conditions in medium supplemented with VEGF-A_{165} prior to serum starvation. Both panels show the effect of the inhibitor of the VEGFR-2 tyrosine kinase (ZM323881). The band intensities were analysed as described in the Section 2.4.6.

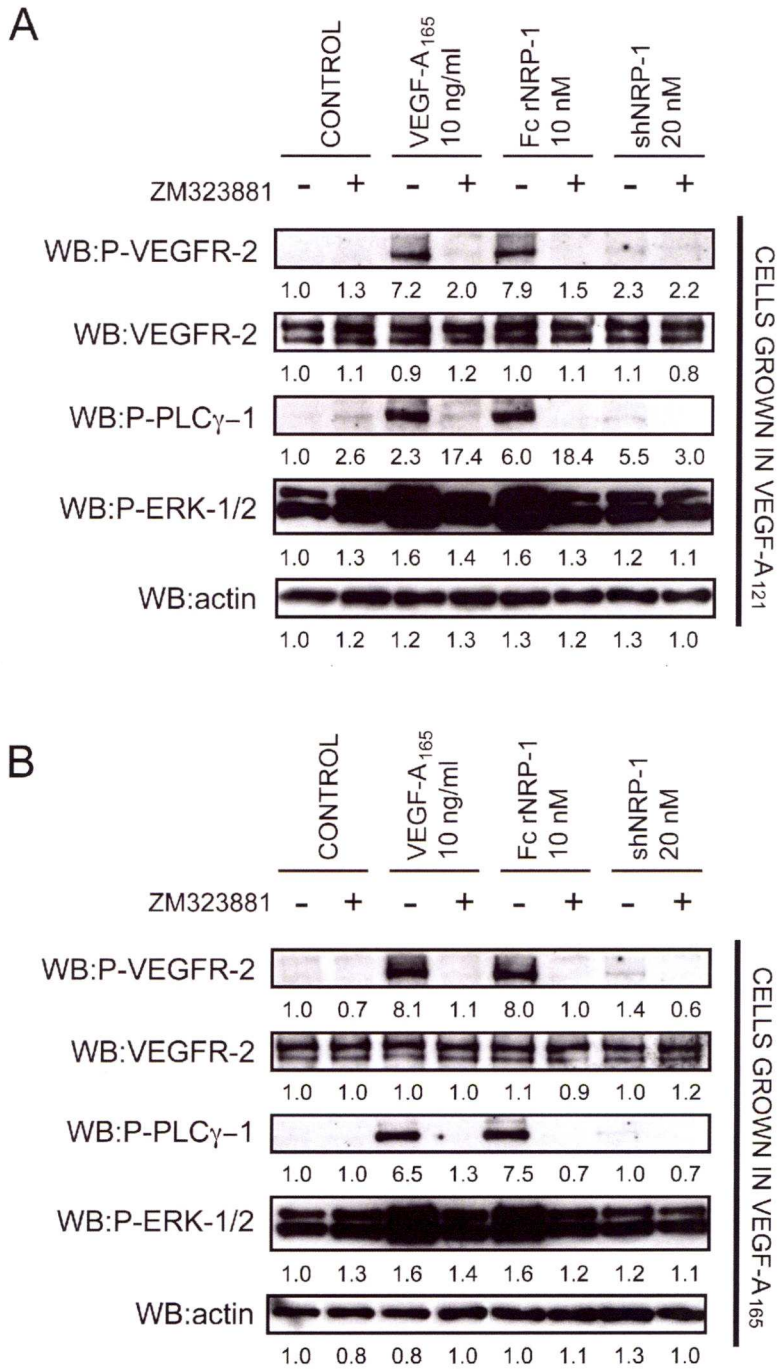

Figure 5.8: Western blot result of the effect of addition of VEGFR-2 inhibitor to the HDMECs cultured on gelatin.

A) The effect of stimulation with VEGF-A_{165} and recombinant NRP-1 proteins on cells grown 7 days prior to serum starvation in medium supplemented with VEGF-A_{121}. B) An analogous experiment with cells grown in standard conditions in medium supplemented with VEGF-A_{165} prior to serum starvation. Both panels show the effect of the inhibitor of the VEGFR-2 tyrosine kinase (ZM323881). The band intensities were analysed as described in the Section 2.4.6.

Cells grown in such conditions are most unlikely to contain any residual VEGF-A_{165} and the response observed is expected to be VEGF-A_{165} independent. In parallel, another batch of cells was grown in the standard conditions containing VEGF-A_{165} for the purpose of comparison. Cells grown in both conditions appeared to be similarly sensitive to Fc rNRP-1 (Figure 5.9). Additionally, they showed exactly the same profile of signalling activation, where VEGF-A_{165}, Fc rNRP-1 and to lesser extent shNRP-1 (whose amount was doubled to 20 nM, whereas Fc rNRP-1 was at 10 nM), caused immediate phosphorylation of VEGFR-2 and activation of PLCγ-1 and ERK-1/2 on collagen (Figure 5.7) and gelatin substrata (Figure 5.8). This shows that cells devoid of VEGF-A_{165} by extended medium depletion are also induced by NRP-1s to undergo a proangiogenic response.

5.5 Sequestration of VEGFs with anti-VEGF-A antibody does not block tube formation

To further eliminate the possibility of endogenous VEGF-A_{165} production contributing to the angiogenic activity of the NRP-1 proteins, a sequestering antibody that targets the N-terminal region of human VEGF-A was introduced into the tube formation assay. The antibody successfully blocked the tube formation of exogenously administered VEGF-A_{165}, however, the stimulation of the formation of tubes by recombinant NRP-1 proteins was completely unaffected by the VEGF-A sequestering antibody (Figure 5.10).

To summarise, the addition of Fc rNRP-1/ shNRP-1 triggered tubular morphogenesis in HDMECs. This early *in vitro* angiogenic response was a consequence of the activation of the VEGFR-2 receptor and was inhibited by a specific inhibitor of the VEGFR-2 tyrosine kinase. At the same time, cells depleted of VEGF-A_{165} or incubated with a sequestering antibody to VEGF-A could still be induced by the NRP-1 proteins to form tubes.

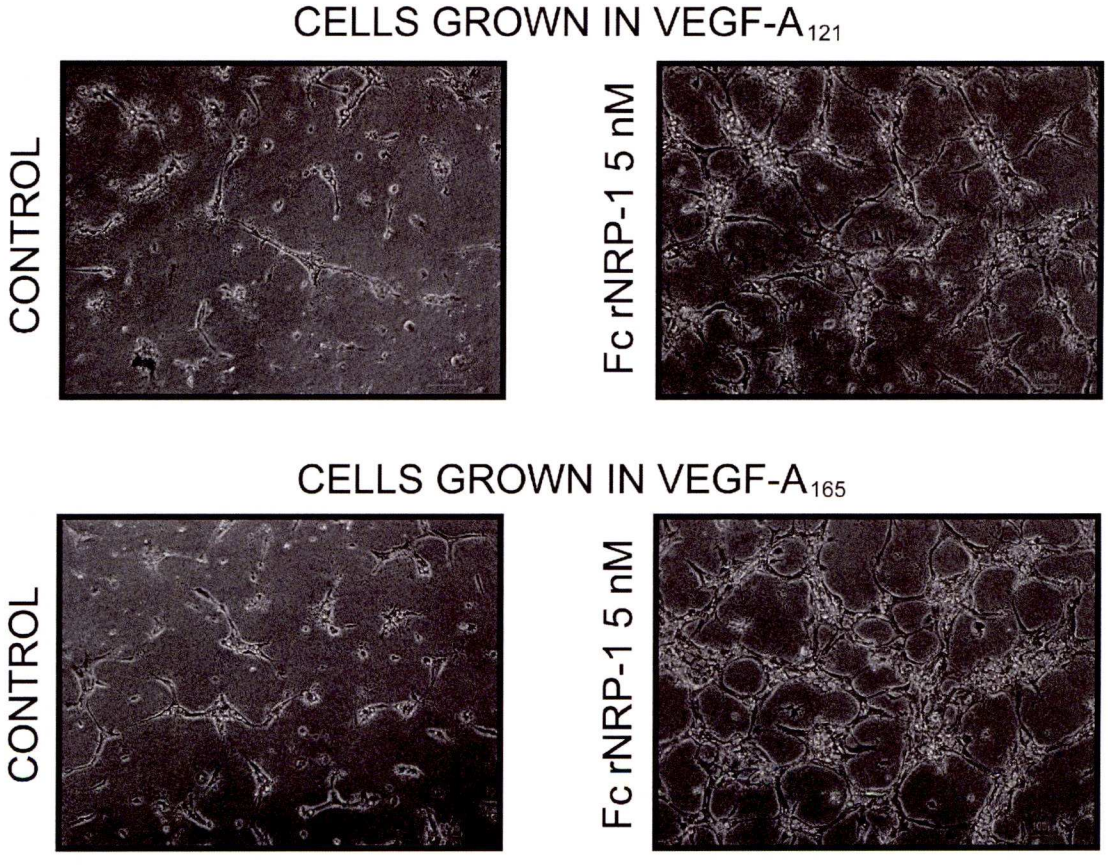

Figure 5.9: The tube formation induced by Fc rNRP-1 depends on VEGFR-2 kinase activity but not on isoform of the VEGF-A in HDMECs.

The angiogenic effect of Fc rNRP-1 on HDMECs grown 7 days prior to serum starvation in medium supplemented with either VEGF-A_{165} or VEGF-A_{121}. The experiment was performed as described in the Section 2.4.3.

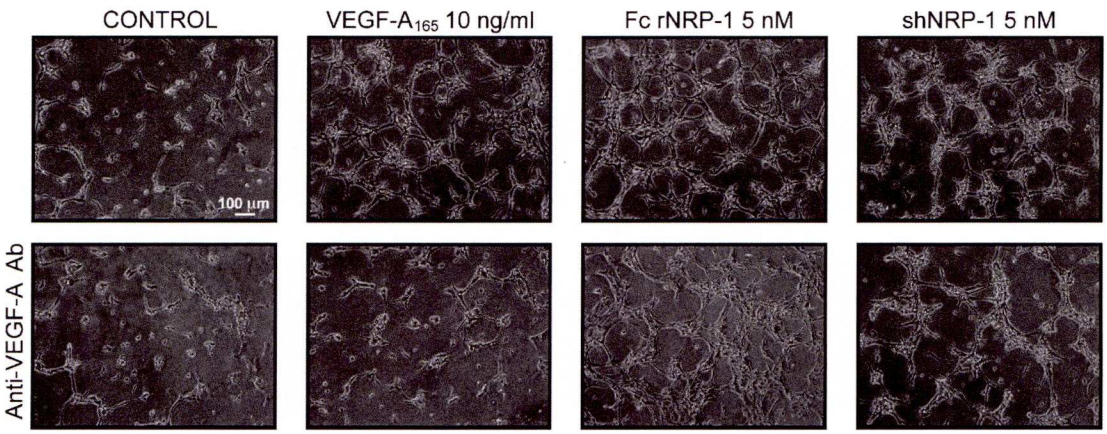

Figure 5.10: Effect of a sequestering antibody to VEGF-A on tube formation by HDMECs.

Top panels present control variants, while the bottom panels present the same conditions but with the addition of the VEGF-A sequestering antibody according to the procedure described in the Section 2.4.3.

Therefore, this study showed that Fc rNRP-1, and to a lesser extent shNRP-1, can behave as a VEGFR-2 agonist, possessing a weaker (shNRP-1) or stronger (Fc rNRP-1) pro-angiogenesis activity in HDMECs. Thus, the present results extend considerably the regulatory potential of NRP-1.

The few studies that have focused on the angiogenic activity of recombinant NRP-1, as opposed to its activity in the presence of VEGF-A_{165}, have provided contradictory views. A study employing monomeric full-length NRP-1 suggested that it inhibited angiogenesis and caused necrosis in chloroma solid tumor in SCID mice. Moreover, localised expression of this dimeric form was able to block tumour progression [74]. However, the inhibitory effect of NRP-1 in these experiments may be due to the NRP-1 sequestering VEGF-A_{165} from the immediate environment of the endothelial cells. A similar effect was observed in another study, conducted in explants of para-aortic splanchnopleural mesoderm cells, where monomeric NRP-1 was found to have an inhibitory effect on vasculogenesis [73]. Further studies of dimeric NRP-1 provide more contradictory data, perhaps related to different experimental systems. According to one study, a chimeric construct similar to the one used here was shown to bind to endothelial cells expressing VEGFR-2 only in the presence of VEGF-A_{165} [11], whereas another study showed that the dimeric form of the protein induced angiogenesis in the presence of VEGF-A_{165} and alone, however even 50 μg/ mL of the dimeric NRP-1 alone had not comparable activity to VEGF-A_{165} [73]. In the presented results the pro-angiogenic activity of Fc rNRP-1 was stronger than in the case of the shNRP-1 protein, which may be explained by the dimerization of the protein by the Fc fusion [74, 194]. Alternatively, the c domain which is known to cause dimerisation of native NRP-1 [25, 34] and may have other functions, may be critical for NRP-1's angiogenic activity.

Overall, the present findings suggest that the dimerisation of NRP-1 by the Fc domain and/ or the presence of the c domain results in a strong VEGFR-2 agonist. Thus, Fc rNRP-1 may be a good candidate for therapeutic angiogenesis in conditions requiring revascularisation such as ischemia [195]. It elicits a strong proangiogenic response and could be an additional/

complementary contribution in the well-studied VEGF-A_{165} based therapies [196]. To become clinically relevant, Fc rNRP-1 would need to undergo two major adaptations: humanisation and reduction of Fc function [197], which are both currently attainable and allow reduction of undesirable immunological response without affecting the benefits of the fusion nature [197]. The practical significance is that the half-life of VEGF-A_{165}, does not exceed one hour [198], limiting the amount of administered agonist, while the modified Fc rNRP-1 may have a considerably longer half-life, as has been found with analogous fusion proteins, which have been already shown successful in preclinical and clinical studies [199], such as etanercept (Fc-p75 TNF receptor) [200], alefacept (Fc-LFA-3) [201], and abatacept (Fc-CTLA-4) [202], Fc-endostatin [203] and VEGF-TRAP (selected VEGFR-1/2 domains trapping VEGF-A independently and Fc) [204]. Thus the discovery that Fc rNRP-1 is a potent VEGFR-2 agonist opens new possibilities for the development of proangiogenic therapies using a powerful approach that so far has been scarcely employed in proangiogenic field [205].

Chapter 6

General Discussion

This study was focused on the molecular mechanism of action and functional characterisation of NRP-1. It used two commercial recombinant NRP-1 proteins, a dimeric rat Fc rNRP-1 and monomeric human shNRP-1. The human and rat NRP-1 sequences are highly conserved, therefore, the main difference between the two proteins was the monomeric and dimeric form, and lack of the c domain in the monomeric human NRP-1. Since several biochemical studies observed dimerisation of NRP-1, it is generally regarded as highly probable that *in vivo* such species are formed. Moreover, it is predicted to especially take place in the membrane location in lipid rafts or via galectin lattices (reviewed in [167] and [41,87]). Also, formation of dimers by soluble species was suggested [82], supported by recently discovered soluble species of NRP-1 containing all extracellular domains including the c domain (120 kDa) [68,69]. Therefore, the Fc rNRP-1 is used mainly as a proxy for the membrane embedded NRP-1 and possibly some fraction of soluble native dimers, while shNRP-1 is one of the soluble monomeric isoforms produced in physiological conditions.

NRP-1, as a membrane receptor, is a component of the pericellular matrix, which is continuous with the ECM. Together with other proteins and proteoglycans, which either share similar membrane localisation (NRP-1, CD44, syndecans), or are membrane attached by a glycosylphosphatidylinositol (GPI) anchor (netrins, glypicans) [206] or just associated to the

cell surface (several growth factors, truncated receptors, perlecan), they create an extremely complex network of the matrix with unique properties, often characteristic for a tissue/ organ [207, 208]. NRP-1, in that respect, is a well-known component of the endothelial ECM of cardiovascular and neural tissues [124], regulatory T lymphocytes [132] and stem cells [122].

NRP-1 is directly involved in protein and polysaccharide interaction networks. On the protein side, not only does it interact with specific function-assigned molecules described in Chapter 1, but also with several extracellular scaffold proteins, such as integrins [45–47]. Additionally, it indirectly controls integrin internalisation and fibronectin function [46]. These results indicate a role for NRP-1 in promoting cell adhesion. In respect to this function, NRP-1 was suggested to dimerise, both *in cis* and *in trans*, and this property, supposedly important for adhesion, was one of the subjects of this thesis.

Unfortunately, although the *in silico* analysis seemed to support dimerisation occuring via the c domains of NRP-1, the crosslinking method applied to the Fc rNRP-1-derived construct containing the c domain, but not the Fc part (crNRP-1), did not show formation of di/ multimerised species. Additionally, the same construct did not have oligosaccharide binding property similar to the Fc rNRP-1. The explanation of this result must take into consideration two possibilities. First of all, the EDC/ NHS method of crosslinking requires in close proximity a carboxyl and an amino group, which might not be present in the c domain interaction interface. In this case the dimerisation might have occurred, but was not detectable by the method. However, such an option would indicate that the actual NRP-1 dimerisation would not result in molecular properties similar to the ones of the Fc rNRP-1. Secondly, it is plausible that the mechanism of dimerisation needs some other structural elements, e.g., within the L2, whose presence in the crNRP-1 was not possible to verify. Such a possibility would be confirmed by the lack of oligosaccharide binding by crNRP-1 in the binding study.

Although the dimerisation of NRP-1 was not successfully confirmed in this study, it is an important issue, since the recombinant dimeric NRP-1, Fc rNRP-1, had very contrasting properties compared to those of the monomeric shNRP-1. Interestingly, applying surface-

based methods it was observed that only Fc rNRP-1 could efficiently bind to heparin, an HS proxy. shNRP-1 and tryptic digests of Fc rNRP-1 comprising either the same set of domains as shNRP-1 or a truncated variant additionally containing the c domain, did not bind to the polysaccharide surfaces. Since shNRP-1 seemed to bind to heparin *in solution* (detected in the stability test) and to heparin immobilised on a column, either surface-based methods were unsuitable to detect shNRP-1 binding to heparin due to conformational or accessibility difficulties or a dissociation rate of the complex resulted in too weak binding to be detected directly on a sensor surface. This suggests that the two proteins had very different mechanisms of interacting with heparin. This has important implications for the putative regulation of NRP-1 function. Namely, the dimerised NRP-1, contrary to its monomer, might be differently affected by the interaction with polysaccharides. These different properties of the two NRP-1s were also seen in *in vitro* studies in endothelial cells. Similarly to the distinct behaviour of the two proteins in the biochemical studies, in early angiogenesis assays, they elicited proangiogenic effects of varied potency, namely, Fc rNRP-1's was more potent than that of shNRP-1. Nonetheless, it is not possible to assess if this property of Fc rNRP-1 could be directly related to its higher affinity for polysaccharide binding.

This observation is important, as heparin is known to be crucial for NRP-1 regulation, although it is not yet clear how the interaction with polysaccharides affects NRP-1 function. Some observations following the presentation of NRP-1 to heparin have been made. It was observed that heparin enhanced VEGF-A_{165} [21,22,24,26,53], PlGF-2 [29,32], and SEMA3A [53,54], and allowed VEGF-C and VEGF-D [31], binding to NRP-1. On the other hand, NRP-1 is known to be a target of glyco-modification itself, which may result in decreased VEGF-A_{165} binding [209], or contrastingly, enhanced VEGF-A_{165} binding to NRP-1 [210]. These discrepancies open a possibility of a tissue specific regulation of NRP-1 function and emphasise the importance of the glycobiological aspect of the regulation of NRP-1 function. Thus, the present study supports the importance of polysaccharides in the regulation of NRP-1 function, and shows that it might be a reason of the major difference between the monomeric and dimeric

NRP-1 species.

However, there could be also another explanation of the varied response of the endothelial cells to the two proteins. Given that NRP-1 was found to interact with galectins (animal lectins) present in the extracellular *milieu* [167, 211], it is tempting to propose that it might be participating in the formation of glycoprotein lattices [41]. Such advanced structures, where galectins crosslink the N-glycans, is postulated to consolidate signalling for more consistent responses across the integrin network, where some form of coordination is proposed to occur among all the crosslinked constituents.

In this respect, the difference between the Fc rNRP-1 and shNRP-1 in exerting their proangiogenic effect could be directly related to their varied scope for engagement in such extracellular structures involved in the global signalling cascade. Fc rNRP-1, as a larger molecule of potentially higher avidity for cell surface epitopes, could be subjected to slower internalisation and at the same time evoke a more potent cellular response, due to its wider and more stable interactions. The comparison of the cell surface interaction and internalisation process of the two proteins could shed some light on the differences between them.

Some of the newly described features of NRP-1 may be involved in the dynamic adaptation of the ECM to the environmental conditions. First of all, as it was shown to interact with a degree of selectivity with variously sulfated heparin derivatives, this selectivity might be a detector of changing populations of the synthesised or enzymatically modified extracellular pools of HS. In this study Fc rNRP-1 was characterised by very high affinity (2.5 nM) for heparin, however, at the same time it bound well both persulfated heparin and triply desulfated heparin, which indicated, that it was not the presence of charge, but more complex conformational output which was a decisive factor for the binding. Although the functional aspect of this selectivity is not known, it seems a probable biophysical mechanism of regulation. An attractive hypothesis explaining the obtained result could be that NRP-1, when bound to the non-sulfated region of HS, is somewhat "blocked" and cannot form a signalling complex with other proteins having a preference for sulfate groups on HS. Consequently, signalling complex can be formed only

after a highly sulfated stretch of HS competes off its non-sulfated counterpart.

Additionally, it is known that NRP-1 is subjected to the enzymatic shedding machinery [68, 69, 71] that produces together with alternative splicing several shorter isoforms of NRP-1. Since according to this study shorter isoforms of NRP-1 were shown to have different heparin-binding properties from the dimerised variant, it is plausible, that alternative splicing and shedding could produce isoforms, which might drive distinct output responses of the cells.

Another novelty identified by this study is the topographical aspect of the heparin-binding site of the Fc rNRP-1. The characterisation of the protein side of the heparin interaction was performed using a P&L methodology. This approach revealed that lysines within large areas of the Fc rNRP-1 were involved in the interaction, which supported previously discovered requirement for large chains of oligosaccharides to efficiently bind to the protein (at least dp 26). The identified peptides covered fragments of the NRP-1 a1, b1, c domains, and the L2 linker region, but also fragments within the Fc part of the protein. The result implied that NRP-1 might interact with heparin via more binding sites than the hitherto identified one in the b1b2 domain, which was only partially confirmed in the P&L experiments, and that there are other areas within the multidomain structure of NRP-1 that can mediate this interaction. Still, it was surprising that both Fc part and the c domain were identified as heparin-binding sites, since neither were expected to interact with the polysaccharide. However, since the method does not distinguish between the areas of the Fc rNRP-1 that are directly involved in the interaction, and those which are indirectly undergoing a heparin-driven protection as a consequence of conformation change elicited by binding of the sugar, an analysis of the interaction surface of the c domain was made. By means of *homology modelling* and docking analysis, it was discovered that one of the P&L identified peptides was highly likely to be actually involved in a protein-protein interaction. Basing on this discovery, a model of the dimerised c domain was presented with the remaining P&L peptides creating a consistent surface interface that could be further involved in heparin interaction. Therefore, it was tempting to suggest that the P&L approach made it possible to indicate crucial regions of the Fc rNRP-1 involved in direct and

indirect interaction of heparin binding. Unfortunately, an attempt to experimentally validate the proposed model of a dimer of the c domains was not successful. Therefore, unless the method was not suitable for the confirmation of interaction for this particular protein, the *in silico* prediction remains a hypothesis, which will require an additional experimental approach to validate it.

The work on endothelial cells identified a novel function of NRP-1. As described before, both Fc rNRP-1 and shNRP-1 were able to drive proangiogenic responses in primary endothelial cells. A fascinating aspect of this finding is that the data indicated that this response is driven solely by the NRP-1 proteins through VEGFR-2, without requirement for VEGF-A, the growth factor that NRP-1 is believed to enhance the response to. In this study the recombinant NRP-1 proteins, activated VEGFR-2 and downstream signalling on their own. This discovery is important as it opens another mode of action of NRP-1 and adds one more mechanism responsible for driving the angiogenic responses in cells.

Future directions

Altogether, the data include novel observations and it will be important to follow the suggested hypothesis. In particular, the issue of the diversity of the soluble isoforms should be addressed to verify if any species of properties similar to Fc rNRP-1 are present *in vivo*. Secondly, the similarity of the Fc rNRP-1 and membrane oligomerised NRP-1 needs to be confirmed.

Next issue to investigate is the ability of the membrane and soluble NRP-1 isoforms to dimerise. This would shed some light on the membrane and soluble pools of NRP-1, and would facilitate design and interpretation of the research projects applying recombinant proxies of the particular isoforms. Additionally, it could confirm the predicted functional variability among the distinct isoforms, pronounced in this study by different heparin-binding properties. Possible functional differences between isoforms could also help analyse the dynamics of the changing pools of NRP-1 in response to certain stimuli.

Next, the experiments in cells that could clarify if the biophysical data on NRP-1 require-

ments of polysaccharide binding have implications on the functional regulation of NRP-1. This would require designing challenging cell biology experiments where the effect of particular heparan-sulfate mimetic structures on signalling/ responses could be investigated independently of each other.

Another issue, this time derived from the endothelial cells study, is the surprising proangiogenic effect of the shNRP-1. As currently, both anti- or proangigenic properties of soluble NRP-1 are documented, a localised context-dependent activity of the soluble NRP-1s is tempting to propose and should be tested. The issue of the shNRP-1 biotransport and *in vivo* interaction with polysaccharides could additionally help to create a model on its mechanism of function and possible modulation of activity.

Also, the fact that dimerised NRP-1 can mediate angiogenesis alone without VEGF ligands needs to be further explored, and, the final outputs should be included in the mathematical models of angiogenesis [93]. This could uncover more comprehensive picture of the dynamics of the angiogenesis.

Finally, several structural aspects of NRP-1, while being indicated and discussed in the study, still require further research. First of all, the c domain with the adjacent important linkers awaits crystallisation and presentation of its most complete structure. In a larger scale, an assembly of the full set of the domains into a comprehensive structure needs to be done. As a consequence, the interpretation of the P&L experiment and design of the validating experiments would become easier. At the same time, general understanding how large proteins, such as NRP-1, may interact with polysaccharides would be better.

Hopefully, elucidation of some of these mysterious aspects of NRP-1 biology will be achieved and soon, the picture of NRP-1 will bring some order into the more chaos-driven NRP-1 field at the moment.

Supplemental paper 1

Uniewicz, K. A. & Fernig, D. G. **2008**. Neuropilins: a versatile partner of extracellular molecules that regulate development and disease. *Front Biosci*, 13: 4339-4360.

Authors contributions:

Uniewicz, K. A. wrote the paper

Fernig, D. G. supervised the writing

[Frontiers in Bioscience 13, 4339-4360, May 1, 2008]

Neuropilins: a versatile partner of extracellular molecules that regulate development and disease

Katarzyna Adela Uniewicz [1], David Garth Fernig [1]

[1] *School of Biological Sciences, University of Liverpool, Crown Street, Liverpool L69 7ZB*

TABLE OF CONTENTS

1. Abstract
2. Introduction
2.1. Neuropilins' splice variants
2.2. Neuropilins' expression and function
3. Sequence analysis
3.1. Origins of the domains of neuropilins
3.2. Neuropilins' in sillico sequence analysis
4. Neuropilins' interactome
4.1. Structural features of neuropilins' interactions
4.2. Functional aspect of neuropilin interactions
4.3. Functional significance of neuropilins' interactions
5. Perspective: neuropilins in molecular networks
6. Acknowledgements
7. References

1. ABSTRACT

Neuropilins are a vertebrate-specific family of membrane multidomain proteins. They are crucial for the embryonic development of neural and vascular systems, whereas in the adult organism they are implicated in many processes, such as angiogenesis and the immune response. Additionally, it has been shown that they are overexpressed in numerous types of tumours, which results in higher microvessel density and correlates with poor prognosis. Their functions have been linked to their binding partners: semaphorins/collapsins, vascular endothelial growth factors (VEGFs), fibroblast growth factors (FGFs), hepatocyte growth factor/scatter factor and heparin/heparan sulfate (HS). Multiplicity of ligands alongside complex formation with several membrane receptors makes neuropilins potential 'hub' proteins, which act as a scaffold for multimeric associations. This review focuses on the structural features of neuropilins that underpin their multiple molecular interactions and hence their functions.

2. INTRODUCTION

Neuropilin 1 (NRP-1) was first identified as antigen A5, which was proposed to be a recognition molecule in the visual centre's neural cells (1) and a promoter of neural overgrowth (2). Subsequently, it was found to be a receptor for a family of semaphorins/collapsins responsible mainly for chemorepulsive neuronal responses, causing the collapse of the growth cone in nervous system development (2-4), however, a mediation of chemoattractive stimuli was also suggested (5). Additionally, the interaction of semaphorins with neuropilin-1 was linked to conveying an apoptotic response in neurons (6), which was dependent on the presence of neuropilin-1. A homologoue to the neuropilin-1 receptor for semaphorins was identified and named neuropilin-2 (NRP-2) (7-9). Similarly to neuropilin-1, neuropilin-2 was identified as playing a part in nervous system development (10).

2.1. Neuropilins' splice variants

In humans the gene encoding neuropilin-1 maps to chromosome 10 and that encoding neuropilin-2 to chromosome 2 (11). Both proteins are around 140 kDa and can be glycosylated. The two neuropilins, although encoded by distinct genes, arose from gene duplication and are structurally related, and consist of the same set of domains, the a1, a2, b1, b2 and c extracellular domains, a transmembrane domain and a short intracellular domain (12), where the a1 and a2 domains belong to the CUB (for complement C1r/C1s, Uegf, Bmp1) family, the b1 and b2 domains belong to the FA58C (for coagulation factor 5/8 C-terminal domain) family and the c domain belongs to the MAM (for meprin/A5-protein/PTPmu) family.

As a result of alternative splicing, there are several splice variants of both neuropilins (7, 11, 13, 14). Human neuropilin-1 has six splice variants, where four of them are soluble forms (Figure 1), while neuropilin-2 has five splice variants, but only one encodes a soluble form (Figure 2) (11, 15, 16). The highest diversity in sequence is observed in the C-terminal part of the proteins (starting where the b2 domain ends), which results in soluble forms that lack fragments of sequence or possess different sequence as a consequence of alternative splicing or the use of different open reading frames. In the case of neuropilin-1, all isoforms share the a1, a2 and b1 domains. The longest one (923 amino acids, isoform a) has also the b2 and c domains. Similar to isoform a is neuropilin-1 (906 amino acids, delta exon 16), which lacks small fragment between the c and the transmembrane domains. Among the soluble isoforms, there are two truncated neuropilin-1 proteins, lacking the C-terminus, including the c domain. These are $_{s12}$neuropilin-1 (644 amino acids, isoform b) and $_{sIV}$neuropilin-1 (609 amino acids, isoform c), where the latter also lacks a small fragment within the b-c linker, but they both contain intron 12 derived C-terminal 3 amino acid sequence (GIK). The other two soluble neuropilin-1s differ substantially in C-terminal sequences with respect to the other isoforms. The $_{s11}$neuropilin-1 isoform shares with other neuropilin-1 isoforms a fragment in the b-c linker, while further sequence is intron 11 derived, although it still shows some sequence similarity to the linker and c domain. The last soluble form (551 aa, $_{sIII}$neuropilin-1) is the only one lacking part of the b2 domain and the rest of the C-terminal sequence, and it uses a different reading frame in exon 12, which results some sequence similarity with the b2 domain.

Among the neuropilin-2 isoforms it is interesting that all but one share all 5 domains (a1, a2, b1, b2, c). The shortest isoform (555 amino acids, s9, isoform 6) is soluble, lacks part of b2 domain together with the rest of the C-terminus and similarly to $_{s11}$neuropilin-1, it has an intron 9 derived C-terminus, which shows similarity with the b-c linker. The longest isoform (931 amino acids, 2a22, isoform 1) has the full set of domains with transmembrane and intracellular domains. The 926 amino acids isoform (2a17, isoform 2) is missing 5 amino acids between the c domain and the transmembrane domain. The remaining two isoforms (grouped as isoforms b in contrast to the previously described two full-length isoforms a) have a distinct C-terminus, which is a result of alternative splicing and is suggested to encode a functional transmembrane and intracellular domain. The difference in length is due to a short fragment after the c domain that the longer isoform encodes (906 amino acids, 2b5, isoform 4), but not this shorter isoform (901 amino acids, 2b0, isoform 5).

Analysis of mRNA expression patterns of variants has revealed that the isoforms are not equally expressed in human tissues. The tissue specific expression pattern of neuropilin-1 isoforms seems to be largely overlapping (brain, heart, kidney, liver, lung, pancreas, placenta, trachea), however, the mRNA level of isoforms IIIs and IVs of neuropilin-1 is 3 and 10 times less abundant, respectively (11, 15). Contrary to neuropilin-1, the isoforms of neuropilin-2 seem to have a more diversified pattern of expression. While isoforms a of neuropilin-2 are dominating in liver, small intestine and placenta, the isoforms b dominate in heart, skeletal muscles and lung. Interestingly, difference in expression levels between the two known isoforms a (2a22 and 2a17) was also observed with significant predominance of 2a17 isoform and 2a22 isoform expressed in smaller amounts in lung, placenta and trachea (11). The mechanism of the control of the expression of specific isoforms is not known.

The protein sequence differences between neuropilins indicate putative modes of action. Firstly, the multiplicity of truncated/soluble isoforms suggests competition and titration mechanisms, where soluble isoforms would be responsible for binding of potential ligands and, therefore, would diminish the local concentration of the ligand available to form signalling complexes with membrane-bound neuropilins. The ligands of neuropilins titrated out by competing soluble isoforms are not known. However, this has been questioned, as the level of these isoforms may not always be physiologically significant (15). Nevertheless, a competition related antitumour property was confirmed *in vivo* with a $_{s12}$neuropilin-1 overexpression system. In addition, the difference between transmembrane and cytoplasmic fragments gives rise to a potentially greater multiplicity of interacting partners. The various short length insertions could possibly disrupt domain structure and consequently structure-dependent interactions, e.g., dimerisation. However, in several studies, no difference in binding features between the short and full length isoforms was detected. Thus, $_{sIII/sIV/s12}$neuropilin-1s interaction with VEGF165 and SEMA3A was confirmed in binding assays (15), independently interaction of VEGF165 with $_{s12}$neuropilin-1 in crosslinking experiments was demonstrated (16) and neuropilin-1(deltaexon16) VEGF165 interaction was confirmed as well (13).

Together with the varied expression pattern, these features expand the possibilities of the mechanism of action of these related proteins. Moreover, it seems that a similar set of functional domains is not only characteristic of neuropilins. One other protein was discovered in human coronary arterial cells, ESDN (endothelial and smooth muscle cell-derived neuropilin-like molecule), which contains CUB and FA58C domains and it was suggested to play a variety of roles akin to those of neuropilins (17).

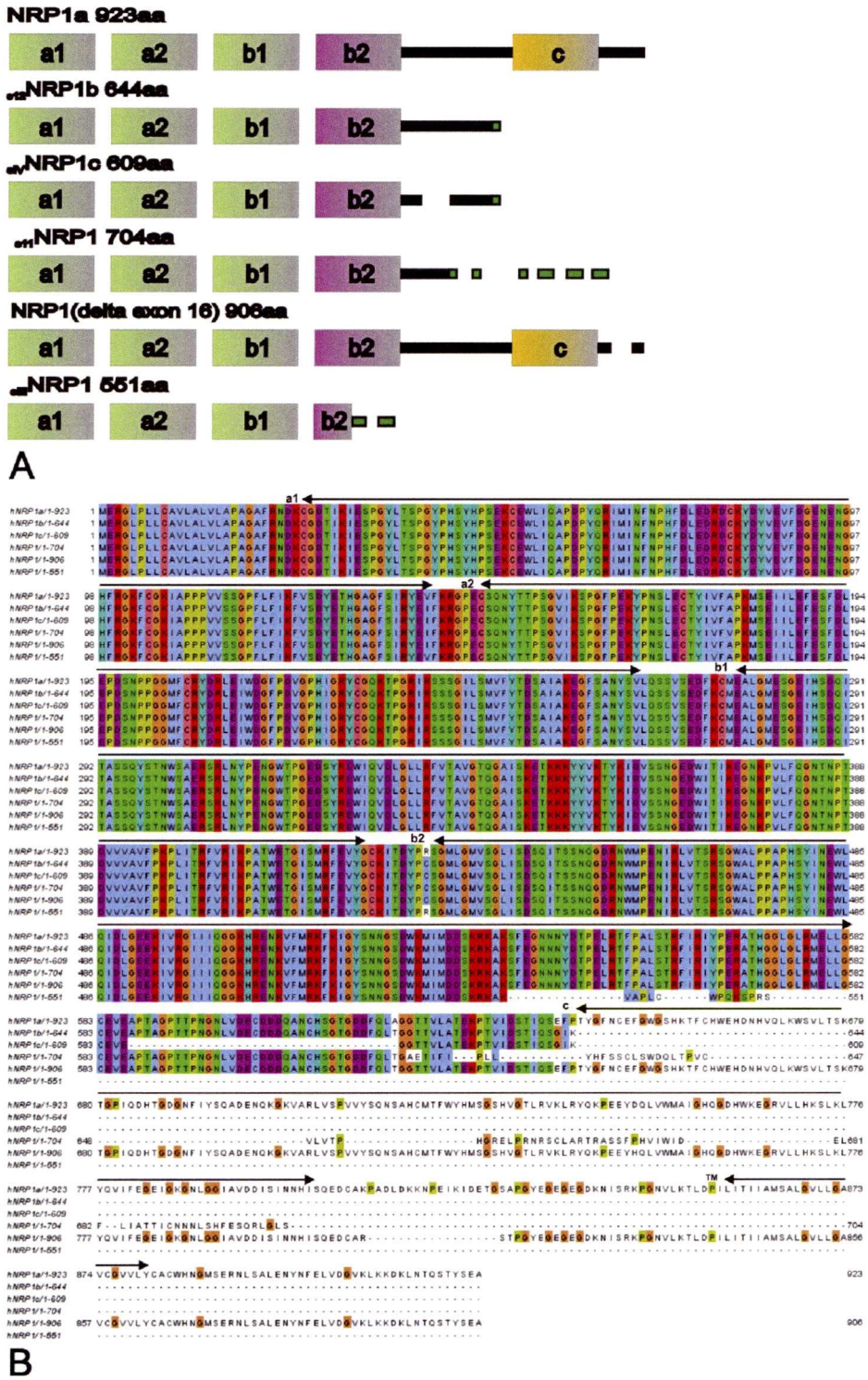

Figure 1. Human neuropilin-1 isoforms analysis; a) schematic representation of multiple alignment, the names of isoforms and domains are indicated, alternative sequences are labelled in green; b) detailed multiple alignment in ClustalW color mode, the sizes of isoforms are indicated together with their symbols and the domains are marked above the sequence.

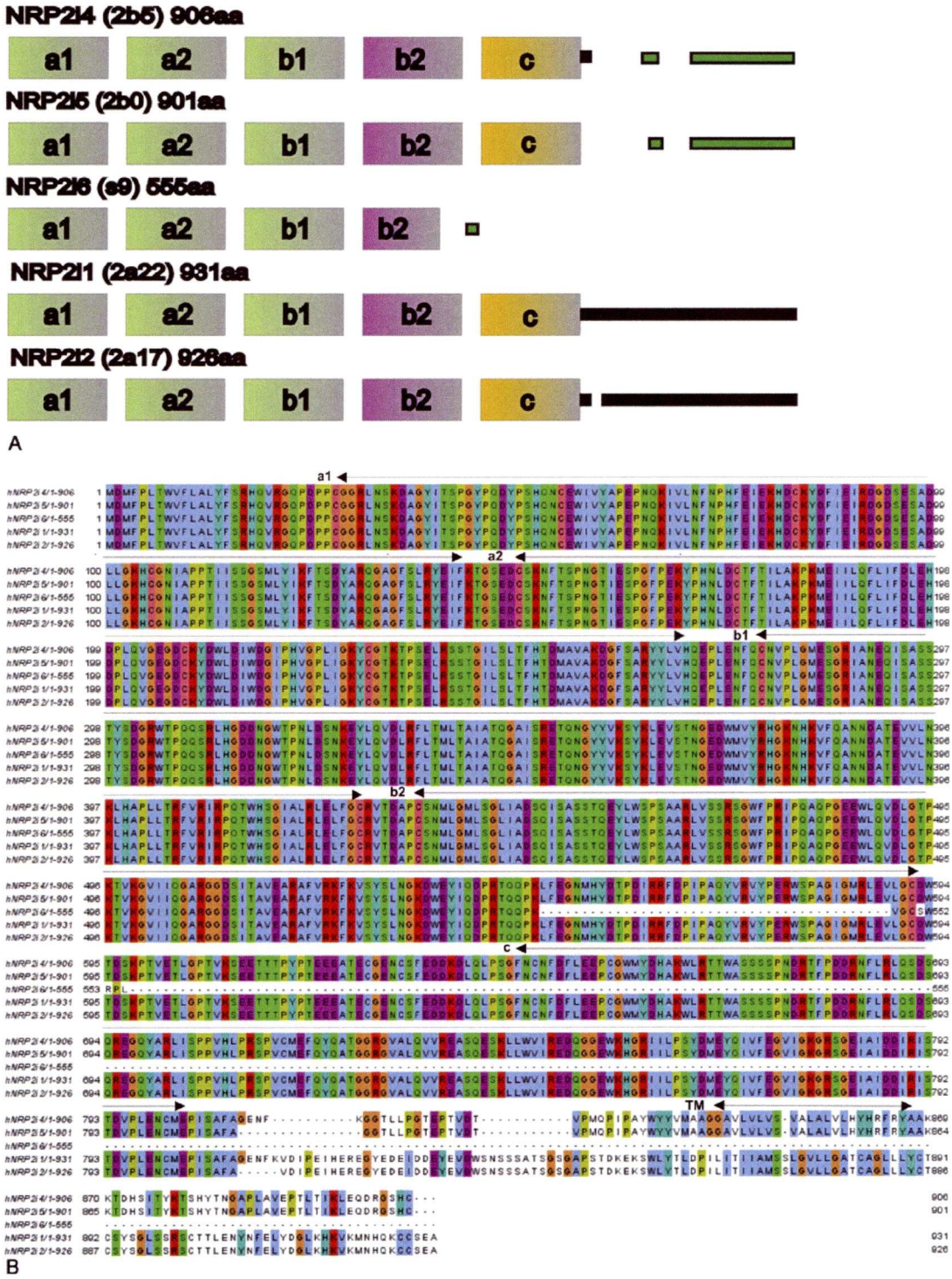

Figure 2. Human neuropilin-2 isoforms analysis; a) schematic representation of multiple alignment, the names of isoforms and domains are indicated, alternative sequences are labelled in green; b) detailed multiple alignment in ClustalW color mode, the sizes of isoforms are indicated together with their symbols, and the domains are marked above the sequence.

2.2. Neuropilins' expression and function

Genetic studies aiming to elucidate functions of neuropilins have been carried out. In mice, deletion of neuropilin-1 is embryonically lethal in E12.5, and causes defective neural patterning and vascular regression (2, 18). Interestingly, the neural phenotype resembled the knockout of Sema3A, while the vascular phenotype in comparison to VEGFR2 knockout suggested a requirement for neuropilin-1 in late embryonic vasculogenesis and the early development of the cardiovascular system. Neuropilin-1 overexpression also has severe consequences, namely heart and blood-vessel formation abnormalities such as excess capilaries and vessels and hemorrhaging and malformation of heart, as well as defects in the nervous system and limbs (19). Significantly, it was shown that neuropilin-1 and neuropilin-2 knockouts do not have the same phenotypes. Neuropilin-2 knockouts have a 40% death rate occurring close to birth and survivors, apart from being smaller in size, have reduction of lymphatic vessels and capillaries or their missposition and neuronal defects (10, 20, 21). In these mutants no change in the blood vessel system was observed. Interestingly, it was shown that both knockouts, neuropilin-1 and neuropilin-2, became unresponsive towards their semaphorin ligands, Sema3A and Sema3F, respectively (2, 10). Simultaneous knockouts of both genes causes E8.5 embryonic lethality (22).

Although these most severe defects after interference with native levels of neuropilins affect mainly blood-vessel and neural systems, neuropilins have been confirmed to be expressed in many other tissues, often in a specific manner. Generally, both neuropilins have been shown to be expressed by several types of organs and tissues, which makes them a wide ranging interacting partner, however, their mRNA expression patterns are often not overlapping (7, 23). This emphasizes the issue of the likelihood of neuropilin-1 and neuropilin-2 possessing distinct functions. In the case of endothelial cells it has even been suggested that, while arterial areas express neuropilin-1, veins produce mainly neuropilin-2, and that this pattern of expression might affect tissue identity (24). A hormone driven interplay between neuropilin-1 and neuropilin-2 in human endometrium was also observed. Under the natural menstuation cycle an estradiol-dependent upregulation of neuropilin-1 in the proliferation phase was followed by neuropilin-2 upregulation in the secretion phase, which is also indicative of distinct functions for the two proteins (25).

Information about the function of neuropilins can be also deduced from data on the regulation of the expression of their mRNAs. There have been several transcription and growth factors identified that influence their expression (reviewed in (23)). Ets-1 (26), dHAND (27), SP1 (28) and AP1 (28) increase expression of neuropilin-1 mRNA. Ets-1 and dHAND upregulation of neuropilin mRNA is generally linked to vascularisation processes, whereas the upregulatory effects of SP1 and AP1 have been obtained from promoter sequence analysis in cell culture. Growth factors identified that upregulate neuropilin-1 mRNA include TNFα(29), VEGF, EGF (30-32) and IL-6 (33). TNFα has angiogenic properties *in vivo*, and at the molecular level it has been shown to upregulate both VEGFR2 and neuropilin-1, which has been suggested as the mechanism whereby it potentiates VEGF action though, in another study this effect was not observed (30). Upregulation of neuropilin-1 has also been observed to be associated with VEGF and EGF – presence of these growth factors in tissue is associated with increases in the amount of mRNA encoding neuropilin-1. In pancreatic cancer cells IL-6 has been found to upregulate neuropilin-1 mRNA. An orphan receptor, Nurr1, was shown to upregulate the levels of neuropilin-1, in the course of the formation of dopamine neurons in midbrain (34). Cyclophilin A, a protein known to be involved in the regulation of vascularisation and cell growth, was shown to upregulate neuropilin-1 mRNA levels in aorta smooth muscle cells (35). Among the transcription factors responsible for downregulation of mRNA encoding neuropilin-1 are COUP-TFII (36), Prox-1 (37), HEX (38) and NRSF/REST (39). NRSF/REST was found to suppress the expression of neuropilin-1 mRNA in keratinocytes. COUP-TFII, by suppressing neuropilin-1 mRNA expression within the vasculature, permits arterial-venial differentiation. In this process, COUP-TFII dependent downregulation of neuropilin-1 mRNA in presumptive veins enables them to acquire the characteristics of vein. Prox1 controls an analogous switch in differentiation of blood and lymphatic endothelium. Here, the downregulation of neuropilin-1 is a characteristic of developing lymphatic vasculature from classical blood vessels. Altogether, these results indicate that the expression of mRNA encoding neuropilin-1 is subjected to a variety of regulatory inputs, though a regulatory signalling network responsible for the control of the levels of neuropilin mRNA has yet to emerge. The extent to which these changes in expression of mRNA encoding neuropilin-1 may be affected by neuropilin-2 is not known. Moreover, in the event of co-expression of the two neuropilins changes in their relative expression may also affect the cellular response, though this has yet to be documented directly.

Much less is known about mRNAs encoding neuropilin-2. High levels of neuropilin-2 mRNA were suggested to be major drive of axonal regeneration. Consistently, neuropilin-2 blocking antibodies prevented first step of regeneration, which is axonal aggregation. Moreover, forskolin, the axon aggregation mimetic, was able to downregulate neuropilin-2 mRNA and thus, confirm its role in regeneration process (40).

It is worth noting that expression of neuropilins is also dependent on the cell microenvironment. Hypoxia, which results in acidic pH has been found to upregulate neuropilin mRNA. This is important, as hypoxia is a major driver of angiogenesis and commonly occurs upon tumour development, when a shortage of oxygen results in the accumulation of lactate and CO_2 in the extracellular compartment and causes pH values to be as low as 5.5 (41, 42). Hypoxic conditions upregulate several mRNAs of angiogenesis-related proteins, including neuropilin-1 and neuropilin-2, which lead to enhanced vascularisation (21, 43-45). However, it is noteworthy that so far a direct link

between the expression of the neuropilins' mRNA and HIF (hypoxia-inducible factor), a key molecular regulator of the hypoxic response, has not been confirmed.

Initial studies aiming to characterise mouse gene expression during embryonic and early postnatal development show that neuropilin-1 mRNA is expressed in the cardiovascular system, nervous system and mesenchymal tissues surrounding them (19, 46). A general pattern is that rather than being generally expressed in these tissues, neuropilin-1 expression is instead focused to certain types of cells and this localised expression is often temporally regulated. Interestingly, initial observations suggested that neuropilin-1 might be an auto-recognition molecule, as it was abundant in actively growing axons and the target of these axons also expressed neuropilin-1. Subsequently, interactions with other molecules were identified. Consequently, another function postulated for neuropilin was neuronal circuit formation (46). In the cardiovascular system high levels of neuropilin-1 are found in vessel system epithelium and also in the surrounding blood vessel mesenchymal cells. Additionally, expression is detected in endocardial cells in developing heart. Interestingly, in adult mouse the expression drops and is mainly localised to heart atria. Neuropilin-1 expression is also pivotal in limb development, where initial high levels in mesenchymal cells are replaced by only connective tissue expression (19). In human adult tissues neuropilin-1 is highly expressed in heart and placenta and at lower levels in lung, skeletal muscles, kidney and pancreas (14). Mouse neuropilin-2 expression is also dynamically regulated and is largely separable from that of neuropilin-1 in the nervous system. Additional locations of neuropilin-2 expression are limb bud muscle masses, bones, smooth muscle of the gut, intestinal epithelium, kidney, lung, inner ear, submandibular glands and whisker follicles of the snout (7).

Neuropilin mRNAs share a feature of being overexpressed in a number of cancers, although usually not in a redundant manner (reviewed in (23, 47, 48)). High levels of neuropilin-1 or neuropilin-2 often correlate with increased tumour size, neovascularisation, decreased tumour apoptosis, tumour cell migration and clinically is often associated with poor prognosis (49, 50). However, the association between the levels of expression of neuropilin-1 and patient prognosis is somewhat contradictory. Thus, in colon cancer one study that measured the level of expression of mRNA encoding both soluble and membrane bound neuropilin-1 suggested that neuropilin-1 expression correlated with a better patient prognosis (51), whereas another study that used immunocytochemistry and presumably was biased towards the detection of cell-associated neuropilin-1 protein suggested that neuropilin-1 was associated with a poor disease outcome (52).

3. SEQUENCE ANALYSIS

3.1. Origins of the domains of neuropilins

Both neuropilins are comprised of the same set of domains, a1, a2, b1, b2 and c, where a1 and a2 belong to the CUB (for complement C1r/C1s, uEGF, BMP1) family (53), b1 and b2 belong to the FA58C (coagulation factor 5/8 C-terminal domain) family (54) and the c domain belongs to the MAM (for meprin/A5-protein/PTPmu) family. CUB domains have been for some time recognised as important elements of developmentally significant proteins, e.g., bone morphogenic protein (BMP1), sea urchin endothelial growth factor (uEGF) and subcomponents of complement (C1r/C1s), spermadhesins, some vertebrate proteases and mammalian hyaluronate-binding protein TSG-6. The function of CUB is related to binding sugars, dimerisation (55) and protein-protein interactions (56). The FA58C domains are characteristic of coagulation factors and of discoidin proteins. They are found in milk fat globule membrane proteins, receptor tyrosine kinases and contactin-associated proteins. The function suggested for these domains is binding of anionic phospholipids on the surface of cells, and a consequent role in adhesion and cell-cell recognition. The MAM domain was found in a surface glycoprotein called meprin and a receptor-like tyrosine protein phosphatase (RPTP mu). MAM domains have been suggested to play a role in protein dimerisation (57) and cell-cell adhesion (58). Importantly, none of the neuropilins has an intracellular domain with clear interaction or signalling motif.

According to the Blast search engine the organisation the domains found in neuropilins evolved relatively late and is not present in any group of organisms other than vertebrates. However, the individual domain families are commonly represented in many systematic groups. CUB-like domains are found in viruses, bacteria, euglenozoa and across metazoa; FA58C is found in wide range of bacteria, archea, metazoa, mycetozoa, fungi, parabasalidea, viridiplantae, haptophyceae; MAM domain is not found in viruses, but is present in many groups of bacteria, in alveolata and metazoa. Therefore, neuropilins arose from old evolutionary motifs that in this particular juxtaposition formed a protein of new functions related to vertebrate-specificity.

3.2. Neuropilins' *in silico* sequence analysis

Although neuropilins show domain structure similarity, comparison of the amino acid sequence between human neuropilin-1a (923 amino acids, Fig.1) and neuropilin-2 (2a17, isoform 2, Fig.2) reveals 44% identity (Figure 3). Moreover, the level of conservation is not uniform throughout the sequence. The highest similarity is observed in the transmembrane region, whereas the lowest is in the c domain and its flanking regions that link it to adjacent domains. In fact, analysis of the C-terminal part of the sequence (the transmembrane and intracellular domains) reveals that neuropilin-2a isoforms show more sequence similarity with neuropilin-1 than neuropilin-2b isoforms (11). Interestingly, analysis of charged residues in sequences of both human neuropilins shows, that although some of the charged residues are similar in the alignment, there are a good number of residues of opposite charges in the two proteins, which may be associated with important differences in function (Figure 4). Comparison of human, mouse, rat and zebrafish sequences of most similar length gives interesting insights into evolutionary conservation. The zebrafish sequences of both neuropilins vary substantially from the others, which is apparent in the

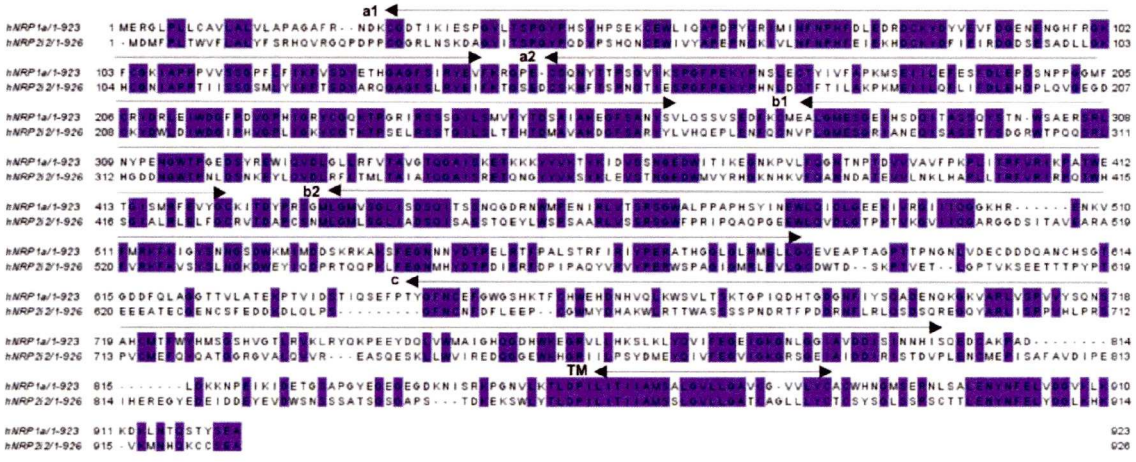

Figure 3. Comparison of most similar human isoforms of neuropilin-1 (isoform a) and neuropilin-2 (isoform 2); the sizes of isoforms are indicated together with their symbols, the domains are marked above the sequence, the residues marked in blue are identical.

number of mismatches, insertions and deletions, especially in the neuropilin-2 b-c linker and c domain and to lesser extent in the same region in neuropilin-1. However, another isoform of zebrafish neuropilin-1, isoform b, has several larger insertions, e.g., 23 amino acids in the b-c linker and 19 amino acids in the c domain (not shown). Overall, the transmembrane and cytoplasmic fragments seem to be most conserved between species, which suggests that the intracellular part of neuropilins may interact with intracellular signalling cascade proteins (59), despite this region having no obvious signalling motifs. When the number of mismatches is considered, the a and b domains are more conserved in neuropilin-2 (21 mismatches versus 55 in the a and b domains in neuropilin-1), while in neuropilin-1 it is c domain that has the lowest number of substitutions (8 mismatches versus 20 in the same region in neuropilin-2) (Figure 5, 6). To summarise, sequence analysis shows that the sequence of zebrafish variants of neuropilins differ to some extent from those of other organisms. Comparison between human, mouse and rat sequences and also between human neuropilin-1 and neuropilin-2 show distinct conservation patterns in different parts of the protein, which is a good indication of putative diverse functions.

Interestingly, the *in silico* analysis of neuropilin sequences in search of putative N-glycosylation and O-glycosylation sites reveals one possible important feature of the multiple splice variants (Figure 7, 8) (60, 61). Most N-glycosylation sites are located in the regions shared by all neuropilin-1 and neuropilin-2 isoforms. Thus, among neuropilin-1 isoforms, four out of six N-glycosylation sites are shared, whereas the sites in the flanking regions of transmembrane domain are shared only by the two longest variants of neuropilin-1. In neuropilin-2 isoforms, two out of four sites are common, one site is absent only in the most truncated isoform 6, and another is only present in the two longest variants of neuropilin-2. Analysis of potential O-glycosylation sites reveals that there are two such sites in both proteins and they localise in both cases to the b-c linker, the least conserved part of the sequence. In neuropilin-2 both predicted sites are shared by all isoforms except for isoform 6. In neuropilin-1 there are also two potential O-glycosylation sites and the shortest isoform sIII lacks both, while the s11 and sIV isoforms have just one, but each of them has a different one. Isoforms a, b (s12) and delta exon 16 share both putative sites. Serine 612 of neuropilin-1 isoform a, which has been suggested to be facultatively glycanated by the glycosaminoglycans heparan sulfate and chondroitin sulfate (62), is located very closely to the region containing the predicted O-glycosylation sites. It is important to note that the interdomain linkers in both neuropilins have no recognised structure. These are likely to be important in mediating domain orientation, interactions with other proteins and contain posttranslational modification sites (63). Thus, these putative posttranslational modification sites could be a part of the regulation of the function of neuropilins.

4. NEUROPILINS' INTERACTOME

The number of different molecular interactions that neuropilins make describe an ever-increasing catalogue of partners. These interactions are, where it is known, associated with particular domains of neuropilin. Alongside the large number of normal and pathological events where neuropilins have been suggested to play important regulatory functions, this suggests that the domains of neuropilins may provide a set of modules involved in multiple molecular interactions. Thus, one view of neuropilins is as a scaffold for cell-cell and cell guidance signalling.

Initially, molecules related to the function of neuropilins were discovered in the neural system, e.g., plexins, semaphorins (firstly SEMA3A) (64). Subsequently, more interacting partners were discovered, like L1-CAM, which is an adhesion molecule that can

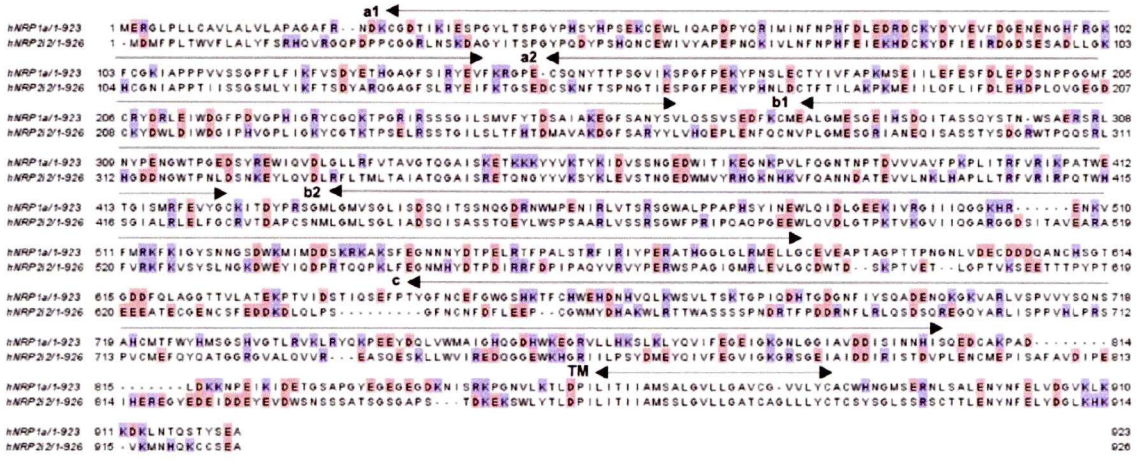

Figure 4. Comparison of charged residues pattern in human neuropilin-1 (isoform a) and neuropilin-2 (isoform 2); the sizes of isoforms are indicated together with their symbols, the domains are marked above the sequence, the basic and acidic residues are marked blue and red, respectively.

modify the SEMA3 repulsive signals (65). The next group of partners of neuropilins were the glycosaminoglycans heparan sulfate, the dominant scaffold and long-range integrator of extracellular signals (66) and members of the VEGF family that bind to heparan sulfate (67). The latest group of partners of neuropilins are prion protein, several members of the FGF family (fibroblast growth factor) and HGF/SF (hepatocyte growth factor/scatter factor) and receptors such as FGF receptor 1 (68), VEGF receptors (69-71) and integrins (72). These proteins are structurally unrelated and apart from integrins they possess in common only one feature: binding to sulfated glycosaminoglycans such as heparan sulfate. Not typical was the discovery of NIP (neuropilin-1 interacting protein), a protein containing the common protein interaction motif PDZ that binds the intracellular part of neuropilin-1 (59). Adding to this complexity are dimerisation and possibly higher order oligomers of neuropilins that have been observed (9, 68, 73, 74). Interaction with heparan sulfate may modify binding affinities and is likely to bring neuropilin into proximity with many complexes involved in cell adhesion and cell-cell communication. In some cases the protein-protein interactions were suggested to occur upon heparin binding, e.g. interaction of neuropilin-1 with VEGFR2 (75) or neuropilin-1/2 with VEGFD (76). Additionally, it has been hypothesised that heparin/heparan sulfate might cause multimerisation of neuropilin-1 (69), however, a mechanism whereby heparin/heparan sulfate serves as a docking molecule for multivalent interactions with neuropilin-1 has also been suggested (77).

4.1. Structural features of neuropilin interactions

The structure of neuropilins suggests they might be a scaffold for protein-protein interactions. This idea is supported by an increasing body of evidence from studies using a variety of approaches such as deletion analysis, mutagenesis, crystallography and biophysics.

Investigation of semaphorin binding until recently had no underpinning from structural biology. Thus, what was initially suggested from deletion studies was that the sema domain of semaphorins bound the a1a2 domains and that these interactions defined the specificity of binding, whilst basic C-terminal region of semaphorins binds to a1a2 and b1b2 (4, 78, 79). In another study the semaphorin specificity was attributed to both regions of a1a2 and b1b2 domains (9). In parallel, it was shown for neuropilin-2 that binding SEMA3F required both a1a2 and b1b2 domains (80). Subsequent work refined the identification of potential semaphorin binding sites by mutational analysis. Basing on structural alignment of the neuropilin-1 a1 domain and bovine spermadhesin CUB domain, residues likely to be exposed to solvent in the a1 predicted loop regions were identified and mutated into residues of opposite charge (residues 46, 47, 51, 52, 53, 79, 80, 128, 129, 130). The introduced mutations inhibited binding of semaphorin, but not that of VEGF. Importantly, these mutations had inhibited the binding of both SEMA3C and F, indicating that the discrimination between these two semaphorins was lost. Also, no effect of these mutations was observed on the interactions with plexin and VEGFR2 (79). Recently, this body of data could be compared to a crystallographic model of neuropilin-2 domains a1 to b2 in complex with a semaphorin-specific blocking antibody (77). The region where the antibody is binding neuropilin-2 is in a1 (residues 39, 45-47, 72-77, 107, 138) and is highly conserved in the neuropilin-1 a1 domain. The antibody binding area appears to be adjacent to the region characterised by Gu et al. as a semaphorin binding region, therefore, together these data span the semaphorin binding site on a larger interface of the a1 domain. Moreover, as a putative calcium binding motif was discovered in crystal models of the a1 domain in close approximity to the characterised semaphorin binding site, it was shown that the interaction with semaphorins is indeed calcium dependent (77).

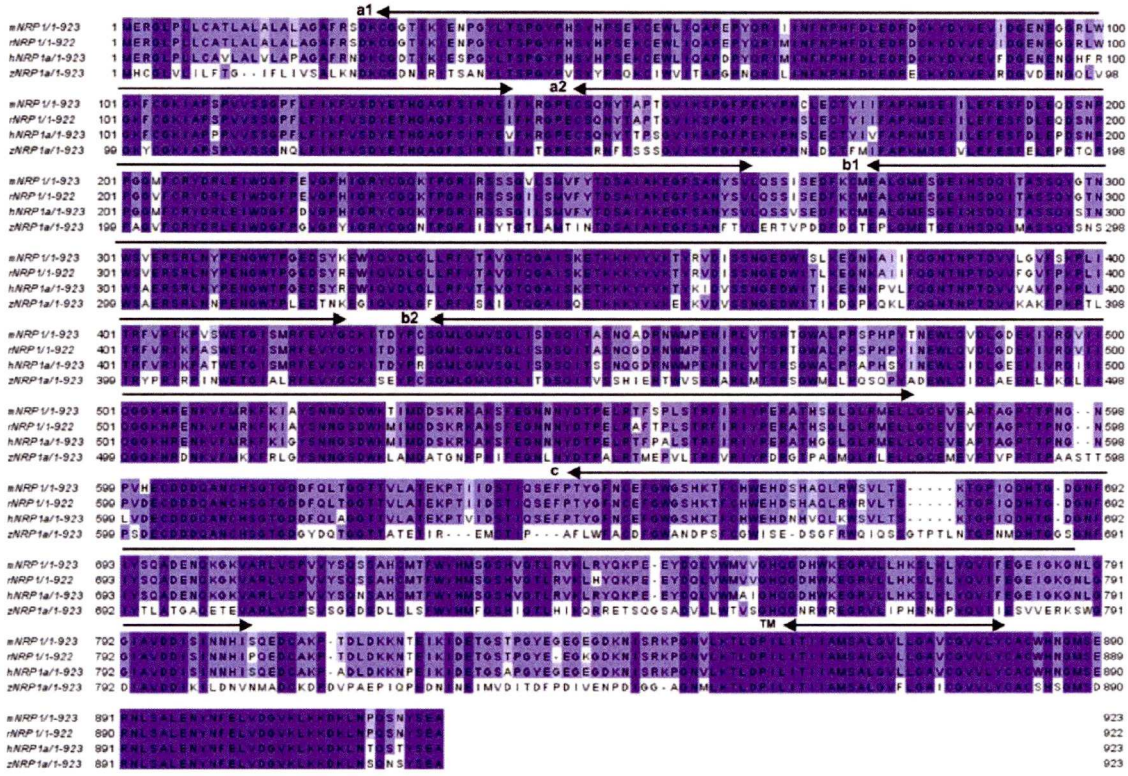

Figure 5. Comparison of most similar human (isoform a), mouse, rat, zebrafish (isoform a) neuropilin-1 sequence; the sizes of isoforms are indicated together with their symbols, the domains are marked above the sequence, the residues marked in blue are identical.

By and large the analysis of VEGF165 binding structures in neuropilins has been supported by subsequent crystallographic models, initially of the human b1 domain and then of rat b1b2 domains (81, 82). Similarly to semaphorins, it was shown by deletion analysis that the b1b2 domain is crucial for the binding of VEGF165 to neuropilin and that the additional presence of the a1a2 domain enhanced the binding (79, 83). Similar results were obtained for the interaction of VEGF165 and neuropilin-2 (80). On the other hand the related PlGF was suggested to bind to only the b1b2 domain of neuropilin-1 and its binding sites in the b domains was thought to overlap with that of VEGF165 (83). Mutational analysis of neuropilin-2, based on sequence similarity with the known neuropilin-1 b1 domain crystal structure, indicated the electronegative loop in the b1 domain as the putative binding site of VEGF165 (residues 284, 287, 290, 291). As the interaction between neuropilin-1 and VEGF165 was suggested to occur via the positively charged heparin binding domain of VEGF (68), the mutation of electronegative residues reduced the binding of VEGF165, whilst mutations introducing more electronegative residues enhanced binding of the growth factor. No change in the Kd for SEMA3F binding was observed as a consequence of these mutations (80). The crystal of the b1b2 domain with tuftsin, a peptide analogue of the basic heparin binding domain in the C-terminus of VEGF, suggests a binding site for this domain of VEGF 165 in a part of b1 (residues 297, 301, 320, 353, 346, 349) adjacent to the area mutated in neuropilin-2 (80). Interestingly, the binding pocket identified in the crystallographic model fits the basic tail that of VEGF165, tuftsin and SEMA3A, however, the latter lacks the C-terminal arginine, which seems to be crucial for the binding. Consequently, it has been suggested that several modes of ligand binding are possible (82). This binding site was further confirmed in a study where a crystal of neuropilin-1 b1 domain with VEGF165 blocking antibody was obtained, however, a broader interface between these molecules was suggested, spanning the b1b2 domain of neuropilin-1 towards putative heparin binding site (77).

The physical and functional relationship of the binding sites semaphorins and VEGF in neuropilin is contentious. A competition effect of SEMA3A and VEGF165 was observed in cell migration and growth cone collapse assays (84). Functionally, in lung cancer VEGF was suggested to promote tumour development while semaphorins were suggested to act as inhibitors of this process (85). Additionally, mechanism of VEGF dependent neuropilin-1 internalisation was observed and explained as a support of preferential VEGF signalling inhibiting

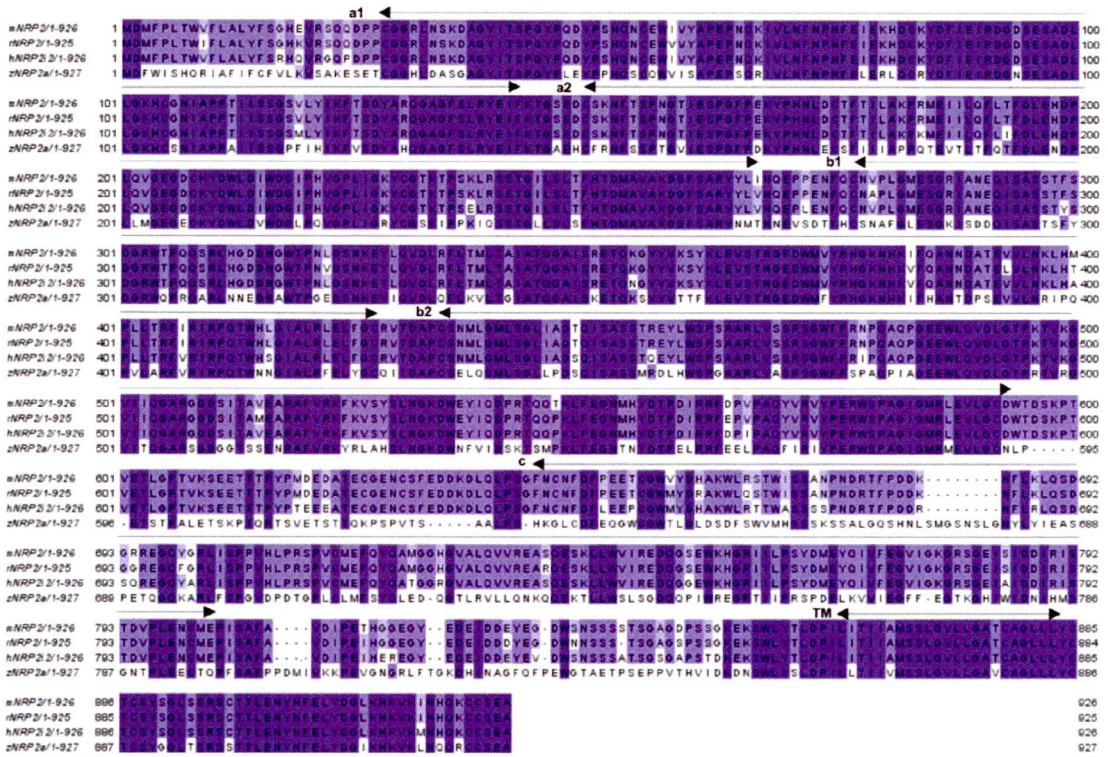

Figure 6. Comparison of most similar human (isoform 2), mouse, rat, zebrafish (isoform a) neuropilin-2 sequence; the sizes of isoforms are indicated together with their symbols, the domains are marked above the sequence, the residues marked in blue are identical.

neuropilin-semaphorin interactions (86). Interestingly, competition with semaphorins was not observed for VEGF121, VEGFB and FGF2 (86). Similarily, it was shown that neuropilin-2 complexed with VEGFR2/3 promotes cell survival by interaction with VEGFA/C, which is functionally inhibited by interaction of neuropilin with SEMA3F (87). This idea was supported by a crystallographic study of the b1 domain of neuropilin-1, and it was suggested that a pocket binding C-terminal arginine of VEGF analog tuftsin can possibly accommodate also basic tail of semaphorins (82). Nevertheless, recent studies argue against a physical overlap of the VEGF and semaophorin bidning sites. Firstly, mutation and deletion studies aimed at characterising the VEGF and the semaphorin binding sites indicate that these are locateD within different domains of neuropilin, i.e. while VEGF binds mainly b1b2 domains, the semaphorins interact with a1a2 domains (79, 80). Secondly, the ability of semaphorin binding to the same pocket as VEGF was excluded because of a lack of the highly conserved arginine as the very C-terminal residue, which is crucial for interaction with the VEGF analog tuftsin (77). Thirdly, crystal structure study depicting binding sites for both ligands by analysis of structures of neuropilin domains with ligand binding blocking antibodies suggests that the biding sites are separated by 65 Angstrom. This independence of binding is also supported by optical biosensor experiments in which footprinting of SEMA3A and VEGF165 binding sites in neuropilin was attempted and interpreted as independent event (77). Finally, functional independence is indicated by experiments in mouse developmental. A study in branchiomotor neurons expressing neuropilin-1 showed that the axon and somata have distinct affinities for VEGF165 and semaphorins and it was suggested that the somata is controlled by VEGF165, while the axon by semaphorins in a neuropilin-1 dependent manner without competition between tehse ligands (88). In other mouse developmental studies only selective preference for distinct ligands was observed during development of vascular and neural systems without direct competition (89). Taken together, it seems as if physical competition for binding to neuropilin may not occur, but that it is possible to engineer a situation where instances functional competition does take place. A comprehensive and quantitative analysis of the interactions of neuropilin with these and other ligands would certainly help to determine the circumstances necessary for competition (functional or otherwise) between VEGF and semaphorins to occur.

Qualitative binding studies have suggested that a tetradecasaccharide is the minimal structure able to bind the b1b2 domain of neuropilin-1. It has been further suggested that a mechanim of dimerisation of neuropilin is mediated by heparin at a 2:2 ratio of heparin:neuropilin.

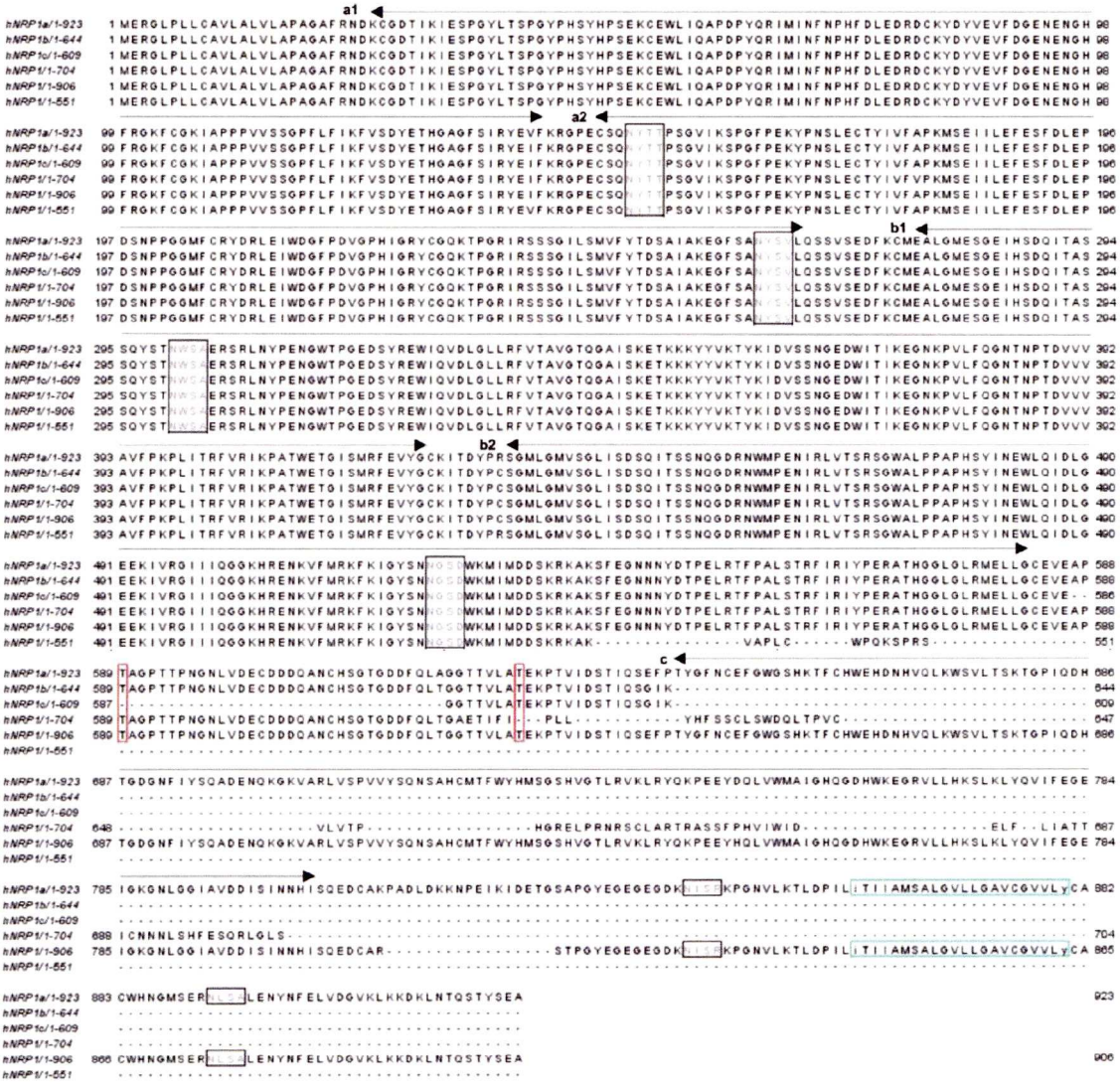

Figure 7. *In silico* analysis of human isoforms of neuropilin-1; the sizes of isoforms are indicated together with their symbols, the domains are marked above the sequence, sequences in black frame are putative N-glycosylation sites, sequences in red frame are putative O-glysylation sites, sequence in green frame is transmembrane region.

However, given that there is no direct evidence for an interaction between neuropilin molecules in such polysaccharide-protein complexes, it remains to be seen whether heparin does in fact cause neuropilin dimerisation or whether, by virtue of this polysaccharide possessing multiple overlapping binding sites it simply "bridges" neuropilins. The residues involved in heparin interaction based on the crystal structure are 359, 373, 513, 514, 516 and locate on the surface of b1b2 adjacent to tuftsin binding pocket, therefore, such proximity may support a mechanim of increased affinity for VEGF165 mediated by neuropilin-1 (77, 82).

Dimerisation of neuropilins has been also suggested to occur through the c domain. However, mutants without c domains still show a degree of dimerisation and, therefore, another domain may also mediate neuropilin homophilic interactions (4). Moreover, it has been shown that interactions between neuropilins are likely to be driven by ionic bonding (68). In crystallographic studies an additional dimerisation role was ascribed to the a1 domain, due to its conserved putative interface and flexible character. A model where dimerisation via the a1 and c domains together with heparin interaction take place was suggested. Consistent with this model is enhanced VEGF binding and independent location of semaphorin binding site in such a dimer (77).

As neuropilins mediate cellular responses, requirements for signal transduction were studied. It was

Figure 8. *In silico* analysis of human isoforms of neuropilin-2; the sizes of isoforms are indicated together with their symbols, the domains are marked above the sequence, sequences in black frame are putative N-glycosylation sites, sequences in red frame are putative O-glysylation sites, sequence in green frame is transmembrane region.

shown in chick neural growth cone assay that the elicited response is strongly dependent firstly on the presence of the a1a2 semaphorin binding domain, secondly on the c domain, and to lesser extent it was observed that full potency of signal requires the b1b2 domain. Interestingly, it was also shown that transmembrane and intracellular parts of neuropilins, even upon deletion, were completely irrelevant for signal transduction in this model (3, 4).

An important feature of neuropilin-1 is its so-called adhesive function (90, 91), which structural requirements were also studied (78). This has been mapped by deletion experiments and synthetic peptide binding assays. The adhesion region was found within the b1b2 domain (residues 347-364 in b1 and 504-521 in b2) and its function was neither enhanced nor competed by VEGF165, SEMA3A and plexins. Intriguingly, this suggested region responsible for the adhesion function of neuropilin-1 overlaps with the putative heparin binding site of the protein (82), suggesting that neuropilin interactions with proteoglycans may be responsible for at least part of the neuropilin's adhesion function.

4.2. Functional aspect of neuropilin interactions

The main functions of neuropilins that have been identified with certainty are associated with vessel and neural systems. In mouse development, both neuropilins are essential in embryonic angiogenesis (18, 22) and similarly for neural system development (92, 93). Also, both of them were confirmed to be important for neural migration (93-95) and they are involved in endothelial cell migration (87, 96), cell survival (87, 97) and vascular permeability (25, 98). Endothelial neuropilin-1 in adult organisms is also involved in wound angiogenesis (99). Related to neuropilins' endothelial localisation is a developmental role in kidney morphogenesis, where they seem to provide a morphogenetic guide plan (100). Similar developmental roles of neuropilin-1 were observed in salivary gland formation and lung development (101, 102). This shows that neuropilins have pivotal functions in development. Another field where neuropilins seem to play

Table 1. Neuropilins expression

Localisation	neuropilin-1	s12 neuropilin-1	neuropilin-2
Vessel systems	18		24
Retina	149		21
Neural system	90		7, 10, 40
Hepatocytes		16	
Kidney	100, 150	16	100
Liver	16		
Keratinocytes	16, 39		
Melanocytes	151		
Chondrocytes	152		
Osteoblasts	153		
Schwann cells			40
T cells	103, 154		
Basophils	106		106
Bone marrow	107		
Dendritic cells			155
Intervertebral disc			156
Aorta smooth muscle cells	35		

an important role is the immune system (103). Neuropilin-1 was shown to be involved in the primary immune response (104) and the migration of thymocytes (105). The presence of neuropilin-1 in basophils is interpreted as a possible means whereby basophils regulate angiogenesis (106). Other studies suggest that neuropilin-1 is involved in the regulation of hematopoiesis (107). A tissue/organ specific summary table presents neuropilin expression data (Table 1). Despite such widespread expression and a wealth of data suggesting that neuropilins play important roles in vertebrate development and homeostasis, the mechanisms whereby neuropilins exert these functions are not well defined. What is known is largely focused around the molecular partners of neuropilins and the association of these interactions of neuropilins with biological activities.

The original partners of neuropilins, the class III semaphorins, require neuropilin co-receptors such as plexins or L1 subfamily molecules to transduce intracellular signals (65, 108). Semaphorins are a versatile group of membrane-associated or soluble proteins classified into eight families, where class 3 in humans consists of 7 members, named A to G. It is noteworthy that neuropilins do not interact with all isoforms equally and within those that interact, the affinities have different values. Thus, the main ligand for neuropilin-1 is SEMA3A, while for neuropilin-2 it is SEMA3F (109). Additionally, proteolytic modifications may influence the binding properties of semaphorins (110). The expression pattern, interactions and signalling mechanism of semaphorins has been thoroughly studied (reviewed in (111)). The interaction with neuropilins seems to be crucial for neural development by causing a chemorepulsive signal in axon guidance (reviewed in (64)) and the expression of semaphorins and neuropilins in neural systems reveals high level of complementarity, which suggests semaphorin function in defining repulsive regions (8, 9). Importantly, it is suggested in different subpopulations of cells at different stages of embryonic and postnatal development the same semaphorins (SEMA3A/E/F) could have either repulsive or no effect on axonal response due to differential expression of partners such as neuropilins (112).

In the neural system several functions of class III semaphorins were observed. The main function related to neuropilins acting as receptors for semaphorins is to generate a repulsive signal for growing axons, which is best studied for SEMA3A (3, 74, 113). Also for SEMA3E/F mediation of a repulsive function was suggested though no direct link with neuropilins was identified for this activity (113, 114). Semaphorins have diverse functions and in fact they are able to antagonise each other, e.g., SEMA3A inhibits neural overgrowth via neuropilin-1, whereas other semaphorins, such as SEMA3C and B, cannot induce such a response and may even block it. Interestingly, while SEMA3B/C act as antagonists of neuropilin-1, they are agonists of neuropilin-2 and via this molecule they can induce growth cone collapse (74, 115). It is noteworthy in the latter respect that only SEMA3A does not interact with neuropilin-2 (7). Similarly, it was shown in zebrafish that SEMA3D elicits both repulsive or attractive signals, depending on subset of neuropilins expressed in cells (116). Other important developmental roles have been observed for SEMA3B, which together with neuropilin-2 is involved in positioning the anterior/posterior orientation of the anterior commissure, a major brain commissural projection (71). Non neural developmental function is ascribed to SEMA3A/C and SEMA3C/F, where they are involved in regulating the processes of salivary gland formation and lung branching, respectively (101, 102). Also SEMA3G in zebrafish was shown to have a function in heart formation (117). Additionally, SEMA3C has been observed to elicit prosurvival responses in neurons, which correlates with the presence of neuropilins (118). SEMA3F, the main interacting ligand of neuropilin-2, was shown in rat cerebellar cone cells, which only express neuropilin-2, to elicit a chemoattractive rather than a repulsive signal (119). SEMA3F was also shown to be important for axonal wiring in guanylate cyclase-D expressing olfactory neurons together with neuropilin-2 (120). SEMA3F is also suggested to control neural crest cells migration together with neuropilin-2 (93). Therefore, a set of functions of semaphorins related to their interaction with neuropilins emerges, as they can elicit not only antagonising guidance signals, but direct also important developmental functions. The complexity of the signalling network, which is a result of multiple members of semaphorin family, permits a very

Table 2. Neuropilins interacting partners

Name	References
Neuropilin-1	
VEGFR1/Flt-1	69
VEGFR2/KDR/Flk-1	70
FGFR-1	68
Plexins	157
L1-CAM	158
Integrin beta-1	72
c-Met	147
SEMA3A	3
SEMA3C, D, E	159
VEGFA121	138
VEGFA165	69, 83, 160
VEGFB	144, 160
VEGFC/D	76
FGF-1,2,4,7	68
PlGF-2	83, 143, 160
HGF/SF	68, 148
NIP	59
FGFBP	68
Prion protein	68
Neuropilin-1/2	68, 73
Heparin	82, 83
Neuropilin-2	
VEGFR2	87
VEGFR3	76, 87
SEMA3C, F	7
VEGFA145 (	160
VEGF165	160
VEGFC	76, 160
VEGFD	76
PlGF-2	160
Neuropilin-1	73

fine mechanism of control and, thus, implicates an important role for neuropilins.

As neuropilins are implicated in the formation and progression of tumours, the impact of semaphorins in these processes has been studied. In human pancreatic cancer, high levels of SEMA3A were suggested to be associated with an increase in the malignancy of the tumours and also correlated with higher levels of expression of neuropilin-1 (121). In contrast, in endothelial cells SEMA3A was suggested to decrease cell proliferation in a neuropilin-dependent manner and the inhibition of expression of both neuropilins resulted in the cells losing their sensitivity to pro-apoptotic signals caused by Sema3A (122). SEMA3F expression has been linked to reduced tumorigenicity and tumour formation, which was attributed to its interaction with neuropilin-2 and the inhibition of the activities of VEGF165 and FGF-2 (123-125). Another semaphorin, SEMA3B, was shown to enhance apoptosis and reduce mitosis in a neuropilin dependent way in lung and breast cancer cells (126). This finding is important, as it relates neuropilins to the cancer field where sets of proteins of given properties can drive pathological process, and therefore expands the potential complexity of the molecular networks that drive tumour progression and metastasis.

Another large group of neuropilin interacting ligands are members of the VEGF family. This family consists of five members in mammals, VEGFA, B, C, D and PlGF (reviewed in (127)). The functional importance of the interaction of neuropilins and VEGFs is related to angiogenesis (128-130) and neural development (131). Several mechanisms such as alternative splicing and proteolytic processing (by matrix metalloproteinases or plasmin) diversify the number of bioavailable VEGF isoforms (132-134). Interactions with neuropilins involve a specific subset of these variants (Table 2), while signal transduction is thought to occur via the canonical VEGF receptor tyrosine kinases (127). It is noteworthy that much less is known about neuropilin-2 function and VEGF family members than about neuropilin-1. The feature that seems to be required for VEGF to bind to both neuropilins are exons 7-8, where exon 7 encodes the heparin binding site in VEGF. Thus, the VEGF121 isoform that lacks the ability to bind heparin does not interact with neuropilins (14, 135). An absence of interaction with neuropilin-1 was also shown for isoforms lacking only exon 8, such as VEGF165b and VEGF159 (136). Another unusual isoform is VEGF145, which also lacks exon 7, however, it can bind heparin and is able to interact with neuropilin-2, but not neuropilin-1 (137). In one study VEGF121 was found to interact with neuropilin-1 with an affinity similar to that of VEGF165, which was explained by the fact that commercial VEGF121 lacks the C-terminus, which is crucial for the interaction with neuropilin-1 (138). However, not all studies with VEGF121 have used C-terminally truncated protein, for example, full-length VEGF121 produced in baculovirus also fails to bind to neuropilins (70). Nevertheless, in two independent studies similar concentration of VEGF121 was observed to elicit either similar effect as VEGF165 or much weaker (138-140).

Next, neuropilins can bind to VEGF receptors and it was shown that neuropilin-1 can interact with VEGFR2 (141) and VEGFR1 (69), while neuropilin-2 can interact with VEGFR1, VEGFR2 and VEGFR3 (76, 87, 142). Apart from VEGFs which can bind both VEGFR1/2, neuropilin-1 can also bind VEGFR1 specific PlGF and VEGFB, and VEGFR2 specific viral VEGFE (143-145). The interesting feature of neuropilins is that they may participate in the formation of signalling complexes not only in *cis*, but also in *trans*, between two cells (75). The formation of complexes between neuropilins and ligands and receptors for VEGF has been suggested to have several effects. Thus, it was shown that VEGF165 may possess a higher signalling potency, compared to that of VEGF121 although they both bind VEGFR2 with similar affinity, due to interaction with neuropilin-1 and formation a ternary complex neuropilin-1-VEGF165-VEGFR2 (141). Moreover, it was shown that mutagenesis of VEGF165, which blocked its binding to VEGFR2, but not to neuropilin-1, resulted in the phosphorylation of VEGFR2 (70). Interaction of neuropilin-1 with VEGFR2 was suggested to result in an enhancement of signalling potency, however two possible mechanisms explaining this were proposed. In one this enhancement was thought to be due to the formation of a complex without affecting the complex affinity for ligand (14, 141). Whereas in a different study, a mechanism whereby neuropilin enhanced ligand affinity was proposed (69). Interestingly, in case of neuropilin-1 and VEGFR1 complex no influence on VEGF165 complex affinity was observed (69). Importantly, the formation of complexes between

neuropilin-1 and VEGFR2 was questioned and a VEGF165-dependent, but not VEGF121, mechanism was suggested (75).

The formation of complexes between neuropilins, VEGF ligand and receptor is complicated by the fact that all three types of proteins also interact with heparan sulfate/heparin. Some work has focused on identifying the relationship between these four partners. In one study it was suggested that neuropilin-1-VEGF binding is strongly enhanced by the addition of heparin, in a manner dependent on the size of the heparin oligosaccharides. This was explained by longer fragments of heparin affecting the avidity of the complex (69, 135). Heparin may also be important for the interaction of neuropilin-2 and VEGF165 (76). It is also suggested to inhibit binding of neuropilin-1 and VEGFR1, which is consistent as the VEGFR1:neuropilin-1 binding site overlaps with the heparin binding site. Interestingly, an interplay between VEGF165 and VEGFR1 to bind neuropilin-1 was shown, which implicates overlapping binding sites for these two targets in neuropilin. Consequently heparin was suggested to have negative regulating effect as it interferes with VEGFR1 binding but enhances VEGF165 binding (69). A related study demonstrated that glycanylated neuropilin-1 may increase VEGF165 binding and signalling, thus showing the importance of the sugar-modified isoforms in the mechanism of signalling control (62). Another heparin function is possibily to mediate neuropilin-1 multimerisation (69).

Other VEGFs were also shown to be important interacting partners of neuropilins. VEGFB similarly to VEGFA possesses a heparin binding site and via this region it interacts with neuropilin-1 (144). VEGFC and VEGFD bind both neuropilins, however, only interaction of VEGFC with neuropilin-2 occures in the absence of heparin, while the others require heparin. Importantly, VEGFC/D do not contain typical VEGFA heparin binding sites, which is thought to mediate interaction with neuropilins. Indeed, it was shown that VEGFC uses its N-terminal to bind neuropilins. On the other hand, in order to bind VEGFC neuropilin-1 requires the b1b2 domain and heparin, while neuropilin-2 requires the b1b2 domain and either heparin or a1a2, which may make the a1a2 domain functional eqivalent to heparin in this respect (76).

The role of neuropilins' interactions with other growth factors is much less understood. PlGF-2 is suggested to potentiate VEGF signalling (146) and increased motility (143). FGF2 together with neuropilin-1 has stimulating effect on endothelial cells (68). Another neuropilin interacting partner, HGF/SF, is suggested to promote cancer progression in two independent studies (147, 148). It was shown that neuropilin-1 is essential for successful signalling and response in both cases and thus, enhances cell survival and invasion through activation of c-MET pathway through direct c-MET interaction.

Collectively, the structural data reviewed here together with a set of interactions and associated functions enriched by genetic studies enable this initial compilation of facts about neuropilins that present contemporary knowledge about this family of proteins. According to the historical profile of neuropilins the first publication concerning neuropilin-1 (1) was in 1991, and at the moment there are around 700 available publications. However, the complexity of the action of neuropilins seem to grow proportionally to the number of studies devoted to these proteins. Therefore, the current approaches for elucidating the function of neuropilins needs to be replaced by novel approaches to characterise protein functions which would accommodate the flexible and multifunctionality of proteins such as neuropilins.

4.3. Functional significance of neuropilins' interactions

Neuropilins have established cellular functions such as cell guidance, angiogenesis and cell adhesion. In the simplified models the cell guiding function is ascribed to the interaction of neuropilin with semaphorins and angiogenic function to the interaction with VEGF. The basis of the adhesive property of neuropilin are still not known. Contemporary knowledge of neuropilins permits their schematised characterisation, however, there are still many missing elements in the puzzle.

A first key element still not fully understood is the issue of neuropilin oligo/multimerisation. The question of its functional importance and a putative switch between the action of monomeric and oligo/multimeric forms could play a significant role in the regulation of responses elicited via neuropilins. Moreover, this mechanism could be allied to the hypothesised competition between soluble and membrane bound neuropilins. Evidently, such a switch would be dependent on protein interactions that involve neuropilin and, therefore, could determine their ability to form homophilic associations.

Another mystery is the influence of heparin on neuropilin function. Interactions with glycosaminoglycans (heparin being a common experimental proxy) is a hallmark of many extracellular regulatory molecules, yet the diversity of data presented so far on neuropilin is substantial and leaves open any discussion of the functional signalificance of the interaction of neuropilin with the polysaccharide. Firstly, the issue of the structural role of heparin as a molecule involved in the formation of signalling complexes in which neuropilin is involved needs resolution. Secondly, the question of heparin-dependent signal transduction and modulation of signalling requires clarification. Many of the partners of neuropilins bind heparin/heparan sulfate and the polysaccharide is an integral part of their ligand-receptor complex. How neuropilin fits into such complexes and the role of its interaction with the polysaccharide is not known. Thirdly, as a holistic functional consequence *in vivo*, the relation between neuropilin dependent responses and the differential expression of specific protein-binding structures by heparan sulfate observed in tissues may provide a means to speficify particular signalling outcomes and the selection of partners by neuropilin.

Next, the membrane localisation of neuropilins indicates that they possess interactions in three different

compartments, namely the extracellular, intracellular and transmembrane environments. Therefore, neuropilin is a target of extracellular signalling molecules, an integral part of the signalling complexes that are formed at the cell surface and a molecule that triggeris directly inracellular signalling cascades.

Last but not least is the involvement of neuropilin in cell-cell contact. Since it is confirmed that neuropilins can act *in trans* between distinct cells, another field of neuropilin function emerges, which ascribes to neuropilins the important function of maintaining the physical and functional connectivity of tissue. Therefore, neuropilins apart from bridging cells may also play a part in communication between them.

5. PERSPECTIVES: NEUROPILINS IN MOLECULAR NETWORKS

Neuropilins have a large number of structurally unrelated molecular partners, though the biological functions of a number of these interactions remain to be elucidated. Neuropilins should thus perhaps be considered as multifunctional proteins. The functions of neuropilins at any given time will depend on the localisation of the neuropilins in plasma membrane domains, and their association with membrane bound and pericellular proteins and glycosaminoglycans or glycans, thus their functions depend ultimately on the cellular proteome and glycome. However, individual neuropilin molecules are likely to partition between different partners or groups of partners. Thus, on a single cell, not all neuropilin molecules may be engaged in the same functionality. This complexity is founded on a protein structure, which seems able to accommodate multiple partners. Different parts of the neuropilin protein interact with members of VEGF family, semaphorins, signalling receptors and heparin. Neuropilins possess considerable unstructured regions in the interdomain linkers and loops joining secondary structural elements. Such unstructured regions are a hallmark of sites of interaction, which often become structured in the molecular complex. The discovery of the the first partner of the intracellular domain of neuropilin-1, the PDZ motif containing NIP, suggests that, like other transmembrane proteins with small cytoplasmic stubs, such as syndecans, neuropilins may possess a reasonably complex intracellular interactome. However, a complete description of the partners of the intracellular domain remains to be established. The picture of neuropilin function is perhaps somewhat confounding, which is a consequence of its multifunctionality and complexity. Thus, it is expressed by many cell types; as a co-receptor of several other receptors it modifies their signalling potency; it interacts with and is probably regulated by heparan sulfate; its developmental role is clearly significant, but there is no obvious single molecular mechanism that can explain, for example, the phenotypes of neuropilins knockout mice. Collectively, these data suggest that a simple "A interacts with B, causing signals X, Y and Z" does not explain the biological functions we can observe. This problem requires a modification of our models of molecular function that incorporate the idea of a protein interactome. Thus, instead of focusing on one protein, a model where sets of proteins cooperating in the same moment and in the same place determine the functionality of the components of the complexes may provide a more adequate explanation of molecular function. Therefore, the overall cell response is a result of the cooperation of multiple molecules working in concerted networks to generate intracellular signals.

A major challenge for this field, as for much of postgenome biology, is to define molecular function. However, molecules such as neuropilins, which seem to represent complex regulatory nodes in molecular networks pose major analytical problems. Thus, the challenge is one of resolving complexity in the context of different individual neuropilin molecules performing different functions at the same time in a single cell. Current approaches will simply average the functions across the population of neuropilins. It seems likely that an individual molecule approach may be required to resolve the intricacies of the functions of neuropilins.

6. ACKNOWLEDGEMENTS

The work is supported by Marie Curie Early Stage Training Programme, The Cancer and Polio Research Fund Laboratories and the North West Cancer Research Fund.

7. REFERENCES

1. S. Takagi, T. Hirata, K. Agata, M. Mochii, G. Eguchi and H. Fujisawa: The A5 antigen, a candidate for the neuronal recognition molecule, has homologies to complement components and coagulation factors. *Neuron*, 7, 295-307 (1991)

2. T. Kitsukawa, M. Shimizu, M. Sanbo, T. Hirata, M. Taniguchi, Y. Bekku, T. Yagi and H. Fujisawa: Neuropilin-semaphorin III/D-mediated chemorepulsive signals play a crucial role in peripheral nerve projection in mice. *Neuron*, 19, 995-1005 (1997)

3. Z. He and M. Tessier-Lavigne: Neuropilin is a receptor for the axonal chemorepellent Semaphorin III. *Cell*, 90, 739-51 (1997)

4. F. Nakamura, M. Tanaka, T. Takahashi, R. G. Kalb and S. M. Strittmatter: Neuropilin-1 extracellular domains mediate semaphorin D/III-induced growth cone collapse. *Neuron*, 21, 1093-100 (1998)

5. D. Bagnard, M. Lohrum, D. Uziel, A. W. Puschel and J. Bolz: Semaphorins act as attractive and repulsive guidance signals during the development of cortical projections. *Development*, 125, 5043-53 (1998)

6. A. Shirvan, I. Ziv, G. Fleminger, R. Shina, Z. He, I. Brudo, E. Melamed and A. Barzilai: Semaphorins as mediators of neuronal apoptosis. *J Neurochem*, 73, 961-71 (1999)

7. H. Chen, A. Chedotal, Z. He, C. S. Goodman and M. Tessier-Lavigne: Neuropilin-2, a novel member of the neuropilin family, is a high affinity receptor for the semaphorins Sema E and Sema IV but not Sema III. *Neuron*, 19, 547-59 (1997)

8. A. L. Kolodkin and D. D. Ginty: Steering clear of semaphorins: neuropilins sound the retreat. *Neuron*, 19, 1159-62 (1997)
9. R. J. Giger, E. R. Urquhart, S. K. Gillespie, D. V. Levengood, D. D. Ginty and A. L. Kolodkin: Neuropilin-2 is a receptor for semaphorin IV: insight into the structural basis of receptor function and specificity. *Neuron*, 21, 1079-92 (1998)
10. R. J. Giger, J. F. Cloutier, A. Sahay, R. K. Prinjha, D. V. Levengood, S. E. Moore, S. Pickering, D. Simmons, S. Rastan, F. S. Walsh, A. L. Kolodkin, D. D. Ginty and M. Geppert: Neuropilin-2 is required in vivo for selective axon guidance responses to secreted semaphorins. *Neuron*, 25, 29-41 (2000)
11. M. Rossignol, M. L. Gagnon and M. Klagsbrun: Genomic organization of human neuropilin-1 and neuropilin-2 genes: identification and distribution of splice variants and soluble isoforms. *Genomics*, 70, 211-22 (2000)
12. H. Fujisawa: From the discovery of neuropilin to the determination of its adhesion sites. *Adv Exp Med Biol*, 515, 1-12 (2002)
13. Q. Tao, S. C. Spring and B. I. Terman: Characterization of a new alternatively spliced neuropilin-1 isoform. *Angiogenesis*, 6, 39-45 (2003)
14. S. Soker, S. Takashima, H. Q. Miao, G. Neufeld and M. Klagsbrun: Neuropilin-1 is expressed by endothelial and tumor cells as an isoform-specific receptor for vascular endothelial growth factor. *Cell*, 92, 735-45 (1998)
15. F. C. Cackowski, L. Xu, B. Hu and S. Y. Cheng: Identification of two novel alternatively spliced Neuropilin-1 isoforms. *Genomics*, 84, 82-94 (2004)
16. M. L. Gagnon, D. R. Bielenberg, Z. Gechtman, H. Q. Miao, S. Takashima, S. Soker and M. Klagsbrun: Identification of a natural soluble neuropilin-1 that binds vascular endothelial growth factor: In vivo expression and antitumor activity. *Proc Natl Acad Sci U S A*, 97, 2573-8 (2000)
17. K. Kobuke, Y. Furukawa, M. Sugai, K. Tanigaki, N. Ohashi, A. Matsumori, S. Sasayama, T. Honjo and K. Tashiro: ESDN, a novel neuropilin-like membrane protein cloned from vascular cells with the longest secretory signal sequence among eukaryotes, is up-regulated after vascular injury. *J Biol Chem*, 276, 34105-14 (2001)
18. T. Kawasaki, T. Kitsukawa, Y. Bekku, Y. Matsuda, M. Sanbo, T. Yagi and H. Fujisawa: A requirement for neuropilin-1 in embryonic vessel formation. *Development*, 126, 4895-902 (1999)
19. T. Kitsukawa, A. Shimono, A. Kawakami, H. Kondoh and H. Fujisawa: Overexpression of a membrane protein, neuropilin, in chimeric mice causes anomalies in the cardiovascular system, nervous system and limbs. *Development*, 121, 4309-18 (1995)
20. L. Yuan, D. Moyon, L. Pardanaud, C. Breant, M. J. Karkkainen, K. Alitalo and A. Eichmann: Abnormal lymphatic vessel development in neuropilin 2 mutant mice. *Development*, 129, 4797-806 (2002)
21. J. Shen, R. Samul, J. Zimmer, H. Liu, X. Liang, S. Hackett and P. A. Campochiaro: Deficiency of neuropilin 2 suppresses VEGF-induced retinal neovascularization. *Mol Med*, 10, 12-18 (2004)
22. S. Takashima, M. Kitakaze, M. Asakura, H. Asanuma, S. Sanada, F. Tashiro, H. Niwa, J. Miyazaki Ji, S. Hirota, Y. Kitamura, T. Kitsukawa, H. Fujisawa, M. Klagsbrun and M. Hori: Targeting of both mouse neuropilin-1 and neuropilin-2 genes severely impairs developmental yolk sac and embryonic angiogenesis. *Proc Natl Acad Sci U S A*, 99, 3657-62 (2002)
23. D. R. Bielenberg, C. A. Pettaway, S. Takashima and M. Klagsbrun: Neuropilins in neoplasms: expression, regulation, and function. *Exp Cell Res*, 312, 584-93 (2006)
24. D. Moyon, L. Pardanaud, L. Yuan, C. Breant and A. Eichmann: Plasticity of endothelial cells during arterial-venous differentiation in the avian embryo. *Development*, 128, 3359-70 (2001)
25. A. Germeyer, A. E. Hamilton, L. S. Laughlin, B. L. Lasley, R. M. Brenner, L. C. Giudice and N. R. Nayak: Cellular expression and hormonal regulation of neuropilin-1 and -2 messenger ribonucleic Acid in the human and rhesus macaque endometrium. *J Clin Endocrinol Metab*, 90, 1783-90 (2005)
26. D. Watanabe, H. Takagi, K. Suzuma, I. Suzuma, H. Oh, H. Ohashi, S. Kemmochi, A. Uemura, T. Ojima, E. Suganami, N. Miyamoto, Y. Sato and Y. Honda: Transcription factor Ets-1 mediates ischemia- and vascular endothelial growth factor-dependent retinal neovascularization. *Am J Pathol*, 164, 1827-35 (2004)
27. H. Yamagishi, E. N. Olson and D. Srivastava: The basic helix-loop-helix transcription factor, dHAND, is required for vascular development. *J Clin Invest*, 105, 261-70 (2000)
28. M. Rossignol, J. Pouyssegur and M. Klagsbrun: Characterization of the neuropilin-1 promoter; gene expression is mediated by the transcription factor Sp1. *J Cell Biochem*, 88, 744-57 (2003)
29. E. Giraudo, L. Primo, E. Audero, H. P. Gerber, P. Koolwijk, S. Soker, M. Klagsbrun, N. Ferrara and F. Bussolino: Tumor necrosis factor-alpha regulates expression of vascular endothelial growth factor receptor-2 and of its co-receptor neuropilin-1 in human vascular endothelial cells. *J Biol Chem*, 273, 22128-35 (1998)
30. A. A. Parikh, W. B. Liu, F. Fan, O. Stoeltzing, N. Reinmuth, C. J. Bruns, C. D. Bucana, D. B. Evans and L. M. Ellis: Expression and regulation of the novel vascular endothelial growth factor receptor neuropilin-1 by epidermal growth factor in human pancreatic carcinoma. *Cancer*, 98, 720-9 (2003)
31. M. Akagi, M. Kawaguchi, W. Liu, M. F. McCarty, A. Takeda, F. Fan, O. Stoeltzing, A. A. Parikh, Y. D. Jung, C. D. Bucana, P. F. Mansfield, D. J. Hicklin and L. M. Ellis: Induction of neuropilin-1 and vascular endothelial growth factor by epidermal growth factor in human gastric cancer cells. *Br J Cancer*, 88, 796-802 (2003)
32. H. Oh, H. Takagi, A. Otani, S. Koyama, S. Kemmochi, A. Uemura and Y. Honda: Selective induction of neuropilin-1 by vascular endothelial growth factor (VEGF): a mechanism contributing to VEGF-induced angiogenesis. *Proc Natl Acad Sci U S A*, 99, 383-8 (2002)
33. L. W. Feurino, Y. Zhang, U. Bharadwaj, R. Zhang, F. Li, W. E. Fisher, F. C. Brunicardi, C. Chen, Q. Yao and M. Li: IL-6 Stimulates Th2 Type Cytokine Secretion and Upregulates VEGF and NRP-1 Expression in Pancreatic Cancer Cells. *Cancer Biol Ther*, 6, (2007)
34. E. Hermanson, L. Borgius, M. Bergsland, E. Joodmardi and T. Perlmann: Neuropilin1 is a direct downstream target

of Nurr1 in the developing brain stem. *J Neurochem*, 97, 1403-11 (2006)
35. H. Yang, M. Li, H. Chai, S. Yan, P. Lin, A. B. Lumsden, Q. Yao and C. Chen: Effects of cyclophilin A on cell proliferation and gene expressions in human vascular smooth muscle cells and endothelial cells. *J Surg Res*, 123, 312-9 (2005)
36. L. R. You, F. J. Lin, C. T. Lee, F. J. DeMayo, M. J. Tsai and S. Y. Tsai: Suppression of Notch signalling by the COUP-TFII transcription factor regulates vein identity. *Nature*, 435, 98-104 (2005)
37. Y. K. Hong, N. Harvey, Y. H. Noh, V. Schacht, S. Hirakawa, M. Detmar and G. Oliver: Prox1 is a master control gene in the program specifying lymphatic endothelial cell fate. *Dev Dyn*, 225, 351-7 (2002)
38. T. Nakagawa, M. Abe, T. Yamazaki, H. Miyashita, H. Niwa, S. Kokubun and Y. Sato: HEX acts as a negative regulator of angiogenesis by modulating the expression of angiogenesis-related gene in endothelial cells in vitro. *Arterioscler Thromb Vasc Biol*, 23, 231-7 (2003)
39. P. Kurschat, D. Bielenberg, M. Rossignol-Tallandier, A. Stahl and M. Klagsbrun: Neuron restrictive silencer factor NRSF/REST is a transcriptional repressor of neuropilin-1 and diminishes the ability of semaphorin 3A to inhibit keratinocyte migration. *J Biol Chem*, 281, 2721-9 (2006)
40. J. Ara, P. Bannerman, F. Shaheen and D. E. Pleasure: Schwann cell-autonomous role of neuropilin-2. *J Neurosci Res*, 79, 468-75 (2005)
41. P. R. Young and S. M. Spevacek: Substratum acidification and proteinase activation by murine B16F10 melanoma cultures. *Biochim Biophys Acta*, 1182, 69-74 (1993)
42. G. Helmlinger, F. Yuan, M. Dellian and R. K. Jain: Interstitial pH and pO2 gradients in solid tumors in vivo: high-resolution measurements reveal a lack of correlation. *Nat Med*, 3, 177-82 (1997)
43. C. W. Pugh and P. J. Ratcliffe: Regulation of angiogenesis by hypoxia: role of the HIF system. *Nat Med*, 9, 677-84 (2003)
44. I. Nilsson, C. Rolny, Y. Wu, B. Pytowski, D. Hicklin, K. Alitalo, L. Claesson-Welsh and S. Wennstrom: Vascular endothelial growth factor receptor-3 in hypoxia-induced vascular development. *Faseb J*, 18, 1507-15 (2004)
45. P. Ottino, J. Finley, E. Rojo, A. Ottlecz, G. N. Lambrou, H. E. Bazan and N. G. Bazan: Hypoxia activates matrix metalloproteinase expression and the VEGF system in monkey choroid-retinal endothelial cells: Involvement of cytosolic phospholipase A2 activity. *Mol Vis*, 10, 341-50 (2004)
46. A. Kawakami, T. Kitsukawa, S. Takagi and H. Fujisawa: Developmentally regulated expression of a cell surface protein, neuropilin, in the mouse nervous system. *J Neurobiol*, 29, 1-17 (1996)
47. N. Guttmann-Raviv, O. Kessler, N. Shraga-Heled, T. Lange, Y. Herzog and G. Neufeld: The neuropilins and their role in tumorigenesis and tumor progression. *Cancer Lett*, 231, 1-11 (2006)
48. L. M. Ellis: The role of neuropilins in cancer. *Mol Cancer Ther*, 5, 1099-107 (2006)
49. T. Kawakami, T. Tokunaga, H. Hatanaka, H. Kijima, H. Yamazaki, Y. Abe, Y. Osamura, H. Inoue, Y. Ueyama and M. Nakamura: Neuropilin 1 and neuropilin 2 co-expression is significantly correlated with increased vascularity and poor prognosis in nonsmall cell lung carcinoma. *Cancer*, 95, 2196-201 (2002)
50. H. Q. Miao, P. Lee, H. Lin, S. Soker and M. Klagsbrun: Neuropilin-1 expression by tumor cells promotes tumor angiogenesis and progression. *Faseb J*, 14, 2532-9 (2000)
51. T. Kamiya, T. Kawakami, Y. Abe, M. Nishi, N. Onoda, N. Miyazaki, Y. Oida, H. Yamazaki, Y. Ueyama and M. Nakamura: The preserved expression of neuropilin (NRP) 1 contributes to a better prognosis in colon cancer. *Oncol Rep*, 15, 369-73 (2006)
52. T. Ochiumi, Y. Kitadai, S. Tanaka, M. Akagi, M. Yoshihara and K. Chayama: Neuropilin-1 is involved in regulation of apoptosis and migration of human colon cancer. *Int J Oncol*, 29, 105-16 (2006)
53. P. Bork and G. Beckmann: The CUB domain. A widespread module in developmentally regulated proteins. *J Mol Biol*, 231, 539-45 (1993)
54. S. Baumgartner, K. Hofmann, R. Chiquet-Ehrismann and P. Bucher: The discoidin domain family revisited: new members from prokaryotes and a homology-based fold prediction. *Protein Sci*, 7, 1626-31 (1998)
55. A. Romero, M. J. Romao, P. F. Varela, I. Kolln, J. M. Dias, A. L. Carvalho, L. Sanz, E. Topfer-Petersen and J. J. Calvete: The crystal structures of two spermadhesins reveal the CUB domain fold. *Nat Struct Biol*, 4, 783-8 (1997)
56. A. L. Sieron, A. Tretiakova, B. A. Jameson, M. L. Segall, S. Lund-Katz, M. T. Khan, S. Li and W. Stocker: Structure and function of procollagen C-proteinase (mTolloid) domains determined by protease digestion, circular dichroism, binding to procollagen type I, and computer modeling. *Biochemistry*, 39, 3231-9 (2000)
57. F. T. Ishmael, V. K. Shier, S. S. Ishmael and J. S. Bond: Intersubunit and domain interactions of the meprin B metalloproteinase. Disulfide bonds and protein-protein interactions in the MAM and TRAF domains. *J Biol Chem*, 280, 13895-901 (2005)
58. G. C. Zondag, G. M. Koningstein, Y. P. Jiang, J. Sap, W. H. Moolenaar and M. F. Gebbink: Homophilic interactions mediated by receptor tyrosine phosphatases mu and kappa. A critical role for the novel extracellular MAM domain. *J Biol Chem*, 270, 14247-50 (1995)
59. H. Cai and R. R. Reed: Cloning and characterization of neuropilin-1-interacting protein: a PSD-95/Dlg/ZO-1 domain-containing protein that interacts with the cytoplasmic domain of neuropilin-1. *J Neurosci*, 19, 6519-27 (1999)
60. A. Gattiker, E. Gasteiger and A. Bairoch: ScanProsite: a reference implementation of a PROSITE scanning tool. *Appl Bioinformatics*, 1, 107-8 (2002)
61. J. E. Hansen, O. Lund, N. Tolstrup, A. A. Gooley, K. L. Williams and S. Brunak: NetOglyc: prediction of mucin type O-glycosylation sites based on sequence context and surface accessibility. *Glycoconj J*, 15, 115-30 (1998)
62. Y. Shintani, S. Takashima, Y. Asano, H. Kato, Y. Liao, S. Yamazaki, O. Tsukamoto, O. Seguchi, H. Yamamoto, T. Fukushima, K. Sugahara, M. Kitakaze and M. Hori: Glycosaminoglycan modification of neuropilin-1 modulates VEGFR2 signaling. *Embo J*, 25, 3045-55 (2006)

63. D. Devos and R. B. Russell: A more complete, complexed and structured interactome. *Curr Opin Struct Biol*, 17, 370-7 (2007)
64. H. Fujisawa and T. Kitsukawa: Receptors for collapsin/semaphorins. *Curr Opin Neurobiol*, 8, 587-92 (1998)
65. V. Castellani: The function of neuropilin/L1 complex. *Adv Exp Med Biol*, 515, 91-102 (2002)
66. M. Delehedde, M. Lyon, J. T. Gallagher, P. S. Rudland and D. G. Fernig: Fibroblast growth factor-2 binds to small heparin-derived oligosaccharides and stimulates a sustained phosphorylation of p42/44 mitogen-activated protein kinase and proliferation of rat mammary fibroblasts. *Biochem J*, 366, 235-44 (2002)
67. T. Tammela, B. Enholm, K. Alitalo and K. Paavonen: The biology of vascular endothelial growth factors. *Cardiovasc Res*, 65, 550-63 (2005)
68. D. C. West, C. G. Rees, L. Duchesne, S. J. Patey, C. J. Terry, J. E. Turnbull, M. Delehedde, C. W. Heegaard, F. Allain, C. Vanpouille, D. Ron and D. G. Fernig: Interactions of multiple heparin binding growth factors with neuropilin-1 and potentiation of the activity of fibroblast growth factor-2. *J Biol Chem*, 280, 13457-64 (2005)
69. G. Fuh, K. C. Garcia and A. M. de Vos: The interaction of neuropilin-1 with vascular endothelial growth factor and its receptor flt-1. *J Biol Chem*, 275, 26690-5 (2000)
70. N. Shraga-Heled, O. Kessler, C. Prahst, J. Kroll, H. Augustin and G. Neufeld: Neuropilin-1 and neuropilin-2 enhance VEGF121 stimulated signal transduction by the VEGFR-2 receptor. *Faseb J* (2006)
71. J. Falk, A. Bechara, R. Fiore, H. Nawabi, H. Zhou, C. Hoyo-Becerra, M. Bozon, G. Rougon, M. Grumet, A. W. Puschel, J. R. Sanes and V. Castellani: Dual functional activity of semaphorin 3B is required for positioning the anterior commissure. *Neuron*, 48, 63-75 (2005)
72. M. Fukasawa, A. Matsushita and M. Korc: Neuropilin-1 Interacts with Integrin beta1 and Modulates Pancreatic Cancer Cell Growth, Survival and Invasion. *Cancer Biol Ther*, 6, (2007)
73. H. Chen, Z. He, A. Bagri and M. Tessier-Lavigne: Semaphorin-neuropilin interactions underlying sympathetic axon responses to class III semaphorins. *Neuron*, 21, 1283-90 (1998)
74. T. Takahashi, F. Nakamura, Z. Jin, R. G. Kalb and S. M. Strittmatter: Semaphorins A and E act as antagonists of neuropilin-1 and agonists of neuropilin-2 receptors. *Nat Neurosci*, 1, 487-93 (1998)
75. S. Soker, H. Q. Miao, M. Nomi, S. Takashima and M. Klagsbrun: VEGF165 mediates formation of complexes containing VEGFR-2 and neuropilin-1 that enhance VEGF165-receptor binding. *J Cell Biochem*, 85, 357-68 (2002)
76. T. Karpanen, C. A. Heckman, S. Keskitalo, M. Jeltsch, H. Ollila, G. Neufeld, L. Tamagnone and K. Alitalo: Functional interaction of VEGF-C and VEGF-D with neuropilin receptors. *Faseb J*, 20, 1462-72 (2006)
77. B. A. Appleton, P. Wu, J. Maloney, J. Yin, W. C. Liang, S. Stawicki, K. Mortara, K. K. Bowman, J. M. Elliott, W. Desmarais, J. F. Bazan, A. Bagri, M. Tessier-Lavigne, A. W. Koch, Y. Wu, R. J. Watts and C. Wiesmann: Structural studies of neuropilin/antibody complexes provide insights into semaphorin and VEGF binding. *Embo J* (2007)
78. M. Shimizu, Y. Murakami, F. Suto and H. Fujisawa: Determination of cell adhesion sites of neuropilin-1. *J Cell Biol*, 148, 1283-93 (2000)
79. C. Gu, B. J. Limberg, G. B. Whitaker, B. Perman, D. J. Leahy, J. S. Rosenbaum, D. D. Ginty and A. L. Kolodkin: Characterization of neuropilin-1 structural features that confer binding to semaphorin 3A and vascular endothelial growth factor 165. *J Biol Chem*, 277, 18069-76 (2002)
80. E. Geretti, A. Shimizu, P. Kurschat and M. Klagsbrun: Site-directed Mutagenesis in the B-Neuropilin-2 Domain Selectively Enhances Its Affinity to VEGF165, but Not to Semaphorin 3F. *J Biol Chem*, 282, 25698-707 (2007)
81. C. C. Lee, A. Kreusch, D. McMullan, K. Ng and G. Spraggon: Crystal structure of the human neuropilin-1 b1 domain. *Structure*, 11, 99-108 (2003)
82. C. W. Vander Kooi, M. A. Jusino, B. Perman, D. B. Neau, H. D. Bellamy and D. J. Leahy: Structural basis for ligand and heparin binding to neuropilin B domains. *Proc Natl Acad Sci U S A*, 104, 6152-7 (2007)
83. R. Mamluk, Z. Gechtman, M. E. Kutcher, N. Gasiunas, J. Gallagher and M. Klagsbrun: Neuropilin-1 binds vascular endothelial growth factor 165, placenta growth factor-2, and heparin via its b1b2 domain. *J Biol Chem*, 277, 24818-25 (2002)
84. H. Q. Miao, S. Soker, L. Feiner, J. L. Alonso, J. A. Raper and M. Klagsbrun: Neuropilin-1 mediates collapsin-1/semaphorin III inhibition of endothelial cell motility: functional competition of collapsin-1 and vascular endothelial growth factor-165. *J Cell Biol*, 146, 233-42 (1999)
85. J. Roche, H. Drabkin and E. Brambilla: Neuropilin and its ligands in normal lung and cancer. *Adv Exp Med Biol*, 515, 103-14 (2002)
86. M. Narazaki and G. Tosato: Ligand-induced internalization selects use of common receptor neuropilin-1 by VEGF165 and semaphorin3A. *Blood*, 107, 3892-901 (2006)
87. B. Favier, A. Alam, P. Barron, J. Bonnin, P. Laboudie, P. Fons, M. Mandron, J. P. Herault, G. Neufeld, P. Savi, J. M. Herbert and F. Bono: Neuropilin-2 interacts with VEGFR-2 and VEGFR-3 and promotes human endothelial cell survival and migration. *Blood*, 108, 1243-50 (2006)
88. Q. Schwarz, C. Gu, H. Fujisawa, K. Sabelko, M. Gertsenstein, A. Nagy, M. Taniguchi, A. L. Kolodkin, D. D. Ginty, D. T. Shima and C. Ruhrberg: Vascular endothelial growth factor controls neuronal migration and cooperates with Sema3A to pattern distinct compartments of the facial nerve. *Genes Dev*, 18, 2822-34 (2004)
89. J. M. Vieira, Q. Schwarz and C. Ruhrberg: Selective requirements for NRP1 ligands during neurovascular patterning. *Development*, 134, 1833-43 (2007)
90. S. Takagi, Y. Kasuya, M. Shimizu, T. Matsuura, M. Tsuboi, A. Kawakami and H. Fujisawa: Expression of a cell adhesion molecule, neuropilin, in the developing chick nervous system. *Dev Biol*, 170, 207-22 (1995)
91. M. Murga, O. Fernandez-Capetillo and G. Tosato: Neuropilin-1 regulates attachment in human endothelial

cells independently of vascular endothelial growth factor receptor-2. *Blood*, 105, 1992-9 (2005)
92. R. Bron, B. J. Eickholt, M. Vermeren, N. Fragale and J. Cohen: Functional knockdown of neuropilin-1 in the developing chick nervous system by siRNA hairpins phenocopies genetic ablation in the mouse. *Dev Dyn*, 230, 299-308 (2004)
93. L. S. Gammill, C. Gonzalez and M. Bronner-Fraser: Neuropilin 2/semaphorin 3F signaling is essential for cranial neural crest migration and trigeminal ganglion condensation. *Dev Neurobiol*, 67, 47-56 (2007)
94. A. Cariboni, J. Hickok, S. Rakic, W. Andrews, R. Maggi, S. Tischkau and J. G. Parnavelas: Neuropilins and their ligands are important in the migration of gonadotropin-releasing hormone neurons. *J Neurosci*, 27, 2387-95 (2007)
95. R. McLennan and P. M. Kulesa: In vivo analysis reveals a critical role for neuropilin-1 in cranial neural crest cell migration in chick. *Dev Biol*, 301, 227-39 (2007)
96. L. Wang, H. Zeng, P. Wang, S. Soker and D. Mukhopadhyay: Neuropilin-1-mediated vascular permeability factor/vascular endothelial growth factor-dependent endothelial cell migration. *J Biol Chem*, 278, 48848-60 (2003)
97. W. U. Kim, S. S. Kang, S. A. Yoo, K. H. Hong, D. G. Bae, M. S. Lee, S. W. Hong, C. B. Chae and C. S. Cho: Interaction of vascular endothelial growth factor 165 with neuropilin-1 protects rheumatoid synoviocytes from apoptotic death by regulating Bcl-2 expression and Bax translocation. *J Immunol*, 177, 5727-35 (2006)
98. P. M. Becker, J. Waltenberger, R. Yachechko, T. Mirzapoiazova, J. S. Sham, C. G. Lee, J. A. Elias and A. D. Verin: Neuropilin-1 regulates vascular endothelial growth factor-mediated endothelial permeability. *Circ Res*, 96, 1257-65 (2005)
99. A. M. Matthies, Q. E. Low, M. W. Lingen and L. A. DiPietro: Neuropilin-1 participates in wound angiogenesis. *Am J Pathol*, 160, 289-96 (2002)
100. G. Villegas and A. Tufro: Ontogeny of semaphorins 3A and 3F and their receptors neuropilins 1 and 2 in the kidney. *Mech Dev*, 119 Suppl 1, S149-53 (2002)
101. L. Chung, T. L. Yang, H. R. Huang, S. M. Hsu, H. J. Cheng and P. H. Huang: Semaphorin signaling facilitates cleft formation in the developing salivary gland. *Development*, 134, 2935-45 (2007)
102. M. Kagoshima and T. Ito: Diverse gene expression and function of semaphorins in developing lung: positive and negative regulatory roles of semaphorins in lung branching morphogenesis. *Genes Cells*, 6, 559-71 (2001)
103. P. H. Romeo, V. Lemarchandel and R. Tordjman: Neuropilin-1 in the immune system. *Adv Exp Med Biol*, 515, 49-54 (2002)
104. S. Moretti, A. Procopio, M. Boemi and A. Catalano: Neuronal semaphorins regulate a primary immune response. *Curr Neurovasc Res*, 3, 295-305 (2006)
105. Y. Lepelletier, S. Smaniotto, R. Hadj-Slimane, D. M. Villa-Verde, A. C. Nogueira, M. Dardenne, O. Hermine and W. Savino: Control of human thymocyte migration by Neuropilin-1/Semaphorin-3A-mediated interactions. *Proc Natl Acad Sci U S A*, 104, 5545-50 (2007)
106. A. de Paulis, N. Prevete, I. Fiorentino, F. W. Rossi, S. Staibano, N. Montuori, P. Ragno, A. Longobardi, B. Liccardo, A. Genovese, D. Ribatti, A. F. Walls and G. Marone: Expression and functions of the vascular endothelial growth factors and their receptors in human basophils. *J Immunol*, 177, 7322-31 (2006)
107. R. Tordjman, N. Ortega, L. Coulombel, J. Plouet, P. H. Romeo and V. Lemarchandel: Neuropilin-1 is expressed on bone marrow stromal cells: a novel interaction with hematopoietic cells? *Blood*, 94, 2301-9 (1999)
108. H. Fujisawa: Discovery of semaphorin receptors, neuropilin and plexin, and their functions in neural development. *J Neurobiol*, 59, 24-33 (2004)
109. G. Neufeld, T. Cohen, N. Shraga, T. Lange, O. Kessler and Y. Herzog: The neuropilins: multifunctional semaphorin and VEGF receptors that modulate axon guidance and angiogenesis. *Trends Cardiovasc Med*, 12, 13-9 (2002)
110. R. H. Adams, M. Lohrum, A. Klostermann, H. Betz and A. W. Puschel: The chemorepulsive activity of secreted semaphorins is regulated by furin-dependent proteolytic processing. *Embo J*, 16, 6077-86 (1997)
111. U. Yazdani and J. R. Terman: The semaphorins. *Genome Biol*, 7, 211 (2006)
112. E. Pozas, M. Pascual, K. T. Nguyen Ba-Charvet, P. Guijarro, C. Sotelo, A. Chedotal, J. A. Del Rio and E. Soriano: Age-dependent effects of secreted Semaphorins 3A, 3F, and 3E on developing hippocampal axons: in vitro effects and phenotype of Semaphorin 3A (-/-) mice. *Mol Cell Neurosci*, 18, 26-43 (2001)
113. A. Chedotal, J. A. Del Rio, M. Ruiz, Z. He, V. Borrell, F. de Castro, F. Ezan, C. S. Goodman, M. Tessier-Lavigne, C. Sotelo and E. Soriano: Semaphorins III and IV repel hippocampal axons via two distinct receptors. *Development*, 125, 4313-23 (1998)
114. M. Steffensky, K. Steinbach, U. Schwarz and B. Schlosshauer: Differential impact of semaphorin 3E and 3A on CNS axons. *Int J Dev Neurosci*, 24, 65-72 (2006)
115. S. P. Niclou, E. H. Franssen, E. M. Ehlert, M. Taniguchi and J. Verhaagen: Meningeal cell-derived semaphorin 3A inhibits neurite outgrowth. *Mol Cell Neurosci*, 24, 902-12 (2003)
116. M. A. Wolman, Y. Liu, H. Tawarayama, W. Shoji and M. C. Halloran: Repulsion and attraction of axons by semaphorin3D are mediated by different neuropilins in vivo. *J Neurosci*, 24, 8428-35 (2004)
117. M. Sato, H. J. Tsai and H. J. Yost: Semaphorin3D regulates invasion of cardiac neural crest cells into the primary heart field. *Dev Biol*, 298, 12-21 (2006)
118. M. T. Moreno-Flores, E. Martin-Aparicio, M. J. Martin-Bermejo, M. Agudo, S. McMahon, J. Avila, J. Diaz-Nido and F. Wandosell: Semaphorin 3C preserves survival and induces neuritogenesis of cerebellar granule neurons in culture. *J Neurochem*, 87, 879-90 (2003)
119. S. Ding, J. H. Luo and X. B. Yuan: Semaphorin-3F attracts the growth cone of cerebellar granule cells through cGMP signaling pathway. *Biochem Biophys Res Commun*, 356, 857-63 (2007)
120. A. Walz, P. Feinstein, M. Khan and P. Mombaerts: Axonal wiring of guanylate cyclase-D-expressing olfactory neurons is dependent on neuropilin 2 and semaphorin 3F. *Development*, 134, 4063-72 (2007)
121. M. W. Muller, N. A. Giese, J. M. Swiercz, G. O. Ceyhan, I. Esposito, U. Hinz, P. Buchler, T. Giese, M. W.

Buchler, S. Offermanns and H. Friess: Association of axon guidance factor Semaphorin 3A with poor outcome in pancreatic cancer. *Int J Cancer*, 121, 2421-33 (2007)
122. N. Guttmann-Raviv, N. Shraga-Heled, A. Varshavsky, C. Guimaraes-Sternberg, O. Kessler and G. Neufeld: Semaphorin-3A and semaphorin-3F work together to repel endothelial cells and to inhibit their survival by induction of apoptosis. *J Biol Chem*, 282, 26294-305 (2007)
123. D. R. Bielenberg, Y. Hida, A. Shimizu, A. Kaipainen, M. Kreuter, C. C. Kim and M. Klagsbrun: Semaphorin 3F, a chemorepulsant for endothelial cells, induces a poorly vascularized, encapsulated, nonmetastatic tumor phenotype. *J Clin Invest*, 114, 1260-71 (2004)
124. S. Kusy, P. Nasarre, D. Chan, V. Potiron, D. Meyronet, R. M. Gemmill, B. Constantin, H. A. Drabkin and J. Roche: Selective suppression of in vivo tumorigenicity by semaphorin SEMA3F in lung cancer cells. *Neoplasia*, 7, 457-65 (2005)
125. O. Kessler, N. Shraga-Heled, T. Lange, N. Gutmann-Raviv, E. Sabo, L. Baruch, M. Machluf and G. Neufeld: Semaphorin-3F is an inhibitor of tumor angiogenesis. *Cancer Res*, 64, 1008-15 (2004)
126. E. Castro-Rivera, S. Ran, P. Thorpe and J. D. Minna: Semaphorin 3B (SEMA3B) induces apoptosis in lung and breast cancer, whereas VEGF165 antagonizes this effect. *Proc Natl Acad Sci U S A*, 101, 11432-7 (2004)
127. A. K. Olsson, A. Dimberg, J. Kreuger and L. Claesson-Welsh: VEGF receptor signalling - in control of vascular function. *Nat Rev Mol Cell Biol*, 7, 359-71 (2006)
128. H. Q. Miao and M. Klagsbrun: Neuropilin is a mediator of angiogenesis. *Cancer Metastasis Rev*, 19, 29-37 (2000)
129. M. Klagsbrun, S. Takashima and R. Mamluk: The role of neuropilin in vascular and tumor biology. *Adv Exp Med Biol*, 515, 33-48 (2002)
130. G. Neufeld, T. Cohen, S. Gengrinovitch and Z. Poltorak: Vascular endothelial growth factor (VEGF) and its receptors. *Faseb J*, 13, 9-22 (1999)
131. C. Gu, E. R. Rodriguez, D. V. Reimert, T. Shu, B. Fritzsch, L. J. Richards, A. L. Kolodkin and D. D. Ginty: Neuropilin-1 conveys semaphorin and VEGF signaling during neural and cardiovascular development. *Dev Cell*, 5, 45-57 (2003)
132. J. Dai and A. B. Rabie: VEGF: an essential mediator of both angiogenesis and endochondral ossification. *J Dent Res*, 86, 937-50 (2007)
133. S. Lee, S. M. Jilani, G. V. Nikolova, D. Carpizo and M. L. Iruela-Arispe: Processing of VEGF-A by matrix metalloproteinases regulates bioavailability and vascular patterning in tumors. *J Cell Biol*, 169, 681-91 (2005)
134. J. E. Park, G. A. Keller and N. Ferrara: The vascular endothelial growth factor (VEGF) isoforms: differential deposition into the subepithelial extracellular matrix and bioactivity of extracellular matrix-bound VEGF. *Mol Biol Cell*, 4, 1317-26 (1993)
135. S. Soker, H. Fidder, G. Neufeld and M. Klagsbrun: Characterization of novel vascular endothelial growth factor (VEGF) receptors on tumor cells that bind VEGF165 via its exon 7-encoded domain. *J Biol Chem*, 271, 5761-7 (1996)
136. S. Cebe Suarez, M. Pieren, L. Cariolato, S. Arn, U. Hoffmann, A. Bogucki, C. Manlius, J. Wood and K. Ballmer-Hofer: A VEGF-A splice variant defective for heparan sulfate and neuropilin-1 binding shows attenuated signaling through VEGFR-2. *Cell Mol Life Sci*, 63, 2067-77 (2006)
137. Z. Gluzman-Poltorak, T. Cohen, Y. Herzog and G. Neufeld: Neuropilin-2 is a receptor for the vascular endothelial growth factor (VEGF) forms VEGF-145 and VEGF-165 *J Biol Chem*, 275, 18040-5 (2000)
138. Q. Pan, Y. Chathery, Y. Wu, N. Rathore, R. K. Tong, F. Peale, A. Bagri, M. Tessier-Lavigne, A. W. Koch and R. J. Watts: Neuropilin-1 binds to VEGF121 and regulates endothelial cell migration and sprouting. *J Biol Chem*, 282, 24049-56 (2007)
139. S. Ogawa, A. Oku, A. Sawano, S. Yamaguchi, Y. Yazaki and M. Shibuya: A novel type of vascular endothelial growth factor, VEGF-E (NZ-7 VEGF), preferentially utilizes KDR/Flk-1 receptor and carries a potent mitotic activity without heparin-binding domain. *J Biol Chem*, 273, 31273-82 (1998)
140. S. Soker, S. Gollamudi-Payne, H. Fidder, H. Charmahelli and M. Klagsbrun: Inhibition of vascular endothelial growth factor (VEGF)-induced endothelial cell proliferation by a peptide corresponding to the exon 7-encoded domain of VEGF165. *J Biol Chem*, 272, 31582-8 (1997)
141. G. B. Whitaker, B. J. Limberg and J. S. Rosenbaum: Vascular endothelial growth factor receptor-2 and neuropilin-1 form a receptor complex that is responsible for the differential signaling potency of VEGF(165) and VEGF(121). *J Biol Chem*, 276, 25520-31 (2001)
142. Z. Gluzman-Poltorak, T. Cohen, M. Shibuya and G. Neufeld: Vascular endothelial growth factor receptor-1 and neuropilin-2 form complexes. *J Biol Chem*, 276, 18688-94 (2001)
143. M. Migdal, B. Huppertz, S. Tessler, A. Comforti, M. Shibuya, R. Reich, H. Baumann and G. Neufeld: Neuropilin-1 is a placenta growth factor-2 receptor. *J Biol Chem*, 273, 22272-8 (1998)
144. T. Makinen, B. Olofsson, T. Karpanen, U. Hellman, S. Soker, M. Klagsbrun, U. Eriksson and K. Alitalo: Differential binding of vascular endothelial growth factor B splice and proteolytic isoforms to neuropilin-1. *J Biol Chem*, 274, 21217-22 (1999)
145. L. M. Wise, T. Veikkola, A. A. Mercer, L. J. Savory, S. B. Fleming, C. Caesar, A. Vitali, T. Makinen, K. Alitalo and S. A. Stacker: Vascular endothelial growth factor (VEGF)-like protein from orf virus NZ2 binds to VEGFR2 and neuropilin-1. *Proc Natl Acad Sci U S A*, 96, 3071-6 (1999)
146. J. E. Park, H. H. Chen, J. Winer, K. A. Houck and N. Ferrara: Placenta growth factor. Potentiation of vascular endothelial growth factor bioactivity, in vitro and in vivo, and high affinity binding to Flt-1 but not to Flk-1/KDR. *J Biol Chem*, 269, 25646-54 (1994)
147. A. Matsushita, T. Gotze and M. Korc: Hepatocyte growth factor mediated cell invasion in pancreatic cancer cells is dependent on neuropilin-1. *Cancer Res*, 67, 10309-16 (2007)
148. B. Hu, P. Guo, I. Bar-Joseph, Y. Imanishi, M. J. Jarzynka, O. Bogler, T. Mikkelsen, T. Hirose, R. Nishikawa and S. Y. Cheng: Neuropilin-1 promotes human

glioma progression through potentiating the activity of the HGF/SF autocrine pathway. *Oncogene*, 26, 5577-86 (2007)
149. J. I. Lim, C. Spee, M. Hangai, J. Rocha, H. S. Ying, S. J. Ryan and D. R. Hinton: Neuropilin-1 expression by endothelial cells and retinal pigment epithelial cells in choroidal neovascular membranes. *Am J Ophthalmol*, 140, 1044-1050 (2005)
150. S. J. Harper, C. Y. Xing, C. Whittle, R. Parry, D. Gillatt, D. Peat and P. W. Mathieson: Expression of neuropilin-1 by human glomerular epithelial cells in vitro and in vivo. *Clin Sci (Lond)*, 101, 439-46 (2001)
151. E. J. Kim, H. Y. Park, M. Yaar and B. A. Gilchrest: Modulation of vascular endothelial growth factor receptors in melanocytes. *Exp Dermatol*, 14, 625-33 (2005)
152. G. Bluteau, M. Julien, D. Magne, F. Mallein-Gerin, P. Weiss, G. Daculsi and J. Guicheux: VEGF and VEGF receptors are differentially expressed in chondrocytes. *Bone*, 40, 568-76 (2007)
153. J. Harper, L. C. Gerstenfeld and M. Klagsbrun: Neuropilin-1 expression in osteogenic cells: down-regulation during differentiation of osteoblasts into osteocytes. *J Cell Biochem*, 81, 82-92 (2001)
154. H. Yi, Y. Zhen, L. Jiang, J. Zheng and Y. Zhao: The phenotypic characterization of naturally occurring regulatory CD4+CD25+ T cells. *Cell Mol Immunol*, 3, 189-95 (2006)
155. S. Curreli, Z. Arany, R. Gerardy-Schahn, D. Mann and N. M. Stamatos: Polysialylated neuropilin-2 is expressed on the surface of human dendritic cells and modulates dendritic cell-T lymphocyte interactions. *J Biol Chem*, 282, 30346-56 (2007)
156. H. E. Gruber, J. L. Mougeot, G. Hoelscher, J. A. Ingram and E. N. Hanley, Jr.: Microarray analysis of laser capture microdissected-anulus cells from the human intervertebral disc. *Spine*, 32, 1181-7 (2007)
157. T. Takahashi, A. Fournier, F. Nakamura, L. H. Wang, Y. Murakami, R. G. Kalb, H. Fujisawa and S. M. Strittmatter: Plexin-neuropilin-1 complexes form functional semaphorin-3A receptors. *Cell*, 99, 59-69 (1999)
158. V. Castellani, E. De Angelis, S. Kenwrick and G. Rougon: Cis and trans interactions of L1 with neuropilin-1 control axonal responses to semaphorin 3A. *Embo J*, 21, 6348-57 (2002)
159. L. Feiner, A. M. Koppel, H. Kobayashi and J. A. Raper: Secreted chick semaphorins bind recombinant neuropilin with similar affinities but bind different subsets of neurons in situ. *Neuron*, 19, 539-45 (1997)
160. G. Neufeld, O. Kessler and Y. Herzog: The interaction of Neuropilin-1 and Neuropilin-2 with tyrosine-kinase receptors for VEGF. *Adv Exp Med Biol*, 515, 81-90 (2002)

Abbreviations: FGF: Fibroblas Growth Factor; HGF/SF: Hepatocyte Growth Factor/ Scatter Factor; HS: Heparan Sulfate, NRP-1/-2: Neuropilin-1/-2; PlGF: Plancenta Growth Factor; VEGF: Vascular Endothelial Growth Factor; VEGFR: VEGF Receptor.

Key Words: Neuropilins, Development, Structure, Interactions, Review

Send correspondence to: Katarzyna Adela Uniewicz, David Garth Fernig, Biosciences Building, Crown Street, University of Liverpool, Liverpool L69 7ZB, E-mail: katuni@liverpool.ac.uk

http://www.bioscience.org/current/vol13.htm

Supplemental paper 2

Uniewicz, K. A., Ori, A., Xu, R., Ahmed, Y., Wilkinson, M. C., Fernig, D. G., & Yates, E. A. **2010**. Differential scanning fluorimetry measurement of protein stability changes upon binding to glycosaminoglycans: a screening test for binding specificity. *Analytical Chemistry*, 82(9): 3796-3802.

Authors contributions:

Uniewicz, K. A. designed the research, performed the experiments, analysed the data, and wrote the paper

Ori, A. performed the experiments, analysed the data

Xu, R. contributed to reagents

Ahmed, Y. contributed to reagents

Wilkinson, M. C. provided technical training and equipment

Fernig, D. G. supervised the writing

Yates, E. A. supervised the writing

Anal. Chem. **2010**, *82*, 3796–3802

Differential Scanning Fluorimetry Measurement of Protein Stability Changes upon Binding to Glycosaminoglycans: A Screening Test for Binding Specificity

Katarzyna A. Uniewicz, Alessandro Ori, Ruoyan Xu, Yassir Ahmed, Mark C. Wilkinson, David G. Fernig, and Edwin A. Yates*

School of Biological Sciences, University of Liverpool, Liverpool, L69 7ZB, United Kingdom

The interaction between glycosaminoglycans (GAGs) and proteins is important for the regulation of protein transport and activity. Here we present a novel method for the measurement of protein−GAG interactions suitable for high-throughput screening, able to discriminate between the interactions of a protein with GAGs of different structures. Binding of proteins to the GAG heparin, a proxy for sulfated regions of extracellular heparan sulfate, was found to enhance the stability of three test proteins, fibroblast growth factors (FGFs)-1, -2, and -18. Chemically modified heparins and heparin oligosaccharides of different lengths stabilized the three FGFs to different extents, depending on the pattern of sugar binding specificity. The method is based on a differential scanning fluorescence approach. It uses a Sypro Orange dye, which binds to exposed core residues of a denatured protein and results in an increased fluorescence signal. It is convenient, requiring low micromolar amounts of protein and ligand compared to other interaction assays, employing only a real-time polymerase chain reaction (PCR) instrument.

Heparan sulfate (HS) is a member of the glycosaminoglycan (GAG) family of highly anionic linear polysaccharides. It is synthesized as a homogeneous polymer of glucuronic acid linked to *N*-acetyl glucosamine ((-4)D-GlcA β(1-4)D-GlcNAc α(1-)), which is then modified by a series of sulfation and epimerization reactions. N-Deacetylation and N-sulfation of glucosamine residues indicates regions for further modifications, which include epimerization of D-glucuronate to L-iduronate and 2-O-sulfation of iduronic acid, 6-O-sulfation, and more rarely, 3-O-sulfation of glucosamine.[1] The resulting HS polymer is of high sequence variability comprising subunits bearing distinct sulfation patterns.[1] Heparin can be considered a specialized form of HS and consists predominantly of highly modified, sulfated stretches.

HS functions as an extracellular mechanical support molecule[2−4] but is also a regulator of the functions of a vast array of proteins, ranging from the fibroblast growth factors (FGFs),[5−7] β-amyloid cleavage enzyme-1 (BACE-1),[8] antithrombin,[9] and neuropilin-1 (NRP-1).[10] The interaction of HS with its protein partners alter their activity and often serves as a means of assembling functional complexes.[1,11] One of the plausible explanations of the function of HS within complexes is to enhance the stability of the proteins with which it is involved.[12] The functional importance of protein interactions with HS and the potential consequences for glycotherapies[13] has led to the development of many assay systems.[14] These include surface-based methods[15] (enzyme-linked immunosorbent assay (ELISA), surface plasmon resonance (SPR)), calorimetric (isothermal titration calorimetry (ITC),[16] differential scanning calorimetry (DSC)[16,17]), and spectroscopic approaches such as NMR,[18] circular dichroism (CD),[19,20] and Fourier transform-infrared (FT-IR).[16] However, these approaches do not lend themselves to a comprehensive high-throughput screen of sugar structures involved in the interactions, may suffer from surface based artifacts,[21] or may require large amounts of sample and complex instrumentation.

* To whom correspondence should be addressed. E-mail: E.A.Yates@liverpool.ac.uk. Fax: +44-151-795-4406.

(1) Esko, J. D.; Selleck, S. B. *Annu. Rev. Biochem.* **2002**, *71*, 435–471.
(2) Scott, J. E. *J. Anat.* **1995**, *187* (Part 2), 259–269.
(3) Florian, J. A.; Kosky, J. R.; Ainslie, K.; Pang, Z.; Dull, R. O.; Tarbell, J. M. *Circ. Res.* **2003**, *93*, e136–142.
(4) Rodgers, K. D.; San Antonio, J. D.; Jacenko, O. *Dev. Dyn.* **2008**, *237*, 2622–2642.
(5) Pye, D. A.; Vives, R. R.; Turnbull, J. E.; Hyde, P.; Gallagher, J. T. *J. Biol. Chem.* **1998**, *273*, 22936–22942.
(6) Sugaya, N.; Habuchi, H.; Nagai, N.; Ashikari-Hada, S.; Kimata, K. *J. Biol. Chem.* **2008**, *283*, 10366–10376.
(7) Guimond, S.; Maccarana, M.; Olwin, B. B.; Lindahl, U.; Rapraeger, A. C. *J. Biol. Chem.* **1993**, *268*, 23906–23914.
(8) Patey, S. J.; Edwards, E. A.; Yates, E. A.; Turnbull, J. E. *J. Med. Chem.* **2006**, *49*, 6129–6132.
(9) Hovingh, P.; Piepkorn, M.; Linker, A. *Biochem. J.* **1986**, *237*, 573–581.
(10) Uniewicz, K. A.; Fernig, D. G. *Front. Biosci.* **2008**, *13*, 4339–4360.
(11) Gallagher, J. T. *Biochem. Soc. Trans.* **2006**, *34*, 438–441.
(12) Roy, S.; Fortin, M.; Gagnon, J.; Ghinet, M. G.; Lehoux, J. G.; Dupuis, G.; Brzezinski, R. *Biochim. Biophys. Acta* **2007**, *1774*, 975–984.
(13) Patey, S. J.; Edwards, E. A.; Yates, E. A.; Turnbull, J. E. *Neurodegener. Dis.* **2008**, *5*, 197–199.
(14) Hamel, D. J.; Sielaff, I.; Proudfoot, A. E.; Handel, T. M. *Methods Enzymol.* **2009**, *461*, 71–102.
(15) Delehedde, M.; Lyon, M.; Gallagher, J. T.; Rudland, P. S.; Fernig, D. G. *Biochem. J.* **2002**, *366*, 235–244.
(16) Guzman-Casado, M.; Cardenete, A.; Gimenez-Gallego, G.; Parody-Morreale, A. *Int. J. Biol. Macromol.* **2001**, *28*, 305–313.
(17) McPherson, J. M.; Sawamura, S. J.; Condell, R. A.; Rhee, W.; Wallace, D. G. *Coll. Relat. Res.* **1988**, *8*, 65–82.
(18) Gettins, P.; Wooten, E. W. *Biochemistry* **1987**, *26*, 4403–4408.
(19) Svensson, G.; Linse, S.; Mani, K. *Biochemistry* **2009**, *48*, 9994–10004.
(20) Zakrzewska, M.; Wiedlocha, A.; Szlachcic, A.; Krowarsch, D.; Otlewski, J.; Olsnes, S. *J. Biol. Chem.* **2009**, *284*, 25388–25403.
(21) Powell, A. K.; Zhi, Z. L.; Turnbull, J. E. *Methods Mol. Biol.* **2009**, *534*, 313–329.

10.1021/ac100188x
Published on Web 03/30/2010

Since the interaction of HS with its protein partners can alter their activity and often serves as a means of assembling functional complexes, it has been suggested that this may occur by stabilization of the protein structure, illustrated, for example, by antithrombin III[22] and also by the FGFs.[20,23−27] Consequently, we have employed a recently described technique, which measures protein stability,[28] to develop a new method for determining the specificity of protein−polysaccharide interactions.

The method uses a sensitive dye (Sypro Orange), which when bound to exposed core residues of denatured proteins exhibits high fluorescence. Small volumes (10 μL) and protein concentrations (low micromolar range) are used, and the assay can be adapted to a multiwell format, taking less than 1 h, making it suitable for high-throughput screening. The assay utilizes heparin as an internal control, allowing the comparison of the tested compounds with heparin and calculation of their relative stabilizing effects. In this study, we determined the minimal length of oligosaccharide and the sulfation pattern required for the interaction of the three illustrative proteins: FGF-1, FGF-2 (prototypical HS binding proteins), and FGF-18, with a range of homogenously modified polysaccharides employed widely as probes of structure−function relationships in HS. The method can also be applied to the measurement of melting temperatures of protein−GAG complexes. The results with FGF-1 and FGF-2 are in good agreement with published data demonstrating that this method can be used to establish the specificity of the interactions between GAGs and proteins.

EXPERIMENTAL SECTION

Protein and Polysaccharide Preparation. Recombinant FGF-1 (aFGF) (UniProt Accession, P05230; residues, 16−155) and FGF-2 (bFGF) (UniProt Accession, P09038-2; residues, 1−155) were expressed in C41 *Escherichia coli* cells using a pET-14b system (Novagen, Merck Chemical Ltd., Nottingham, Notts, U.K.).[29] FGF-2 was purified as described previously,[30] and the same procedure was employed to purify FGF-1. FGF-18 (zFGF5) (UniProt Accession, O76093; residues, 28−207) (Figure S-1 in the Supporting Information) was cloned in a modified pET-24b vector (pETM-11, kind gift of Dr. Paul Elliott, University of Liverpool) and expressed in C41 *E. coli* cells. Bacteria were grown under standard conditions and, following induction (1 mM IPTG, 16 h at 16 °C), cells were collected by centrifugation at 3000*g* for 7 min, washed with 50 mM Tris pH 7.5, 0.15 M NaCl, and sonicated in buffer A (50 mM Tris pH 7.5, 0.5 M NaCl, 50 mM imidazole) on ice. When a clear solution had been obtained, the lysate was applied to a 3 mL ProBond nickel-chelating resin (Invitrogen, Paisley, Scotland, U.K.) column equilibrated with buffer A. Following extensive washing with buffer A, protein was eluted using 50 mM Tris pH 7.5, 0.5 M NaCl, 500 mM imidazole. The histidine tag of the eluted protein was cleaved with a histidine-tagged TEV protease (also a kind gift from Dr. Paul Elliot) at 4 °C. Following overnight digestion, the sample was reapplied to the ProBond nickel-chelating resin column to separate the cleaved tag, TEV protease, and impurities from the FGF-18. The cleaved protein (unbound fraction) was further purified using a HiTrap Heparin HP 1 mL column (GE Healthcare, Amersham, Bucks, U.K.). All proteins were prepared as 10 times concentrated stocks in 50 mM Tris pH 7.5, 2 M NaCl.

The same heparin (17 kDa average molecular weight) (Celsus Lab, Cincinnati, OH) was used in the assay and as a starting material for the production of modified derivatives[8,31] (Figure S-2 in the Supporting Information) and oligosaccharides,[32] all of which were used as 10 times concentrated stock solutions (1.75 mg/mL) in HPLC grade water.

Differential Scanning Fluorimetry (DSF). The experiment was performed using a 7500 Fast Real Time PCR System (software version 1.4.0) (Applied Biosystems, Warrington, Cheshire, U.K.), and the samples were subjected to the heating cycle as described previously.[28] Briefly, heparin derivatives (10% v/v), protein stock solutions (10% v/v), and Dulbecco's phosphate-buffered saline without $CaCl_2/MgCl_2$ (Gibco-Europe, Paisley, Scotland, U.K.) (70% v/v) were added to a Fast Optical 96 Well Reaction Plate (Applied Biosystems) maintained on ice. Freshly prepared 100× water based dilution of Sypro Orange 5000× (Invitrogen, Paisley, Scotland, U.K.) was added as 10% v/v. The final volume of the reaction mixture was either 10 or 25 μL. Final concentrations of the proteins were 10 μM (FGF-1 and FGF-2 in screens of oligosaccharides and chemically modified heparin derivatives and all FGF-18 assays) or 5 μM (FGF-2 and gradient of heparin concentrations). For experiments with ranges of heparin concentrations, the final concentrations of heparin were calculated according to the molar ratio of the heparin versus the protein within a range 0.5−500 μM. In oligosaccharide and chemically modified heparin derivative assays, the species under examination comprised pools of defined oligosaccharides, which made molarity difficult to define. In addition, as the mechanism of binding of the saccharides to the protein is unclear, the concentration range expressed in micrograms per milliliter was selected to compare the bestowed stabilization effects. Thus, the effective concentration of heparin was chosen (for instance, 175 μg/mL corresponding to ~10 μM), and all other heparin-derived compounds were used at the same w/v ratio (175 μg/mL). In the case of FGF-18, the same mass ratio was maintained for the screen of oligosaccharides. For chemically modified heparin derivatives, their concentration was doubled (to 350 μg/mL, analogous to 20 μM concentration of heparin) as 175 μg/mL was insufficient to bestow any stabilizing effect by any of the compounds and compared with 350 μg/mL of heparin. After sealing with Optical Adhesive Film (Applied Biosystems), the plate was gently vortexed and

(22) Busby, T. F.; Atha, D. H.; Ingham, K. C. *J. Biol. Chem.* **1981**, *256*, 12140–12147.
(23) Vemuri, S.; Beylin, I.; Sluzky, V.; Stratton, P.; Eberlein, G.; Wang, Y. J. *J. Pharm. Pharmacol.* **1994**, *46*, 481–486.
(24) Prestrelski, S. J.; Fox, G. M.; Arakawa, T. *Arch. Biochem. Biophys.* **1992**, *293*, 314–319.
(25) Copeland, R. A.; Ji, H.; Halfpenny, A. J.; Williams, R. W.; Thompson, K. C.; Herber, W. K.; Thomas, K. A.; Bruner, M. W.; Ryan, J. A.; Marquis-Omer, D.; et al. *Arch. Biochem. Biophys.* **1991**, *289*, 53–61.
(26) Fan, H.; Li, H.; Zhang, M.; Middaugh, C. R. *J. Pharm. Sci.* **2007**, *96*, 1490–1503.
(27) Culajay, J. F.; Blaber, S. I.; Khurana, A.; Blaber, M. *Biochemistry* **2000**, *39*, 7153–7158.
(28) Niesen, F. H.; Berglund, H.; Vedadi, M. *Nat. Protoc.* **2007**, *2*, 2212–2221.
(29) Duchesne, L.; Gentili, D.; Comes-Franchini, M.; Fernig, D. G. *Langmuir* **2008**, *24*, 13572–13580.
(30) Ke, Y.; Wilkinson, M. C.; Fernig, D. G.; Smith, J. A.; Rudland, P. S.; Barraclough, R. *Biochim. Biophys. Acta* **1992**, *1131*, 307–310.
(31) Yates, E. A.; Santini, F.; Guerrini, M.; Naggi, A.; Torri, G.; Casu, B. *Carbohydr. Res.* **1996**, *294*, 15–27.
(32) Turnbull, J. E. *Methods Mol. Biol.* **2001**, *171*, 141–147.

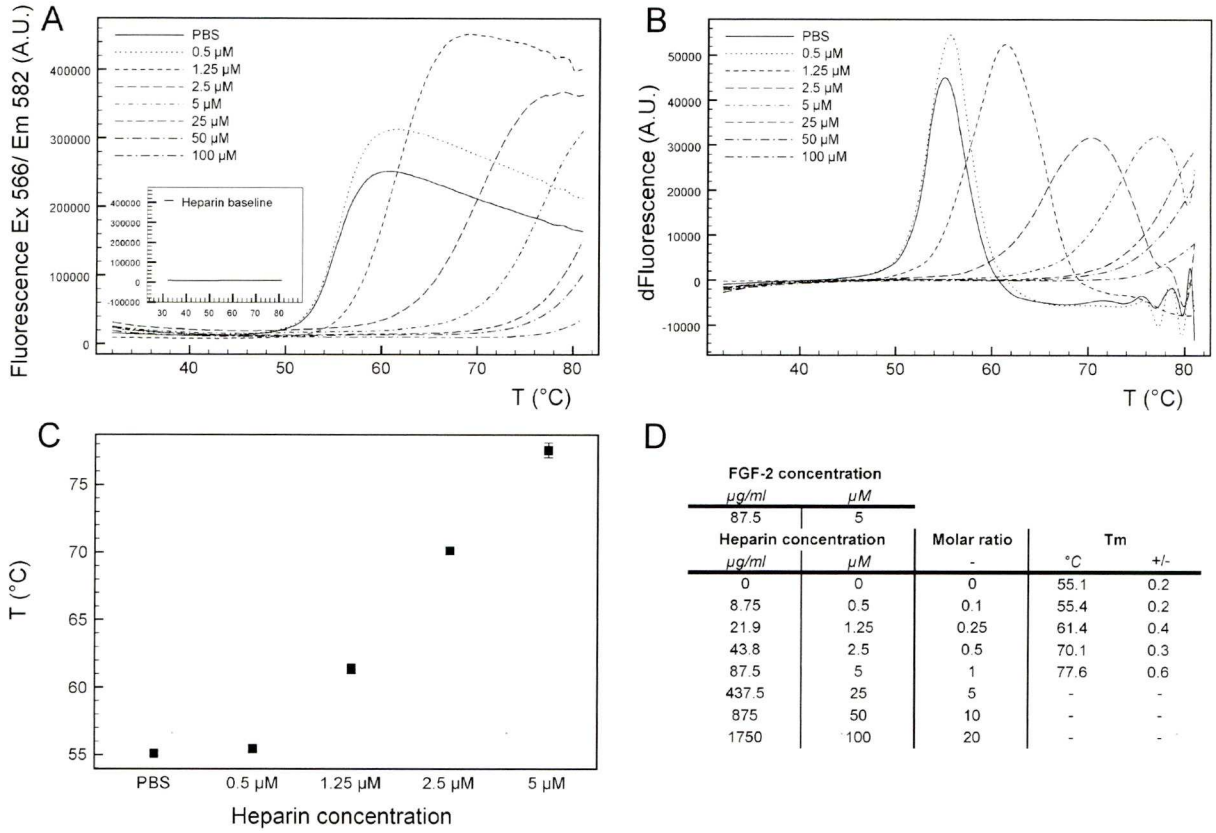

FGF-2 concentration				
µg/ml	µM			
87.5	5			
Heparin concentration		Molar ratio	Tm	
µg/ml	µM	-	°C	+/-
0	0	0	55.1	0.2
8.75	0.5	0.1	55.4	0.2
21.9	1.25	0.25	61.4	0.4
43.8	2.5	0.5	70.1	0.3
87.5	5	1	77.6	0.6
437.5	25	5	-	-
875	50	10	-	-
1750	100	20	-	-

Figure 1. Concentration dependent effect of heparin on thermal stabilization of FGF-2. (A) Melting curve profile of 5 μM FGF-2 in the presence of various concentrations of heparin ligand (0, 0.5−100 μM). (B) The first derivatives of each melting curve where each maximum of the first derivative indicates the Tm (melting temperature). (C) Mean Tm values plotted from the maxima of the derivatives calculated from three repeats of at least two experiments performed in triplicate (±SD). (D) Ratios of assayed concentrations of FGF-2 and heparin juxtaposed with their corresponding mean Tm values (±SD) from at least two independent experiments performed in triplicate.

directly analyzed in the real-time polymerase chain reaction (RT-PCR) instrument. The heating cycle comprised a 120 s prewarming step at 31 °C and a subsequent gradient between 32 and 81 °C in 99 steps of 20 s, each of 0.5 °C ramp. Data were collected using the calibration setting for TAMRA dye detection (λ_{ex} 560 nm; λ_{em} 582 nm) installed on the instrument.

Data Analysis. The data were analyzed using the Plot v. 0.997 software for Mac OS X (plot.micw.eu) by application of an exponential correlation function approximation of the first derivative for each melting curve. For each heparin derivative, three distinct melting curves were analyzed. However, the figures include only one melting curve/derivative per polysaccharide variant tested for clarity. The maxima of distinct derivatives were used to calculate the mean Tm (melting temperature) and the standard deviation (SD) of each Tm was based on three repeats. Subsequently, data were normalized to allow comparison between the stabilization effects of assayed heparin derivatives with that of heparin. To perform normalization, each compound was characterized by the difference between the Tm of the protein in PBS (Tm PBS) and the Tm of the protein in the presence of the heparin derivative (Tm x) according to eq 1

$$\text{Tm x} - \text{Tm PBS} \tag{1}$$

Next, the comparison of stabilization potency versus heparin was obtained from eq 2

$$\frac{\text{Tm x} - \text{Tm PBS}}{\text{Tm hep} - \text{Tm PBS}} \tag{2}$$

where Tm hep is the mean Tm of the protein in the presence of heparin. Thus, the relative stability of protein in PBS was set to 0, while the relative stabilizing effect of heparin was set to 1. To calculate absolute Tm of FGF-1 and FGF-2, at least two independent experiments in triplicate were analyzed and the final Tm is the mean of all obtained values.

RESULTS AND DISCUSSION

Suitability of DSF for Detecting Heparin Dependent Thermostabilizing Effects on FGF-2. The interaction of FGF-2 with heparin has been studied extensively and the stabilizing effect of the interaction is well documented.[23,24] To establish whether DSF has the potential to measure protein−sugar interactions, a screen was performed, in which a range of heparin concentrations (0.5−100 μM) was tested against a constant amount of FGF-2 (5 μM). The denaturation curves show that a stabilizing effect is apparent from 1.25 μM heparin (heparin−FGF-2 molar ratio 1:4) with concentrations of heparin of 25 μM or more sufficient to prevent full denaturation in the temperature range used (Figure

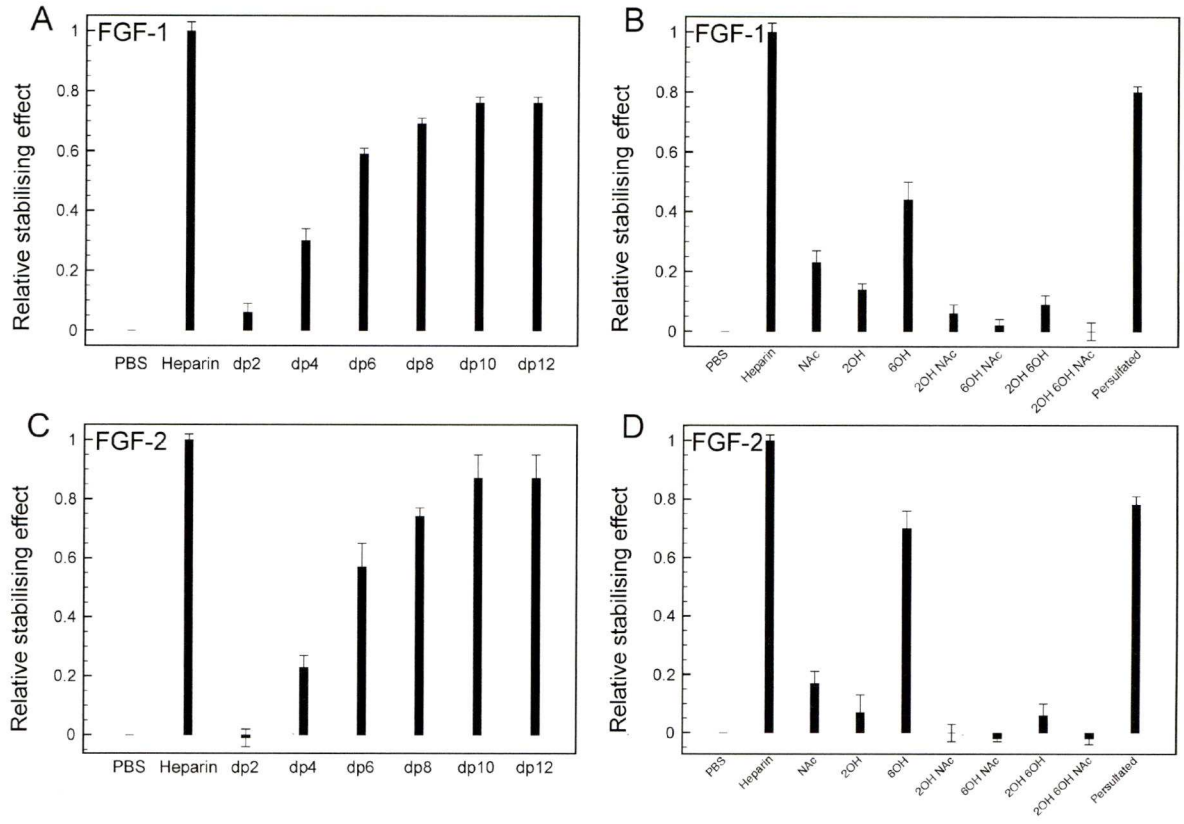

Figure 2. Relative thermostabilizing effect of heparin, heparin-derived oligosaccharides, and chemically modified heparins on FGF-1 and FGF-2, calculated according to eq 2. (A) Thermostabilizing effect on FGF-1 caused by heparin-derived oligosaccharides and (B) chemically modified heparins. (C) Thermostabilizing effect on FGF-2 caused by heparin-derived oligosaccharides and (D) chemically modified heparins. Results are the mean ± SD of three repeats after normalization.

1A). The first derivatives of the denaturation curves were plotted, where the maxima defined the Tm (Figure 1B). This experiment clearly showed that heparin had a concentration dependent effect on FGF-2 stability (Figure 1B–D). Importantly, there was no background signal arising from heparin–Sypro Orange interactions (inset of Figure 1A); therefore, the method is suitable for measuring the interactions of proteins with polysaccharides through the stabilization effect, since all the signal derives from the denatured protein.

Application of DSF to Probe the Structural Requirements of Heparin-Derived Compounds for Protein Stabilization. Having shown that DSF could identify the interaction between heparin and FGF-2, the ability of DSF to discriminate between the binding specificity of structurally different heparins was tested. To verify DSF against published data, the interactions of FGF-1 and FGF-2 with heparin, oligosaccharides of various lengths and full-length homogenously modified heparin derivatives bearing a range of different sulfation patterns were tested (Figure S-2 in the Supporting Information). The data were collected at a 1:1 molar ratio of protein to heparin, because at this ratio the stabilization effect was in the medium to high range, so providing a good dynamic range. For other saccharide ligands, the same concentration (175 μg/mL) was employed, under the assumption that the differences between the potency of the compounds should be detectable at this ratio. Data were then analyzed as before and normalized to reveal the ability of each compound to stabilize the protein relative to heparin, whose potency was defined as 1 (referred to as 0, with no ligand present). The minimal length of oligosaccharide required to stabilize FGF-1 or FGF-2 at the same level as heparin was established using a library of various oligosaccharides of varying lengths defined as degree of polymerization, dp, where dp 2 is a basic repeating disaccharide unit. The data clearly showed that even dp 2 had a small effect on FGF-1 thermostability, which thereafter increased as the length of the oligosaccharides increased to reach a maximum around dp 8–dp 10 (Figure 2A,C). In contrast, there was a detectable effect of dp 4 but not dp 2 on FGF-2 thermostability in accord with published data that indicated a tetrasaccharide as the minimal binding unit.[15,33] This experiment confirmed the published data, that binding sites of FGF-1 and FGF-2 can accommodate oligosaccharides of up to dp 10.[34,35]

The experiment in which various desulfated heparins were tested employed chemically modified heparin derivatives in which sulfate groups had been systematically removed to homogeneity, to give eight variants.[31] In addition, a persulfated heparin derivative bearing two additional sulfate groups (3-O-sulfate at uronic acid and 3-O-sulfate at glucosamine) was also

(33) Faham, S.; Hileman, R. E.; Fromm, J. R.; Linhardt, R. J.; Rees, D. C. *Science* **1996**, *271*, 1116–1120.
(34) Fromm, J. R.; Hileman, R. E.; Weiler, J. M.; Linhardt, R. J. *Arch. Biochem. Biophys.* **1997**, *346*, 252–262.
(35) DiGabriele, A. D.; Lax, I.; Chen, D. I.; Svahn, C. M.; Jaye, M.; Schlessinger, J.; Hendrickson, W. A. *Nature* **1998**, *393*, 812–817.

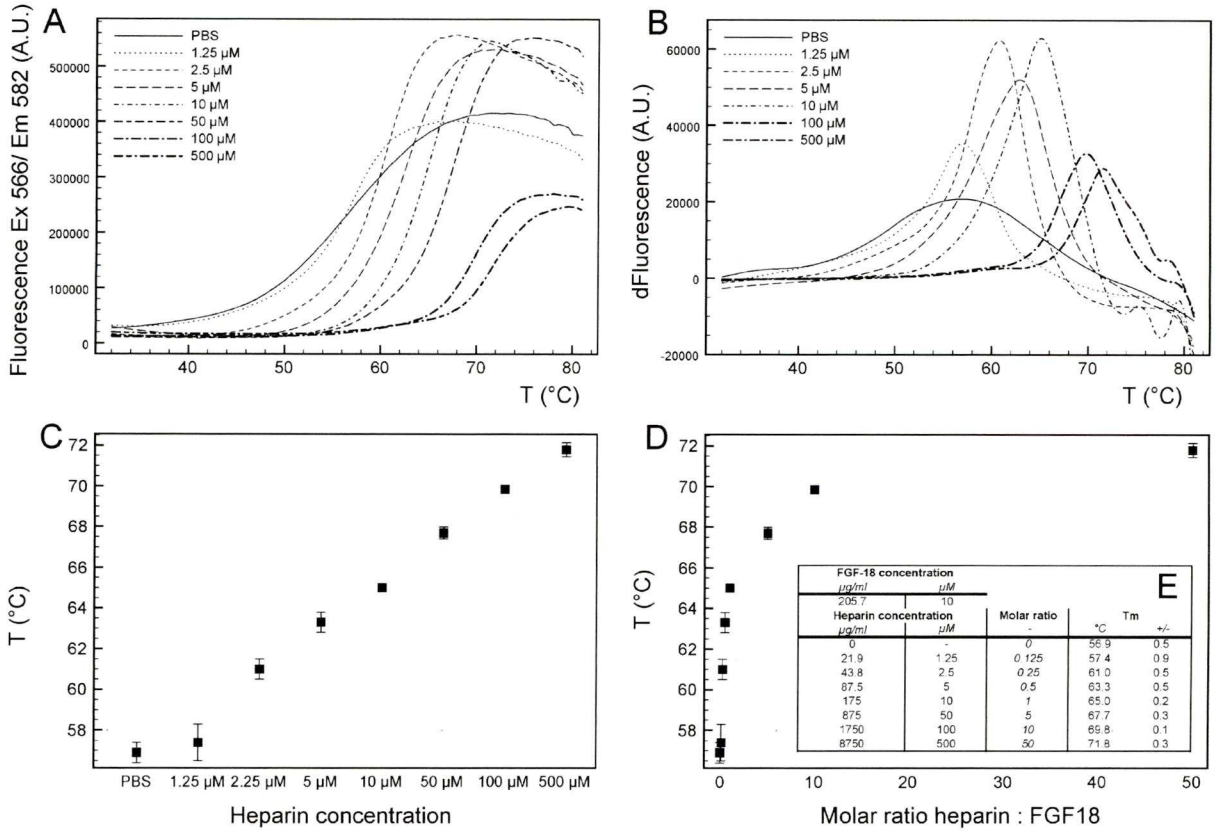

Figure 3. Concentration dependent effect of heparin on thermal stabilization of FGF-18. (A) Melting curve profile of 10 μM FGF-18 in the presence of various concentrations of heparin ligand (0, 1.25−500 μM). (B) The first derivatives of each melting curve where each maximum of the first derivative indicates the Tm (melting temperature). (C) Plotted mean Tm values calculated from three repeats (±SD). (D) The Tm values as in panel C plotted against molar ratio of present species. (E) Ratios of assayed concentrations of FGF-18 and heparin and their corresponding mean Tm values calculated from three repeats (±SD).

assayed, as a control for processes driven essentially by high charge density. The results again confirmed the published data, showing that sulfation is important for the interaction of the polysaccharide with both FGF-1 and FGF-2 (Figure 2B,D). Nevertheless, the potency of the persulfated heparin derivative did not exceed that of heparin, supporting the notion that although the interaction of these proteins with the sugars require sulfate groups, it is the disposition of the sulfates and their overall conformational consequences that are critical for the interactions. As shown using other approaches, the singley desulfated species had contrasting effects on FGF-1 and FGF-2, revealing distinct specificity profiles. Thus, it was shown that for FGF-1 all three sulfate groups, N-sulfate, 6-O-sulfate and 2-O-sulfate are required for interaction, while in the case of FGF-2, only N-sulfate and 2-O-sulfate play important roles[7,33,36−38] in these homogeneous derivatives. These findings were confirmed by the DSF method, as the presence of the 6-O-sulfate group contributed much less to the heparin-dependent stability of FGF-2 than of FGF-1 (Figure 2B,D). It was, therefore, possible to differentiate between two specific binding requirements of FGF-1 and FGF-2 and to show that this method could be applied to an assay of protein binding specificity.

Characterization of the Thermostabilizing Effect of Heparin, Heparin Oligosaccharides and Modified Heparin Derivatives on FGF-18. FGF-18 was chosen as a test protein to be characterized using this method because limited data are available concerning its interaction with heparin and HS. In contrast to FGF-1 and FGF-2, which both belong to the same FGF-1 subfamily, FGF-18 belongs to the FGF-8 subfamily, together with FGF-8 and FGF-17.[39] The published data describe FGF-18 as a heparin-binding growth factor that binds octasaccharides (dp 8) and requires both 2-O-sulfate and 6-O-sulfates, with an apparent preference for 2-O-sulfate groups.[40] First, the effect of heparin on FGF-18 stability was characterized. Interestingly, the protein alone had a very shallow denaturing curve, suggesting aggregation rather than unfolding following temperature elevation (Figure 3A). Nevertheless, addition of only 0.125 mol equiv of heparin was sufficient to sharpen the denaturation curve while, at the same

(36) Kreuger, J.; Salmivirta, M.; Sturiale, L.; Gimenez-Gallego, G.; Lindahl, U. *J. Biol. Chem.* **2001**, *276*, 30744–30752.
(37) Guglier, S.; Hricovini, M.; Raman, R.; Polito, L.; Torri, G.; Casu, B.; Sasisekharan, R.; Guerrini, M. *Biochemistry* **2008**, *47*, 13862–13869.
(38) Ashikari-Hada, S.; Habuchi, H.; Sugaya, N.; Kobayashi, T.; Kimata, K. *Glycobiology* **2009**, *19*, 644–654.
(39) Itoh, N.; Ornitz, D. M. *Trends Genet.* **2004**, *20*, 563–569.
(40) Ashikari-Hada, S.; Habuchi, H.; Kariya, Y.; Itoh, N.; Reddi, A. H.; Kimata, K. *J. Biol. Chem.* **2004**, *279*, 12346–12354.

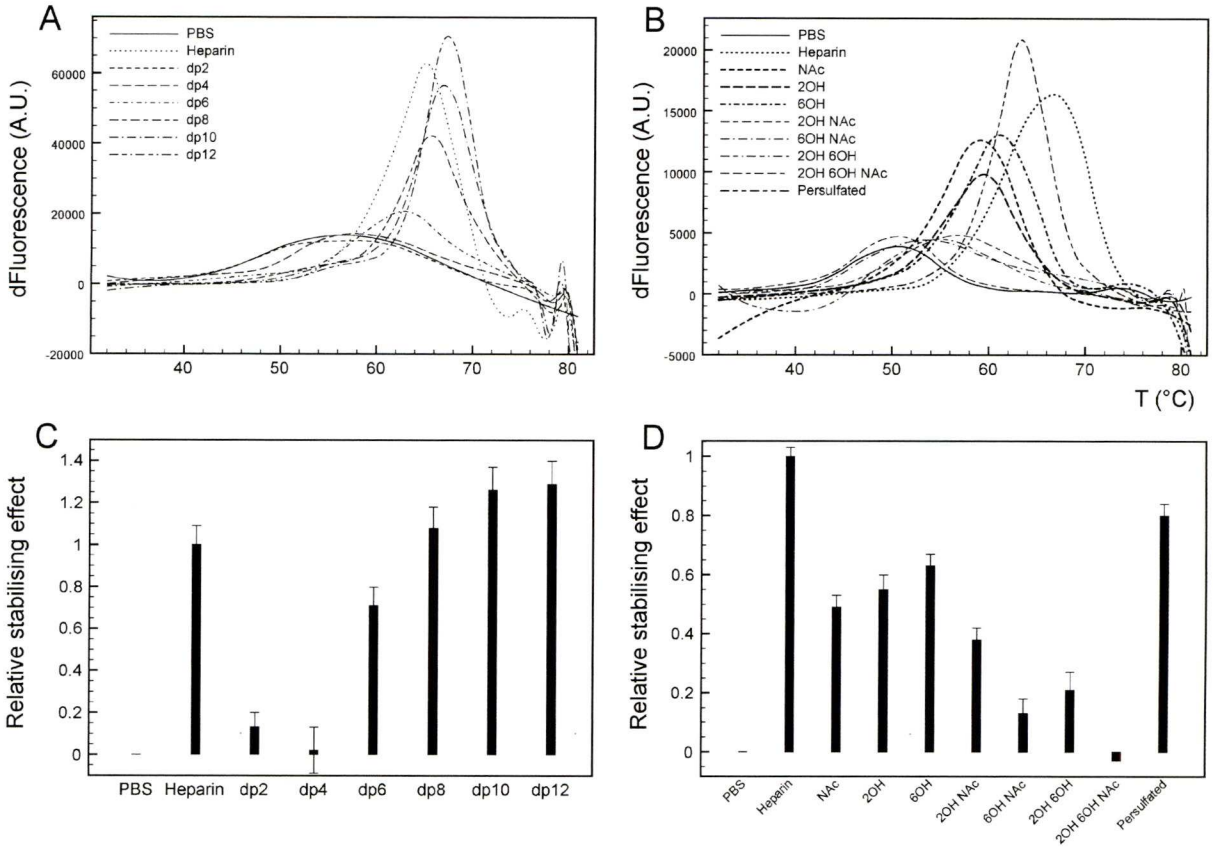

Figure 4. Relative thermostabilizing effect of heparin, heparin-derived oligosaccharides, and chemically modified heparins on FGF-18, calculated according to eq 2. (A, C) The first derivatives of each melting curve and relative thermostabilizing effect of heparin-derived oligosaccharides, respectively. (B, D) The first derivatives of each melting curve and relative thermostability effect of chemically modified heparins, respectively. (C, D) Results are the mean ± SD of three repeats after normalization.

time, affecting the Tm value only subtly (Figure 3A,B). Subsequent heparin concentrations modified the thermostability of the complex gradually, resulting in a thermostability shift from 57 to 71 °C at 1:50 molar ratio of FGF-18 to heparin. It is important to note that this difference was broadly comparable with, albeit somewhat lower than, that observed with FGF-2 and heparin (Figure 1), in which a 1:1 (protein−heparin) molar ratio was the final condition covered by the temperature range of the experiment. To conclude, the interaction between FGF-18 and heparin resulted in a less pronounced stabilization effect than with FGF-1 and FGF-2 but, nonetheless, even low heparin concentrations affected the protein behavior, as indicated by the visibly steeper denaturation curves (Figure 3A,B; compare PBS and 1.25 μM curves).

The potency of oligosaccharide derivatives in mediating the stability effect on FGF-18 were then examined. The shorter oligosaccharides dp 2−dp 6 were ineffective at altering the Tm of FGF-18 and neither did they affect the denaturation curve of the putatively aggregating FGF-18. In contrast, dp 8 oligosaccharides not only managed to sharpen the denaturation curve of FGF-18 but also significantly influenced its stability (Figure 4A,C). This size requirement correlated with the published data, where an octasaccharide library was used to characterize FGF-18 sulfate group binding specificity.[40] The sulfation requirements of saccharide binding were examined using the same set of heparin derivatives. However, in order to obtain reproducible denaturation curves, FGF-18 had to be incubated with increased amounts of the heparin derivatives, otherwise the stabilization effect was not detectable (data not shown). This modification highlights the importance for all three sulfate groups in mediating the structure affecting/stabilizing property of heparin. Under the new conditions, FGF-18, in contrast to FGF-1 and FGF-2, was equally stabilized by three singly desulfated heparin derivatives though to a lesser extent than with heparin (Figure 4B,D). These data suggest that FGF-18 interactions are altered by loss of any of the three sulfate groups of heparin at comparable levels, which results in a reduction of the stabilizing effect.

DSF Characterization of FGF-1 and FGF-2 Stability. The method described permits the comparison between the effects of various carbohydrate ligands on protein−polysaccharide complex stability to be made by conducting an experiment under defined conditions and including appropriate controls. Although such an approach allows virtual independence from external data, because the Tm values so obtained are normalized against the Tm of internal controls, it was decided to check whether the DSF Sypro method was consistent with other published data concerning the stability of FGF-1 and of FGF-2. It should be noted that the final Tm obtained in various experiments was dependent on many variables, including the protein, buffer conditions, protein concentration, intervals between data collection, and the method of

Table 1. Comparison of Experimentally Obtained Melting Temperatures of FGF-1 and FGF-2 Using Various Methods, Buffer Types, and Protein Constructs with Appropriate References[a]

	method	T [°C]	buffer type	ref	residues	additional ref
FGF-1	CD	40.3	0.7 M guanidine-Cl	20	21−154	
	Trp fluorescence	39.8	0.7 M guanidine-Cl	20	21−154	
	CD	40.7	1.5 M urea	20	21−154	
	Trp fluorescence	35	Na phosphate pH 7.4	25	1−155	41
	CD	42	Na phosphate pH 7.4	25	1−155	
	DSC	42	Na phosphate pH 7.4	25	1−155	
	ANS fluorescence	52	Na phosphate Na citrate 0.15 M NaCl	26	2−155	Human Phage Biotechnology Corporation patent info
	DSC	39.45	0.7 M guanidine-Cl	27	16−155	42
	DSF Sypro	48.5	Na phosphate pH 7.4 0.35 M NaCl		16−155	
FGF-2	DSC	59	K phosphate pH 6.5	23	10−155	43
	FT-IR	57	Tris-Cl pH 8.5	24	10−155	
	DSF Sypro	55.4	Na phosphate pH 7.4 0.35 M NaCl		1−155	

[a] The values obtained using the DSF Sypro method are the mean value of at least two independent experiments performed in triplicate.

calculation. Table 1 shows juxtaposed melting temperatures of FGF-1 and FGF-2 obtained by different methods and employing distinct protein constructs in various buffer systems. For FGF-1, the Tm values covered a wide range of temperatures from 35 to 52 °C, while for FGF-2, the temperature range was limited to between 55 and 59 °C. Our experimental approach provided Tm values comparable with those obtained in the previous studies, also in the case of heparin-induced stability showing an approximately 20 °C rise in the melting temperatures (data not shown for FGF-1).[20,23−26]

However, it is emphasized that experimental variability can result in diverse Tm measurements and, while relative values are informative, the absolute values should be interpreted with caution.

CONCLUSIONS

A new method for the elucidation of the specificity of the interactions between proteins and GAGs is presented. The method enables calculation of protein melting temperatures in complexes with various heparin-derived molecules and can provide important structure−function information. The assay comprises a multicompound array consisting of internal controls (protein with and without heparin) and tested ligands, which permits normalization within a defined set of ligands. The assay requires a hydrophobic dye, Sypro Orange, which interacts with the protein core residues exposed upon denaturation, altering its emission spectrum and permits denaturation curves to be recorded as a function of temperature. It was confirmed that heparin derivatives do not interact with Sypro Orange, which excluded the possibility of nonspecific background signals. The assay requires low volumes (10 μL per well) and low concentrations of protein and ligand, 5 μM in the case of FGF-2 (17 kDa). It is convenient because the denaturation cycle takes only ~30 min and is entirely compatible with multiwell plates and automation. The screen requires a standard RT-PCR machine compatible with multiwell plates and can be used without specific calibration by employing the common TAMRA dye setting generally available. The method can be standarized easily and produces valuable data concerning the biophysical properties of protein interactions. This approach will shed new light on the role of GAGs in signaling complexes, or as extracellular buffers regulating transportation and the availability of the proteins. It could be applied to other polysaccharides and a range of hydrophilic ligands, or small molecules as a means of characterizing their interactions.

(41) Linemeyer, D. L.; Menke, J. G.; Kelly, L. J.; DiSalvo, J.; Soderman, D.; Schaeffer, M. T.; Ortega, S.; Gimenez-Gallego, G.; Thomas, K. A. *Growth Factors* **1990**, *3*, 287–298.

(42) Gimenez-Gallego, G.; Conn, G.; Hatcher, V. B.; Thomas, K. A. *Biochem. Biophys. Res. Commun.* **1986**, *138*, 611–617.

(43) Abraham, J. A.; Mergia, A.; Whang, J. L.; Tumolo, A.; Friedman, J.; Hjerrild, K. A.; Gospodarowicz, D.; Fiddes, J. C. *Science* **1986**, *233*, 545–548.

ACKNOWLEDGMENT

The work was supported by the European Commission (Marie Curie Early Stage Training Fellowships to Katarzyna Uniewicz and Alessandro Ori), the North West Cancer Research Fund, and the Cancer and Polio Research Fund. The authors thank James Ross, Dr. Pryank Patel, and Prof. Lu-Yun Lian for technical assistance and helpful discussions.

NOTE ADDED AFTER ASAP PUBLICATION

This paper was published on the Web March 30, 2010 with some errors in the volumes and concentrations in the Experimental Section and typographical errors. The corrected version was reposted April 16, 2010.

SUPPORTING INFORMATION AVAILABLE

Additional information as noted in text. This material is available free of charge via the Internet at http://pubs.acs.org.

Received for review January 21, 2010. Accepted March 11, 2010.

AC100188X

Supplemental data 3

Supplemental data 3 contains the spectra of the peptides analysed by MALDI-Q-TOF for the P&L experiment of the Fc rNRP-1 binding to heparin (Table 4.2, Section 4.4).

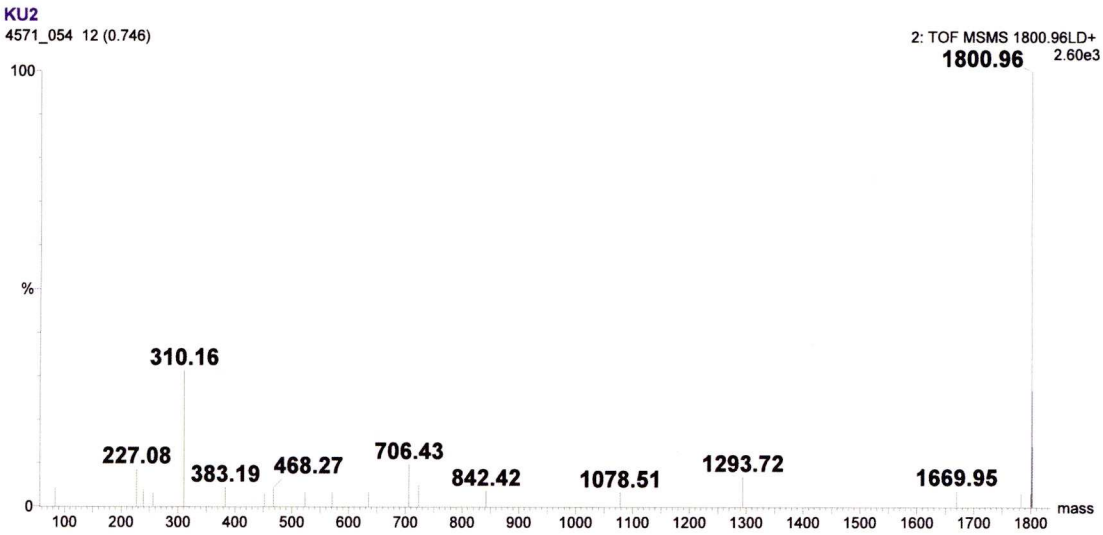

1800.96	*2.60E+03*	*VRIK(Biotin)PASWETGISM*
Ion fragment mass (m/z)	**Intensity**	**Assignment (error - ppm)**
84.07	1.11E+02	K(-128)
227.08	2.23E+02	Biotin(0)
239.15	9.89E+01	b_2-NH_3(-1.1)
256.17	8.07E+01	b_2(-27) / PAS(159) / SW-H_2O(242)
310.16	8.10E+02	K(Biotin)(0)
383.19	1.13E+02	ETGI-H_2O(-6.6)
452.24	7.84E+01	K(Biotin)P(16)
468.27	1.11E+02	IK(Biotin)(13)
523.28	8.38E+01	K(Biotin)PA(20)
571.26	8.44E+01	PASWE(16)
635.36	8.28E+01	
706.43	2.51E+02	b_4-NH3(33) / IK(Biotin)PAS-NH_3(100)
723.48	1.28E+02	b_4(64) / IK(Biotin)PAS(130)
842.42	9.22E+01	PASWETGI(19)
1078.51	8.40E+01	y_{10}(21)
1293.72	1.78E+02	b_9(33)
1669.95	9.57E+01	b_{13}+H_2O(46)
1783.01	7.92E+01	MH-H_2O(60)
1799.83	7.92E+01	
1800.96	2.60E+03	MH(26)

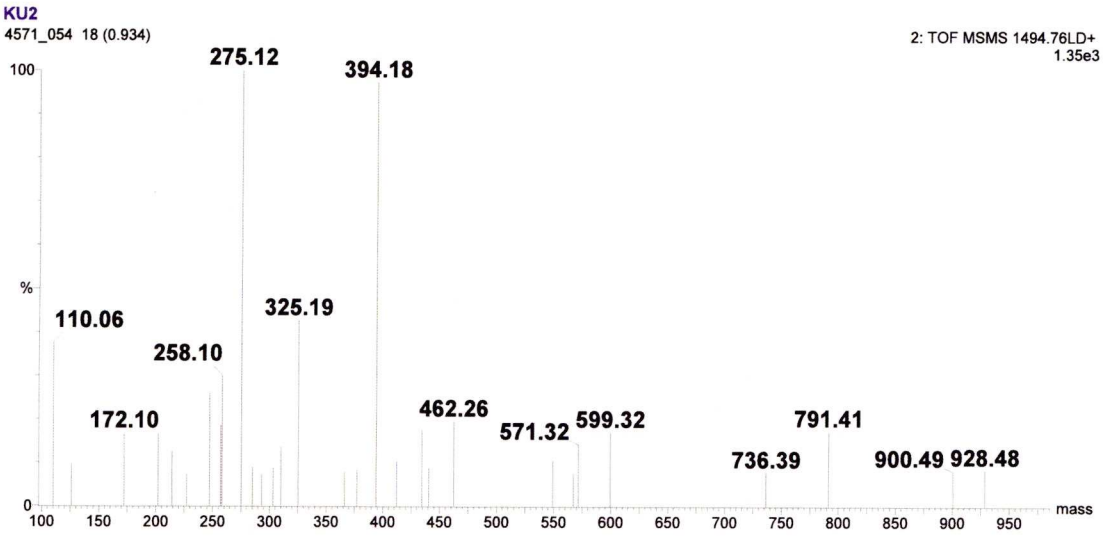

1494.76.	*1.35E+03*	*AGAFR(Acetyl)SDK(Biotin)C(Carbamidomethyl)GGT*
Ion fragment mass (m/z)	**Intensity**	**Assignment (error - ppm)**
110.06	5.10E+02	
126.08	1.29E+02	K(-90)
172.1	2.25E+02	a_3(-47)
202.1	2.24E+02	
214.1	1.69E+02	
227.09	9.94E+01	Biotin(44)
247.13	3.49E+02	C(Carbamidomethyl)GG-28(178)
257.11	2.52E+02	
258.1	4.06E+02	
275.12	1.35E+03	C(Carbamidomethyl)GG(142)
285.11	1.21E+02	
293.14	9.84E+01	
303.12	1.18E+02	
310.16	1.84E+02	K(Biotin) (0)
325.19	5.77E+02	
366.18	1.08E+02	
377.16	1.13E+02	
394.18	1.32E+03	y_4(104)
412.22	1.41E+02	
434.26	2.40E+02	
440.19	1.20E+02	
462.26	2.63E+02	
549.26	1.43E+02	
567.27	1.01E+02	
571.32	1.91E+02	
599.32	2.29E+02	
736.39	1.04E+02	
791.41	2.33E+02	
900.49	1.08E+02	
928.48	1.12E+02	

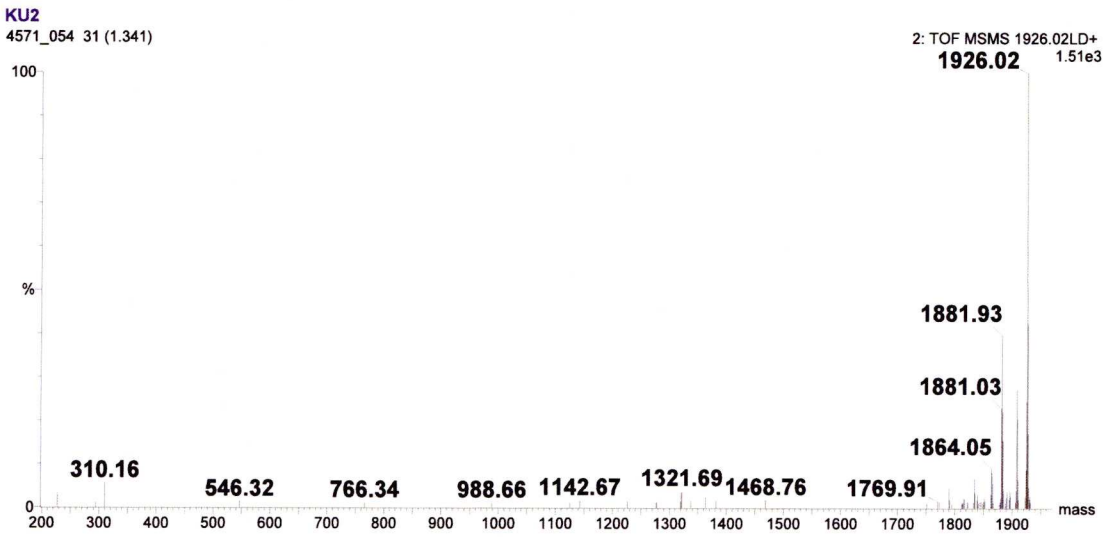

1926.02	*1.51E+03*	*DK(Biotin)NISRKPGNVLKTL(Ammonium)*
Ion fragment mass (m/z)	**Intensity**	**Assignment (error - ppm)**
227.08	4.68E+01	Biotin(0)
294.15	1.68E+01	
310.16	8.42E+01	K(Biotin)(0)
546.32	1.99E+01	
766.34	1.62E+01	b_5-H2O(-20)
988.66	1.64E+01	
1125.65	1.56E+01	y_{10}-NH3(-54)
1142.67	2.53E+01	y_{10}(-58)
1225.68	2.08E+01	
1276.69	1.62E+01	
1319.63	2.09E+01	b_{10}-NH3(-17)
1337.74	2.35E+01	
1363.73	3.65E+01	
1381.71	2.62E+01	
1468.76	2.67E+01	
1750.95	1.60E+01	
1769.91	2.24E+01	
1789.98	7.06E+01	
1812.03	1.58E+01	
1832.87	1.88E+01	
1862.96	4.89E+01	
1877.99	1.71E+01	
1905.84	1.91E+01	
1923	3.95E+01	

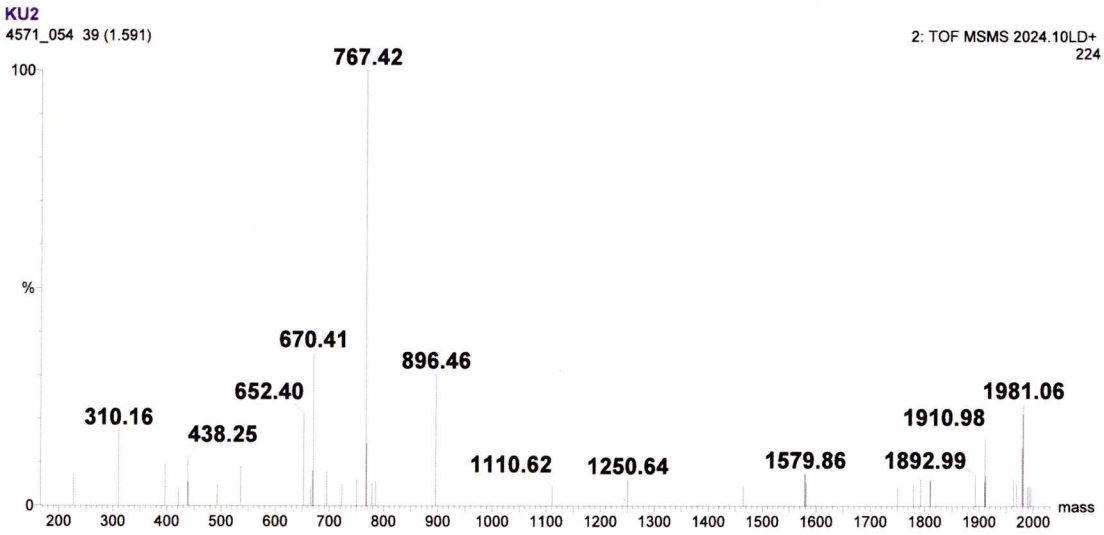

2024.10	*224*	*TLPPSRDELTK(Biotin)NQVSL*
Ion fragment mass (m/z)	**Intensity**	**Assignment (error - ppm)**
227.08	1.60E+01	Biotin(0)
310.16	3.86E+01	K(Biotin)(0)
396.23	2.09E+01	
421.22	9.04E+00	PPSR-NH_3(1.4)
438.25	2.52E+01	PPSR(9.3) / TK(Biotin)-H_2O(75) / PSRD-H_2O(92)
493.25	1.08E+01	
536.27	2.05E+01	PPSRD-NH_3(44)
652.4	4.72E+01	b_6(34)
665.29	9.50E+00	PPSRDE-NH_3(1.6) / LTK(Biotin)N-H2O(-81)
669.43	1.80E+01	
695.44	1.72E+01	
723.38	1.11E+01	
750.37	1.34E+01	b_7-NH_3(-11)
767.42	2.24E+02	PPSRDEL-28(20) / b_7(20) / LPPSRDE-28(20)
778.42	1.10E+01	LPPSRDE-NH_3(60) / PPSRDEL-NH3(60)
785.41	1.25E+01	DELTK(Biotin)-28(30)
896.46	6.77E+01	y_6-H_2O(-6.5) / PPSRDELT(14) / b_8(14)
1110.62	9.71E+00	y_8-H_2O(20) / b_{10}(37)
1250.64	1.34E+01	PPSRDELTK(Biotin)(16) / PSRDELTK(Biotin)N-NH_3(45)
1464.77	1.01E+01	b_{11}(13) / PPSRDELTK(Biotin)NQ-28(30)
1578.81	1.62E+01	b_{12}(9.8)
1749.9	9.31E+00	
1778.93	1.13E+01	
1791.97	1.37E+01	LPPSRDELTK(Biotin)NQVS(36) / y_{14}-H_2O(36)
1810	1.27E+01	y_{14}(46)
1892.99	1.65E+01	b_{15}(19)
1910.06	1.21E+01	
1963.1	1.37E+01	
1968.98	1.15E+01	
1979.15	2.99E+01	
1989	9.74E+00	
1995.08	9.66E+00	

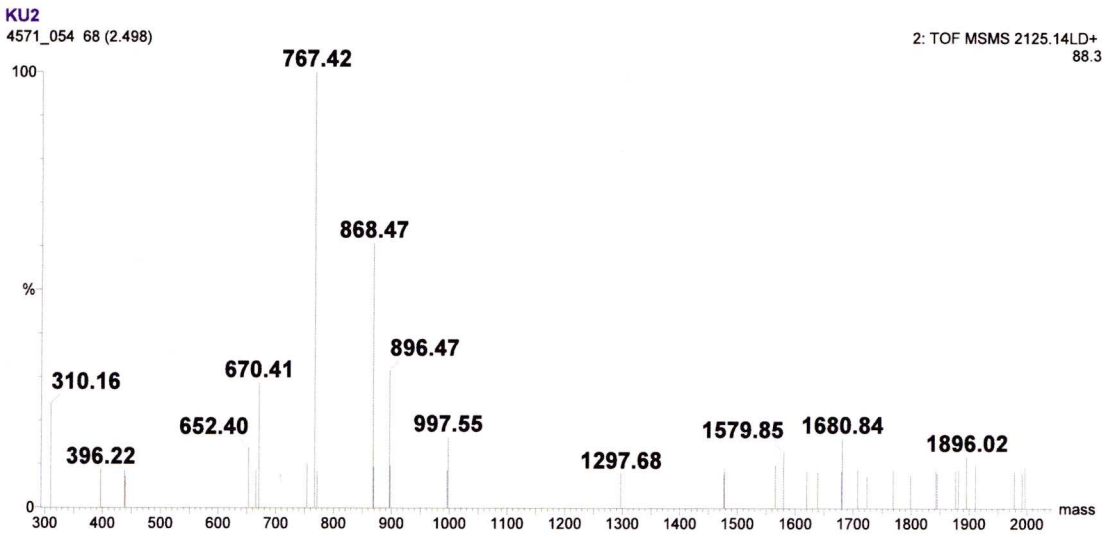

2125.14	*88.30*	*VVVDVSHEDPEVK(Biotin)FNW*
Ion fragment mass (m/z)	**Intensity**	**Assignment (error - ppm)**
310.16	2.10E+01	K(Biotin)(0)
396.22	7.65E+00	
438.25	7.50E+00	
652.4	1.19E+01	PEVK(Biotin)-28(79)
665.29	7.35E+00	VSHEDP(1.6) / DVSHED-H_2O(56)
670.41	2.53E+01	
753.44	8.94E+00	
767.42	8.83E+01	DPEVK(Biotin)-28(58)
771.49	7.40E+00	
868.47	5.37E+01	
896.47	2.79E+01	EDPEVK(Biotin)-28(58)
996.48	7.55E+00	
1297.68	6.86E+00	
1476.73	6.81E+00	
1565.76	8.62E+00	
1579.85	1.13E+01	
1619.84	7.36E+00	
1638.8	7.27E+00	
1679.94	7.36E+00	VVDVSHEDPEVK(Biotin)F-28(78)
1708.02	7.71E+00	VVDVSHEDPEVK(Biotin)F(126)
1723.92	6.52E+00	
1768.98	7.58E+00	
1798.82	6.59E+00	
1842.84	7.47E+00	
1876.88	7.62E+00	
1881.84	7.78E+00	
1896.02	1.04E+01	
1911.03	8.83E+00	
1978.9	7.34E+00	
1991.94	6.89E+00	
1996.97	8.44E+00	

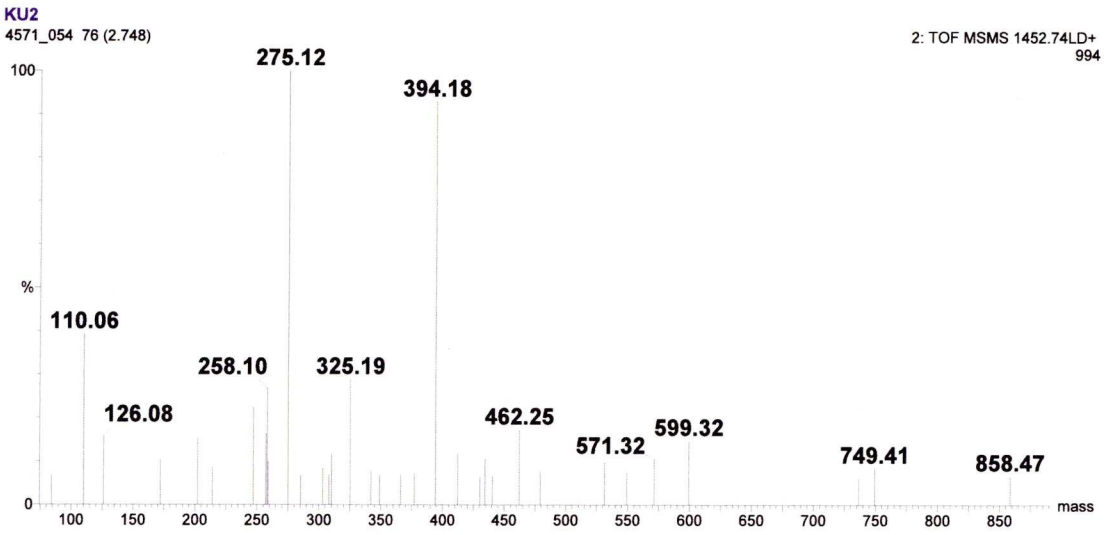

1452.74	*994*	*AGAFRSDK(Biotin)C(Carbamidomethyl)GGT*
Ion fragment mass (m/z)	**Intensity**	**Assignment (error - ppm)**
84.07	6.80E+01	K(-128)
110.06	3.90E+02	
126.08	1.56E+02	K(-90)
172.1	1.02E+02	a_3(-47)
202.1	1.52E+02	
214.1	8.64E+01	
247.13	2.22E+02	C(Carbamidomethyl)GG-28(178)
257.11	1.63E+02	
275.12	9.94E+02	C(Carbamidomethyl)GG(142)
285.11	6.76E+01	
303.12	8.27E+01	
308.17	6.77E+01	
310.16	1.16E+02	K(Biotin)(0)
325.19	2.86E+02	
342.21	7.69E+01	RSD-NH_3(202)
349.15	6.73E+01	
366.18	6.80E+01	
377.15	7.16E+01	
394.18	9.24E+02	y_4(104)
412.21	1.17E+02	
430.2	6.30E+01	
434.26	1.05E+02	AFRS-28(21)
440.19	6.48E+01	
462.25	1.71E+02	AFRS(8.8)
479.29	7.63E+01	
531.27	9.69E+01	
549.29	7.51E+01	AFRSD-28(22)
571.32	1.05E+02	
599.32	1.46E+02	
736.39	6.08E+01	
749.41	8.32E+01	
858.47	6.56E+01	

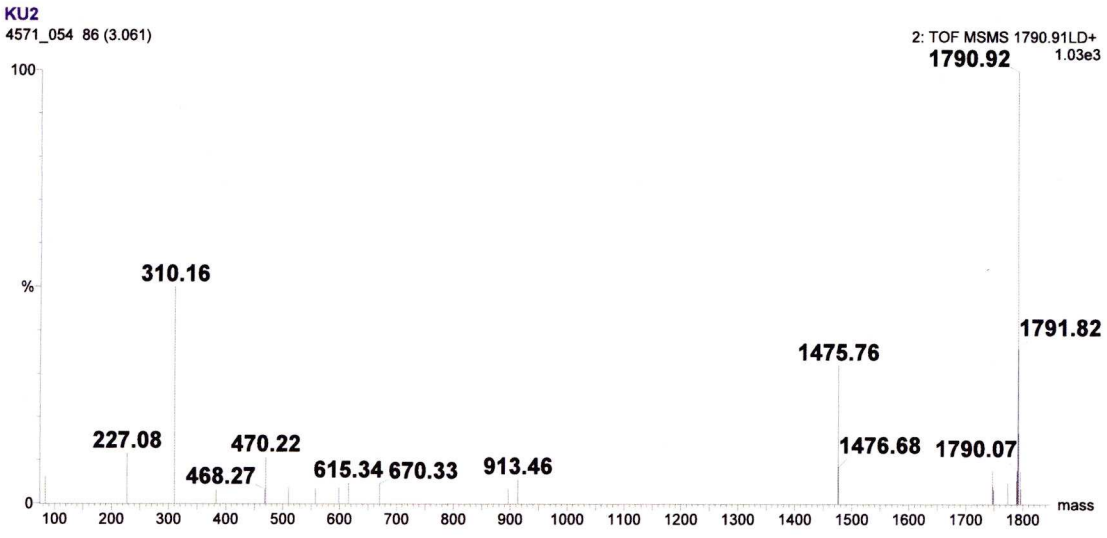

1790.92	*1.03E+03*	*TVDK(Biotin)SRWQQGNVF*
Ion fragment mass (m/z)	**Intensity**	**Assignment (error - ppm)**
84.07	6.36E+01	K(-128) Q(-128)
227.08	1.19E+02	Biotin(0)
310.16	5.17E+02	K(Biotin)(0)
383.17	3.11E+01	
468.27	3.36E+01	
510.23	3.86E+01	QQGNV-NH_3(-1.3)
557.26	3.54E+01	DK(Biotin)S(38)
598.33	3.69E+01	K(Biotin)SR(28)
615.34	4.90E+01	
670.33	4.64E+01	b_4(11)
896.43	3.45E+01	b_6-NH_3(0.60)
913.46	5.76E+01	b_6(4.4)
1475.76	3.30E+02	y_{10}(26)
1746.86	7.88E+01	
1773.88	4.91E+01	MH-NH_3(24)
1788.84	5.40E+01	

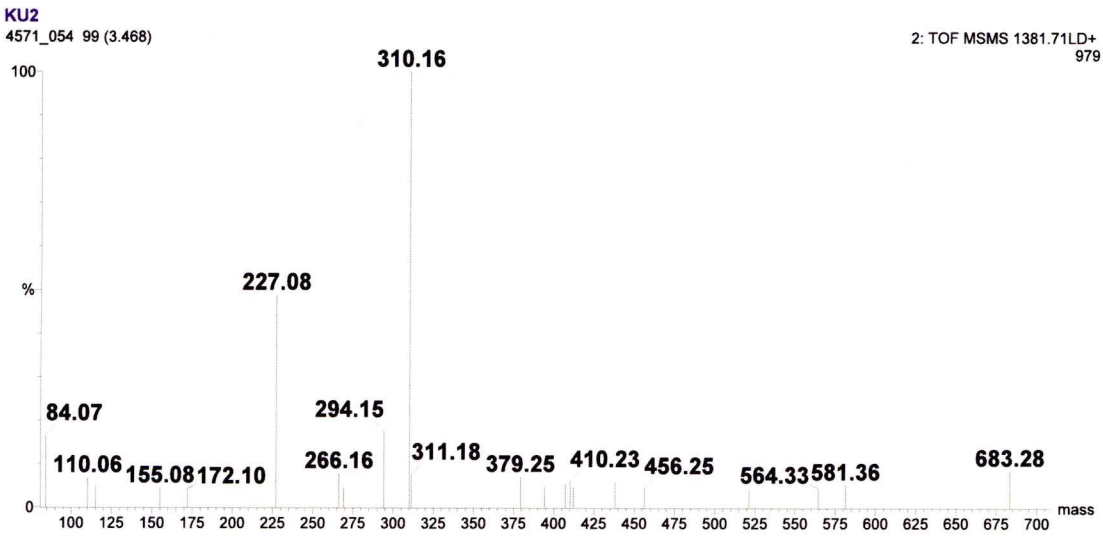

1381.71	*979*	*NGK(Biotin)EYKCKVS*
Ion fragment mass (m/z)	**Intensity**	**Assignment (error - ppm)**
84.07	1.63E+02	K(-128)
110.06	6.61E+01	
115.08	4.71E+01	
155.08	4.28E+01	b_2-NH_3(225)
172.1	4.09E+01	b_2(165)
227.08	4.78E+02	Biotin(0)
266.16	7.58E+01	
269.16	4.50E+01	
294.15	1.71E+02	
310.16	9.80E+02	K(Biotin)(0)
379.25	6.82E+01	
394.23	4.65E+01	
407.25	5.35E+01	
438.22	5.87E+01	
456.25	4.39E+01	K(Biotin)E-28(49)
521.33	4.06E+01	
564.33	4.34E+01	y_5(22)
581.36	5.02E+01	
683.28	8.24E+01	

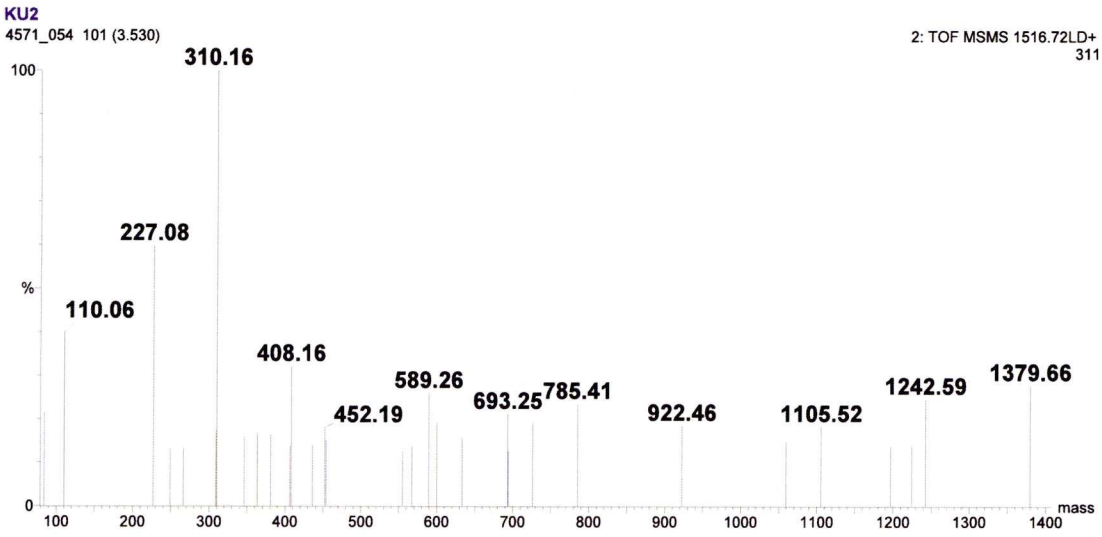

1516.72	*311*	*QVIFEGEIGK(Biotin)GN*
Ion fragment mass (m/z)	**Intensity**	**Assignment (error - ppm)**
84.07	6.59E+01	Q(-128) / K(-128)
110.06	1.24E+02	
227.08	1.86E+02	Biotin(0)
249.09	4.07E+01	FE-28(-134)
266.12	4.16E+01	
310.16	3.11E+02	K(Biotin)(0)
346.12	4.94E+01	
363.14	5.14E+01	
381.15	5.12E+01	
406.18	4.23E+01	
436.15	4.36E+01	
452.19	5.58E+01	GK(Biotin)G-NH_3(-14)
567.26	4.28E+01	
589.26	8.03E+01	a_5(-126)
600.26	5.91E+01	b_5-NH_3(-71)
633.24	4.85E+01	FEGEIG(-76)
693.25	6.56E+01	EIGK(Biotin)G-H_2O(-128) / GEIGK(Biotin)-H_2O(-128)
726.32	5.89E+01	
785.41	7.28E+01	b_7-H_2O(35)
922.46	5.72E+01	
1059.5	4.59E+01	
1105.52	5.66E+01	
1196.57	4.29E+01	
1224.61	4.29E+01	
1242.59	7.62E+01	
1379.66	8.61E+01	

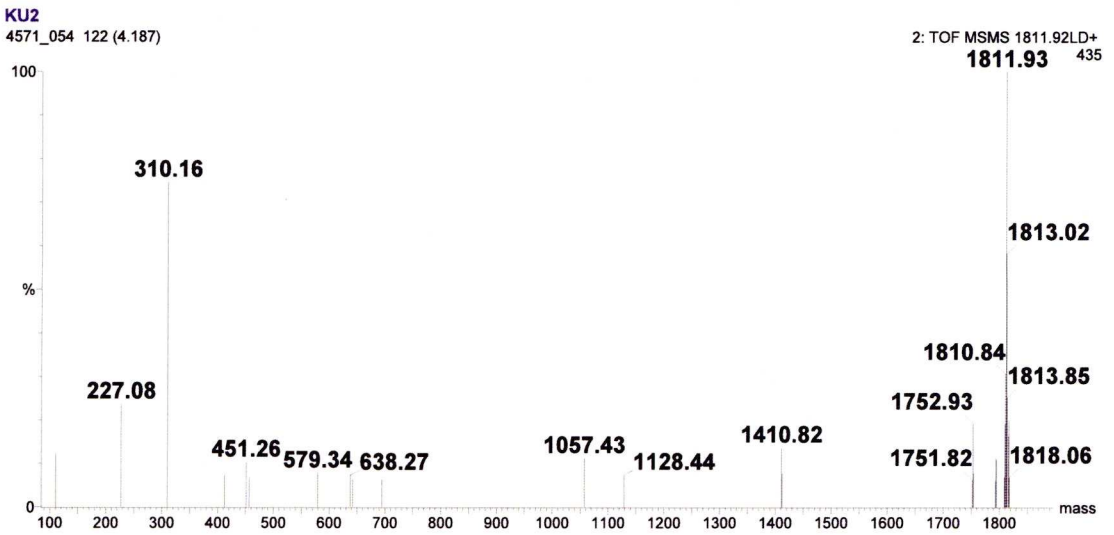

1811.92	*435*	*SQADENQK(Biotin)GK(Acetyl)VARL*
Ion fragment mass (m/z)	**Intensity**	**Assignment (error - ppm)**
110.06	5.30E+01	
227.08	1.03E+02	Biotin(0)
310.16	3.24E+02	K(Biotin)(0)
412.21	3.14E+01	K(Biotin)G(21) / ADEN-H_2O(155)
451.26	4.48E+01	
456.15	2.92E+01	
579.34	3.41E+01	
638.27	3.20E+01	
642.24	2.81E+01	
694.37	2.75E+01	
1057.43	4.88E+01	
1128.44	3.21E+01	
1410.82	5.93E+01	y_{10}(48)
1751.82	2.70E+01	
1792.99	2.64E+01	
1808.83	3.02E+01	
1813.02	2.53E+02	

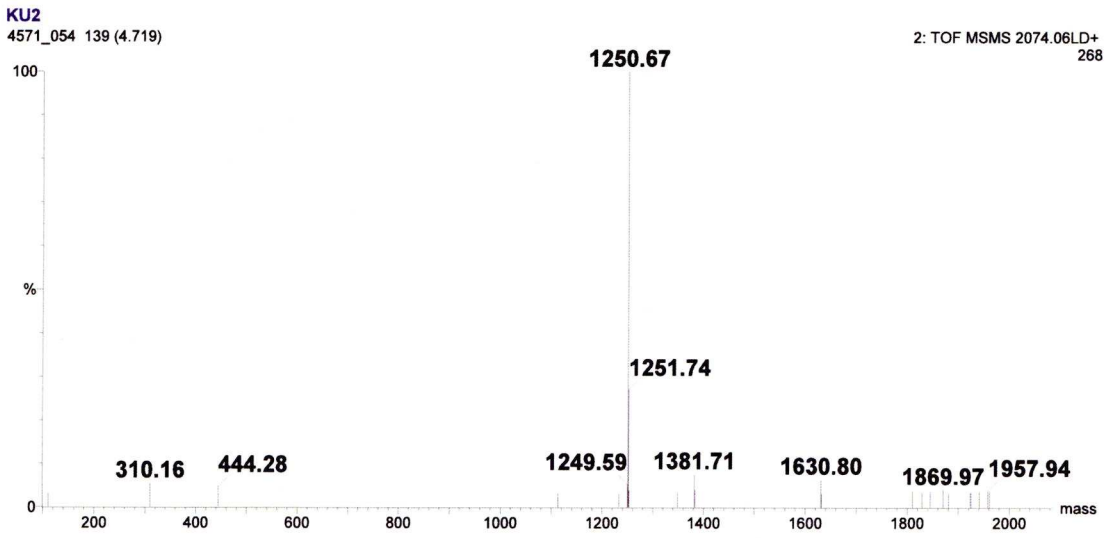

2074.06	*268*	*MVVGHQGDHWK(Biotin)EGRVL*
Ion fragment mass (m/z)	**Intensity**	**Assignment (error - ppm)**
110.06	8.21E+00	H(-102)
310.16	1.45E+01	K(Biotin)(0)
444.28	1.26E+01	y_4(-29)
1113.68	8.41E+00	y_7(83)
1233.62	8.10E+00	y_8-NH_3(0.22)
1249.59	1.41E+01	
1348.77	9.12E+00	y_9-NH_3(91)
1381.71	2.02E+01	
1630.8	1.71E+01	b_{12}(46)
1809.94	9.99E+00	
1828.9	9.11E+00	
1845	9.63E+00	
1869.97	1.08E+01	
1880.93	8.29E+00	
1923.14	9.60E+00	
1940.98	9.75E+00	
1957.94	1.03E+01	
1961.06	1.01E+01	b_{15}+H_2O(68)

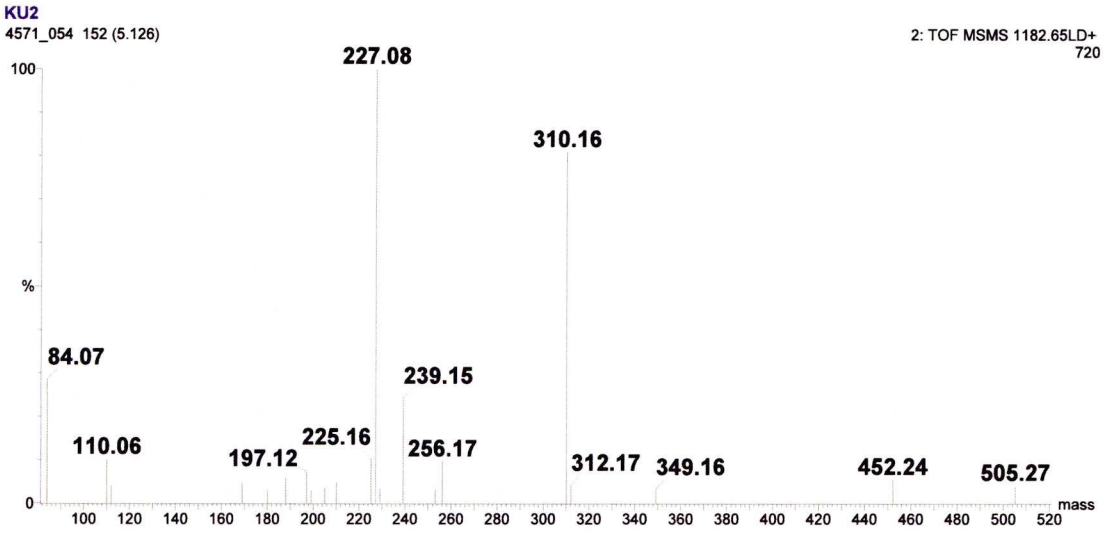

1182.65	*720*	*VRIK(Biotin)PASW*
Ion fragment mass (m/z)	**Intensity**	**Assignment (error - ppm)**
84.07	2.06E+02	K(-128)
110.06	7.22E+01	
169.12	3.38E+01	PA(135)
180.09	2.26E+01	
188.06	4.23E+01	
197.12	5.23E+01	
205.1	2.56E+01	y_1(14)
210.15	3.43E+01	
225.16	7.30E+01	
227.08	7.20E+02	Biotin(0)
239.15	1.74E+02	b_2-NH_3(-1.1)
253.16	2.22E+01	RI-NH_3(-23)
256.17	6.88E+01	b_2(-27) / PAS(159)
310.16	5.82E+02	K(Biotin)(0)
349.16	2.34E+01	
452.24	3.88E+01	K(Biotin)P(16)
505.27	2.89E+01	

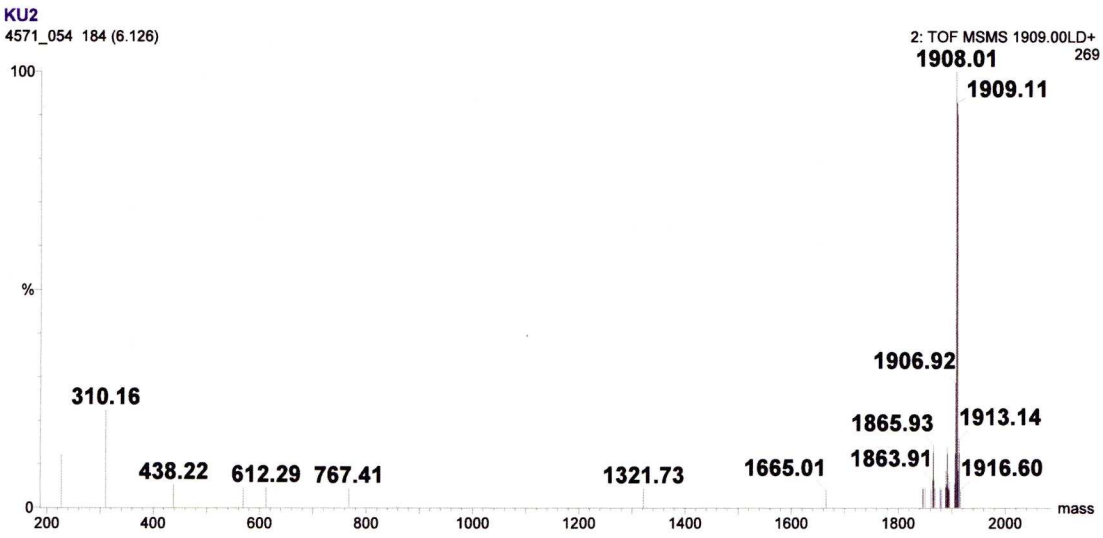

1909.00	*269*	*DK(Biotin)NISRKPGNVLKTL*
Ion fragment mass (m/z)	**Intensity**	**Assignment (error - ppm)**
227.08	3.23E+01	Biotin(0)
310.16	6.01E+01	K(Biotin)(0)
438.22	1.40E+01	NVLK-NH_3(-117)
569.27	1.19E+01	
612.29	1.23E+01	SRKPGN-28(-110)
767.41	1.17E+01	b_5-NH_3(92)
1321.73	1.17E+01	
1665.01	1.08E+01	
1845.97	1.13E+01	
1860.93	1.09E+01	
1877.95	1.25E+01	
1880.95	1.18E+01	
1887.98	1.25E+01	
1904.95	1.49E+01	
1911.01	2.42E+02	
1916.6	1.08E+01	

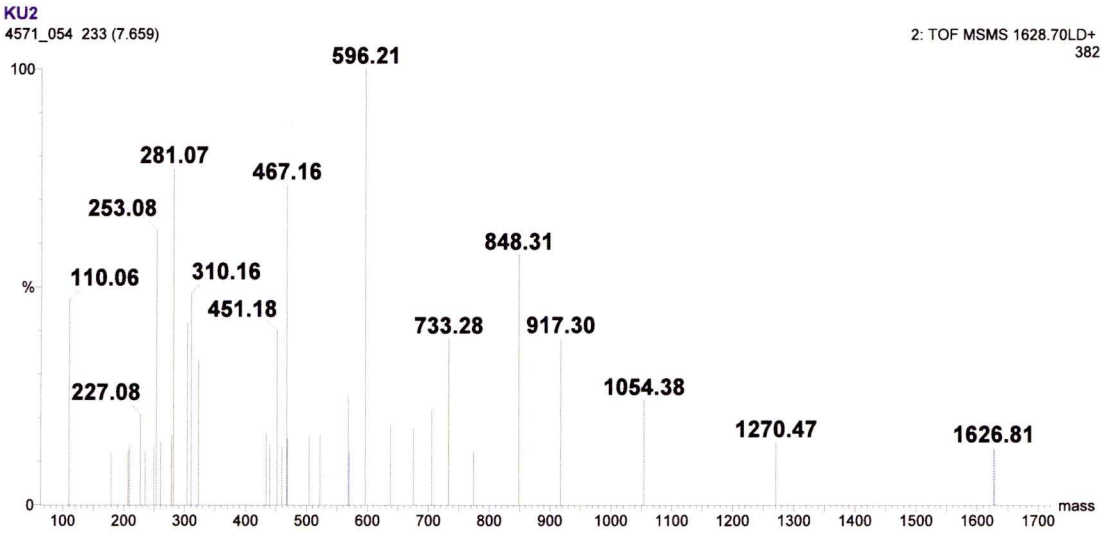

1628.70	*382*	*HSYHPSEK(Biotin)CEW*
Ion fragment mass (m/z)	**Intensity**	**Assignment (error - ppm)**
110.06	1.80E+02	H(-102)
179.09	4.61E+01	a_2-H_2O(-15)
207.08	4.71E+01	b_2-H_2O(-37) / HP-28(-213)
227.08	7.94E+01	Biotin(0)
235.09	4.71E+01	HP(-123)
249.1	5.08E+01	
253.08	2.41E+02	
260.11	5.52E+01	
278.12	6.09E+01	
281.07	2.95E+02	
304.1	1.60E+02	HPS-H_2O(-133)
310.16	1.85E+02	K(Biotin)(0)
322.12	1.27E+02	HPS(-96)
433.15	6.31E+01	HPSE-H_2O(-76)
439.16	5.39E+01	
451.18	1.52E+02	HPSE(-30)
459.18	5.16E+01	
467.16	2.80E+02	EK(Biotin)-NH_3(-77) / YHPS-H_2O(-94) / SYHP-H_2O(-94)
504.2	6.07E+01	
522.23	6.12E+01	
568.23	9.65E+01	
596.21	3.82E+02	YHPSE-H_2O(-61)
637.26	7.01E+01	
675.3	6.73E+01	
705.27	8.34E+01	
733.28	1.45E+02	
774.31	4.73E+01	y_4-NH_3(19)
848.31	2.19E+02	
917.3	1.46E+02	
1054.38	9.17E+01	YHPSEK(Biotin)C-NH_3(-30)
1270.47	5.47E+01	SYHPSEK(Biotin)CE-NH_3(-13)
1626.81	5.02E+01	

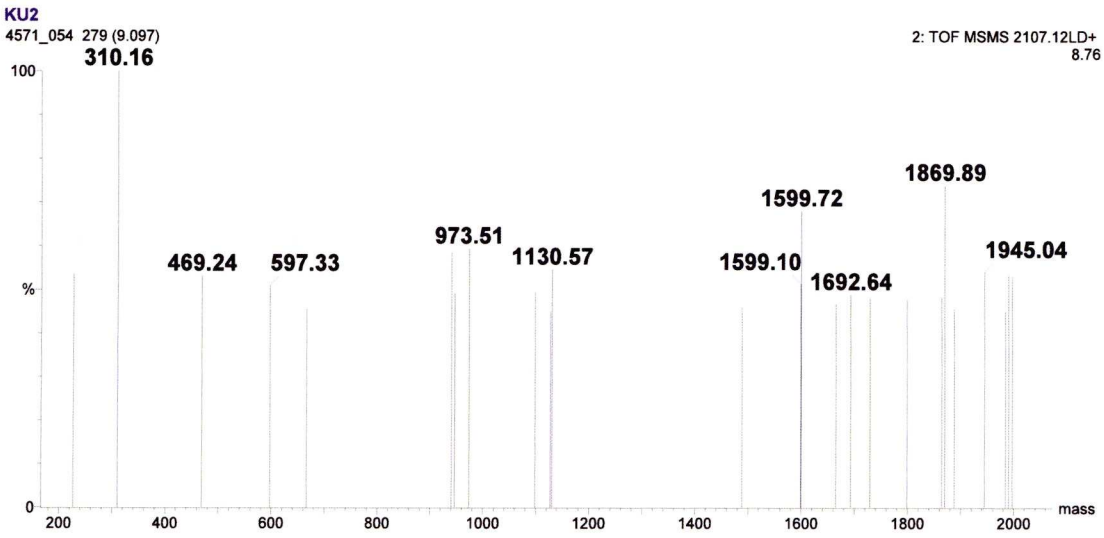

2107.12	*8.76*	*VVVDVSHEDPEVK(Biotin)FNW -H_2O*
Ion fragment mass (m/z)	**Intensity**	**Assignment (error - ppm)**
469.24	4.64E+00	
597.33	4.46E+00	
666.29	3.98E+00	
940.45	5.11E+00	
946.45	4.30E+00	
973.51	5.19E+00	
1098.54	4.33E+00	
1127.55	3.95E+00	y_7-H_2O(14)
1130.57	4.77E+00	SHEDPEVK(Biotin)-H_2O(68)
1488.52	4.03E+00	
1599.1	4.49E+00	
1664.88	4.10E+00	
1692.64	4.27E+00	
1729	4.21E+00	
1799.09	4.18E+00	
1864.16	4.22E+00	
1869.89	6.47E+00	
1887.92	3.99E+00	
1945.04	4.74E+00	
1983.99	3.96E+00	
1990.07	4.68E+00	y_{15}-H_2O(77)
1997.1	4.64E+00	

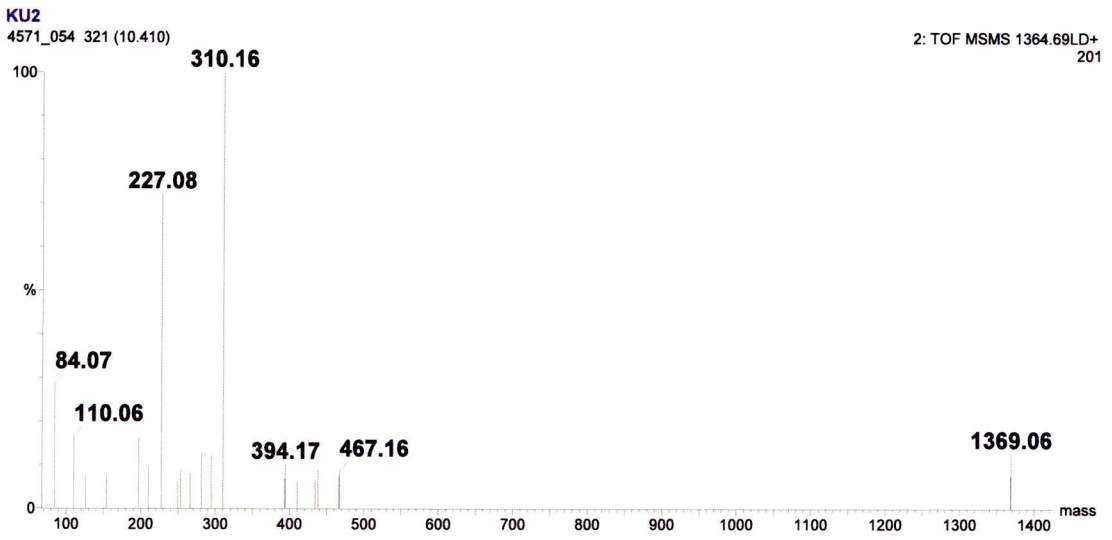

1364.69	*201*	*NGK(Biotin)EYKCKVS -NH_3*
Ion fragment mass (m/z)	**Intensity**	**Assignment (error - ppm)**
84.07	5.77E+01	K(-128)
110.06	3.35E+01	
126.08	1.55E+01	K(-90)
154.08	1.50E+01	
197.12	3.27E+01	
210.16	1.90E+01	
227.08	1.45E+02	Biotin(0)
249.09	1.25E+01	
253.08	1.82E+01	
266.16	1.62E+01	
281.07	2.53E+01	
294.16	2.46E+01	
310.16	2.01E+02	K(Biotin)(0)
393.2	1.38E+01	EYK-28(-34)
410.26	1.24E+01	
434.15	1.24E+01	
438.23	1.74E+01	
466.22	1.51E+01	K(Biotin)E-H_2O(17)

Bibliography

[1] Appleton, B. A. *et al.* Structural studies of neuropilin/antibody complexes provide insights into semaphorin and VEGF binding. *EMBO J* **26**, 4902–12 (2007).

[2] Fujisawa, H., Takagi, S. & Hirata, T. Cell surface molecule A5: a putative involvement in retinal central connection. *Neurosci Res Suppl* **13**, S11–7 (1990).

[3] Takagi, S. *et al.* The A5 antigen, a candidate for the neuronal recognition molecule, has homologies to complement components and coagulation factors. *Neuron* **7**, 295–307 (1991).

[4] Uniewicz, K. A. & Fernig, D. G. Neuropilins: a versatile partner of extracellular molecules that regulate development and disease. *Front Biosci* **13**, 4339–60 (2008).

[5] Ward, N. L. & Lamanna, J. C. The neurovascular unit and its growth factors: coordinated response in the vascular and nervous systems. *Neurol Res* **26**, 870–83 (2004).

[6] Fantin, A., Maden, C. H. & Ruhrberg, C. Neuropilin ligands in vascular and neuronal patterning. *Biochem Soc Trans* **37**, 1228–32 (2009).

[7] Zachary, I. C., Frankel, P., Evans, I. M. & Pellet-Many, C. The role of neuropilins in cell signalling. *Biochem Soc Trans* **37**, 1171–8 (2009).

[8] Ellis, L. M. The role of neuropilins in cancer. *Mol Cancer Ther* **5**, 1099–107 (2006).

[9] Jiang, S. X. *et al.* Neuropilin 1 directly interacts with Fer kinase to mediate semaphorin3A-induced death of cortical neurons. *J Biol Chem* **285**, 9908–9918 (2010).

[10] Sasaki, Y. *et al.* Fyn and Cdk5 mediate semaphorin-3A signaling, which is involved in regulation of dendrite orientation in cerebral cortex. *Neuron* **35**, 907–20 (2002).

[11] Soker, S. *et al.* VEGF165 mediates formation of complexes containing VEGFR-2 and neuropilin-1 that enhance VEGF165-receptor binding. *J Cell Biochem* **85**, 357–68 (2002).

[12] Pan, Q. *et al.* Neuropilin-1 binds to VEGF121 and regulates endothelial cell migration and sprouting. *J Biol Chem* **282**, 24049–56 (2007).

[13] Salikhova, A. *et al.* Vascular endothelial growth factor and semaphorin induce neuropilin-1 endocytosis via separate pathways. *Circ Res* **103**, e71–9 (2008).

[14] Ball, S. G., Bayley, C., Shuttleworth, C. A. & Kielty, C. M. Neuropilin-1 regulates platelet-derived growth factor receptor signaling in mesenchymal stem cells. *Biochem J* **427**, 29–40 (2010).

[15] Holmes, D. I. & Zachary, I. C. Vascular endothelial growth factor regulates Stanniocalcin-1 expression via Neuropilin-1-dependent regulation of KDR and synergism with fibroblast growth Factor-2. *Cell Signal* **20**, 569–79 (2008).

[16] Ng, S. K., Zhang, Z., Tan, S. H. & Lin, K. InterDom: a database of putative interacting protein domains for validating predicted protein interactions and complexes. *Nucleic Acids Res* **31**, 251–4 (2003).

[17] Ori, A., Wilkinson, M. C. & Fernig, D. G. The heparanome and regulation of cell function: structures, functions and challenges. *Front Biosci* **13**, 4309–38 (2008).

[18] Whitaker, G. B., Limberg, B. J. & Rosenbaum, J. S. Vascular endothelial growth factor receptor-2 and neuropilin-1 form a receptor complex that is responsible for the differential signaling potency of VEGF(165) and VEGF(121). *J Biol Chem* **276**, 25520–31 (2001).

[19] von Wronski, M. A. *et al.* Tuftsin binds neuropilin-1 through a sequence similar to that encoded by exon 8 of vascular endothelial growth factor. *J Biol Chem* **281**, 5702–10 (2006).

[20] Jia, H. *et al.* Characterization of a bicyclic peptide neuropilin-1 (NP-1) antagonist (EG3287) reveals importance of vascular endothelial growth factor exon 8 for NP-1 binding and role of NP-1 in KDR signaling. *J Biol Chem* **281**, 13493–502 (2006).

[21] Gitay-Goren, H., Soker, S., Vlodavsky, I. & Neufeld, G. The binding of vascular endothelial growth factor to its receptors is dependent on cell surface-associated heparin-like molecules. *J Biol Chem* **267**, 6093–8 (1992).

[22] Soker, S., Fidder, H., Neufeld, G. & Klagsbrun, M. Characterization of novel vascular endothelial growth factor (VEGF) receptors on tumor cells that bind VEGF165 via its exon 7-encoded domain. *J Biol Chem* **271**, 5761–7 (1996).

[23] Soker, S. *et al.* Inhibition of vascular endothelial growth factor (VEGF)-induced endothelial cell proliferation by a peptide corresponding to the exon 7-encoded domain of VEGF165. *J Biol Chem* **272**, 31582–8 (1997).

[24] Soker, S. *et al.* Neuropilin-1 is expressed by endothelial and tumor cells as an isoform-specific receptor for vascular endothelial growth factor. *Cell* **92**, 735–45 (1998).

[25] Giger, R. J. *et al.* Neuropilin-2 is a receptor for semaphorin IV: insight into the structural basis of receptor function and specificity. *Neuron* **21**, 1079–92 (1998).

[26] Fuh, G., Garcia, K. C. & de Vos, A. M. The interaction of neuropilin-1 with vascular endothelial growth factor and its receptor flt-1. *J Biol Chem* **275**, 26690–5 (2000).

[27] Gagnon, M. L. *et al.* Identification of a natural soluble neuropilin-1 that binds vascular endothelial growth factor: In vivo expression and antitumor activity. *Proc Natl Acad Sci U S A* **97**, 2573–8 (2000).

[28] Gu, C. *et al.* Characterization of neuropilin-1 structural features that confer binding to semaphorin 3A and vascular endothelial growth factor 165. *J Biol Chem* **277**, 18069–76 (2002).

[29] Mamluk, R. *et al.* Neuropilin-1 binds vascular endothelial growth factor 165, placenta growth factor-2, and heparin via its b1b2 domain. *J Biol Chem* **277**, 24818–25 (2002).

[30] Makinen, T. *et al.* Differential binding of vascular endothelial growth factor B splice and proteolytic isoforms to neuropilin-1. *J Biol Chem* **274**, 21217–22 (1999).

[31] Karpanen, T. *et al.* Functional interaction of VEGF-C and VEGF-D with neuropilin receptors. *FASEB J* **20**, 1462–72 (2006).

[32] Migdal, M. *et al.* Neuropilin-1 is a placenta growth factor-2 receptor. *J Biol Chem* **273**, 22272–8 (1998).

[33] He, Z. & Tessier-Lavigne, M. Neuropilin is a receptor for the axonal chemorepellent Semaphorin III. *Cell* **90**, 739–51 (1997).

[34] Nakamura, F. *et al.* Neuropilin-1 extracellular domains mediate semaphorin D/III-induced growth cone collapse. *Neuron* **21**, 1093–100 (1998).

[35] Miao, H. Q. *et al.* Neuropilin-1 mediates collapsin-1/semaphorin III inhibition of endothelial cell motility: functional competition of collapsin-1 and vascular endothelial growth factor-165. *J Cell Biol* **146**, 233–42 (1999).

[36] West, D. C. *et al.* Interactions of multiple heparin binding growth factors with neuropilin-1 and potentiation of the activity of fibroblast growth factor-2. *J Biol Chem* **280**, 13457–64 (2005).

[37] Sulpice, E. *et al.* Neuropilin-1 and neuropilin-2 act as coreceptors, potentiating proangiogenic activity. *Blood* **111**, 2036–45 (2007).

[38] Glinka, Y. & Prud'homme, G. J. Neuropilin-1 is a receptor for transforming growth factor beta-1, activates its latent form, and promotes regulatory T cell activity. *J Leukoc Biol* **84**, 302–10 (2008).

[39] Chen, H., He, Z., Bagri, A. & Tessier-Lavigne, M. Semaphorin-neuropilin interactions underlying sympathetic axon responses to class III semaphorins. *Neuron* **21**, 1283–90 (1998).

[40] Takahashi, T. *et al.* Semaphorins A and E act as antagonists of neuropilin-1 and agonists of neuropilin-2 receptors. *Nat Neurosci* **1**, 487–93 (1998).

[41] Hsieh, S. H. *et al.* Galectin-1, a novel ligand of neuropilin-1, activates VEGFR-2 signaling and modulates the migration of vascular endothelial cells. *Oncogene* **27**, 3746–53 (2008).

[42] Prahst, C. *et al.* Neuropilin-1-VEGFR-2 complexing requires the PDZ-binding domain of neuropilin-1. *J Biol Chem* **283**, 25110–4 (2008).

[43] Shraga-Heled, N. *et al.* Neuropilin-1 and neuropilin-2 enhance VEGF121 stimulated signal transduction by the VEGFR-2 receptor. *FASEB J* **21**, 915–26 (2007).

[44] Matsushita, A., Gotze, T. & Korc, M. Hepatocyte growth factor mediated cell invasion in pancreatic cancer cells is dependent on neuropilin-1. *Cancer Res* **67**, 10309–16 (2007).

[45] Fukasawa, M., Matsushita, A. & Korc, M. Neuropilin-1 Interacts with Integrin beta1 and Modulates Pancreatic Cancer Cell Growth, Survival and Invasion. *Cancer Biol Ther* **6**, 1173–80 (2007).

[46] Valdembri, D. *et al.* Neuropilin-1/GIPC1 signaling regulates alpha5beta1 integrin traffic and function in endothelial cells. *PLoS Biol* **7**, e25 (2009).

[47] Robinson, S. D. *et al.* Alphavbeta3-integrin limits the contribution of neuropilin-1 to VEGF-induced angiogenesis. *J Biol Chem* **284**, 33966–81 (2009).

[48] Castellani, V. The function of neuropilin/L1 complex. *Adv Exp Med Biol* **515**, 91–102 (2002).

[49] Takahashi, T. *et al.* Plexin-neuropilin-1 complexes form functional semaphorin-3A receptors. *Cell* **99**, 59–69 (1999).

[50] Rohm, B., Ottemeyer, A., Lohrum, M. & Puschel, A. W. Plexin/neuropilin complexes mediate repulsion by the axonal guidance signal semaphorin 3A. *Mech Dev* **93**, 95–104 (2000).

[51] Cai, H. & Reed, R. R. Cloning and characterization of neuropilin-1-interacting protein: a PSD-95/Dlg/ZO-1 domain-containing protein that interacts with the cytoplasmic domain of neuropilin-1. *J Neurosci* **19**, 6519–27 (1999).

[52] Wang, L., Mukhopadhyay, D. & Xu, X. C terminus of RGS-GAIP-interacting protein conveys neuropilin-1-mediated signaling during angiogenesis. *FASEB J* **20**, 1513–5 (2006).

[53] Narazaki, M. & Tosato, G. Ligand-induced internalization selects use of common receptor neuropilin-1 by VEGF165 and semaphorin3A. *Blood* **107**, 3892–901 (2006).

[54] De Wit, J., De Winter, F., Klooster, J. & Verhaagen, J. Semaphorin 3A displays a punctate distribution on the surface of neuronal cells and interacts with proteoglycans in the extracellular matrix. *Mol Cell Neurosci* **29**, 40–55 (2005).

[55] Cohen, T. *et al.* VEGF121, a vascular endothelial growth factor (VEGF) isoform lacking heparin binding ability, requires cell-surface heparan sulfates for efficient binding to the VEGF receptors of human melanoma cells. *J Biol Chem* **270**, 11322–6 (1995).

[56] Lake, A. C. *et al.* Low molecular weight fucoidan increases VEGF165-induced endothelial cell migration by enhancing VEGF165 binding to VEGFR-2 and NRP1. *J Biol Chem* **281**, 37844–52 (2006).

[57] Di Benedetto, M. *et al.* Distinct heparin binding sites on VEGF165 and its receptors revealed by their interaction with a non sulfated glycoaminoglycan (NaPaC). *Biochim Biophys Acta* **1780**, 723–32 (2008).

[58] Narazaki, M., Segarra, M. & Tosato, G. Sulfated polysaccharides identified as inducers of neuropilin-1 internalization and functional inhibition of VEGF165 and semaphorin3A. *Blood* **111**, 4126–36 (2008).

[59] Gray, M. J. *et al.* Neuropilin-1 suppresses tumorigenic properties in a human pancreatic adenocarcinoma cell line lacking neuropilin-1 coreceptors. *Cancer Res* **65**, 3664–70 (2005).

[60] Bachelder, R. E. *et al.* Vascular endothelial growth factor is an autocrine survival factor for neuropilin-expressing breast carcinoma cells. *Cancer Res* **61**, 5736–40 (2001).

[61] Murga, M., Fernandez-Capetillo, O. & Tosato, G. Neuropilin-1 regulates attachment in human endothelial cells independently of vascular endothelial growth factor receptor-2. *Blood* **105**, 1992–9 (2005).

[62] Wang, L. *et al.* Neuropilin-1-mediated vascular permeability factor/vascular endothelial growth factor-dependent endothelial cell migration. *J Biol Chem* **278**, 48848–60 (2003).

[63] Guttmann-Raviv, N. *et al.* The neuropilins and their role in tumorigenesis and tumor progression. *Cancer Lett* **231**, 1–11 (2006).

[64] Neufeld, G. *et al.* The neuropilins: multifunctional semaphorin and VEGF receptors that modulate axon guidance and angiogenesis. *Trends Cardiovasc Med* **12**, 13–9 (2002).

[65] Renzi, M. J., Feiner, L., Koppel, A. M. & Raper, J. A. A dominant negative receptor for specific secreted semaphorins is generated by deleting an extracellular domain from neuropilin-1. *J Neurosci* **19**, 7870–80 (1999).

[66] Williams, G. *et al.* A complementary peptide approach applied to the design of novel semaphorin/neuropilin antagonists. *J Neurochem* **92**, 1180–90 (2005).

[67] Vander Kooi, C. W. *et al.* Structural basis for ligand and heparin binding to neuropilin B domains. *Proc Natl Acad Sci U S A* **104**, 6152–7 (2007).

[68] Lu, Y. *et al.* Identification of circulating neuropilin-1 and dose-dependent elevation following anti-neuropilin-1 antibody administration. *MAbs* **1**, 364–9 (2009).

[69] Swendeman, S. *et al.* VEGF-A stimulates ADAM17-dependent shedding of VEGFR2 and crosstalk between VEGFR2 and ERK signaling. *Circ Res* **103**, 916–8 (2008).

[70] Cackowski, F. C., Xu, L., Hu, B. & Cheng, S. Y. Identification of two novel alternatively spliced Neuropilin-1 isoforms. *Genomics* **84**, 82–94 (2004).

[71] Xu, D. *et al.* Novel MMP-9 substrates in cancer cells revealed by a label-free quantitative proteomics approach. *Mol Cell Proteomics* **7**, 2215–28 (2008).

[72] Goshima, Y. *et al.* Growth cone neuropilin-1 mediates collapsin-1/Sema III facilitation of antero- and retrograde axoplasmic transport. *J Neurobiol* **39**, 579–89 (1999).

[73] Yamada, Y. *et al.* Exogenous clustered neuropilin 1 enhances vasculogenesis and angiogenesis. *Blood* **97**, 1671–8 (2001).

[74] Schuch, G. *et al.* In vivo administration of vascular endothelial growth factor (VEGF) and its antagonist, soluble neuropilin-1, predicts a role of VEGF in the progression of acute myeloid leukemia in vivo. *Blood* **100**, 4622–8 (2002).

[75] Hong, T. M. *et al.* Targeting Neuropilin 1 as an Antitumor Strategy in Lung Cancer. *Clin Cancer Res* **13**, 4759–4768 (2007).

[76] Bartsch, J., G. *et al.* Combined antiangiogenic therapy is superior to single inhibitors in a model of renal cell carcinoma. *J Urol* **179**, 326–32 (2008).

[77] Li, H. *et al.* Possible participation of pICln in the regulation of angiogenesis through alternative splicing of vascular endothelial growth factor receptor mRNAs. *Endothelium* **11**, 293–300 (2004).

[78] Miao, H. Q. *et al.* Neuropilin-1 expression by tumor cells promotes tumor angiogenesis and progression. *FASEB J* **14**, 2532–9 (2000).

[79] Osborne, N. J. *et al.* Semaphorin/neuropilin signaling influences the positioning of migratory neural crest cells within the hindbrain region of the chick. *Dev Dyn* **232**, 939–49 (2005).

[80] Bates, D. *et al.* Neurovascular congruence results from a shared patterning mechanism that utilizes Semaphorin3A and Neuropilin-1. *Dev Biol* **255**, 77–98 (2003).

[81] Tao, Q., Spring, S. C. & Terman, B. I. Characterization of a new alternatively spliced neuropilin-1 isoform. *Angiogenesis* **6**, 39–45 (2003).

[82] Neufeld, G., Kessler, O. & Herzog, Y. The interaction of Neuropilin-1 and Neuropilin-2 with tyrosine-kinase receptors for VEGF. *Adv Exp Med Biol* **515**, 81–90 (2002).

[83] Jin, Q., Alkhatib, B., Cornetta, K. & Alkhatib, G. Alternate receptor usage of neuropilin-1 and glucose transporter protein 1 by the human T cell leukemia virus type 1. *Virology* **396**, 203–12 (2010).

[84] Castellani, V., Falk, J. & Rougon, G. Semaphorin3A-induced receptor endocytosis during axon guidance responses is mediated by L1 CAM. *Mol Cell Neurosci* **26**, 89–100 (2004).

[85] Teesalu, T., Sugahara, K. N., Kotamraju, V. R. & Ruoslahti, E. C-end rule peptides mediate neuropilin-1-dependent cell, vascular, and tissue penetration. *Proc Natl Acad Sci U S A* **106**, 16157–62 (2009).

[86] Piper, M. *et al.* Endocytosis-dependent desensitization and protein synthesis-dependent resensitization in retinal growth cone adaptation. *Nat Neurosci* **8**, 179–86 (2005).

[87] Guirland, C. *et al.* Lipid rafts mediate chemotropic guidance of nerve growth cones. *Neuron* **42**, 51–62 (2004).

[88] Moretti, S. *et al.* Semaphorin3A signaling controls Fas (CD95)-mediated apoptosis by promoting Fas translocation into lipid rafts. *Blood* **111**, 2290–9 (2008).

[89] Mukherjee, S., Tessema, M. & Wandinger-Ness, A. Vesicular trafficking of tyrosine kinase receptors and associated proteins in the regulation of signaling and vascular function. *Circ Res* **98**, 743–56 (2006).

[90] Lantuejoul, S. *et al.* Expression of VEGF, semaphorin SEMA3F, and their common receptors neuropilins NP1 and NP2 in preinvasive bronchial lesions, lung tumours, and cell lines. *J Pathol* **200**, 336–47 (2003).

[91] Guttmann-Raviv, N. *et al.* Semaphorin-3A and semaphorin-3F work together to repel endothelial cells and to inhibit their survival by induction of apoptosis. *J Biol Chem* **282**, 26294–305 (2007).

[92] Vieira, J. M., Schwarz, Q. & Ruhrberg, C. Selective requirements for NRP1 ligands during neurovascular patterning. *Development* **134**, 1833–43 (2007).

[93] Wu, F. T. *et al.* Computational kinetic model of VEGF trapping by soluble VEGF receptor-1: Effects of transendothelial and lymphatic macromolecular transport. *Physiol Genomics* **38**, 29–41 (2009).

[94] Whittles, C. E. *et al.* ZM323881, a novel inhibitor of vascular endothelial growth factor-receptor-2 tyrosine kinase activity. *Microcirculation* **9**, 513–22 (2002).

[95] Ori, A. *et al.* Identification of heparin binding sites in proteins by selective labelling. *Mol Cell Proteomics* **10**, 2256–65 (2009).

[96] Uniewicz, K. A. *et al.* Differential scanning fluorimetry measurement of protein stability changes upon binding to glycosaminoglycans: a screening test for binding specificity. *Anal Chem* **82**, 3796–802 (2010).

[97] Yates, E. A. *et al.* 1H and 13C NMR spectral assignments of the major sequences of twelve systematically modified heparin derivatives. *Carbohydr Res* **294**, 15–27 (1996).

[98] Patey, S. J., Edwards, E. A., Yates, E. A. & Turnbull, J. E. Heparin derivatives as inhibitors of BACE-1, the Alzheimer's beta-secretase, with reduced activity against factor Xa and other proteases. *J Med Chem* **49**, 6129–32 (2006).

[99] Turnbull, J. E. Analytical and preparative strong anion-exchange HPLC of heparan sulfate and heparin saccharides. *Methods Mol Biol* **171**, 141–7 (2001).

[100] Popplewell, J. F. *et al.* Fabrication of carbohydrate surfaces by using nonderivatised oligosaccharides, and their application to measuring the assembly of sugar-protein complexes. *Chembiochem* **10**, 1218–26 (2009).

[101] Ornitz, D. M. *et al.* Receptor specificity of the fibroblast growth factor family. *J Biol Chem* **271**, 15292–7 (1996).

[102] Mellberg, S. *et al.* Transcriptional profiling reveals a critical role for tyrosine phosphatase VE-PTP in regulation of VEGFR2 activity and endothelial cell morphogenesis. *FASEB J* **23**, 1490–502 (2009).

[103] Heukeshoven, J. & Dernick, R. Improved silver staining procedure for fast staining in PhastSystem Development Unit. I. Staining of sodium dodecyl sulfate gels. *Electrophoresis* **9**, 28–32 (1988).

[104] Turnbull, J. E., Hopwood, J. J. & Gallagher, J. T. A strategy for rapid sequencing of heparan sulfate and heparin saccharides. *Proc Natl Acad Sci U S A* **96**, 2698–703 (1999).

[105] Soding, J., Biegert, A. & Lupas, A. N. The HHpred interactive server for protein homology detection and structure prediction. *Nucleic Acids Res* **33**, W244–8 (2005).

[106] Aricescu, A. R. *et al.* Molecular analysis of receptor protein tyrosine phosphatase mu-mediated cell adhesion. *EMBO J* **25**, 701–12 (2006).

[107] Aricescu, A. R. *et al.* Structure of a tyrosine phosphatase adhesive interaction reveals a spacer-clamp mechanism. *Science* **317**, 1217–20 (2007).

[108] Holm, L. & Park, J. DaliLite workbench for protein structure comparison. *Bioinformatics* **16**, 566–7 (2000).

[109] Thompson, J. D., Higgins, D. G. & Gibson, T. J. CLUSTAL W: improving the sensitivity of progressive multiple sequence alignment through sequence weighting, position-specific gap penalties and weight matrix choice. *Nucleic Acids Res* **22**, 4673–80 (1994).

[110] Eswar, N. *et al.* Protein structure modeling with MODELLER. *Methods Mol Biol* **426**, 145–59 (2008).

[111] Bradford, J. R. & Westhead, D. R. Improved prediction of protein-protein binding sites using a support vector machines approach. *Bioinformatics* **21**, 1487–94 (2005).

[112] Qin, S. & Zhou, H. X. meta-PPISP: a meta web server for protein-protein interaction site prediction. *Bioinformatics* **23**, 3386–7 (2007).

[113] de Vries, S. J., van Dijk, A. D. & Bonvin, A. M. WHISCY: what information does surface conservation yield? Application to data-driven docking. *Proteins* **63**, 479–89 (2006).

[114] Niesen, F. H., Berglund, H. & Vedadi, M. The use of differential scanning fluorimetry to detect ligand interactions that promote protein stability. *Nat Protoc* **2**, 2212–21 (2007).

[115] Somers, W., Stahl, M. & Seehra, J. S. 1.9 A crystal structure of interleukin 6: implications for a novel mode of receptor dimerization and signaling. *EMBO J* **16**, 989–97 (1997).

[116] Sugio, S. *et al.* Crystal structure of human serum albumin at 2.5 A resolution. *Protein Eng* **12**, 439–46 (1999).

[117] Pathuri, P., Vogeley, L. & Luecke, H. Crystal structure of metastasis-associated protein S100A4 in the active calcium-bound form. *J Mol Biol* **383**, 62–77 (2008).

[118] Anderson, B. F. *et al.* Structure of human lactoferrin at 3.2-A resolution. *Proc Natl Acad Sci U S A* **84**, 1769–73 (1987).

[119] Arakawa, T. & Kita, Y. Stabilizing effects of caprylate and acetyltryptophanate on heat-induced aggregation of bovine serum albumin. *Biochim Biophys Acta* **1479**, 32–6 (2000).

[120] Mata, L., Sanchez, L., Headon, D. R. & Calvo, M. Thermal Denaturation of Human Lactoferrin and Its Effect on the Ability To Bind Iron. *J Agric Food Chem* **46**, 3964–3970 (1998).

[121] Takagi, S. *et al.* Specific cell surface labels in the visual centers of Xenopus laevis tadpole identified using monoclonal antibodies. *Dev Biol* **122**, 90–100 (1987).

[122] Gualandris, A. *et al.* Microenvironment drives the endothelial or neural fate of differentiating embryonic stem cells coexpressing neuropilin-1 and Flk-1. *FASEB J* **23**, 68–78 (2009).

[123] Schwarz, Q., Maden, C. H., Vieira, J. M. & Ruhrberg, C. Neuropilin 1 signaling guides neural crest cells to coordinate pathway choice with cell specification. *Proc Natl Acad Sci U S A* **106**, 6164–9 (2009).

[124] Kitsukawa, T. *et al.* Overexpression of a membrane protein, neuropilin, in chimeric mice causes anomalies in the cardiovascular system, nervous system and limbs. *Development* **121**, 4309–18 (1995).

[125] Bron, R. *et al.* Functional knockdown of neuropilin-1 in the developing chick nervous system by siRNA hairpins phenocopies genetic ablation in the mouse. *Dev Dyn* **230**, 299–308 (2004).

[126] Kitsukawa, T. *et al.* Neuropilin-semaphorin III/D-mediated chemorepulsive signals play a crucial role in peripheral nerve projection in mice. *Neuron* **19**, 995–1005 (1997).

[127] Kawasaki, T. *et al.* A requirement for neuropilin-1 in embryonic vessel formation. *Development* **126**, 4895–902 (1999).

[128] Matthies, A. M., Low, Q. E., Lingen, M. W. & DiPietro, L. A. Neuropilin-1 participates in wound angiogenesis. *Am J Pathol* **160**, 289–96 (2002).

[129] Zhang, Z. G. *et al.* Up-regulation of neuropilin-1 in neovasculature after focal cerebral ischemia in the adult rat. *J Cereb Blood Flow Metab* **21**, 541–9 (2001).

[130] Staton, C. A., Kumar, I., Reed, M. W. & Brown, N. J. Neuropilins in physiological and pathological angiogenesis. *J Pathol* **212**, 237–48 (2007).

[131] Romeo, P. H., Lemarchandel, V. & Tordjman, R. Neuropilin-1 in the immune system. *Adv Exp Med Biol* **515**, 49–54 (2002).

[132] Bruder, D. *et al.* Neuropilin-1: a surface marker of regulatory T cells. *Eur J Immunol* **34**, 623–30 (2004).

[133] Sarris, M. *et al.* Neuropilin-1 expression on regulatory T cells enhances their interactions with dendritic cells during antigen recognition. *Immunity* **28**, 402–13 (2008).

[134] Gitay-Goren, H. *et al.* Selective binding of VEGF121 to one of the three vascular endothelial growth factor receptors of vascular endothelial cells. *J Biol Chem* **271**, 5519–23 (1996).

[135] Gluzman-Poltorak, Z., Cohen, T., Herzog, Y. & Neufeld, G. Neuropilin-2 is a receptor for the vascular endothelial growth factor (VEGF) forms VEGF-145 and VEGF-165. *J Biol Chem* **275**, 18040–5 (2000).

[136] Castellani, V., De Angelis, E., Kenwrick, S. & Rougon, G. Cis and trans interactions of L1 with neuropilin-1 control axonal responses to semaphorin 3A. *EMBO J* **21**, 6348–57 (2002).

[137] Rabenstein, D. L. Heparin and heparan sulfate: structure and function. *Nat Prod Rep* **19**, 312–31 (2002).

[138] Rodgers, K. D., San Antonio, J. D. & Jacenko, O. Heparan sulfate proteoglycans: a GAGgle of skeletal-hematopoietic regulators. *Dev Dyn* **237**, 2622–42 (2008).

[139] Mach, H. *et al.* Partially structured self-associating states of acidic fibroblast growth factor. *Biochemistry* **32**, 7703–11 (1993).

[140] Linding, R. *et al.* Protein disorder prediction: implications for structural proteomics. *Structure* **11**, 1453–9 (2003).

[141] Gunasekaran, K. *et al.* Enhancing antibody Fc heterodimer formation through electrostatic steering effects: applications to bispecific molecules and monovalent IgG. *J Biol Chem* **285**, 19637–46 (2010).

[142] Fernig, D. G. Optical biosensor techniques to analyze protein-polysaccharide interactions. *Methods Mol Biol* **171**, 505–18 (2001).

[143] Powell, A. K., Yates, E. A., Fernig, D. G. & Turnbull, J. E. Interactions of heparin/heparan sulfate with proteins: appraisal of structural factors and experimental approaches. *Glycobiology* **14**, 17R–30R (2004).

[144] Edwards, P. R. *et al.* Kinetics of protein-protein interactions at the surface of an optical biosensor. *Anal Biochem* **231**, 210–7 (1995).

[145] Rudd, T. R. *et al.* Influence of substitution pattern and cation binding on conformation and activity in heparin derivatives. *Glycobiology* **17**, 983–93 (2007).

[146] Mulloy, B. *et al.* The effect of variation of substitution on the solution conformation of heparin: a spectroscopic and molecular modelling study. *Carbohydr Res* **255**, 1–26 (1994).

[147] Mulloy, B. & Forster, M. J. Conformation and dynamics of heparin and heparan sulfate. *Glycobiology* **10**, 1147–56 (2000).

[148] Thompson, L. D., Pantoliano, M. W. & Springer, B. A. Energetic characterization of the basic fibroblast growth factor-heparin interaction: identification of the heparin binding domain. *Biochemistry* **33**, 3831–40 (1994).

[149] Lindahl, U., Kusche-Gullberg, M. & Kjellen, L. Regulated diversity of heparan sulfate. *J Biol Chem* **273**, 24979–82 (1998).

[150] Rabenstein, D. L., Robert, J. M. & Peng, J. Multinuclear magnetic resonance studies of the interaction of inorganic cations with heparin. *Carbohydr Res* **278**, 239–56 (1995).

[151] Rudd, T. R. *et al.* Site-specific interactions of copper(II) ions with heparin revealed with complementary (SRCD, NMR, FTIR and EPR) spectroscopic techniques. *Carbohydr Res* **343**, 2184–93 (2008).

[152] Alter, S. C. & Schwartz, L. B. Effect of histamine and divalent cations on the activity and stability of tryptase from human mast cells. *Biochim Biophys Acta* **991**, 426–30 (1989).

[153] Young, T. N., Edelberg, J. M., Stack, S. & Pizzo, S. V. Ionic modulation of the effects of heparin on plasminogen activation by tissue plasminogen activator: the effects of ionic strength, divalent cations, and chloride. *Arch Biochem Biophys* **296**, 530–8 (1992).

[154] Skidmore, M. A. *et al.* The activities of heparan sulfate and its analogue heparin are dictated by biosynthesis, sequence, and conformation. *Connect Tissue Res* **49**, 140–4 (2008).

[155] Sasaki, T. *et al.* Structural basis and potential role of heparin/heparan sulfate binding to the angiogenesis inhibitor endostatin. *EMBO J* **18**, 6240–8 (1999).

[156] Faham, S. *et al.* Heparin structure and interactions with basic fibroblast growth factor. *Science* **271**, 1116–20 (1996).

[157] Shaw, J. P. *et al.* The X-ray structure of RANTES: heparin-derived disaccharides allows the rational design of chemokine inhibitors. *Structure* **12**, 2081–93 (2004).

[158] Mohammadi, M., Olsen, S. K. & Goetz, R. A protein canyon in the FGF-FGF receptor dimer selects from an a la carte menu of heparan sulfate motifs. *Curr Opin Struct Biol* **15**, 506–16 (2005).

[159] Nakagawa, Y., Capetillo, S. & Jirgensons, B. Effect of chemical modification of lysine residues on the conformation of human immunoglobulin G. *J Biol Chem* **247**, 5703–8 (1972).

[160] Fazili, K. M., Mir, M. M. & Qasim, M. A. Changes in protein stability upon chemical modification of lysine residues of bovine serum albumin by different reagents. *Biochem Mol Biol Int* **31**, 807–16 (1993).

[161] Costa, B., Giusti, L., Martini, C. & Lucacchini, A. Chemical modification of the dihydropyridines binding sites by lysine reagent, pyridoxal 5'-phosphate. *Neurochem Int* **32**, 361–4 (1998).

[162] Turnbull, J., Powell, A. & Guimond, S. Heparan sulfate: decoding a dynamic multifunctional cell regulator. *Trends Cell Biol* **11**, 75–82 (2001).

[163] Vanpouille, C. *et al.* The heparin/heparan sulfate sequence that interacts with cyclophilin B contains a 3-O-sulfated N-unsubstituted glucosamine residue. *J Biol Chem* **282**, 24416–29 (2007).

[164] Chang, J. Y. Binding of heparin to human antithrombin III activates selective chemical modification at lysine 236. Lys-107, Lys-125, and Lys-136 are situated within the heparin-binding site of antithrombin III. *J Biol Chem* **264**, 3111–5 (1989).

[165] Filizola, M. & Weinstein, H. The structure and dynamics of GPCR oligomers: a new focus in models of cell-signaling mechanisms and drug design. *Curr Opin Drug Discov Devel* **8**, 577–84 (2005).

[166] Miyoshi, J. & Takai, Y. Structural and functional associations of apical junctions with cytoskeleton. *Biochim Biophys Acta* **1778**, 670–91 (2008).

[167] Lajoie, P., Goetz, J. G., Dennis, J. W. & Nabi, I. R. Lattices, rafts, and scaffolds: domain regulation of receptor signaling at the plasma membrane. *J Cell Biol* **185**, 381–5 (2009).

[168] Molina, E. *et al.* The functional properties of a truncated form of endothelial cell protein C receptor generated by alternative splicing. *Haematologica* **93**, 878–84 (2008).

[169] Koyama, H., Yamamoto, H. & Nishizawa, Y. RAGE and soluble RAGE: potential therapeutic targets for cardiovascular diseases. *Mol Med* **13**, 625–35 (2007).

[170] Chitteti, B. R. *et al.* Impact of interactions of cellular components of the bone marrow microenvironment on hematopoietic stem and progenitor cell function. *Blood* (2010).

[171] Lambert, S. *et al.* HTLV-1 uses HSPG and neuropilin-1 for entry by molecular mimicry of VEGF165. *Blood* **113**, 5176–85 (2009).

[172] Herzog, Y. *et al.* Differential expression of neuropilin-1 and neuropilin-2 in arteries and veins. *Mech Dev* **109**, 115–9 (2001).

[173] Bielenberg, D. R., Pettaway, C. A., Takashima, S. & Klagsbrun, M. Neuropilins in neoplasms: expression, regulation, and function. *Exp Cell Res* **312**, 584–93 (2006).

[174] Kawakami, T. *et al.* Neuropilin 1 and neuropilin 2 co-expression is significantly correlated with increased vascularity and poor prognosis in nonsmall cell lung carcinoma. *Cancer* **95**, 2196–201 (2002).

[175] Geretti, E. & Klagsbrun, M. Neuropilins: novel targets for anti-angiogenesis therapies. *Cell Adh Migr* **1**, 56–61 (2007).

[176] Barr, M. P. *et al.* A peptide corresponding to the neuropilin-1-binding site on VEGF(165) induces apoptosis of neuropilin-1-expressing breast tumour cells. *Br J Cancer* **92**, 328–33 (2005).

[177] Starzec, A. *et al.* Structure-function analysis of the antiangiogenic ATWLPPR peptide inhibiting VEGF(165) binding to neuropilin-1 and molecular dynamics simulations of the ATWLPPR/neuropilin-1 complex. *Peptides* **28**, 2397–402 (2007).

[178] Liang, W. C. *et al.* Function Blocking Antibodies to Neuropilin-1 Generated from a Designed Human Synthetic Antibody Phage Library. *J Mol Biol* **366**, 815–29 (2006).

[179] Jarvis, A. *et al.* Small Molecule Inhibitors of the Neuropilin-1 Vascular Endothelial Growth Factor A (VEGF-A) Interaction. *J Med Chem* **53**, 2215–26 (2010).

[180] Sugahara, K. N. *et al.* Tissue-penetrating delivery of compounds and nanoparticles into tumors. *Cancer Cell* **16**, 510–20 (2009).

[181] Bechet, D. *et al.* Neuropilin-1 Targeting Photosensitization-Induced Early Stages of Thrombosis via Tissue Factor Release. *Pharm Res* **27**, 468–79 (2010).

[182] Slimani, H. *et al.* Lipopeptide-based liposomes for DNA delivery into cells expressing neuropilin-1. *J Drug Target* **14**, 694–706 (2006).

[183] Unger, R. E., Krump-Konvalinkova, V., Peters, K. & Kirkpatrick, C. J. In vitro expression of the endothelial phenotype: comparative study of primary isolated cells and cell lines, including the novel cell line HPMEC-ST1.6R. *Microvasc Res* **64**, 384–97 (2002).

[184] Harper, S. J. & Bates, D. O. VEGF-A splicing: the key to anti-angiogenic therapeutics? *Nat Rev Cancer* **8**, 880–7 (2008).

[185] Peirce, S. M. Computational and mathematical modeling of angiogenesis. *Microcirculation* **15**, 739–51 (2008).

[186] Montesano, R., Orci, L. & Vassalli, P. In vitro rapid organization of endothelial cells into capillary-like networks is promoted by collagen matrices. *J Cell Biol* **97**, 1648–52 (1983).

[187] Hesser, B. A. *et al.* Down syndrome critical region protein 1 (DSCR1), a novel VEGF target gene that regulates expression of inflammatory markers on activated endothelial cells. *Blood* **104**, 149–58 (2004).

[188] Fuentes, J. J., Pritchard, M. A. & Estivill, X. Genomic organization, alternative splicing, and expression patterns of the DSCR1 (Down syndrome candidate region 1) gene. *Genomics* **44**, 358–61 (1997).

[189] Holmes, K., Roberts, O. L., Thomas, A. M. & Cross, M. J. Vascular endothelial growth factor receptor-2: structure, function, intracellular signalling and therapeutic inhibition. *Cell Signal* **19**, 2003–12 (2007).

[190] Gupta, K. *et al.* VEGF prevents apoptosis of human microvascular endothelial cells via opposing effects on MAPK/ERK and SAPK/JNK signaling. *Exp Cell Res* **247**, 495–504 (1999).

[191] Abcouwer, S. F., Marjon, P. L., Loper, R. K. & Vander Jagt, D. L. Response of VEGF expression to amino acid deprivation and inducers of endoplasmic reticulum stress. *Invest Ophthalmol Vis Sci* **43**, 2791–8 (2002).

[192] Bartoli, M. *et al.* VEGF differentially activates STAT3 in microvascular endothelial cells. *FASEB J* **17**, 1562–4 (2003).

[193] Uchida, K. *et al.* Glomerular endothelial cells in culture express and secrete vascular endothelial growth factor. *Am J Physiol* **266**, F81–8 (1994).

[194] Schneider, P. Production of recombinant TRAIL and TRAIL receptor: Fc chimeric proteins. *Methods Enzymol* **322**, 325–45 (2000).

[195] Cristofaro, B. & Emanueli, C. Possible novel targets for therapeutic angiogenesis. *Curr Opin Pharmacol* **9**, 102–8 (2009).

[196] Ferrara, N. Role of vascular endothelial growth factor in the regulation of angiogenesis. *Kidney Int* **56**, 794–814 (1999).

[197] An, Z. *et al.* IgG2m4, an engineered antibody isotype with reduced Fc function. *MAbs* **1**, 572–9 (2009).

[198] Eppler, S. M. *et al.* A target-mediated model to describe the pharmacokinetics and hemodynamic effects of recombinant human vascular endothelial growth factor in humans. *Clin Pharmacol Ther* **72**, 20–32 (2002).

[199] Huang, C. Receptor-Fc fusion therapeutics, traps, and MIMETIBODY technology. *Curr Opin Biotechnol* **20**, 692–9 (2009).

[200] Scallon, B. *et al.* Binding and functional comparisons of two types of tumor necrosis factor antagonists. *J Pharmacol Exp Ther* **301**, 418–26 (2002).

[201] da Silva, A. J. *et al.* Alefacept, an immunomodulatory recombinant LFA-3/IgG1 fusion protein, induces CD16 signaling and CD2/CD16-dependent apoptosis of CD2(+) cells. *J Immunol* **168**, 4462–71 (2002).

[202] Fiocco, U. *et al.* Co-stimulatory modulation in rheumatoid arthritis: the role of (CTLA4-Ig) abatacept. *Autoimmun Rev* **8**, 76–82 (2008).

[203] Lee, T. Y. *et al.* Linking antibody Fc domain to endostatin significantly improves endostatin half-life and efficacy. *Clin Cancer Res* **14**, 1487–93 (2008).

[204] Holash, J. *et al.* VEGF-Trap: a VEGF blocker with potent antitumor effects. *Proc Natl Acad Sci U S A* **99**, 11393–8 (2002).

[205] Foubert, P. *et al.* PSGL-1-mediated activation of EphB4 increases the proangiogenic potential of endothelial progenitor cells. *J Clin Invest* **117**, 1527–37 (2007).

[206] Chatterjee, S. & Mayor, S. The GPI-anchor and protein sorting. *Cell Mol Life Sci* **58**, 1969–87 (2001).

[207] Kolonin, M. G. Tissue-specific targeting based on markers expressed outside endothelial cells. *Advances in Genetics* **67**, 61–102 (2009).

[208] Mythreye, K. & Blobe, G. C. Proteoglycan signaling co-receptors: roles in cell adhesion, migration and invasion. *Cell Signal* **21**, 1548–58 (2009).

[209] Frankel, P. *et al.* Chondroitin sulphate-modified neuropilin 1 is expressed in human tumour cells and modulates 3D invasion in the U87MG human glioblastoma cell line through a p130Cas-mediated pathway. *EMBO Rep* **9**, 983–9 (2008).

[210] Shintani, Y. *et al.* Glycosaminoglycan modification of neuropilin-1 modulates VEGFR2 signaling. *EMBO J* **25**, 3045–55 (2006).

[211] Camby, I., Le Mercier, M., Lefranc, F. & Kiss, R. Galectin-1: a small protein with major functions. *Glycobiology* **16**, 137R–157R (2006).